Alma Mater Studiorum - Università di Bologna

Dottorato di Ricerca in Geofisica - XXI Ciclo

Settore scientifico disciplinare di afferenza: GEO/10

CRUSTAL HETEROGENEITIES AND COMPLEXITIES OF FAULT PROCESSES

Ph.D. Thesis of:

Claudio Ferrari

Tutor:

Prof. Maurizio Bonafede

Coordinator:

Prof. Michele Dragoni

Esame finale anno 2009

To Milena

Aknowledgments

This work is the result of my collaboration with Prof. Maurizio Bonafede. I have to express my gratitude to him for his constructive discussions and suggestions. His guide has been fundamental in the develop of the present work.

Contents

Chapter 1

Introduction

The crust represents the outer part of the solid earth and in this region seismic activity concentrates. The estimated conditions of pressure and temperature in the crust suggest that an elastic-brittle behaviour can be assumed for crustal rocks. This means that the action of tectonic forces can determine the build up of stress in localized regions of the crust. This build up continues until intact rocks fail or suitably oriented preexisting faults are activated. Faults represent surfaces of weakness in the crust that are blocked by the action of friction. If the shear stress on a fault surface overcomes the friction threshold then the fault can slip. The relative movement of the contact surfaces can be of two types: we talk about aseismic slip if the relative movement takes place at slow velocity, while the seismic slip refers to a sudden fast relative movement of the two blocks in contact. If the stress conditions acting on the fault determine the seismic slip, then the elastic deformation energy can be released in the form of elastic waves and the phenomenon known as earthquake takes place. In many regions of the earth, seismic activity presents anomalous features and the interpretation of this activity can represent a difficult task. Complexities in fault processes must be invoked in order to interpret such features and the development of such complexities can be related to the heterogeneous structure of the crust. Therefore the study of crustal heterogeneities is important in order to achieve a better understanding of fault processes and in this work we will refer to two different types of crustal heterogeneities: the first type involves the concept of asperity, while the second is related to the layered structure of the shallow crust.

1.1 Complexities in faulting: the concept of asperity

The term *asperity* is often used in seismology to describe heterogeneity in faulting. This term has been used for the first time in this context in Lay et al. (1981), who used it to describe "*regions within earthquakes*" where relatively high moment release occurred. They interpreted this feature in terms of the rupture of a strong region, which they called an asperity. The asperities in their view are interpreted as permanent, mechanically distinct features of subduction zone interfaces. The mechanics of rupture of a single asperity

represents an external crack problem in which an internal unbroken region is surrounded by a previously broken area (Das and Kostrov , 1983). Rupture through the asperity occurs in a similar way as crack propagation, the major difference being that when a crack ruptures it causes an increase in stress of the surrounding parts of the fault, whereas when an asperity ruptures it causes an increase in slip in the surrounding part. Lay et al. (1980) employed an asperity model in order to describe rupture characteristics of subduction zones, but the asperities in this work are defined in a different way. The asperities are considered as regions that slip seismically with large moment release and Lay et al. (1980) assume that the intervening regions normally slip aseismically. These regions are only ruptured seismically when an adjoining asperity ruptures and dynamically propagates into them. In such a case no inference regarding the relative strength of the different regions can be made, since the asperity can be simply interpreted as a part of the subduction zone interface characterized by an unstable constitutive law (e.g. velocity weakening), while the surrounding regions shows a stable behaviour (velocity strengthening).
In Chapter 2 we propose an asperity model in which high pressure fluids ascending from the brittle-ductile transition plays a preeminent role. In our model, the presence of the asperity is invoked not only to explain the high stress release observed, since the asperity is also considered responsible of a perturbation of the pressure in the region surrounding the asperity. The nature of the asperity will be discussed in terms of the properties of the ascending fluids and the mutual interaction between the fluid and the asperity will be invoked to explain the preparatory processes of the $M_s = 6.6$ earthquake of June 17-th, 2000 in Iceland.

1.2 Complexities of fault processes: the role of layering

Several regions with transcurrent tectonics are characterized by complex distributions of surface fractures which cannot be simply explained in terms of the stress field produced by the seismic fault. An example of these complex patterns is represented by double-en-echelon structures. These structures are characterized by arrays of fractures whose direction is not parallel to the main fault strike direction and furthermore the single fractures are aligned along another direction with respect to the array (Figure 1.1). This kind of observations can be related to the heterogeneous structure of the crust, in fact in this work we shall show how fault processes may be significantly affected by stratification properties of the media.

Bonafede et al. (2002) investigated the case of a planar transcurrent fault developing across the interface between two media characterized by different elastic properties μ, ν with $m = \frac{\mu_2}{\mu_1} > 1$ (Figure 1.2). The welded boundary condition imposes that stress drop must be discontinuous at the interface, since on both crack sections the stress drop must be proportional to the local rigidity value.

$$\frac{\Delta\sigma_1}{\mu_1} = \frac{\Delta\sigma_2}{\mu_2} \tag{1.1}$$

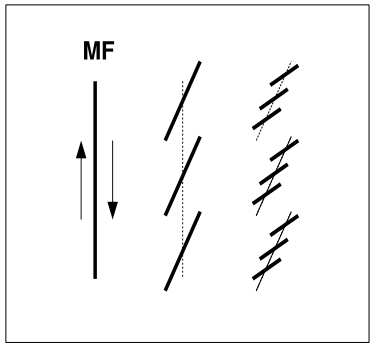

Figure 1.1: Double-en-echelon

This stress drop condition has considerable influence on the style of faulting along a transform margin. In fact we can immediately identify several important cases in which such a condition cannot be satisfied.

Among these we can mention the following three cases:

(a) *Fresh fractures developing in presence of friction.*
In this case the initial stress on each crack surface can be proportional to the local rigidity value, but the residual stress is governed by friction and so stress drop in the shallow layer cannot match the value prescribed by the stress drop condition proper to a vertical planar crack.

(b) *Faults developing across a rheological discontinuity.*
For instance, if layer 2 is Maxwell viscoelastic, the initial stress in the brittle layer is typically much higher than in the ductile layer 2, even if the instantaneous rigidity in the ductile layer is higher than in the brittle layer. In this case the stress drop in the soft layer 1 would be much higher than in the harder (coseismically) but ductile medium 2. The stress drop condition (1.1) cannot be fulfilled in a fault event penetrating the interface.

(c) *Faults developing from a reference configuration in which the stress does not vanish*

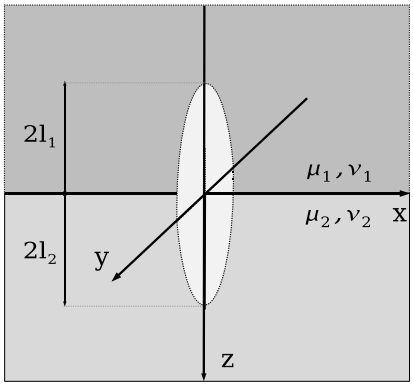

Figure 1.2: Planar fault model

simultaneously in both media.
There are few instances in which the initial shear stress prior to crack failure is not proportional to rigidity. Among these the recent emplacement of sediments or volcanics on top of pre-stressed basement rock is particularly relevant in geophysics. In such cases, the stress drop in the sedimentary layer can be much lower than prescribed by the stress drop discontinuity condition (1.1).

The stress drop condition in these cases cannot be fulfilled, therefore strike-slip faulting cannot be described within the framework of the model of a planar crack surface across a welded boundary. To obtain a crack model suitable to describe strike-slip faulting in cases (a),(b),(c), we must conclude that the failure of the previous model is caused by a violation of one of its assumptions. In our work we shall consider the following possible cases:

- Welded interface: the dip of the fault surface cannot be vertical in both media (Figure 1.3a) or else that fault branching may take place on one side of the interface (Figure 1.3b)
- Unwelded interface: the interface cannot remain welded during crack slip (Figure 1.4).

In Chapter 3 we introduce the basic theory (dislocation theory) upon which crack models are based, since two models of this type are used in Chapters 4-5 in order to describe fault bending and fault branching across a welded interface. In Chapter 6 we consider the case in which the interface become unwelded and we use dislocation models in order to study the conditions for unwelding and for the opening of secondary fractures. In the last chapter, we discuss the results obtained and draw our conclusions.

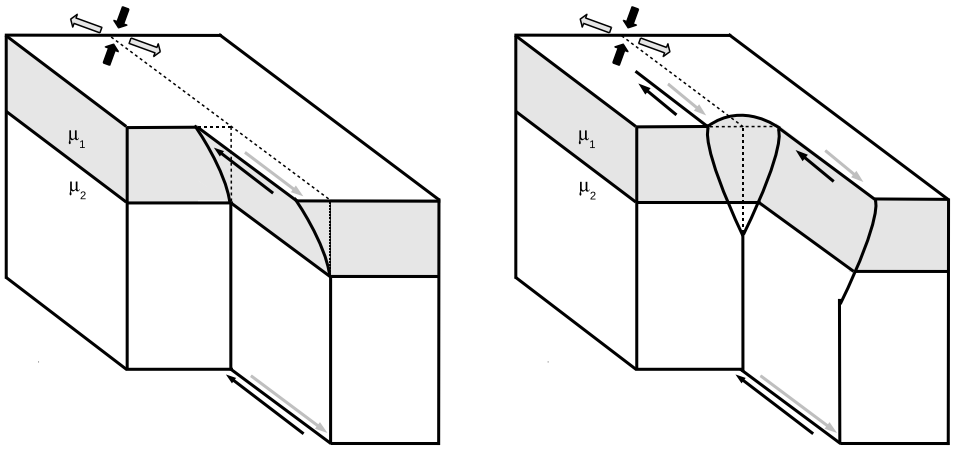

(a) Fault bending (b) Fault branching

Figure 1.3: Welded interface

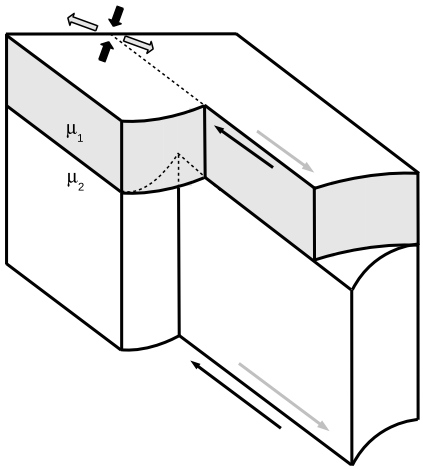

Figure 1.4: Unwelded interface

Chapter 2

Asperity model

In this chapter we investigate the effects induced on stress field by the presence of an asperity in a homogeneous medium. The presence of an asperity in the hypocentral region of the $M_s = 6.6$ earthquake of June 17-th, 2000 in the South Iceland Seismic Zone is invoked to explain two significant features related to this seismic event: the high magnitude of the earthquake with respect to the estimated fault dimensions and the change of seismicity pattern before and after the mainshock. The first model (Elastic model) presented simulates the presence of an asperity in terms of a high rigidity spherical inclusion, within a softer elastic medium in a transform domain with a deviatoric stress field imposed at remote distances. In the second model (Viscoelastic model) we consider the case in which the medium surrounding the inclusion is viscoelastic.

2.1 Geodynamic framework

The South Iceland Seismic Zone (SISZ) is a left-lateral transform zone located between the Reykjanes peninsula and the east volcanic zone, with a length $L \sim 70\,\text{km}$ in the EW direction and a width $w = 10 - 15\,\text{km}$ in the NS direction (Figure 2.1). The depth h of the brittle-ductile (B-D) transition is quite sharp increasing from $8\,\text{km}$ in the E to $12\,\text{km}$ in the W (Stefansson et al. (1993)). The left-lateral motion is estimated by geodetic means as 1.95 cm/yr mostly in the EW direction (De Mets et al. (1994)). One of the peculiar features of the SISZ is that the main faults are all right-lateral strike-slip and oriented NS, with a quite regular parallel spacing of 5-6 km (Figure 2.2b), suggesting a bookshelf failure mechanism (Einarsson et al. (1991)). The historical seismicity is characterized by sequences of large earthquakes, reaching magnitude 7. A sequence lasts up to 30 years and a complete seismic cycle is ∼140 years (Stefansson and Halldorsson (1988)).

The mainshock of June 17-th, 2000 ($M_s = 6.6$) interrupted a period of seismic quiescence since 1912. This event was followed on June 21-th, 2000 by a $M_s = 6.6$ earthquake located 17 km west, which was interpreted as a triggered event (Arnadottir et al. (2003)). Migration of seismicity from east to west during short periods of time (days to weeks) is another characteristic feature of this area. The hypocenter of the June 17-th, 2000 earth-

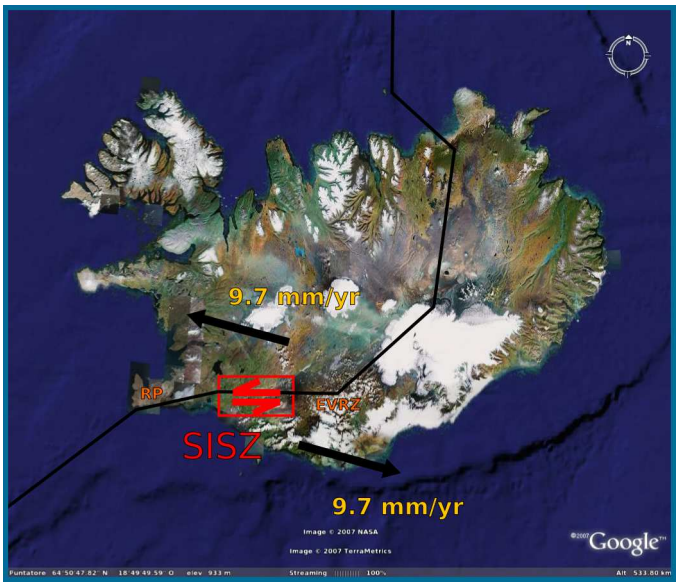

Figure 2.1: Iceland

quake was located at 6.3 km depth and the fault surface had a length of 12.5 km along strike, oriented 7° E from N, and a vertical extension of 10 km (from the surface to the B-D transition), as shown by the local seismic network and by USGS and Harvard CMT solutions (Stefansson et al. (2007)).

A significant feature of the June 17-th mainshock is the high magnitude with respect to the expected magnitude for a fault with these dimensions: the average dimensions expected for the fault of a magnitude 6.6 event are 30 km length and 10 km height, with a slip of 40 cm (Wells et al. (1994)) while the average slip for this fault was $\sim 2\,\mathrm{m}$. This indicates a very high stress drop in the hypocentral region. The accurately located aftershocks were mostly in close proximity of the fault plane and suggest the presence of an asperity with $\sim 3\,\mathrm{km}$ diameter in the middle of the fault (Figure 2.2c). The seismic moment release in the SISZ is in general agreement with the observed strain build up during a 140 year period (Stefansson and Halldorsson (1988)). It was also pointed out by modeling of the historical seismicity (Roth (2004)) that the time and place of successive earthquakes in the SISZ are not predicted by the highest induced stress, with exceptions of events very close in time and space: local strength heterogeneities seem to control the place. The two earthquakes of year 2000 released only 1/4–1/3 of the expected moment (Arnadottir et al. (2005), Stefansson et al. (2007)).

The second significant feature associated with this earthquake is the change of seismicity pattern before and after the mainshock. Deep foreshocks in the area of the impending June 17-th earthquake were continuous in time and nearly uniformly distributed horizontally, between $\sim 8-10$ km depth. They show magnitudes generally $\lesssim 1$, with relatively high b-values $\gtrsim 1.2$ (Wyss and Stefansson (2006)). Their focal mechanisms show P-axes significantly scattered with respect to the regional stress direction (Lund et al. (2005)). Shallower foreshocks (at $\sim 4-8\,\mathrm{km}$ depth) took place episodically in swarms, which be-

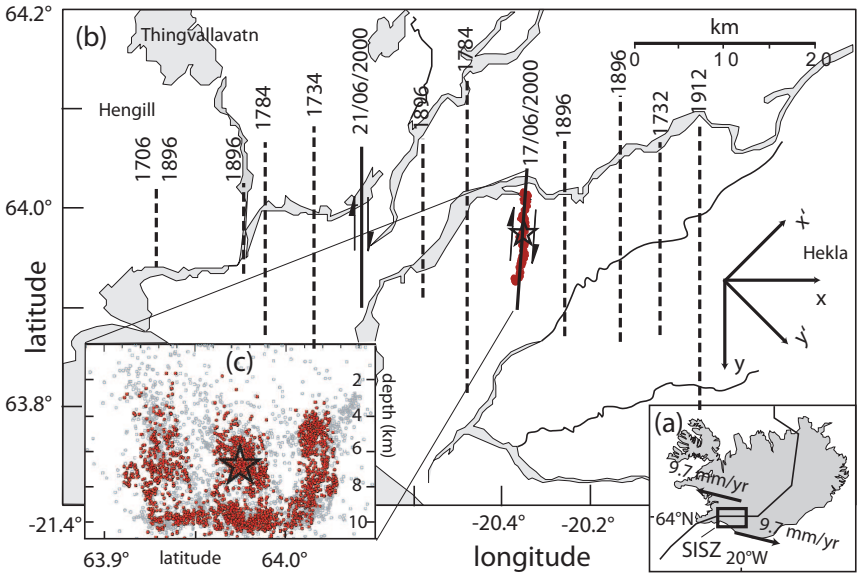

Figure 2.2: SISZ

came more and more frequent while approaching the time of the mainshock, and typically provided low b-values and P-axes coherent with the regional stress. During 9 years of sensitive microearthquake observations before the mainshock the spatial distribution of shallow foreshocks has been progressively concentrating within an elongated volume, oriented $\sim 30°$ W of N and centred on the hypocenter of the impending mainshock (Figure 2.3).

The features of deep foreshocks are generally interpreted in terms of high pressure fluids ascending from the mantle. The widespread presence of fluids permeating the crust in the South Iceland Seismic zone (SISZ) was clearly demonstrated by the post-seismic deformation of the two M_s 6.6 earthquakes of June 2000 (Jonsson et al. (2003)). Many evidences suggest the presence of high pressure fluids down to the base of the crust in the SISZ. Magnetotelluric data (Hersir et al. (1984)) indicate low resistivity (10-20 Ohm m) below the brittle-ductile transition (at 10-20 km depth). This suggests the presence of a fluid reservoir within a solid matrix. The high b-values of deep foreshocks is a typical feature of seismicity induced by high fluid pressure, due to the weakening role of fluids (that lower the effective normal stress) and to the pressure drop accompanying fracture extension.

The pattern associated with shallower foreshocks indicates a perturbation of mean pressure that favours ascending of high pressure fluids only in selected quadrants. So the pattern of shallower foreshocks can be considered as a further suggestion to the presence of an asperity.

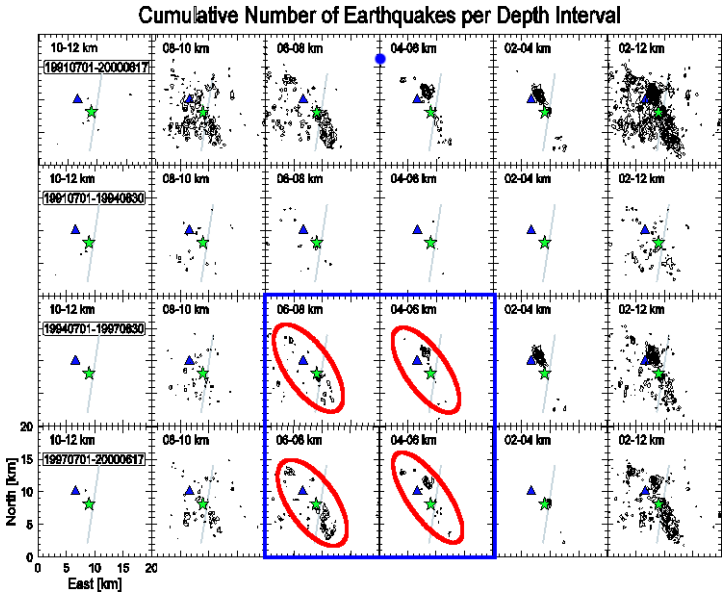

Figure 2.3: Foreshock activity during the period 1991-2000

2.2 Elastic model

We examine the effects induced on the stress field by the presence of a spherical inclusion in a homogeneous medium, assuming an elastic behaviour for both regions but different elastic properties denoted with μ_1, ν_1 for the surrounding media and μ_2, ν_2 for the inclusion. More precisely the asperity is modeled as a spherical inclusion (with radius $a = 1.5$ km) in welded contact with the external medium, so that the following conditions must be imposed on the boundary of the inclusion:

- continuity of the displacement field

$$\begin{cases} {u_r}^1 (a, \theta) = {u_r}^2 (a, \theta) \\ {u_\theta}^1 (a, \theta) = {u_\theta}^2 (a, \theta) \end{cases} \tag{2.1}$$

- continuity of normal and tangential stress components

$$\begin{cases} {\sigma_{rr}}^1 (a, \theta) = {\sigma_{rr}}^2 (a, \theta) \\ {\sigma_{\theta\theta}}^1 (a, \theta) = {\sigma_{\theta\theta}}^2 (a, \theta) \\ {\sigma_{\varphi\varphi}}^1 (a, \theta) = {\sigma_{\varphi\varphi}}^2 (a, \theta) \\ {\sigma_{r\theta}}^1 (a, \theta) = {\sigma_{r\theta}}^2 (a, \theta) \end{cases} \tag{2.2}$$

A deviatoric stress field is imposed at remote distance with a compressive component (-1 MPa) in direction SW, and a tensile component (+1 MPa) acting NW. The geometry of the model is described in Figure 2.4, where the two red arrows indicates the E-W movement of a left-lateral transform zone, like the SISZ.

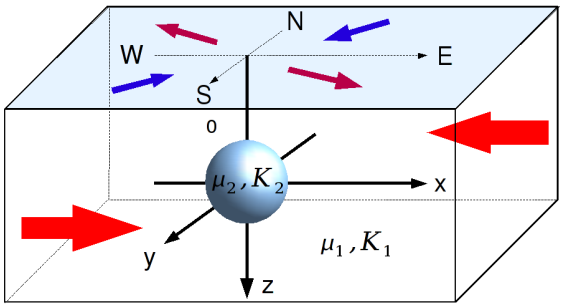

Figure 2.4: Sketch of elastic model

We employ the solution of Goodier (1933) for a spherical inclusion under uniform uniaxial stress and to obtain the solution proper to a transform domain we exploit the linear property of the system superposing two such solutions for two opposite uniaxial stresses acting along NE and NW.
In the surrounding media the solution for a spherical inclusion under uniform uniaxial stress has this form

$$
\begin{cases}
u_r{}^1(r,\theta) = -\dfrac{A}{r^2} - \dfrac{3B}{r^4} + \left[\dfrac{5-4\nu_1}{1-2\nu_1} - \dfrac{C}{r^4} - \dfrac{9B}{r^4}\right]\cos(2\theta) + \dfrac{Ta}{2E_1}\left[(1-\nu_1) + (1+\nu_1)\cos(2\theta)\right] \\
u_\theta{}^1(r,\theta) = -\left[\dfrac{2C}{r^2} + \dfrac{6B}{r^4}\right]\sin(2\theta) - \dfrac{Ta}{2E_1}(1+\nu_1)\sin(2\theta) \\
\sigma_{rr}{}^1(r,\theta) = 2\mu\left\{\dfrac{2A}{r^3} - \dfrac{C^I}{r^3} + 12\,\dfrac{B}{r^5} + \left[-\dfrac{C^{II}}{r^3} + 36\,\dfrac{B}{r^5}\right]\cos(2\theta)\right\} + \dfrac{T}{2}(1+2\cos(2\theta)) \\
\sigma_{\theta\theta}{}^1(r,\theta) = 2\mu\left\{-\dfrac{A}{r^3} - \dfrac{C^I}{r^3} - 3\,\dfrac{B}{r^5} + \left[\dfrac{C}{r^3} - 21\,\dfrac{B}{r^5}\right]\cos(2\theta)\right\} \\
\sigma_{\varphi\varphi}{}^1(r,\theta) = 2\mu\left\{-\dfrac{A}{r^3} - \dfrac{C^{III}}{r^3} - 9\,\dfrac{B}{r^5} + \left[3\,\dfrac{C}{r^3} - 15\,\dfrac{B}{r^5}\right]\cos(2\theta)\right\} \\
\sigma_{r\theta}{}^1(r,\theta) = 2\mu\left\{-\dfrac{C^{IV}}{r^3} + 24\,\dfrac{B}{r^5}\right\}\sin(2\theta) - \dfrac{T}{2}\sin(2\theta)
\end{cases}
$$

where

$$
\begin{aligned}
C^I &= \frac{2\nu_1}{1-2\nu_1}C \\
C^{II} &= \frac{2(5-\nu_1)}{1-2\nu_1}C \\
C^{III} &= \frac{2(1-\nu_1)}{1-2\nu_1}C \\
C^{IV} &= \frac{2(1+\nu_1)}{1-2\nu_1}C
\end{aligned}
$$

Inside the inclusion displacement and stress field have the following form

$$\begin{cases} {u_r}^2(r,\theta) = Hr + Fr + 2\nu_2 G r^3 + \left[3Fr + 6\nu_2 G r^3\right]\cos(2\theta) \\ {u_\theta}^2(r,\theta) = -\left[3Fr + (7-4\nu_2)\,G r^3\right]\sin(2\theta) \\ {\sigma_{rr}}^2(r,\theta) = 2\mu\left\{\dfrac{1+\nu_2}{1-2\nu_2}H + F - \nu_2 G\, r^2 + \left[3F - 3\nu_2 G\, r^2\right]\cos(2\theta)\right\} \\ {\sigma_{\theta\theta}}^2(r,\theta) = 2\mu\left\{\dfrac{1+\nu_2}{1-2\nu_2}H + F - 5\nu_2 G\, r^2 - \left[3F + 7\,(2-\nu_2)\,G\, r^2\right]\cos(2\theta)\right\} \\ {\sigma_{\varphi\varphi}}^2(r,\theta) = 2\mu\left\{\dfrac{1+\nu_2}{1-2\nu_2}H - 2F - (15-7\nu_2)\,G\, r^2 - (7+11\nu_2)\,G\, r^2\cos(2\theta)\right\}\sin(2\theta) \\ {\sigma_{r\theta}}^2(r,\theta) = -2\mu\left\{3F + 7\,(7+2\nu_2)\,G\, r^2\right\}\sin(2\theta) \end{cases}$$

To determine the coefficients A, B, C, F, G, H we have to use the boundary conditions (2.1) and (2.2). The coefficients A, B, C relative to the region surrounding the inclusion have been given by Goodier in the cited paper

$$\frac{A}{R^3} = -\frac{T}{8\mu_1}\left\{\frac{\mu_1-\mu_2}{(7-5\nu_1)\,\mu_1 + (8-10\nu_1)\,\mu_2} \times \frac{(1-2\nu_2)\,(6-5\nu_1)\,2\mu_1 + (3+19\nu_2-20\nu_1\nu_2)\,\mu_2}{(1-2\nu_2)\,2\mu_1 + (1+\nu_2)\,\mu_2} - 2\,\frac{\left[(1-\nu_1)\,\dfrac{1+\nu_2}{1+\nu_1} - \nu_2\right]\mu_2 - (1-2\nu_2)\,\mu_1}{(1-2\nu_2)\,2\mu_1 + (1+\nu_2)\,\mu_2}\right\}$$

$$\frac{B}{R^5} = -\frac{T}{8\mu_1}\,\frac{\mu_1-\mu_2}{(7-5\nu_1)\,\mu_1 + (8-10\nu_1)\,\mu_2}$$

$$\frac{C}{R^3} = -\frac{T}{8\mu_1}\,\frac{5\,(1-2\nu_1)\,(\mu_1-\mu_2)}{(7-5\nu_1)\,\mu_1 + (8-10\nu_1)\,\mu_2}$$

while the coefficients F, G, H relative to the internal region can be easily derived

$$F = -\frac{5T}{4}\,\frac{1-2\nu_1}{(7-5\nu_1)\,\mu_1 + (8-10\nu_1)\,\mu_2}$$

$$G = 0$$

$$H = -\frac{T}{9K_1}\,\frac{4\mu_1 + 3K_1}{4\mu_1 + 3K_2}$$

The computations have been performed assuming $\nu_1 = \nu_2 = 0.25$ and $\mu_1 = 3\mu_2 = 30\text{GPa}$. In 2.5, we show the mean pressure change and the shear stress change computed on the mid-plane ($z = 0$) of the sphere. The mean pressure increases in the NE and SW quadrants, while it decreases in the NW and SE quadrants. Accordingly, the presence of the asperity

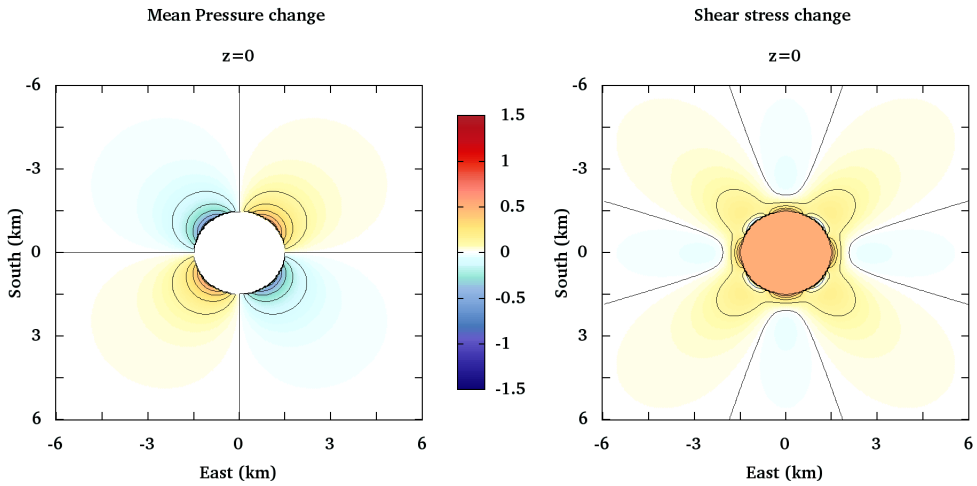

Figure 2.5: Mean pressure change and the shear stress change on the horizontal plane $z = 0$

inhibits hydrofracturing and increases friction in the former case, while hydrofracturing is enhanced and friction decreases in the latter. This result is consistent with the spatial distribution of shallow foreshocks (Figure 2.3). Further a significant increase of $\Delta\sigma_{xy}$ takes place inside the asperity and this high and uniform shear stress is consistent with the high magnitude (M_s=6.6) and slip (2 m) of the earthquake with respect to the values expected from the relatively small fault dimensions.

In Figure 2.6, we show the (a) mean pressure change and (b) the stress component σ_{xy} corresponding to four different levels ($z = 0, \frac{R}{2}, R, \frac{3}{2}R$). For both quantities we can state that the effects determined by the presence of the asperity are important only in its proximity, because the changes induced go to zero at distances of the order of R.

2.3 Nature of the asperity

Considering the results of the previous section, we can state that the elastic model is able to explain both the significant features associated with the earthquake of June 17-th, 2000 in the SISZ. In fact, the concentration of shear stress inside the asperity can justify the high magnitude of this seismic event with respect to the estimated fault dimensions. Furthermore, the presence of the inclusion perturbs the pressure with a pattern that can explain the foreshocks activity, since the ascent of high pressure fluids is favoured SE and NW quadrants, while is inhibited SW and NE quadrants.

In our model the asperity has been modelled as a spherical elastic inclusion embedded in a softer elastic media and calculations have been performed considering a rigidity contrast equal to $m = \mu_2/\mu_1 = 3$. Nevertheless the presence of a high rigidity asperity in the fault region is not supported by seismic tomography studies, which show no major lateral variation of seismic velocities in the hypocentral region (Tryggvason et al. (2002)). To

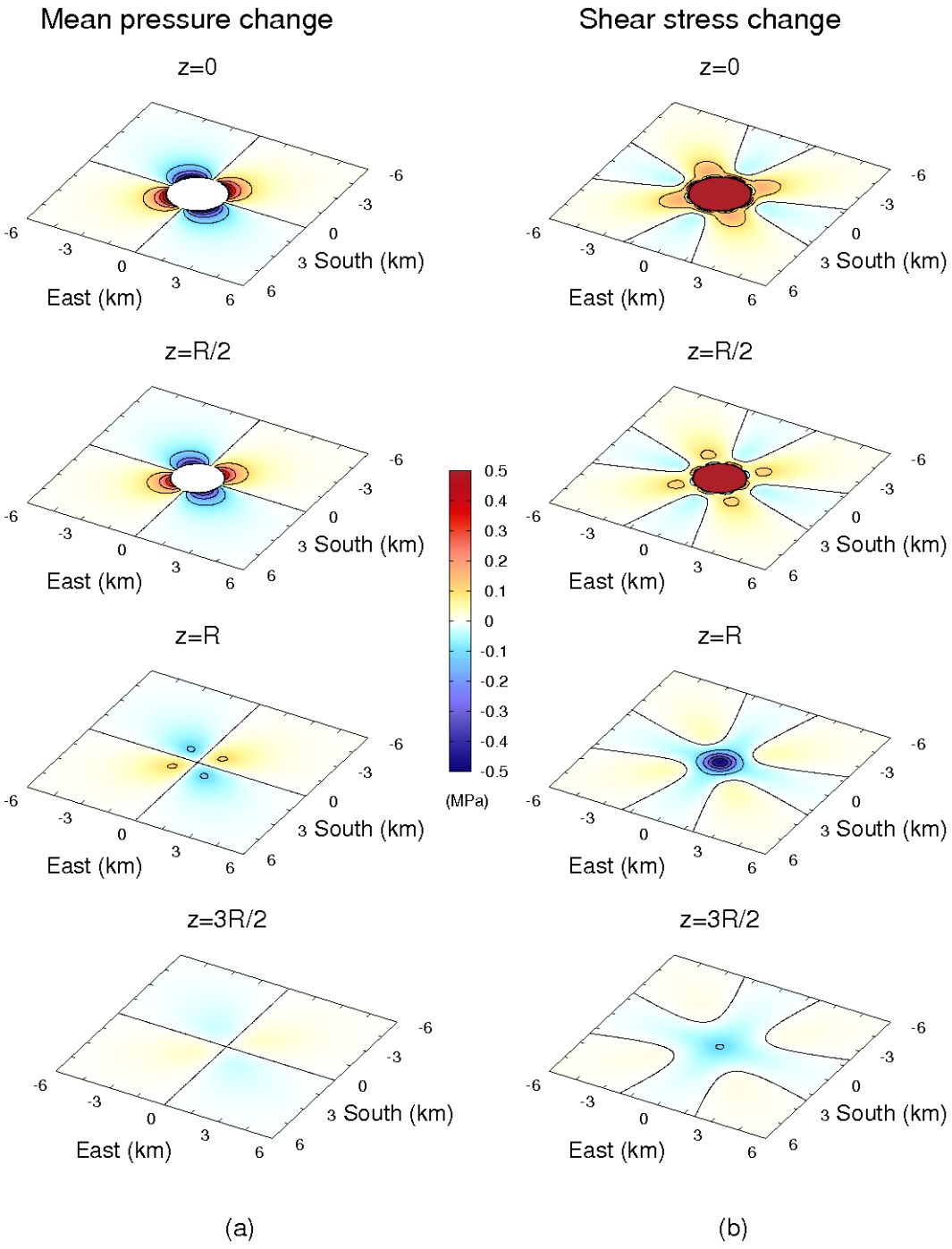

Figure 2.6: Mean pressure and shear stress changes at $z = 0, R/2, R, 3R/2$

be precise, these tomography studies are not resolutive to exclude the presence of a high rigidity asperity, since their resolution ($\sim$ 1 km) is comparable with the dimensions inferred for the asperity. However the presence of a rigidity contrast is not the only way to justify the presence of an asperity. In fact, the asperity and the surrounding medium can have similar short-term rigidities (accounting for the similar seismic velocities), but considering long time deformation processes the two regions can show very different effective rigidities. In order to understand this argument, we have to reconsider the role of high pressure fluids ascending from the mantle. The effect produced by the ascent of these fluids is the opening of several small hydrofractures as envisaged in the effective permeability model proposed by Zencher et al. (2006). The cumulative effects induced on the stress field by the opening of these hydrofractures have been evaluated by Bonafede et al. (2007), employing the solutions for the stress field due to a dislocation opening (with tensile and dip-slip components) close to the interface (the B-D transition) between two different elastic media (Bonafede and Rivalta (1999), Rivalta et al. (2002)). Figure 2.7 shows the stress component $\Delta\sigma_{y'y'}$ induced by the opening of hydrofractures; this stress component enhances fluid flow if positive, while it inhibits fluid flow if negative. The opening of hydrofractures induces compressive stresses laterally (blue areas in Figure 2.7), which are larger along the harder side of the B-D transition. Above the hydrofractures, the induced stress is tensile (yellow areas), and crack opening is favoured. Thus, once hydrofracturing and enhanced fluid migration starts in a region close to the B-D transition, hydrofracturing and fluid flow are inhibited in surrounding regions.
Now we can try to interpret seismic events according the modified Coulomb criterion:

$$|\tau| = S_0 + f\,(\sigma_n - p) \tag{2.3}$$

where τ is the failure stress, S_0 is the inherent rock strength, f is the coefficient of friction, σ_n is the normal stress (positive if compressive), p is the pore pressure. In the interior of a hydrofractured region, p is close to lithostatic and failure may take place at low shear stress; laterally, a high strength asperity is left, since hydrofractures are virtually absent, p is far from lithostatic and failure requires much higher stress. Now the low effective rigidity of the surrounding medium may be due to at least two reasons: the hydrofractured medium can be modelled as viscoelastic, owing to pressure solution processes (e.g. Poirier (1985)) or else the widespread presence of shear cracks (generated seismically or growing subcritically according to the stress-corrosion mechanisms) may produce low effective rigidity at large deviatoric strain (e.g. Jaeger and Cook (1976), Chap. 12). In both cases, the asperity and the surrounding medium would be endowed with similar seismic velocities (sensitive to the short-term/small-amplitude elastic parameters) in agreement with seismic tomography in the SISZ (Tryggvason et al. (2002)). In the following we shall focus on the viscoelastic model for the embedding medium.

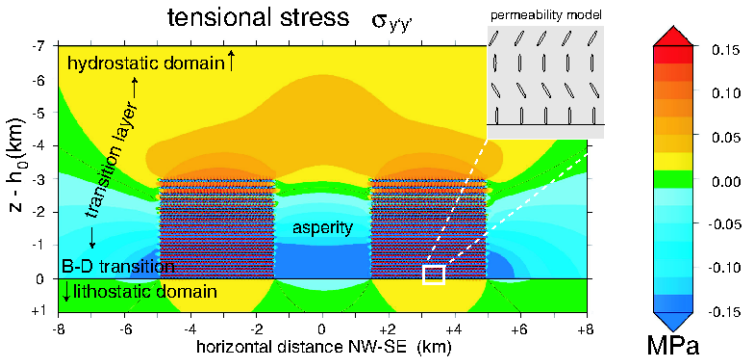

Figure 2.7: Stress field $\sigma_{y'y'}$, acting in the $NW - SE$ direction, induced by a distribution of hydrofractures, opening above the B-D transition under the action of near-lithostatic fluid pressure. The medium below the B-D transition (modeled with effective rigidity $\mu_d = 10^{10}$ Pa) is softer than the brittle medium above (with $\mu_b = 3 \cdot 10^{10}$ Pa). The inset shows the permeability model.

2.4 Viscoelastic model

In this model the asperity, generated by side of a hydrofractured region, is modeled as an elastic spherical inclusion (at the hypocenter of the mainshock, 3 km in diameter) embedded within a medium endowed with much lower effective rigidity. The viscoelastic model has the same geometric configuration of the elastic model and a deviatoric stress field is still imposed at remote distance with a compressive component (-1 MPa) in direction SW, and a tensile component (+1 MPa) acting NW, but with this temporal dependence

$$H(t) = \begin{cases} 0, & t < 0 \\ 1, & t \geq 0 \end{cases} \tag{2.4}$$

Given the solution proper to the elastic model, the viscoelastic (Maxwell) solution in the Laplace transform domain is obtained employing the correspondence principle, with the following substitution for the elastic parameters μ_1, K_1 of the embedding medium

$$\widetilde{\mu_1}(s) = \frac{s\mu_1}{s + \tau^{-1}}, \qquad \widetilde{K}_1(s) = K_1 \tag{2.5}$$

where s is the Laplace transform variable and $\tau = \eta_1/\mu_1$ is the relaxation time (η_1 is the effective viscosity of the medium). The bulk modulus K_1 and the elastic parameters of the inclusion μ_2 and K_2 are assumed to be elastic (with $\mu_2 = \mu_1$ and $K_2 = K_1$). Finally, the stress evolution in the time domain is obtained by inverting Laplace transforms; the coefficients pertinent to the viscoelastic solution are here reported

$$A(t) = \frac{5T}{24}\left\{1 - \frac{8\,\mu_1\,(K_1 - K_2)}{5\,K_1\,(3\,K_2 + 4\,\mu_1)}\,e^{-\frac{3\,K_2}{3\,K_2+4\,\mu_1}\frac{t}{\tau}} + \frac{\mu_1^2\left[135\,K_1^2 + 6\,(19\,\mu_1 + 11\,\mu_2)\,K_1 - 72\,\mu_2\,(\mu_1 - \mu_2)\right]\sinh\left(\frac{a}{2b}\frac{t}{\tau}\right) + a\mu_1\,(14\,\mu_1 + 6\,\mu_2 + 15\,K_1)\cosh\left(\frac{a}{2b}\frac{t}{\tau}\right)}{ab}\,e^{-\frac{c}{2b}\frac{t}{\tau}}\right\}$$

$$B(t) = -\frac{T}{24}\left\{1 - \frac{\mu_1^2\left[135\,K_1^2 + 150\,(\mu_1 + \mu_2)\,K_1 + 40\mu_2\,(\mu_1 + 3\,\mu_2)\right]\sinh\left(\frac{a}{2b}\frac{t}{\tau}\right) + a\mu_1\,(10\,\mu_1 + 10\,\mu_2 + 15\,K_1)\cosh\left(\frac{a}{2b}\frac{t}{\tau}\right)}{ab}\,e^{-\frac{c}{2b}\frac{t}{\tau}}\right\}$$

$$C(t) = -\frac{5T}{4}\,\frac{\mu_1^2\,[3\,(3\,\mu_1 + 7\,\mu_2)\,K_1 + 4\mu_2\,(7\,\mu_1 + 3\,\mu_2)]\sinh\left(\frac{a}{2b}\frac{t}{\tau}\right) - a\mu_1\,(\mu_1 - \mu_2)\cosh\left(\frac{a}{2b}\frac{t}{\tau}\right)}{ab}\,e^{-\frac{c}{2b}\frac{t}{\tau}}$$

$$C^I(t) = -\frac{5T}{24}\left\{1 - \frac{\mu_1^2\left[135\,K_1^2 + 12\,(17\,\mu_1 + 23\,\mu_2)\,K_1 + 16\mu_2\,(13\,\mu_1 + 12\,\mu_2)\right]\sinh\left(\frac{a}{2b}\frac{t}{\tau}\right) + a\mu_1\,(4\,\mu_1 + 16\,\mu_2 + 15\,K_1)\cosh\left(\frac{a}{2b}\frac{t}{\tau}\right)}{ab}\,e^{-\frac{c}{2b}\frac{t}{\tau}}\right\}$$

$$C^{II}(t) = -\frac{15T}{8}\left\{1 - \frac{\mu_1^2\left[405\,K_1^2 + 24\,(18\,\mu_1 + 17\,\mu_2)\,K_1 + 16\mu_2\,(4\,\mu_1 + 21\,\mu_2)\right]\sinh\left(\frac{a}{2b}\frac{t}{\tau}\right) + a\mu_1\,(32\,\mu_1 + 28\,\mu_2 + 45\,K_1)\cosh\left(\frac{a}{2b}\frac{t}{\tau}\right)}{3ab}\,e^{-\frac{c}{2b}\frac{t}{\tau}}\right\}$$

$$C^{III}(t) = -\frac{5T}{24}\left\{1 - \frac{\mu_1^2\left[135\,K_1^2 + 24\,(4\,\mu_1 + \mu_2)\,K_1 - 16\,\mu_2\,(8\,\mu_1 - 3\,\mu_2)\right]\sinh\left(\frac{a}{2b}\frac{t}{\tau}\right) + a\mu_1\,(16\,\mu_1 + 4\,\mu_2 + 15\,K_1)\cosh\left(\frac{a}{2b}\frac{t}{\tau}\right)}{ab}\,e^{-\frac{c}{2b}\frac{t}{\tau}}\right\}$$

$$C^{IV}(t) = -\frac{5T}{8}\left\{1 - \frac{\mu_1^2\left[135\,K_1^2 + 24\,(7\,\mu_1 + 8\,\mu_2)\,K_1 + 48\,\mu_2\,(2\,\mu_1 + 3\,\mu_2)\right]\sinh\left(\frac{a}{2b}\frac{t}{\tau}\right) + a\mu_1\,(8\,\mu_1 + 12\,\mu_2 + 15\,K_1)\cosh\left(\frac{a}{2b}\frac{t}{\tau}\right)}{ab}\,e^{-\frac{c}{2b}\frac{t}{\tau}}\right\}$$

$$F(t) = \frac{5T}{24\mu_2}\left\{1 - \frac{\mu_1^2\left[81\,K_1^2 + 24\,(3\,\mu_1 + 2\,\mu_2)\,K_1 - 16\mu_2\,(2\,\mu_1 - 3\,\mu_2)\right]\sinh\left(\frac{a}{2b}\frac{t}{\tau}\right) + a\mu_1\,(8\,\mu_1 + 4\,\mu_2 + 9\,K_1)\cosh\left(\frac{a}{2b}\frac{t}{\tau}\right)}{ab}\,e^{-\frac{c}{2b}\frac{t}{\tau}}\right\}$$

$$H(t) = \frac{T}{9K_2}\left\{1 - \frac{4\,\mu_1\,(K_1 - K_2)}{K_1\,(3\,K_2 + 4\,\mu_1)}\,e^{-\frac{3\,K_2}{3\,K_2+4\,\mu_1}\frac{t}{\tau}}\right\}$$

where a, b, c have the following form

$$a = \sqrt{3}\mu_1\sqrt{27K_1^2 + 8\mu_2 K_1 + 48\mu_2^2}$$
$$b = (9\mu_1 + 6\mu_2)\,K_1 + (8\mu_1 + 12\mu_2)\,\mu_1$$
$$c = (9\mu_1 + 12\mu_2)\,K_1 + 12\mu_1\mu_2$$

In the case of the viscoelastic model, the computations have been performed assuming $\nu_1 = \nu_2 = 0.25$ and $\mu_1 = \mu_2 = 10$GPa. No rigidity contrast has been imposed between the asperity and the surrounding medium in order to emphasize the role of their different rheological behaviour. In figure 2.8, we can observe the evolution in time ($t' = t/\tau$) of the mean pressure change and of the shear stress change. For (a) $t' < 0$ no deviatoric stress is present, so we have no perturbation in the medium. For (b) $t' \geq 0$ the system is loaded at a constant deviatoric stress and so for $t' = 2$ we can observe that the strength of the perturbation is already increased to a level comparable with the results obtained with the elastic model, in which we have assumed a significant rigidity contrast. For (c) $t' = 2$ we can observe a further increase of both these quantities.

In Figure 2.9, we compare the mean pressure change and the shear stress change

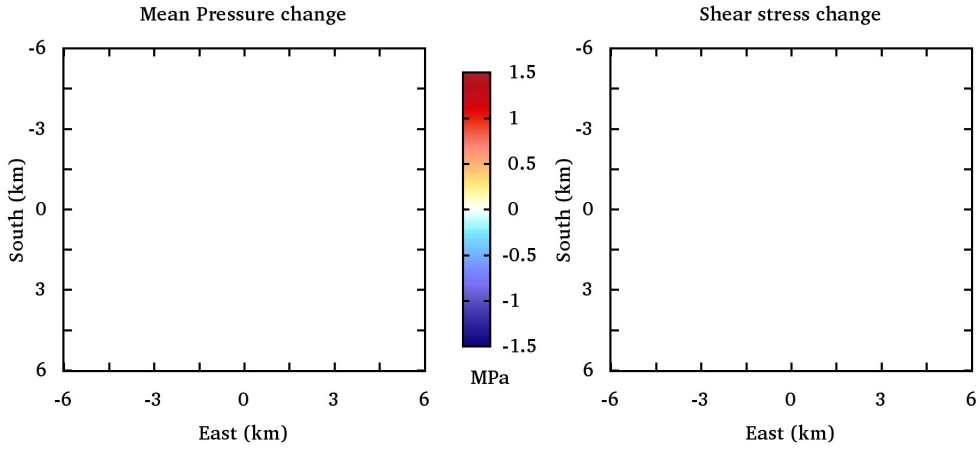

(a) $t' < 0$

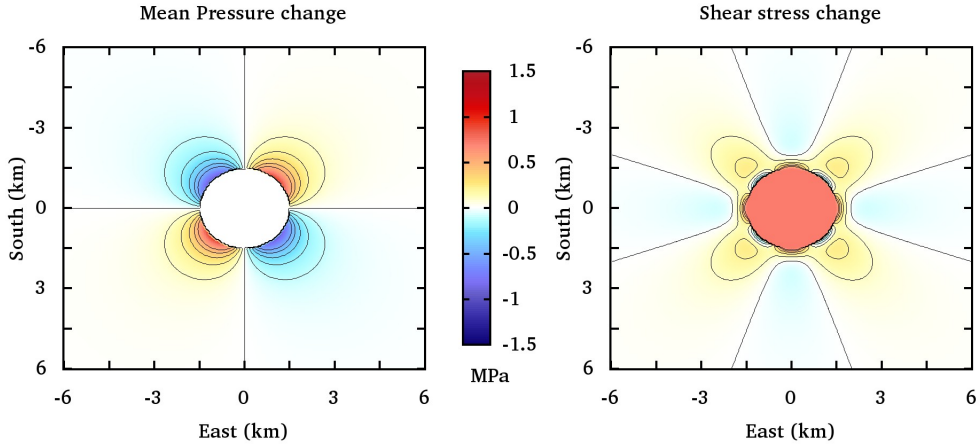

(b) $t' = 2$

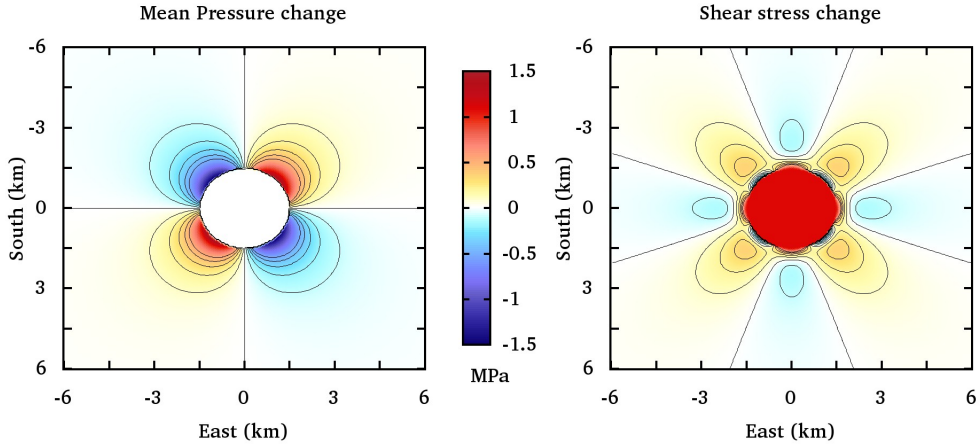

(c) $t' = 4$

Figure 2.8: Mean pressure change and shear stress change computed for three different values of the adimensional time $t' = \frac{t}{\tau}$

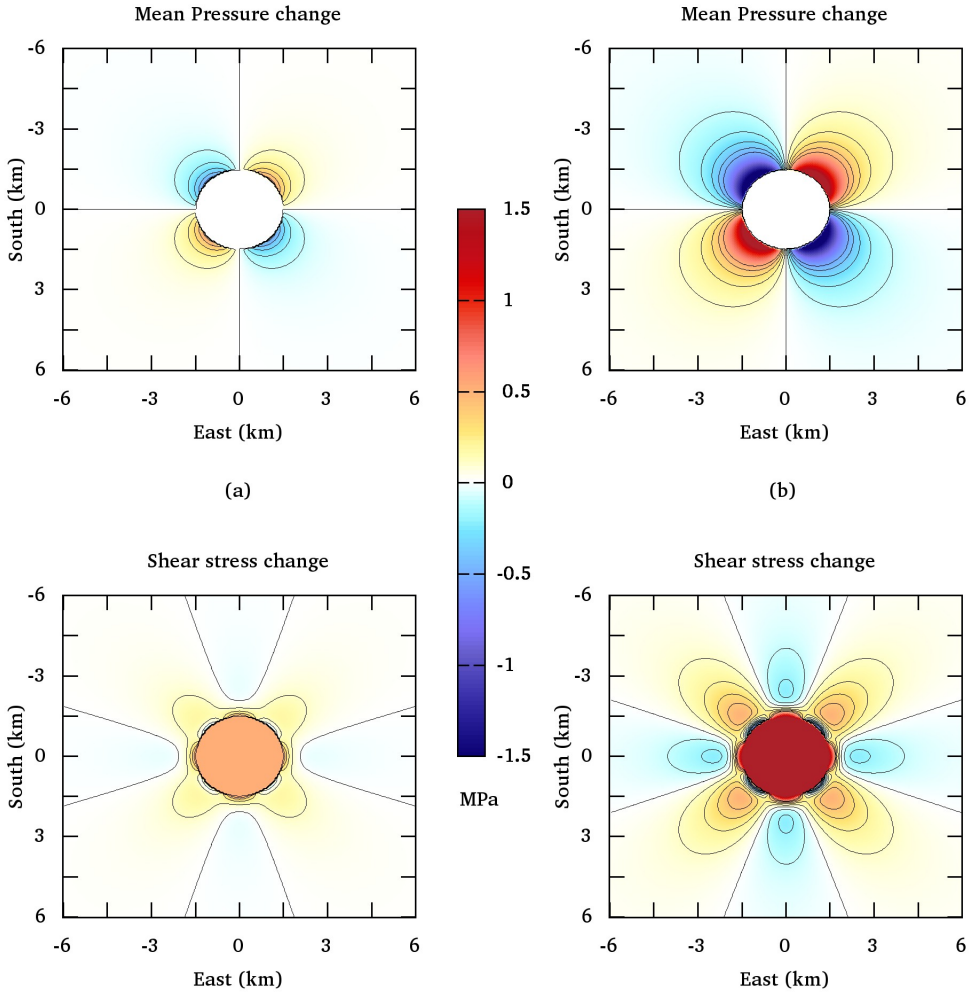

Figure 2.9: Comparison of the results pertinent to (a) the elastic model and (b) the viscoelastic model

computed according to (a) the elastic model, assuming a rigidity contrast $m = 3$, and (b) to the viscoelastic model, considering the fully relaxed response ($t = +\infty$) pertinent to a homogeneous medium ($m = 1$). Although we assume no rigidity contrast, the viscoelastic model is able to explain a much more consistent increase of the shear stress inside the asperity and the same argument is valid for the entity of the perturbation of mean pressure in the surrounding region. We must remark that the system will not necessarily reaches the stress values corresponding to the fully relaxed response since the asperity can fail before and release the shear stress.

2.5 Conclusions

The present model explains several features of the preparatory processes leading to the M_s 6.6 earthquake of June 17-th 2000 in the SISZ. A primary role is envisaged for fluids, ascending at near lithostatic pressure, from below the B-D transition. The cumulative tensile stress induced by the opening of several hydrofractures reinforces lateral variations in fluid flow and asperities are left between two high-flow regions. The different rheological behaviour envisaged between an asperity and the surrounding medium perturbs further the tectonic stress, enhancing foreshock activity in selected quadrants and concentrating a high and uniform deviatoric stress within the asperity, leading to the mainshock. In the previous model the viscoelastic rheology is adopted everywhere outside the asperity; more realistically, this behaviour should be restricted within bounded patches in the crust pervaded by near lithostatic fluid flow. The stress released inelastically within these patches is transferred to the elastic asperities, so that the tectonic strain may match the seismically released moment. Once a fault breaks, that region remains endowed with large permeability, the fluid pressure drops drastically and the next asperities, a few km away are candidates to host the next large earthquakes. The nearly uniform interspace between consecutive faults in the SISZ may be possibly explained in this way. The present model may apply to other tectonically active areas, where fluids of deep origin are present in a low permeability crust. Miller et al. (2004) explain some peculiar features of the aftershocks of the 1997 Colfiorito (Italy) earthquake in terms of high pressure CO_2 released from the mantle; Chiodini et al. (2004) tentatively explain in a similar way the seismic activity along the Apenninic belt in Italy.

Chapter 3

Dislocation theory

Here we present the basic theory of elastic dislocation theory upon which crack models are based. Crack problems will be introduced in Section 3.3 and in this section we also introduce a numerical method (the displacement discontinuity method) suitable to obtain approximate solutions in boundary value problems.

3.1 Dislocation in a homogeneous medium

In mechanics of continuous media, we generally require a continuous and one-valued displacement field, but there is a class of deformation problems requiring a formulation in terms of a multi-valued displacement field. Consider a surface S (Figure 3.1), delimited by a closed curve D (dislocation line), and whose orientation is fixed by versor $\hat{n}$, normal to S. We choose the orientation of curve D to be counter-clockwise with respect to $\hat{n}$. Let's the positive face of surface S moves by a constant quantity $\triangle\mathbf{u} = \mathbf{b}$ with respect to the negative face.

A dislocation with constant Burgers vector $\mathbf{b}$ is defined by the following relation

$$\oint_L du_i = -b_i \tag{3.1}$$

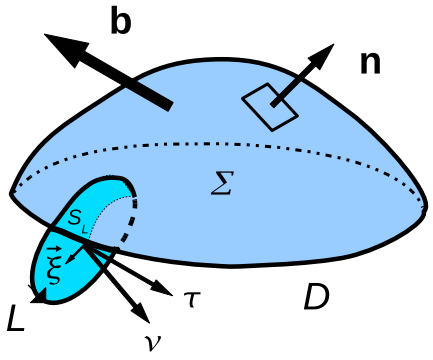

Figure 3.1: *Sketch and notation used to describe a dislocation*

where L is a closed curve shot through by line D.
Displacement field defined by equation (3.1) is a polidrom function because each complete turn around L increases the displacement by a term $+\mathbf{b}$. The displacement can be reduced to a one-valued function making a cut in the media starting from line D and admitting that displacement field is discontinuous on the surface so identified. Furthermore, surface S and dislocation line D are singular domains for $\mathbf{u}$ and its derivates.
Now we can rewrite (3.1) in this way

$$\oint_L du_i = \oint_L \frac{\partial u_i}{\partial x_k}\, dx_k = \oint_L w_{ki}\, dx_k. \tag{3.2}$$

Making use of Stokes theorem for each *i-th* component, we trasform the line integral in a surface integral

$$\oint_L w_{ki}\, dx_k = \int_{S_L} e_{\ell mk} \frac{\partial}{\partial x_m}\, w_{ki}\, \nu_\ell\, dS \tag{3.3}$$

where S_L is an arbitrary surface with normal versor $\hat{\nu}$ and boundary L.
The equation (3.1) can be rewritten to be valid for every L (internal or external to D) making use of Dirac delta function

$$b_i = \int_{S_L} b_i\, \delta(\vec{\xi})\, \tau_\ell\, \nu_\ell\, dS \tag{3.4}$$

where $\vec{\xi}$ identifies a point of S_L with respect to dislocation line D; in that case integral (3.4) gives a result not equal to zero only if curve L is shot through by dislocation line D. The product $\tau_\ell \nu_\ell dS$ is the surface element normal to D. So equation (3.1) can be rewritten making use of (3.3) and (3.4) like one integral on an arbitrary surface S_L.
The integral is equal to zero so we can state

$$e_{\ell mk} \frac{\partial}{\partial x_m} w_{ki} + b_i \tau_\ell\, \delta(\vec{\xi}) = 0 \tag{3.5}$$

Contracting equation (3.5) with $e_{ni\ell}$ and applying the identity e-δ we obtain

$$\frac{\partial}{\partial x_n} w_{kk} - \frac{\partial}{\partial x_i} w_{ni} + e_{ni\ell}\, b_i \tau_\ell\, \delta(\vec{\xi}) = 0. \tag{3.6}$$

If derivative order could be changed (rewriting w_{ki} as $\partial u_i/\partial x_k$), the first two terms of (3.6) will delete each other. Therefore we have to avoid the change of derivative order in singular points $\vec{\xi} = 0$. In absence of volume forces, the elastostatic equation for a homogeneous isotropic medium has this form

$$\lambda \frac{\partial}{\partial x_n} w_{kk} + \mu \frac{\partial}{\partial x_k} w_{kn} + \mu \frac{\partial}{\partial x_k} w_{nk} = 0 \tag{3.7}$$

From (3.7) we obtain $\partial w_{nk}/\partial x_k$ and inserting this in (3.6)

$$\frac{\partial}{\partial x_n} w_{kk} + \frac{\lambda}{\mu} \frac{\partial}{\partial x_n} w_{kk} + \frac{\partial}{\partial x_k} w_{kn} = -e_{ni\ell}\, b_i \tau_\ell\, \delta(\vec{\xi})$$

and rewriting w_{ki} using its definition we obtain

$$\frac{\lambda+\mu}{\mu}\frac{\partial}{\partial x_n}\frac{\partial u_k}{\partial x_k}+\frac{\partial}{\partial x_k}\frac{\partial u_n}{\partial x_k}=-e_{ni\ell}\,b_i\tau_\ell\,\delta(\vec{\xi})$$

Using vectorial formalism and Poisson module ν we can rewrite this equation in this way

$$\frac{1}{1-2\nu}\nabla\left(\nabla\cdot\mathbf{u}\right)+\nabla^2\mathbf{u}=\hat{\tau}\times\mathbf{b}\,\delta(\vec{\xi}) \tag{3.8}$$

3.2 Bidimensional dislocation

In fracture theory, the study of dislocations in condition of plane strain (e.g. $u_x = u_x(x,z), u_z = u_z(x,z), u_y = 0$) or antiplane strain ($u_y = u_y(x,z), u_x = u_z = 0$) plays an important role. In that cases, translation invariance along y axis suggests that dislocation line must be parallel to y axis and dislocation surface can be identified with half-plane $x = 0, z > 0$. These dislocations can be classified according to the direction of Burgers vector

- if $\mathbf{b}$ is parallel to y axis we have a *screw* dislocation
- if $\mathbf{b}$ is normal to the half-plane $x = 0, z > 0$ we have a *tensile* dislocation
- if $\mathbf{b}$ is parallel to z axis we consider a *edge* dislocation

In the following we will consider only screw dislocation because this elementary solution can be used to model transcurrent fault.

3.2.1 Screw dislocation

As dislocation surface we consider the half-plane y, z with $z > 0$, whose orientation is defined by normal versor $\hat{n} = \hat{\jmath}$. y axis is the dislocation line and we take $\hat{\tau} = \hat{j}, \quad \mathbf{b} = b\hat{j}$, where $\hat{j}$ represents y axis versor. The second member of (3.8) is equal to zero. The solution will be indipendent from y for traslational simmetry. Furthermore we suppose $u_x = u_z = 0$; therefore $\nabla\cdot\mathbf{u} = 0$ and equation (3.8) will be reduced to $\nabla^2 u_y = 0$, with the condition $\oint du_y = -b$ attached.
The solution is

$$u_y(x,z) = -\frac{b}{2\pi}\phi, \qquad \phi = \mathrm{Im}\left\{\ln(z+ix)\right\}$$

For simmetry, we sum $b/2$ to displacement field (u_y is equal to $b/2$ in $z > 0$ and $x = 0^+$ while is equal to $-b/2$ in $z > 0$ and $x = 0^-$; this is equivalent to choose the branch of ϕ equal to $-\pi$ in $x = 0^+, z > 0$ and $+\pi$ in $x = 0^-, z > 0$; obviously this traslation does not affect strain and stress fields.

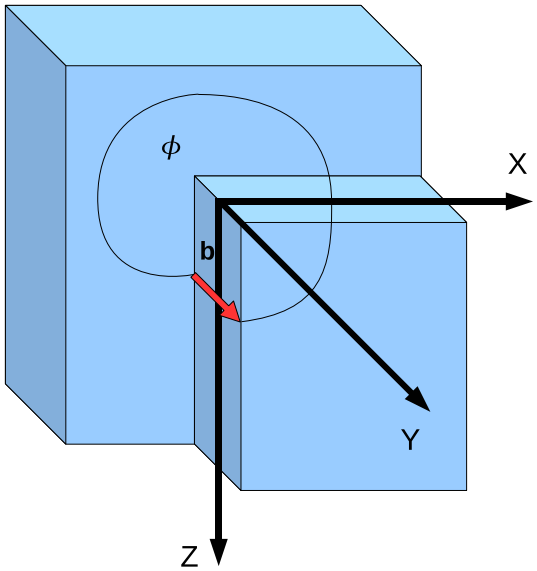

Figure 3.2: *Screw dislocation*

Therefore we can rewrite u_y using real functions

$$u_y = \frac{b}{2\pi}\mathrm{Atan}\left(\frac{z}{x}\right), \qquad \mathrm{Atan}\left(\frac{z}{x}\right) = \begin{cases} \frac{\pi}{2} + \arctan\frac{z}{x} & \text{if } x > 0, \\ -\frac{\pi}{2} + \arctan\frac{z}{x} & \text{if } x < 0 \end{cases} \tag{3.9}$$

It's easy to verify that this function has a jump of finite amplitude b between $x = 0^+$ and $x = 0^-$ for $z > 0$ while it's continuos and derivable everywhere else. Strain and stress can be determined from equation (3.9); the only non-vanishing components are

$$\begin{aligned} e_{yz} = e_{zy} &= \frac{1}{2}\frac{\partial u_y}{\partial z} = \frac{b}{4\pi}\frac{x}{x^2+z^2}, & \sigma_{yz} = \sigma_{zy} &= 2\mu e_{yz} \\ e_{xy} = e_{yx} &= \frac{1}{2}\frac{\partial u_y}{\partial x} = -\frac{b}{4\pi}\frac{z}{x^2+z^2}, & \sigma_{xy} = \sigma_{yx} &= 2\mu e_{xy} \end{aligned} \tag{3.10}$$

3.2.2 Closed rectilinear dislocation

A rectilinear dislocation is closed when its surface opens along a dislocation line and closes along another dislocation line (e.g. a dislocation opening in in $z = z_1$, $x = 0$ and closing in $z = z_2$, $x = 0$ (Figure 3.3)). Solutions of this type can be easily obtained by superimposition, adding a solution with Burgers vector $\mathbf{b}$, dislocation line $z = z_1$, $x = 0$ and an analogous solution with Burgers $-\mathbf{b}$, dislocation line $z = z_2$, $x = 0$. In this way the displacement field is not continuous only on the stripe $z_1 < z < z_2$, $x = 0$. In the case of a homogeneous media, the displacement field proper to a closed screw dislocation can be

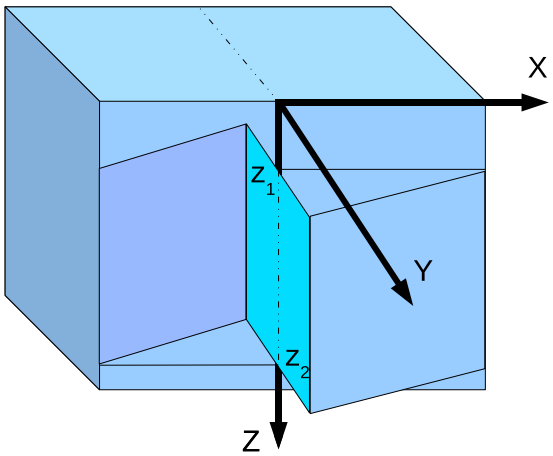

Figure 3.3: *Closed screw dislocation*

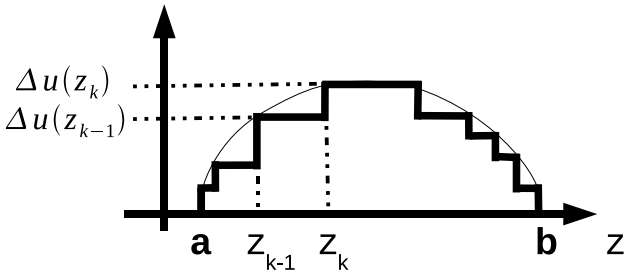

Figure 3.4: *Distribution of dislocations*

derived from (3.9) and has this form

$$u_y = \frac{b}{2\pi}\left[\arctan\frac{z-z_1}{x} - \arctan\frac{z-z_2}{x}\right]$$

Dislocations with constant Burgers vector assigned are defined as *Volterra* dislocations. Instead *Somigliana* dislocations are dislocations with discontinuity of slip assigned but variable on dislocation surface. This kind of dislocations will be introduced in the next section.

3.2.3 Distribution of rectilinear dislocations

The discontinuity of displacement field (Burgers vector) is not necessarily constant on dislocation surface $a < z < b,\ x = 0$. This discontinuity can be described with a function $\Delta u(z)$, derivable (eventually in the sense of generalized functions). Δu can be approximated using a stepwise constant function on the intervals of a finite decomposition of the interval $[a, b]$ $(z_0 = a < z_1 < z_2 < \cdots < z_n = b)$. Displacement is given by

$$\begin{aligned} u_y \quad &\simeq \tfrac{1}{2\pi}\left\{\Delta u(z_0)\arctan\tfrac{z-z_0}{x} + [\Delta u(z_1) - \Delta u(z_0)]\arctan\tfrac{z-z_1}{x} + \right. \\ &\left. + \cdots + [\Delta u(z_n) - \Delta u(z_{n-1})]\arctan\tfrac{z-z_n}{x}\right\} \end{aligned}$$

If $\Delta u(z_0) = 0$, considering the limit $n \to \infty$

$$u_y(x,z) = \frac{1}{2\pi}\int_a^b \rho(z') \arctan\frac{z-z'}{x}\,dz', \qquad \rho(z') = \frac{\partial \Delta u(z')}{\partial z'}. \tag{3.11}$$

The term $\rho(z') = (\partial\Delta u/\partial z')$ is known as *dislocation density*. In the same way we obtain from (3.10) the stress produced by a distribution of screw dislocations

$$\begin{aligned}\sigma_{yz}(x,z) &= \frac{\mu}{2\pi}\int_a^b \rho(z')\,\frac{x}{x^2+(z-z')^2}\,dz' \\ \sigma_{xy}(x,z) &= -\frac{\mu}{2\pi}\int_a^b \rho(z')\,\frac{z-z'}{x^2+(z-z')^2}\,dz'\end{aligned} \tag{3.12}$$

3.3 Crack problems

In the last sections we have assumed to know discontinuity of slip and we have derived resolutive equations for displacement, strain and stress fields in the surrounding medium. In the following we will consider instead *inverse problems*, where we assign the stress drop on the dislocation surface and the unknown function to be determined is the discontinuity of slip on this surface.
In order to solve this kind of problem (called *crack problem*), we start from the determination of induced stress σ^c_{xy} on the dislocation surface by slip of the dislocation: taking the limit for $x \to 0$ we obtain $\sigma_{yz}(0,z) = 0$, while $\sigma_{yz}(0,z)$ is given, for $z < a$ or $z > b$, by the Riemann integral

$$\sigma^c_{xy}(0,z) = \lim_{x\to 0}\left(-\frac{\mu}{2\pi}\int_a^b \rho(z')\,\frac{z-z'}{x^2+(z-z')^2}\,dz'\right) = -\frac{\mu}{2\pi}\int_a^b \frac{\rho(z')}{z-z'}\,dz' \tag{3.13}$$

Nevertheless, for $a<z<b$, the singularity of the integrand does not allow to take the limit under the integral sign; if x is little, but not equal to 0, the integrand is null in $z' = z$; so we can conclude that for $a < z < b$

$$\sigma_{xy}(0^{\pm},z) = -\frac{\mu}{2\pi}\lim_{\epsilon\to 0^+}\left\{\int_a^{z-\epsilon} + \int_{z+\epsilon}^b\right\}\frac{\rho(z')}{z-z'}\,dz' = -\frac{\mu}{2\pi}\,\text{⨍}_a^b \frac{\rho(z')}{z-z'}\,dz' \tag{3.14}$$

where the mark on the sign of integral indicates its principle value.
This is the stress induced by crack slip and that must be added to the stress eventually present before.
Over the crack domain the equilibrium equation is

$$\sigma^0_{xy}(0,z) + \sigma^c_{xy}(0,z) = \sigma^r_{xy}(x,0) \tag{3.15}$$

where σ^r_{xy} is the residual stress after slip occurence. Dislocation density ρ satisfy this singular integral equation

$$-\Delta\sigma(0,z) = \frac{\mu}{2\pi}\int_a^b \frac{\rho(z')}{z-z'}\,dz', \qquad a<z<b \tag{3.16}$$

where the stress $\Delta\sigma = \sigma^0_{xy} - \sigma^r_{xy}$ is assigned.
We consider the following trasformation in order to refer to an adimensional variable

$$\xi = \frac{z-c}{l}$$

where $l = \frac{b-a}{2}$ is the crack half-lenght and $c = \frac{b+a}{2}$ is the depth of its midpoint.
The equation (3.16) become

$$-\Delta\sigma(\xi) = A\int_{-1}^{1} \frac{\rho(\xi')}{\xi-\xi'}\,d\xi', \qquad -1<\xi<1 \tag{3.17}$$

where the integral is valueted in the principle-value sense and

$$\Delta\sigma(\xi) = \sigma^0_{yz}(\ell\xi+c,0) - \sigma^r_{yz}(\ell\xi+c,0), \qquad A=\mu/2\pi, \qquad \rho(\xi') = \rho(\ell\xi'+c)$$

From a mathematical point of view, the equation considered is a singular integral equation of first kind, because the kernel has a simple Cauchy-type singularity. To solve the equation, the first step is to determine the fundamental function $w(\xi)$ which defines the singular nature of dislocation density at the end points $-1, 1$.
As found in Erdogan et al. (1973), the fundamental function must have the following form

$$w(\xi) = (1-\xi)^{\frac{1}{2}+N}\,(1+\xi)^{-\frac{1}{2}+M}, \qquad -1<\xi<+1 \tag{3.18}$$

where N, M are integers.
Thinking about the physical nature of dislocation density, the following restrictions are imposed on N, M

$$-1 < N+\frac{1}{2} < +1, \qquad -1 < M-\frac{1}{2} < +1 \tag{3.19}$$

which means that at a given end (-1 or 1) the dislocation density is either bounded or has an integrable singularity.
The stress drop on dislocation surface must be bounded and therefore dislocation density must have integrable singularities at both ends ($N=-1, M=0$)

$$w(\xi) = (1-\xi)^{-\frac{1}{2}}\,(1+\xi)^{-\frac{1}{2}} \tag{3.20}$$

Once the fundamental function has been determined, its form suggests to expand $\rho(\xi')$ in this way

$$\rho(\xi') = \frac{1}{\sqrt{1-\xi'^2}}\sum_{n=0}^{\infty}\alpha_n T_n(\xi') \tag{3.21}$$

where α_n are coefficients which must be determined and T_n are Chebyshev polynomials of first kind (Appendix A.1). These polynomials are orthogonal polynomials whose weight function corresponds to (3.20), as indicated by relation (A.3).
Inserting this expression in the integral equation we obtain

$$A\,\pi \sum_{n=1}^{\infty} \alpha_n U_{n-1}(\xi) = \Delta\sigma(\xi)$$

where it must be observed that for (A.4) the term corresponding to $n = 0$ is equal to 0 and consequently α_0 is disappered.
Multiplying the last equation by $U_{k-1}(\xi)\sqrt{1-\xi^2}$ and integrating on the interval $(-1, 1)$ we obtain

$$\alpha_k = \frac{2}{A\pi^2} \int_{-1}^{1} \Delta\sigma(\xi)\sqrt{1-\xi^2}\, U_{k-1}(\xi)\, d\xi, \qquad k = 1, 2, \ldots \tag{3.22}$$

The coefficient α_0 still remains unknown, in fact the term $n = 0$ in (3.21) is solution of the homogeneous equation (equation (3.17) with $\Delta\sigma = 0$) and so if $\rho(\xi)$ satisfy (3.17), $\rho(\xi) + \alpha_0\,(1-\xi^2)^{-1/2}$ satisfy this equation too.
Nevertheless $\Delta u(x)$ is related to $\rho(x)$ by (3.11), beeing

$$\rho(x) = \frac{\partial \Delta u}{\partial x}$$

From the previous relation we obtain

$$\begin{aligned} \Delta u(x) &= \int_a^x \rho(x')\, dx' + C = \ell \int_{-1}^{\xi} \rho(\xi')\, d\xi' + C \\ &= \ell \left[\alpha_0 \left(\frac{\pi}{2} + \arcsin \xi \right) - \sqrt{1-\xi^2} \sum_{n=1}^{\infty} \frac{\alpha_n}{n} U_{n-1}(\xi) \right] + C \end{aligned} \tag{3.23}$$

where C is an addictive constant.
To determine C and α_0 we have now to impose the boundary conditions of crack closure at $x = a$ and $x = b$

$$\Delta u(a) = \Delta u(b) = 0$$

finding $C = 0$ and $\alpha_0 = 0$.
The crack problem for an antiplane strain configuration in a homogeneous medium has been completely determined.
The singularity $(1-\xi^2)^{-1/2}$ is typical of homogeneus elastic media; if the crack touches the interface between two media, in addition to the part having a Cuchy singularity, the kernel of the integral equation may contain terms which have a generalized Cauchy kernel.

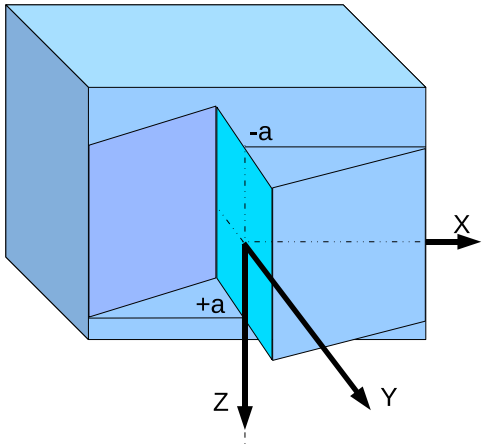

Figure 3.5: Closed screw dislocation

3.3.1 Displacement discontinuity method

The crack problem represents a boundary value problem and in section 3.3 we have shown that the analytical solution can be derived if the crack opens in a homogeneous medium. In more complex cases the analytical solution cannot be obtained and therefore an approximate solution must be found, using a numerical method. The displacement discontinuity method (Crouch et al., 1983) belongs to the class of boundary value methods, an ensemble of numerical techniques developed in order to obtain approximate solutions to boundary value problems. This method is based on the analytical solution to the problem of a constant discontinuity in displacement over a finite line segment and exploits the notion that one can make a discrete approximation to a continuous distribution of displacement discontinuity along a crack (Figure 3.4). Once the distribution of traction applied to the crack surface is known, then the values of the elemental displacement discontinuities that are necessary to produce these tractions are obtained solving a system of algebraic equations.

To illustrate this method, we consider again the case of an antiplane shear crack developing in an infinite elastic media. The following relation defines the displacement field corresponding to a closed bidimensional screw dislocation with Burgers vector $\mathbf{b} = b\hat{j}$, whose dislocation surface is the stripe of the plane $x = 0$, included between the dislocation line $x = 0, z = -a$ and the dislocation line $x = 0, z = +a$ (3.5).

$$u_y = \frac{b}{2\pi}\left[\arctan\frac{z-a}{x} - \arctan\frac{z-a}{x}\right]$$

On the plane ($x = 0$) containing the dislocation surface the only non-vanishing stress component is

$$\sigma_{xy}(0,z) = -\frac{\mu b}{2\pi}\left[\frac{1}{z+a} - \frac{1}{z+a}\right] = \frac{\mu b}{\pi}\frac{a}{z^2-a^2} \tag{3.24}$$

To obtain the numerical solution, we divide the crack into N line segments, or boundary

elements, each of which represents an elemental displacement discontinuity. We suppose that the line segments are small enough so that the displacement discontinuity in the y direction can be assumed as constant over each one. The numerical approximation to the solution of the problem can then be represented by N discrete displacement discontinuities D_i, $i = 1, ..., N$. The values of the N discontinuities are determined by solving a system of N simultaneous linear equations in N unknowns. These equations can be derived from the relation (3.24). If the discontinuity occurs over a line segment of length $2a_j$ centred at the point $x = 0, z = z_j$, then (3.24) can be written as

$$\sigma_{xy}(0, z) = \frac{\mu}{\pi} D_j \frac{a_j}{(z - z_j)^2 - {a_j}^2} \tag{3.25}$$

where D_j is the displacement discontinuity over the interval $|z - z_j| \leq a_j, x = 0$. The stress at the midpoint of the i-th element due to a displacement discontinuity at j-th element is found by setting z to z_i:

$$\sigma_{xy}(0, z_i) = \frac{\mu}{\pi} D_j \frac{a_j}{(z_i - z_j)^2 - {a_j}^2} \tag{3.26}$$

By superimposition, the stress at the midpoint of the i-th element due to displacement discontinuities at all N elements is equal to

$$\sigma_{xy}(0, z_i) = {\sigma_{xy}}^i = \sum_{j=1}^{N} A_{ij} D_j \tag{3.27}$$

where the influence coefficients A_{ij} are

$$A_{ij} = \frac{\mu}{\pi} \frac{a_j}{(z_i - z_j)^2 - {a_j}^2} \tag{3.28}$$

We will suppose that the stress ${\sigma_{xy}}^i$ is representative of the shear stress over the interval $|z - z_i| \leq a_i, x = 0$. A numerical solution to the shear crack problem is then specified be the following linear system of N simultaneous equations in N unknowns

$${\sigma_{xy}}^i = -\sigma_0 = \sum_{j=1}^{N} A_{ij} D_j, \qquad i = 1, ..., N \tag{3.29}$$

These equations can be solved for $D_i, i = 1, .., N$, by standard methods of numerical analysis.

Now we compare the solutions found for the problem of an antiplane shear crack. The analytical solution for the displacement discontinuity distribution is given by (3.23). Two numerical approximations to this solution are shown in Figure 3.6. The first approximation (Figure 3.6a) was found by dividing the crack into 10 equal sized elements, while the second (Figure 3.6b) was found by dividing the crack into 20 equal sized elements. By construction, the discontinuities D_i are constant over each element. From Figure 3.6 we can conclude that the displacement discontinuity method overestimates the relative displacements between the crack surfaces, but that the results tend to the exact solution as N is increased.

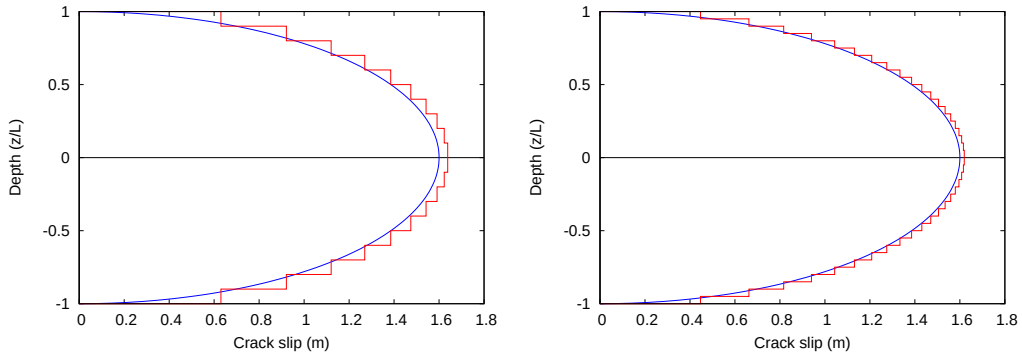

(a) N=10 (b) N=20

Figure 3.6: Numerical and analytical solutions for displacement discontinuity distribution

3.3.2 Crack problems in layered media

We consider a system made up of two half-spaces welded at the interface. The media are homogeneous and isotropic characterised by different elastic properties μ_1, ν_1 and μ_2, ν_2. We consider a crack located in half-space 2 and we want to study how the singularity of the dislocation density is influenced by the position of the crack with respect to the interface. As integral kernel we use the solution for an elementary vertical screw dislocation in a layered media obtained by Rybicki (1971) and the integral equation assumes this form

$$\frac{2\pi}{\mu_2}\Delta\sigma(\xi) = \int_{-1}^{1} \frac{\rho(\xi')}{\xi - \xi'}\, d\xi' + \Gamma \int_{-1}^{1} \frac{\rho(\xi')}{\xi + \xi' + 2 + d}\, d\xi' \tag{3.30}$$

where $d = D/l$, being D the distance of upper tip of the crack from the interface. The previous equation is still a singular Cauchy kernel equation, because the additional term is regular, so the singular behaviour of the dislocation density is still described by the fundamental function

$$w(\xi) = (1-\xi)^{-\frac{1}{2}}\,(1+\xi)^{-\frac{1}{2}} \tag{3.31}$$

Crack touching the interface

If the crack touches the interface (Case (b) in Bonafede et al., 2002), d is equal to 0 so the equation assumes this form

$$\frac{2\pi}{\mu_2}\Delta\sigma(\xi) = \int_{-1}^{1} \frac{\rho(\xi')}{\xi - \xi'}\, d\xi' + \Gamma \int_{-1}^{1} \frac{\rho(\xi')}{\xi + \xi' + 2}\, d\xi' \tag{3.32}$$

where the second term is now singular and precisely become unbounded when ξ, ξ' simultaneously approach the point -1. An equation of this form is classified as a singular integral equation with generalized Cauchy kernel. In the following we will show how the presence of the generalized kernel affects the singular nature of the dislocation density.

First of all, it's necessary to rewrite the equation in this form

$$f(\xi) = \frac{1}{\pi}\int_{-1}^{1}\frac{\rho(\xi')}{\xi'-\xi}\,d\xi' + \frac{1}{\pi}\int_{-1}^{1}\rho(\xi')\sum_{k=0}^{n}c_k\,(\xi+1)^k\,\frac{d^k}{d\xi^k}(\xi'-z_1(\xi))^{-1}\,d\xi' \tag{3.33}$$
$$z_1(\xi) = -1 + (\xi+1)e^{i\theta_1}$$

where c_k (k=0,1,...,n) and θ_1 $(0 < \theta_1 < 2\pi)$ are known constants.
In our case we obtain

$$-\frac{2}{\mu_2}\Delta\sigma(\xi) = \frac{1}{\pi}\int_{-1}^{1}\frac{\rho(\xi')}{\xi'-\xi}\,d\xi' + \frac{1}{\pi}\int_{-1}^{1}\rho(\xi')\frac{c_0}{\xi'-z_1(\xi)}\,d\xi' \tag{3.34}$$
$$z_1(\xi) = -1 + (\xi+1)e^{i\pi}$$

so we have $f(\xi) = -\frac{2}{\mu_2}\Delta\sigma(\xi)$, $\theta_1 = \pi$ and among c_k coefficients only $c_0 = -\Gamma$ is different from 0.
In the case of singular integral equation with generalized Cauchy kernel, the fundamental function $w(\xi)$ can be obtained applying directly the method outlined by Muskhelishvili (1953) to the integral equation.
The most general class of solutions of equation (3.33) is represented by

$$\begin{aligned}\rho(\xi) = w(\xi)R(\xi) &= (1-\xi)^{\alpha}\,(1+\xi)^{\beta}\,R(\xi)\\ &= e^{-i\pi\alpha}\,(\xi-1)^{\alpha}\,(\xi+1)^{\beta}\,R(\xi)\end{aligned} \tag{3.35}$$

where

- $R(\xi)$ is H-continuous in the interval $-1 \le \xi \le 1$
- $(\xi-1)^{\alpha}\,(\xi+1)^{\beta}$ is any definite branch which vary continuously on $-1 < \xi < 1$
- $\alpha = a_1 + ib_1$, $\beta = a_2 + ib_2 \quad -1 < a_1, a_2 < 0$

Now we consider the sectionally holomorphic function $\Phi(z)$

$$\frac{1}{\pi}\int_{-1}^{1}\frac{\rho(\xi')}{\xi'-z}\,d\xi' = \frac{e^{-i\pi\alpha}}{\pi}\int_{-1}^{1}(\xi'-1)^{\alpha}\,(\xi'+1)^{\beta}\,\frac{R(\xi')}{\xi'-z}\,d\xi' \tag{3.36}$$

The singular behaviour of $\Phi(z)$ near the end points may be expressed in this way

$$\Phi(z) = -R(-1)2^{\alpha}\frac{(z+1)^{\beta}}{\sin(\pi\beta)}e^{-i\pi\beta} + R(+1)2^{\beta}\frac{(z-1)^{\alpha}}{\sin(\pi\alpha)} + \Phi_0(z) \tag{3.37}$$

where the function Φ_0 is bounded everywhere except possibly at the ends where

$$|\Phi_0(z)| < \frac{C_k}{|z-c_k|^{d_k}}, \qquad d_k < -a_k,\ k = 1,2, \quad c_1 = -1,\ c_2 = 1 \tag{3.38}$$

C_k and d_k being real constants.
Using Plemelj formula

$$\frac{1}{\pi}\int_{-1}^{1}\frac{\rho(\xi')}{\xi'-\xi}\,d\xi' = \frac{1}{2}\left[\Phi^{+}(\xi) + \Phi^{-}(\xi)\right] \tag{3.39}$$

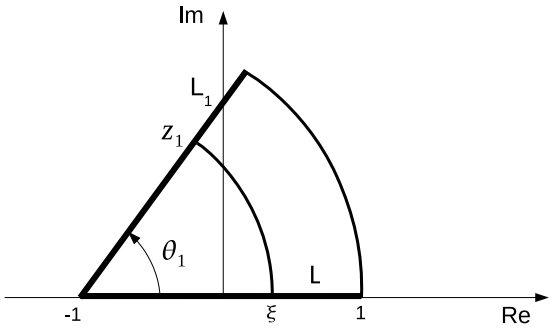

Figure 3.7: The branch cut L and the line L_1 in the complex plane

we obtain for $-1 < \xi < 1$

$$\frac{1}{\pi}\int_{-1}^{1}\frac{\rho(\xi')}{\xi'-\xi}\,d\xi' = -R(-1)2^{\alpha}\cot(\pi\beta)(\xi+1)^{\beta} + R(+1)2^{\beta}\cot(\pi\alpha)(1-\xi)^{\alpha} + F_0(\xi) \tag{3.40}$$

where F_0 has a behaviour similar to to that of Φ_0 given by (3.38).
Now we consider the term

$$\frac{1}{\pi}\int_{-1}^{1}\frac{\rho(\xi')}{\xi'-z_1}\,d\xi' = \Phi(z_1), \quad z_1 \in L_1 \tag{3.41}$$

Substituting $z_1 + 1 = (\xi+1)e^{i\theta_1}$ in equation (3.37) we obtain

$$\Phi(z_1) = -R(-1)2^{\alpha}\frac{e^{-i\pi\beta}}{\sin(\pi\beta)}e^{i\beta\theta_1}(\xi+1)^{\beta} + F_1(\xi), \qquad -1 < \xi < 1 \tag{3.42}$$

where the behaviour of F_1 near $\xi = -1$ is similar to that of Φ_0 given by (3.38).
Since Φ is holomorphic at $z = z_1$, using (3.37), the second group of terms in equation (3.33) can be expressed in this way

$$\begin{aligned}
&\frac{1}{\pi}\int_{-1}^{1}\rho(\xi')\,(\xi+1)^{k}\,\frac{d^k}{d\xi^k}(\xi'-z_1)^{-1}\,d\xi' = \\
&= (\xi+1)^{k}\,\frac{d^k}{d\xi^k}\Phi(z_1) \\
&= -R(-1)2^{\alpha}\frac{e^{-i\pi\beta}}{\sin(\pi\beta)}e^{i\beta\theta_1}\beta(\beta-1)...(\beta-k+1)(\xi+1)^{\beta} + (\xi+1)^{k}\,\frac{d^k}{d\xi^k}F_1(\xi)
\end{aligned} \tag{3.43}$$

for $-1 < \xi < 1$.
Substituting (3.40), (3.37) and (3.43) in equation (3.33) gives for $-1 < \xi < 1$

$$\begin{aligned}
&- R(-1)2^{\alpha}\cot(\pi\beta)(\xi+1)^{\beta} + R(+1)2^{\beta}\cot(\pi\alpha)(1-\xi)^{\alpha} + F_0(\xi) \\
&- c_0 R(-1)2^{\alpha}\frac{e^{-i\pi\beta}}{\sin(\pi\beta)}e^{i\beta\theta_1}(\xi+1)^{\beta} + F_1(\xi) \\
&+ \sum_{k=1}^{n} c_k\left[-R(-1)2^{\alpha}\frac{e^{-i\pi\beta}}{\sin(\pi\beta)}e^{i\beta\theta_1}\beta(\beta-1)...(\beta-k+1)(\xi+1)^{\beta} + (\xi+1)^{k}\,\frac{d^k}{d\xi^k}F_1(\xi)\right] = f(\xi)
\end{aligned} \tag{3.44}$$

Observing that

$$R(-1) \neq 0, \quad R(+1) \neq 0, \quad -1 < \mathrm{Re}(\alpha) < 0, \quad -1 < \mathrm{Re}(\beta) < 0$$
$$\lim_{\xi \to -1} (1+\xi)^{-\beta} \left[f(\xi), F_0(\xi), (\xi+1)^k F_1^{(k)}(\xi) \right] = 0, \qquad k = 0, 1, ..., n$$
$$\lim_{\xi \to -1} (1-\xi)^{-\alpha} \left[f(\xi), F_0(\xi), (\xi+1)^k F_1^{(k)}(\xi) \right] = 0, \qquad k = 0, 1, ..., n$$

From equation (3.44), multiplying both sides by $(1-\xi)^{-\alpha}$ and letting $\xi \to 1$ we obtain

$$\cot(\pi\alpha) = 0 \tag{3.45}$$

Considering again (3.44), but now multiplying both sides by $(1+\xi)^{-\beta}$ and letting $\xi \to -1$

$$\cos(\pi\beta) + e^{i\beta(\theta_1 - \pi)} \left[c_0 + \sum_{k=1}^{n} c_k \beta(\beta-1)...(\beta-k+1) \right] = 0 \tag{3.46}$$

From (3.45) we find $\alpha = -\dfrac{1}{2}$, therefore the singularity of the dislocation density in $\xi = 1$ is the value typical of homogeneous media. Instead from (3.46) we can conclude that the presence of the generalized Cauchy kernel affects the nature of the singularity in $\xi = -1$. In the case of the crack touching the interface we have

$$\theta_1 = \pi, \qquad c_k = \begin{cases} -\Gamma, & k = 0 \\ 0, & k > 0 \end{cases} \tag{3.47}$$

so the equation for β become

$$\cos(\pi\beta) - \Gamma = 0, \tag{3.48}$$

The fundamental function $w(\xi)$ in this case has the following form

$$w(\xi) = (1-\xi)^{-\frac{1}{2}} (1+\xi)^b, \qquad b = -\frac{1}{\pi} \arccos(\Gamma) \tag{3.49}$$

Once the fundamental function $w(\xi)$ is known, an approximate solution for the integral equation can be obtained. The details about the method of solution are related to the form of the fundamental function.

Crack crossing the interface

When the crack crosses the interface(Case (c) in Bonafede et al., 2002), it is convenient to split the crack into two interacting sections, each embedded in one medium and both open at the interface. The main difference with respect to the case of a crack touching the interface is that we have to consider a couple of generalized Cauchy kernel equations, instead of a single equation. In this case the study of the model is based on the following steps:

- an asympthotic study performed generalizing the method presented by Erdogan et

al. (1973) and described in the previous section

- a study of the finite stress drop which have to be assigned on the crack sections in order to derive a stress drop condition
- the research of an approximate solution

The same schema will be adopted in order to study the models presented in Chapters 4-5.

Chapter 4

Fault bending model

In this chapter we employ the asymptotic theory of generalized Cauchy kernel equations in order to study the singular behaviour of a strike-slip fault crossing a material discontinuity. The stress drop condition proper to a vertical planar crack cannot be fulfilled in several cases and in a such a case a strike-slip fault cutting across the interface comes into conflict with the welded boundary conditions. A simple way out of the mentioned problem is assuming that the fault surface is affected by a sharp change of the angle of dip at the intersection with the interface. Therefore the problem will be adressed in terms of a deep vertical planar crack, interacting with a shallower inclined planar crack.

4.1 Model description

We consider an elastic layer of thickness H and rigidity μ_1, bounded by a free surface and welded to an elastic half-space of rigidity μ_2. The origin of the reference system is placed at the intersection between the crack and the interface, with z axis pointing downward. We consider an antiplane strain configuration in which the only non-vanishing component of the displacement field is $u_y(x,z)$, which is independent of the coordinate y.
It is convenient to split the crack into two interacting sections, each embedded in one media and both open at the interface. The section in the upper layer has length $2l_1$, it's inclined of an angle $\alpha \in (-\frac{\pi}{2}, \frac{\pi}{2})$ with respect to the negative z axis and therefore it has $\hat{n} = (\cos\alpha, 0, -\sin\alpha)$ as normal versor. The section embedded in the lower half-space is normal with respect to the interface and its length is equal to $2l_2$. A sketch of the model is presented in figure 4.1.

Consider the equilibrium equation for each of the two crack sections

$$-\Delta\sigma_1(\hat{x},\hat{y}) = (\sigma^c_{ny})^1_1(\hat{x},\hat{y}) + (\sigma^c_{ny})^2_1(\hat{x},\hat{y}), \qquad \begin{cases} \hat{x} = -S\cos\alpha \\ \hat{y} = -S\sin\alpha \end{cases} \qquad (0 < S < 2l_1)$$

$$-\Delta\sigma_2(0,z) = (\sigma^c_{xy})^1_2(0,z) + (\sigma^c_{xy})^2_2(0,z), \qquad (0 < z < 2l_2)$$

where $\Delta\sigma_1(\hat{x},\hat{y})$ is the stress drop in a point of the inclined section, being (S,α) the polar coordinates of the point $(\hat{x},\hat{y})$, and $\Delta\sigma_2(0,z)$ is the stress drop in a point of the vertical

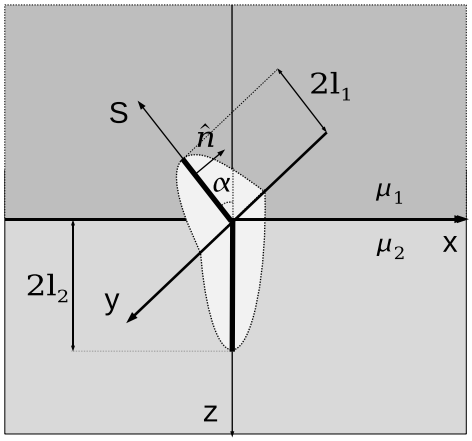

Figure 4.1: Fault bending model

section.
The stress drop on each crack section is equal to to the sum of two contributions. $(\sigma^c_{ny})^1_1, (\sigma^c_{ny})^2_1$ are stress induced on section 1 due to slip of section 1 and slip of section 2, respectively, while $(\sigma^c_{xy})^2_2, (\sigma^c_{xy})^1_2$ are stress induced on section 2 due to slip of section 2 and slip of section 1, respectively.
The two sections have a different inclination with respect to the interface, so we must remark that a different stress component is released on these two sections. On section 2 the stress component released by crack slip is simply σ_{xy}, while on section 1 the component released is σ_{ny} which represents the y component of the traction $\vec{T}^{(\hat{n})}$ relative to a surface with normal versor $\hat{n}$; using the Cauchy relation we obtain

$$\sigma_{ny} = T_y^{(\hat{n})} = \sigma_{iy} n_i = \cos\alpha\, \sigma_{xy} - \sin\alpha\, \sigma_{zy} \tag{4.2}$$

To define a crack model we have to employ suitable superimpositions of elementary solutions. Using a continuous distribution of elementary dislocations with dislocation lines contained in the interval $0 < S < 2l_1$ and an analogous distribution with dislocation lines in the interval $0 < z < 2l_2$, the equilibrium equations can be rewritten in this form

$$-\Delta\sigma_1(S) = \int_0^{2l_1} (\sigma_{ny})^I_1 (S; S_0)\rho_1(S_0)dS_0 + \int_0^{2l_2} (\sigma_{ny})^{II}_1 (S; z_0)\rho_2(z_0)dz_0 \tag{4.3a}$$

$$-\Delta\sigma_2(z) = \int_0^{2l_1} (\sigma_{xy})^I_2 (z; S_0)\rho_1(S_0)dS_0 + \int_0^{2l_2} (\sigma_{xy})^{II}_2 (z; z_0)\rho_2(z_0)dz_0 \tag{4.3b}$$

where the integrals must be evaluated in the principle-value sense.
In case of section 1 to determine the integral kernels $(\sigma_{ny})^I_1, (\sigma_{xy})^I_2$ we use the analytical solutions for an elementary scree dislocation of arbitrary dip (Singh et al., 1994) embedded in the upper layer.

$$(\sigma_{xy})_1^I(x,z;S_0)=\frac{\mu_1}{2\pi}\left\{\frac{z+S_0\cos\alpha}{R^2}-\frac{z-S_0\cos\alpha+2H}{S^2}\right.$$
$$+\sum_{n=1}^{\infty}\Gamma^n\left[-\frac{z-S_0\cos\alpha-2(n-1)H}{T^2}+\frac{z+S_0\cos\alpha+2nH}{V^2}\right.$$
$$\left.\left.+\frac{z+S_0\cos\alpha-2nH}{U^2}-\frac{z-S_0\cos\alpha+2(n+1)H}{W^2}\right]\right\} \tag{4.4}$$

$$(\sigma_{zy})_1^I(x,z;S_0)=-\frac{\mu_1}{2\pi}(x+S_0\sin\alpha)\left\{\frac{1}{R^2}-\frac{1}{S^2}+\sum_{n=1}^{\infty}\Gamma^n\left[-\frac{1}{T^2}+\frac{1}{V^2}+\frac{1}{U^2}-\frac{1}{W^2}\right]\right\} \tag{4.5}$$

$$(\sigma_{xy})_2^I(x,z;S_0)=\frac{\mu_2}{2\pi}\frac{2}{1+m}\left\{\frac{z+S_0\cos\alpha}{R^2}-\frac{z-S_0\cos\alpha+2H}{S^2}\right.$$
$$\left.+\sum_{n=1}^{\infty}\Gamma^n\left[\frac{z+S_0\cos\alpha+2nH}{V^2}-\frac{z-S_0\cos\alpha+2(n+1)H}{W^2}\right]\right\} \tag{4.6}$$

where

$$\begin{cases}R^2=(x+S_0\sin\alpha)^2+(z+S_0\cos\alpha)^2\\ S^2=(x+S_0\sin\alpha)^2+(z-S_0\cos\alpha+2H)^2\\ T^2=(x+S_0\sin\alpha)^2+(z-S_0\cos\alpha-2(n-1)H)^2\\ U^2=(x+S_0\sin\alpha)^2+(z+S_0\cos\alpha-2nH)^2\\ V^2=(x+S_0\sin\alpha)^2+(z+S_0\cos\alpha+2nH)^2\\ W^2=(x+S_0\sin\alpha)^2+(z-S_0\cos\alpha+2(n+1)H)^2\end{cases}\qquad\begin{cases}m=\dfrac{\mu_2}{\mu_1}\\ \\ \Gamma=\dfrac{1-m}{1+m}\end{cases} \tag{4.7}$$

In case of section 2, the integral kernels $(\sigma_{ny})_1^{II}$, $(\sigma_{xy})_2^{II}$ can be derived using the analytical solutions proper to a vertical screw dislocation (Rybicki , 1971).

$$(\sigma_{xy})_1^{II}(x,z;z_0)=\frac{\mu_1}{2\pi}\frac{2m}{1+m}\left[\sum_{n=0}^{\infty}\Gamma^n\left(\frac{z+z_0+2(n+1)H}{x^2+(z+z_0+2(n+1)H)^2}-\frac{z-z_0-2nH}{x^2+(z-z_0-2nH)^2}\right)\right] \tag{4.8}$$

$$(\sigma_{zy})_1^{II}(x,z;z_0)=-\frac{\mu_1}{2\pi}\frac{2m}{1+m}\left[\sum_{n=0}^{\infty}\Gamma^n\left(\frac{x}{x^2+(z+z_0+2(n+1)H)^2}-\frac{x}{x^2+(z-z_0-2nH)^2}\right)\right] \tag{4.9}$$

$$(\sigma_{xy})_2^{II}(z;z_0)=-\frac{\mu_2}{2\pi}\left[\frac{1}{z-z_0}+\Gamma\frac{1}{z+z_0}-\frac{4m}{(1+m)^2}\sum_{n=0}^{\infty}\Gamma^n\frac{1}{z+z_0+2(n+1)H}\right] \tag{4.10}$$

Once the stress drops $\Delta\sigma_1, \Delta\sigma_2$ are assigned, the equilibrium equations become a system of coupled integral equations for the unknown functions ρ_1, ρ_2.
The function ρ is the unknown dislocation density distribution; in this case ρ is splitted into two subdomains in this way

$$\rho = \begin{cases} \rho_1(S_0), & 0 < S_0 < 2l_1 \\ \rho_2(z_0), & 0 < z_0 < 2l_2 \end{cases} \tag{4.11}$$

where ρ_1, ρ_2 are defined through the displacement discontinuity over the crack plane

$$\rho_1 = \left[\frac{\partial \Delta u(S)}{\partial S}\right]_{S=S_0} \tag{4.12}$$

$$\rho_2 = \left[\frac{\partial \Delta u(z)}{\partial z}\right]_{z=z_0} \tag{4.13}$$

From (4.12) and (4.13) we obtain

$$\Delta u_1(S) = \int_0^S \rho(S_0) dS_0 + C_1$$
$$\Delta u_2(z) = \int_0^z \rho(z_0) dz_0 + C_2$$

where C_1, C_2 are constants that can be fixed imposing the condition of crack closure

$$\Delta u_1(2l_1) = 0$$
$$\Delta u_2(2l_2) = 0$$

From these conditions we obtain $C_1, C_2 = 0$.
Once the dislocation density ρ is known, the solution of a crack problem is simply obtained by a superimposition of elementary solutions. In our case, if f denotes any elementary component of displacement or stress, the crack solution is given by

$$f^c(x,z) = \int_0^{2l_1} f(x,z;S_0)\rho_1(S_0)dS_0 + \int_0^{2l_2} f(x,z;z_0)\rho_2(z_0)dz_0 \tag{4.14}$$

After this premise, the first step is to derive the system of integral equations which describe the model presented. The details about the calculations performed are reported

in appendix B.1) and the equilibrium equations 4.3 can be expressed as

$$\begin{aligned}\frac{2\pi}{\mu_1}\Delta\sigma_1(S) = &\int_0^{2l_1}\frac{\rho_1(S_0)dS_0}{S-S_0}\\ &-\Gamma\int_0^{2l_1}\frac{(S-S_0)\sin^2\alpha+(S+S_0)\cos^2\alpha}{(S-S_0)^2\sin^2\alpha+(S+S_0)^2\cos^2\alpha}\rho_1(S_0)dS_0\\ &-\frac{2m}{1+m}\int_0^{2l_2}\frac{z_0\cos\alpha+S}{S^2\sin^2\alpha+(z_0+S\cos\alpha)^2}\rho_2(z_0)dz_0\\ &+\int_0^{2l_1}\mathcal{R}_{11}(S;S_0)\rho_1(S_0)dS_0+\int_0^{2l_2}\mathcal{R}_{12}(S;z_0)\rho_2(z_0)dz_0\end{aligned} \tag{4.15}$$

$$\begin{aligned}\frac{2\pi}{\mu_2}\Delta\sigma_2(z) = &\int_0^{2l_2}\frac{\rho_2(z_0)dz_0}{z-z_0}+\Gamma\int_0^{2l_2}\frac{\rho_2(z_0)dz_0}{z+z_0}\\ &-\frac{2}{1+m}\int_0^{2l_1}\frac{S_0\cos\alpha+z}{S_0^2\sin^2\alpha+(S_0\cos\alpha+z)^2}\rho_1(S_0)dS_0\\ &+\int_0^{2l_1}\mathcal{R}_{21}(z;S_0)\rho_1(S_0)dS_0+\int_0^{2l_2}\mathcal{R}_{22}(z;z_0)\rho_2(z_0)dz_0\end{aligned} \tag{4.16}$$

where singular terms are singled out and $m=\frac{\mu_2}{\mu_1}, \Gamma=\frac{1-m}{1+m}$.
The terms present in the last raw of each integral equation are regular (Fredholm kernels), in fact these terms describe the effects induced by the presence of the free surface. Letting $H\longrightarrow+\infty$ these terms tend to 0, therefore the system obtained describe the case of two half-spaces welded at the interface. Hereafter we choose to concentrate our attention to this case, since the presence of the free surface does not affect the singular nature of the dislocation density. Furthermore, if we consider the following transformations

$$\begin{cases}\xi_1=\dfrac{S-l_1}{l_1}\\ \xi_1^{'}=\dfrac{S_0-l_1}{l_1}\end{cases}\qquad\begin{cases}\xi_2=\dfrac{z-l_2}{l_2}\\ \xi_2^{'}=\dfrac{z_0-l_2}{l_2}\end{cases} \tag{4.17}$$

the system can be rewritten in order to refer to adimensional variables

$$\begin{aligned}\frac{2\pi}{\mu_1}\Delta\sigma_1(\xi_1) = &\int_{-1}^{+1}\frac{\rho_1(\xi_1^{'})d\xi_1^{'}}{\xi_1-\xi_1^{'}}\\ &-\Gamma\int_{-1}^{+1}\frac{(\xi_1-\xi_1^{'})\sin^2\alpha+(\xi_1+\xi_1^{'}+2)\cos^2\alpha}{(\xi_1-\xi_1^{'})^2\sin^2\alpha+(\xi_1+\xi_1^{'}+2)^2\cos^2\alpha}\rho_1(\xi_1^{'})d\xi_1^{'}\\ &-\frac{2m}{1+m}\int_{-1}^{+1}\frac{(\xi_2^{'}+1)\cos\alpha+\dfrac{l_1}{l_2}(\xi_1+1)}{\left(\dfrac{l_1}{l_2}\right)^2(\xi_1+1)^2\sin^2\alpha+\left((\xi_2^{'}+1)+\dfrac{l_1}{l_2}(\xi_1+1)\cos\alpha\right)^2}\rho_2(\xi_2^{'})d\xi_2^{'}\end{aligned} \tag{4.18a}$$

$$\begin{aligned}\frac{2\pi}{\mu_2}\Delta\sigma_2(\xi_2) = &\int_{-1}^{+1}\frac{\rho_2(\xi_2^{'})d\xi_2^{'}}{\xi_2-\xi_2^{'}}+\Gamma\int_{-1}^{+1}\frac{\rho_2(\xi_2^{'})d\xi_2^{'}}{\xi_2+\xi_2^{'}+2}\\ &-\frac{2}{1+m}\int_{-1}^{+1}\frac{(\xi_1^{'}+1)\cos\alpha+\dfrac{l_2}{l_1}(\xi_2+1)}{(\xi_1^{'}+1)^2\sin^2\alpha+\left((\xi_1^{'}+1)\cos\alpha+\dfrac{l_2}{l_1}(\xi_2+1)\right)^2}\rho_1(\xi_1^{'})d\xi_1^{'}\end{aligned} \tag{4.18b}$$

The integral equations can be written in this compact way

$$\begin{cases} \dfrac{2\pi}{\mu_1}\Delta\sigma_1(\xi_1) = I_{11} - \Gamma I_{12} - (1-\Gamma)\, I_{13} \\ \\ \dfrac{2\pi}{\mu_2}\Delta\sigma_2(\xi_2) = I_{21} + \Gamma I_{22} - (1+\Gamma)\, I_{23} \end{cases} \tag{4.19}$$

in order to refer more easily to the terms present on second side of both equations.
Once the explicit form for the equilibrium equations (4.3) is obtained, to study the crack model we perform the following procedure:

- we consider an asymptotic study in order to determine the singular nature of the dislocation density (Sec. 4.2)
- we study the relation between the bounded stress drops on the two crack sections (Sec. 4.3)
- we search a numerical solution for the system of integral equations (Sec. 4.4)

4.2 Study of asymptotic behaviour

The stress drops $\Delta\sigma_1, \Delta\sigma_2$ must be bounded on the crack surface, so the first problem to be solved is the determination of the singular behaviour of the dislocation density at crack tips. To this end, we generalize to the system of coupled equations (4.18) the method proposed by Erdogan et al. (1973), already described in section 3.3.2 on page 31. To determine the asymptotic behaviour of I_{ij} integrals, we introduce the following expressions for ρ_1 and ρ_2

$$\rho_1 = R_1(t)(1-t)^{a_1}(t+1)^{b_1} \tag{4.20}$$

$$\rho_2 = R_2(t)(1-t)^{a_2}(t+1)^{b_2} \tag{4.21}$$

where $R_1(\pm1)$, $R_2(\pm1) \neq 0$, $-1 < a_1, b_1, a_2, b_2 \leqslant 0$ and t denotes either ξ_1' or ξ_2'.
Following Muskhelishvili (1953), we consider the function $\Phi(\zeta)$ of the complex variable ζ

$$\Phi(\zeta) = \frac{1}{\pi}\int_{-1}^{+1}\frac{\rho_k(t)}{t-\zeta}dt = \frac{e^{-i\pi a_k}}{\pi}\int_{-1}^{+1}\frac{R_k(t)(t-1)^{a_k}(t+1)^{b_k}}{t-\zeta}dt, \qquad k=1,2 \tag{4.22}$$

The asymptotic behaviour of $\Phi(\zeta)$ in the neighbourhood of $\zeta = \pm1$ is assigned by the following expression

$$\Phi(\zeta) = -R_k(-1)2^{a_k}\frac{(\zeta+1)^{b_k}}{\sin(\pi b_k)}e^{-i\pi b_k} + R_k(+1)2^{b_k}\frac{(\zeta-1)^{a_k}}{\sin(\pi a_k)} + \Phi_0(\zeta), \qquad k=1,2 \tag{4.23}$$

where the function $\Phi_0(\zeta)$ is bounded everywhere, with the exception of points $\zeta = \pm1$, where however its order of infinity is less than a_k or b_k ($a_k \leqslant 0, b_k \leqslant 0$), depending on the point considered.

4.2.1 Singularities of ρ at crack tips

The details about the evaluation of the asymptothic behaviour of I_{ij} integrals are described in appendix B.2. Here we report only the asymptotic evaluation for the integral equations obtained summing the asymptotic evaluation for each term

$$\begin{aligned}
-\frac{2}{\mu_1}\Delta\sigma_1(\xi) = &-R_1(-1)2^{a_1}\cot(\pi b_1)\,(\xi+1)^{b_1} + R_1(1)2^{b_1}\cot(\pi a_1)\,(1-\xi)^{a_1} \\
&- b_0 R_1(-1)2^{a_1}\frac{1}{\sin(\pi b_1)}\,(\xi+1)^{b_1}\cos(2\alpha(1+b_1)) \\
&- c_0 R_2(-1)2^{a_2}\frac{1}{\sin(\pi b_2)}\left[\frac{l_1}{l_2}\,(\xi+1)\right]^{b_2}\cos(\alpha(1+b_2)) \\
&+ F_0(\xi) + F_1(\xi) + \hat{F}_1(\xi)
\end{aligned} \tag{4.24}$$

$$\begin{aligned}
-\frac{2}{\mu_2}\Delta\sigma_2(\xi) = &-R_2(-1)2^{a_2}\cot(\pi b_2)\,(\xi+1)^{b_2} + R_2(1)2^{b_2}\cot(\pi a_2)\,(1-\xi)^{a_2} \\
&- b_0^{'} R_2(-1)2^{a_2}\frac{1}{\sin(\pi b_2)}\,(\xi+1)^{b_2} \\
&- c_0^{'} R_1(-1)2^{a_1}\frac{1}{\sin(\pi b_1)}\left[\frac{l_2}{l_1}\,(\xi+1)\right]^{b_1}\cos(\alpha(1+b_1)) \\
&+ G_0(\xi) + G_1(\xi) + \hat{G}_1(\xi)
\end{aligned} \tag{4.25}$$

where

$$b_0 = \Gamma, \qquad c_0 = \frac{2m}{1+m}, \qquad b_0^{'} = -\Gamma, \qquad c_0^{'} = \frac{2}{1+m} \tag{4.26}$$

4.2.2 Singularity at $\xi = 1$

To study the singularity of ρ_1 in the crack tip embedded in the upper media, we multiply both sides of equation (4.24) by $(1-\xi)^{-a_1}$ and letting $\xi \to 1$ we find

$$\cot(\pi a_1) = 0 \quad \Longrightarrow \quad a_1 = -\frac{1}{2} \tag{4.27}$$

In the same manner we can study the singularity of ρ_2; multiplying both sides of equation (4.25) by $(1-\xi)^{-a_2}$ and considering the limit $\xi \to 1$ we obtain

$$\cot(\pi a_2) = 0 \quad \Longrightarrow \quad a_2 = -\frac{1}{2} \tag{4.28}$$

The singular nature of dislocation density in these points corresponds to that observed in case of a crack in a homogeneous media.

4.2.3 Singularity at the interface

Multiplying both sides of equation (4.24) by $(\xi+1)^{-b_1}$ and letting $\xi \to -1$

$$\begin{aligned} 0 = & -R_1(-1)2^{a_1}\cot(\pi b_1) \\ & - b_0 R_1(-1)2^{a_1}\frac{1}{\sin(\pi b_1)}\cos(2\alpha(1+b_1)) \\ & - c_0 R_2(-1)2^{a_2}\frac{1}{\sin(\pi b_2)}\left(\frac{l_1}{l_2}\right)^{b_2}(\xi+1)^{b_2-b_1}\cos(\alpha(1+b_1)) \end{aligned} \tag{4.29}$$

we deduce that the following inequality must be fulfilled

$$b_2 \leq b_1 \tag{4.30}$$

Multiplying both sides of equation (4.25) by $(\xi+1)^{-b_2}$ and considering the limit $\xi \to -1$

$$\begin{aligned} 0 = & -R_2(-1)2^{a_2}\cot(\pi b_2) \\ & - b_0^{'} R_2(-1)2^{a_2}\frac{1}{\sin(\pi b_2)} \\ & - c_0^{'} R_1(-1)2^{a_1}\frac{1}{\sin(\pi b_1)}\left(\frac{l_2}{l_1}\right)^{b_1}(\xi+1)^{b_1-b_2}\cos(\alpha(1+b_1)) \end{aligned} \tag{4.31}$$

we find another inequality that must be satisfied

$$b_1 \leq b_2 \tag{4.32}$$

The two inequalities found imply that

$$b_1 = b_2 = \omega \tag{4.33}$$

In order the stress drop on the crack surface can be limited near the interface, the following two conditions must be fulfilled

$$\begin{cases} \left[\cos(\pi\omega) + \Gamma\cos(2\alpha(1+\omega))\right] R_1(-1) + (1-\Gamma)\left(\dfrac{l_1}{l_2}\right)^{\omega}\cos(\alpha(1+\omega))R_2(-1) = 0 \\ (1+\Gamma)\left(\dfrac{l_2}{l_1}\right)^{\omega}\cos(\alpha(1+\omega))R_1(-1) + \left[\cos(\pi\omega) - \Gamma\right] R_2(-1) = 0 \end{cases} \tag{4.34}$$

This is a system whose unknowns are $R_1(-1), R_2(-1)$; in order to have non-vanishing solutions the determinant of this system must vanish and so we find the following equation for ω

$$\left[\cos(\pi\omega) + \Gamma\cos(2\alpha(1+\omega))\right]\cdot\left[\cos(\pi\omega) - \Gamma\right] - (1-\Gamma^2)\cos^2(\alpha(1+\omega)) = 0 \tag{4.35}$$

The roots of this equation can be determined numerically and studying the dependence of ω from the parameters α, m of our model (Figures 4.2, 4.3), we can state that for whatever combinations of acceptable values of these parameters, the equation has only one root. We can observe that the singularity degree ω is always less than -0.5 and this consideration will be useful in section 4.4 where a method of solution for the system of integral equations

is proposed.

For this value of ω, we find the following condition relating $R_1(-1), R_2(-1)$

$$\frac{R_1(-1)}{R_2(-1)} = -m\left(\frac{l_1}{l_2}\right)^{\omega} \frac{\cos(\pi\omega) - \Gamma}{(1-\Gamma)\cdot\cos(\alpha(1+\omega))} \tag{4.36}$$

This condition will be used later in order to constrain the solution of the system of integral equations.

4.3 Stress drop condition

In the previous section, the singular terms for the stress drop have been evaluated in order to study the singular nature of dislocation density; studying the asymptotic behaviour we have found that $\rho_1(\xi_1), \rho_2(\xi_2)$ must have the following form

$$\begin{aligned} &\rho_1(\xi_1) = (1-\xi_1)^{a_1}(1+\xi_1)^{b_1} R_1(\xi_1) && -1 < a_1, b_1, a_2, b_2 \leqslant 0 \\ &\rho_2(\xi_2) = (1-\xi_2)^{a_2}(1+\xi_2)^{b_2} R_2(\xi_2) && R_1(\pm 1), R_2(\pm 1) \neq 0 \end{aligned}$$

where

$$\begin{cases} a_1 = -\dfrac{1}{2} \\ b_1 = \omega \end{cases} \quad \begin{cases} a_2 = -\dfrac{1}{2} \\ b_2 = \omega \end{cases} \tag{4.37}$$

The value for ω is found solving the equation

$$[\cos(\pi\omega) - \Gamma)] \cdot [\cos(\pi\omega) + \Gamma\cos(2\alpha(1+\omega))] - (1-\Gamma^2)\cos^2(\alpha(1+\omega)) = 0 \tag{4.38}$$

Furthermore, the singular nature of $\rho_1(\xi_1), \rho_2(\xi_2)$ suggests to expand $R_1(\xi_1), R_2(\xi_2)$ in this way

$$R_1(\xi_1) = \sum_{k=0}^{\infty} \gamma_k P_k^{(\alpha,\beta)}(\xi_1) \tag{4.39}$$

$$R_2(\xi_2) = \sum_{k=0}^{\infty} \beta_k P_k^{(\alpha,\beta)}(\xi_2) \tag{4.40}$$

since $P_k^{(\alpha,\beta)}$ are orthogonal polynomials whose weight function is $w(\xi) = (1-\xi)^{\alpha}(1+\xi)^{\beta}$. In this section we will compare the stress released on the two crack sections near the interface in order to determine any condition relating the bounded stress drops $\Delta\sigma_1, \Delta\sigma_2$ which must be assigned on these sections.
We use the results obtained in appendix B.3 and we consider the following two relations

$$(1+\xi_1)^{-\omega} \cdot \left[{I_{11}}^S - \Gamma {I_{12}}^S - (1-\Gamma)\,{I_{13}}^S\right] \tag{4.41}$$

$$(1+\xi_2)^{-\omega} \cdot \left[{I_{21}}^S + \Gamma {I_{22}}^S - (1+\Gamma)\,{I_{23}}^S\right] \tag{4.42}$$

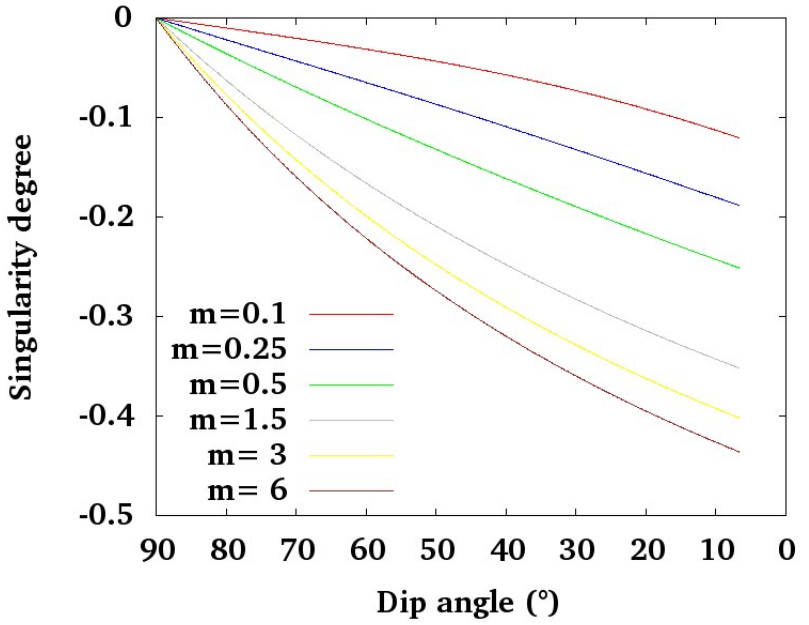

Figure 4.2: Dependence of the singularity ω from the dip angle

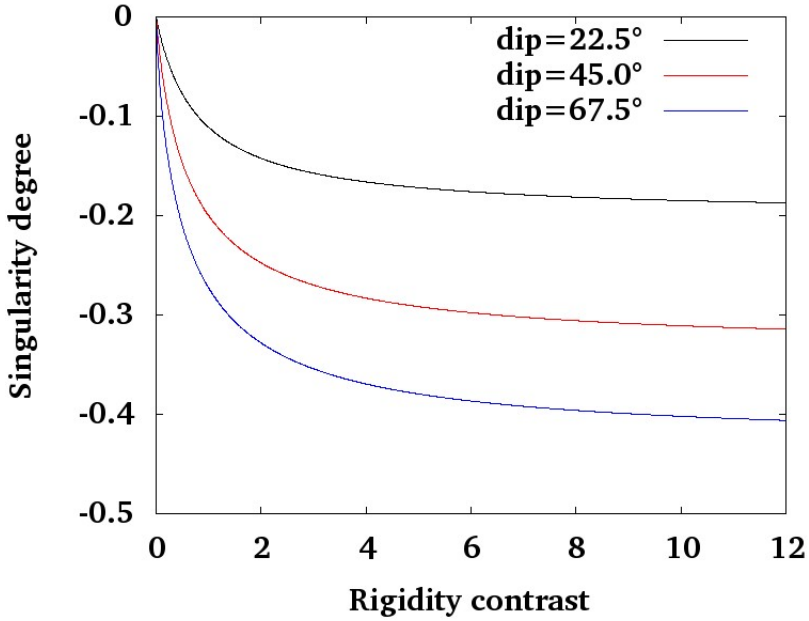

Figure 4.3: Dependence of the singularity ω from the rigidity contrast m

in order to verify the accuracy of the asymptotic study performed in the previous section. Letting $\xi \to -1$, we obtain the following couple of equations

$$[\cos(\pi\omega) + \Gamma\cos(2\alpha(1+\omega))]\, R_1(-1) + \left(\frac{l_1}{l_2}\right)^{\omega} (1-\Gamma)\, R_2(-1) = 0 \tag{4.43}$$

$$[\cos(\pi\omega) - \Gamma]\, R_1(-1) + \left(\frac{l_2}{l_1}\right)^{\omega} (1+\Gamma)\cos(\alpha(1+\omega)) R_2(-1) = 0 \tag{4.44}$$

that correspond effectively to the system (4.34); the compensation of singular terms on each crack sections near the interface is obtained when the system has non-trivial solutions, therefore the admissible value for ω is the root of equation (4.38).
For this value of ω, the following relation between $R_1(-1)$ and $R_2(-1)$ is valid

$$\frac{R_1(-1)}{R_2(-1)} = \frac{\sum_{k=0}^{+\infty} \gamma_k P_k^{(-\frac{1}{2},\omega)}(-1)}{\sum_{k=0}^{+\infty} \beta_k P_k^{(-\frac{1}{2},\omega)}(-1)} = -\left(\frac{l_1}{l_2}\right)^{\omega} \frac{\cos(\pi\omega) - \Gamma}{(1+\Gamma)\cdot\cos(\alpha(1+\omega))} \tag{4.45}$$

From (4.45) and using the linear independence of $P_k^{(\alpha,\beta)}$ polynomials, we find that for every $k \geq 0$

$$\frac{\gamma_k}{\beta_k} = -\left(\frac{l_1}{l_2}\right)^{\omega} \frac{\cos(\pi\omega) - \Gamma}{(1+\Gamma)\cdot\cos(\alpha(1+\omega))} \tag{4.46}$$

Now we have to evaluate the bounded stress drop on each crack section; all the terms have been evaluated in appendix B.3 and in case of section 2, summing all the bounded terms, we find that stress drop can be expressed as

$$\begin{aligned}\frac{2\pi}{\mu_2}\Delta\sigma_2(-1) = {} & 2^{-\frac{1}{2}+\omega}\, \mathbf{\Gamma}(\omega) \sum_{k=0}^{+\infty} \beta_k (-1)^k \frac{\mathbf{\Gamma}(k+1-\frac{1}{2})}{\mathbf{\Gamma}(k+1-\frac{1}{2}+\omega)} \\ & - \Gamma\, 2^{-\frac{1}{2}+\omega}\, \mathbf{\Gamma}(\omega) \sum_{k=0}^{+\infty} \beta_k (-1)^k \frac{\mathbf{\Gamma}(k+1-\frac{1}{2})}{\mathbf{\Gamma}(k+1-\frac{1}{2}+\omega)} \\ & + (1+\Gamma)\, 2^{-\frac{1}{2}+\omega}\, \mathbf{\Gamma}(\omega) \left(\sum_{k=0}^{+\infty} \gamma_k (-1)^k \frac{\mathbf{\Gamma}(k+1-\frac{1}{2})}{\mathbf{\Gamma}(k+1-\frac{1}{2}+\omega)}\right) \cos\alpha\end{aligned} \tag{4.47}$$

Using equation (4.46), the previous equation can be rewritten in this form

$$\frac{2\pi}{\mu_2}\Delta\sigma_2(-1) = \mathcal{S}(\omega)\left[(1-\Gamma) - \left(\frac{l_1}{l_2}\right)^{\omega} \frac{\cos(\pi\omega) - \Gamma}{\cos(\alpha(1+\omega))}\cos\alpha\right] \tag{4.48}$$

where $\mathcal{S}(\omega)$ is so defined

$$\mathcal{S}(\omega) = 2^{-\frac{1}{2}+\omega}\, \mathbf{\Gamma}(\omega) \sum_{k=0}^{+\infty} \beta_k (-1)^k \frac{\mathbf{\Gamma}(k+1-\frac{1}{2})}{\mathbf{\Gamma}(k+1-\frac{1}{2}+\omega)}$$

The bounded stress drop on the inclined section is given by

$$\begin{aligned}\frac{2\pi}{\mu_1}\Delta\sigma_1(-1) = {} & 2^{-\frac{1}{2}+\omega}\,\mathbf{\Gamma}(\omega)\sum_{k=0}^{+\infty}\gamma_k(-1)^k\frac{\mathbf{\Gamma}(k+1-\frac{1}{2})}{\mathbf{\Gamma}(k+1-\frac{1}{2}+\omega)} \\ & + \Gamma\,2^{-\frac{1}{2}+\omega}\,\mathbf{\Gamma}(\omega)\left(\sum_{k=0}^{+\infty}\gamma_k(-1)^k\frac{\mathbf{\Gamma}(k+1-\frac{1}{2})}{\mathbf{\Gamma}(k+1-\frac{1}{2}+\omega)}\right)\cos(2\alpha) \\ & + (1-\Gamma)\,2^{-\frac{1}{2}+\omega}\,\mathbf{\Gamma}(\omega)\left(\sum_{k=0}^{+\infty}\beta_k(-1)^k\frac{\mathbf{\Gamma}(k+1-\frac{1}{2})}{\mathbf{\Gamma}(k+1-\frac{1}{2}+\omega)}\right)\cos\alpha\end{aligned} \tag{4.49}$$

that using (4.46) can be expressed as

$$\frac{2\pi}{\mu_1}\Delta\sigma_1(-1) = \mathcal{S}(\omega)\left[(1-\Gamma)\cos\alpha - \left(\frac{l_1}{l_2}\right)^{\omega}\frac{\cos(\pi\omega)-\Gamma}{(1+\Gamma)\cdot\cos(\alpha(1+\omega))}(1+\Gamma\cos(2\alpha))\right] \tag{4.50}$$

The last relation can be rewritten observing that

$$\begin{aligned}\frac{1+\Gamma\cos(2\alpha)}{1+\Gamma} &= \frac{1}{1+\Gamma}+\frac{\Gamma}{1+\Gamma}\cos(2\alpha) \\ &= \frac{1+m}{2}+\frac{1-m}{2}\cos(2\alpha) \\ &= \frac{1}{2}(1+\cos(2\alpha))+\frac{1}{2}(1-\cos(2\alpha))m \\ &= \cos^2\alpha + m\sin^2\alpha\end{aligned} \tag{4.51}$$

and so the stress drop on section 1 near $\xi=-1$ can be expressed as

$$\begin{aligned}&\frac{2\pi}{\mu_1}\Delta\sigma_1(-1) = \\ &= \mathcal{S}(\omega)\left\{\cos\alpha\left[(1-\Gamma)-\left(\frac{l_1}{l_2}\right)^{\omega}\frac{\cos(\pi\omega)-\Gamma}{\cos(\alpha(1+\omega))}\cos\alpha\right]-\sin\alpha\left[m\left(\frac{l_1}{l_2}\right)^{\omega}\frac{\cos(\pi\omega)-\Gamma}{\cos(\alpha(1+\omega))}\sin\alpha\right]\right\}\end{aligned} \tag{4.52}$$

If we compare the expressions found for $\Delta\sigma_1$ and $\Delta\sigma_2$, we obtain

$$\begin{aligned}\Delta\sigma_1(-1) &= \cos\alpha\,\frac{\Delta\sigma_2(-1)}{m}-\frac{\mu_1}{2\pi}\frac{2m}{1+m}\left(\frac{l_1}{l_2}\right)^{\omega}\frac{\cos(\pi\omega)-\Gamma}{(1+\Gamma)\,\cos(\alpha(1+\omega))}\sin^2\alpha\,\mathcal{S}(\omega) \\ &= \cos\alpha\,\frac{\Delta\sigma_2(-1)}{m}+\frac{\mu_1}{2\pi}\frac{2m}{1+m}\sin^2\alpha\,2^{-\frac{1}{2}+\omega}\,\mathbf{\Gamma}(\omega)\left(\sum_{k=0}^{+\infty}\gamma_k(-1)^k\frac{\mathbf{\Gamma}(k+1-\frac{1}{2})}{\mathbf{\Gamma}(k+1-\frac{1}{2}+\omega)}\right)\end{aligned} \tag{4.53}$$

The relation between stress drops $\Delta\sigma_1, \Delta\sigma_2$ can be finally expressed in this form

$$\frac{\Delta\sigma_1(-1)}{\mu_1} = \cos\alpha\,\frac{\Delta\sigma_2(-1)}{\mu_2}-\sin\alpha\,F(\alpha,m) \tag{4.54}$$

where

$$F(\alpha,m) = -\frac{1}{2\pi}\frac{2m}{1+m}\sin\alpha\,2^{-\frac{1}{2}+\omega}\,\mathbf{\Gamma}(\omega)\left(\sum_{k=0}^{+\infty}\gamma_k(-1)^k\frac{\mathbf{\Gamma}(k+1-\frac{1}{2})}{\mathbf{\Gamma}(k+1-\frac{1}{2}+\omega)}\right) \tag{4.55}$$

This relation generalises the condition corresponding to a planar crack surface

$$\frac{\Delta\sigma_1(-1)}{\mu_1} = \frac{\Delta\sigma_2(-1)}{\mu_2} \tag{4.56}$$

in fact, letting $\alpha \to 0$, the second term on second side of (4.54) vanishes and therefore relation (4.54) reproduces the condition proper to the case of a planar crack.
Remembering that

$$\sigma_{ny} = \cos(\alpha)\sigma_{xy} - \sin(\alpha)\sigma_{zy} \tag{4.57}$$

we can identify $F(\alpha, m)$ as the σ_{zy} stress component induced at the interface by crack slip; the initial stress on section σ^0_{ny} at the interface is given by

$$\sigma^0_{ny}(-1) = \cos(\alpha)\sigma^0_{xy}(-1) - \sin(\alpha)\sigma^0_{zy}(-1) \tag{4.58}$$

where $\sigma^0_{xy}(-1), \sigma^0_{zy}(-1)$ are determined by the reference configuration we decide to use. If we consider the case of a purely transform domain

$$\begin{cases} \sigma^0_{xy} = \sigma^0 \\ \sigma^0_{zy} = 0 \end{cases} \tag{4.59}$$

the stress drop condition becomes

$$\frac{\Delta\sigma_1(-1)}{\mu_1} = \cos\alpha \, \frac{\Delta\sigma_2(-1)}{\mu_2} \tag{4.60}$$

since the stress component σ_{zy} have not to be released and therefore $F(\alpha, m)$ must vanish.
If the media in welded contact are assumed elastic, the stress drops $\Delta\sigma_1, \Delta\sigma_2$ must be proportional to the local rigidity value and so the fault bending model is suitable to describe strike-slip faulting across a structural discontinuity only if $m = \mu_2/\mu_1 > 1$, since the vertical dipping fault at depth may cross the interface with the softer layer, provided that the shallower section is suitably inclined, according to the stress drop condition (4.60).

4.4 Numerical solution

The singular nature of the dislocation density suggests to expand the regular factors $R(\xi')$ through Jacobi polynomials $P_n^{(-1/2,\omega)}(\xi')$, which are the orthogonal polynomials for the weight function $w(\xi') = (1-\xi')^{-\frac{1}{2}}(1+\xi')^{\omega}$; however no convenient analytical expression can be found for the singular integrals in the system of integral equations (4.15) and so we are forced to search an approximate solution.
An approximate solution for this system can be derived if we rewrite the dislocation density in this way

$$\rho(\xi') = \frac{1}{\sqrt{1-\xi'^2}} \left[R(\xi')(1+\xi')^{\frac{1}{2}+\omega} \right] \tag{4.61}$$

where the exponent $\frac{1}{2}+\omega \in \left(-\frac{1}{2}, 0\right)$, since from the asymptotic study performed in section (4.2) we know that the singularity degree is always in the interval $(-0.5, 0]$; in this case $R(\xi')(1+\xi')^{\frac{1}{2}+\omega}$ has a square-integrable singularity and so the expansion in Chebyshev polynomials will be convergent only in the mean.
After these considerations, dislocation density ρ_1, ρ_2 can be written in this form

$$\rho_1(\xi_1^{'}) = \frac{1}{\sqrt{1-\xi_1^{'2}}} \sum_{n=0}^{\infty} \gamma_n T_n(\xi_1^{'}), \tag{4.62}$$

$$\rho_2(\xi_2^{'}) = \frac{1}{\sqrt{1-\xi_2^{'2}}} \sum_{n=0}^{\infty} \beta_n T_n(\xi_2^{'}), \tag{4.63}$$

where T_n are Chebyshev polynomials of the first kind and

$$\sum_{n=0}^{\infty} \gamma_n T_n(\xi_1') = R_1(\xi_1')(1+\xi_1')^{\frac{1}{2}+\omega} \tag{4.64}$$

$$\sum_{n=0}^{\infty} \beta_n T_n(\xi_2') = R_2(\xi_2')(1+\xi_2')^{\frac{1}{2}+\omega} \tag{4.65}$$

Both crack sections are open at the interface, therefore we must supply two supplementary conditions in order that the problem may yield a unique solution.

4.4.1 Supplementary conditions

The first supplementary condition is easily derived from the continuity condition of crack slip at the interface between the media

$$\Delta u_1\left(\xi_1 = -1\right) = \Delta u_2\left(\xi_2 = -1\right) \quad \Longrightarrow \quad -l_1 \int_{-1}^{1} \rho_1(\xi_1^{'}) d\xi_1^{'} = -l_2 \int_{-1}^{1} \rho_2(\xi_2^{'}) d\xi_2^{'} \tag{4.66}$$

The two integrals can be simply evaluated using the orthogonality condition (A.1) and from (4.66) we obtain the following relation between coefficients γ_0, β_0

$$l_1 \gamma_0 = l_2 \beta_0 \tag{4.67}$$

A second condition is needed in order to provide finite stress values over the crack plane near the interface ($z = 0$). From the asymptotic study we have found that compensation of singular terms is possible only when ω is solution of (4.35) and in such a case the following relation must hold

$$\frac{R_1(-1)}{R_2(-1)} = -\left(\frac{l_1}{l_2}\right)^{\omega} \frac{\cos(\pi\omega) - \Gamma}{(1-\Gamma)\cdot\cos(\alpha(1+\omega))} \tag{4.68}$$

Considering the ratio between ρ_1, ρ_2 and letting $t \to -1$ we obtain the second supplementary condition

$$\sum_{n=0}^{\infty} \gamma_n \left(-1\right)^n = Q \sum_{n=0}^{\infty} \beta_n \left(-1\right)^n \tag{4.69}$$

being $T_n(-1) = (-1)^n$ and $Q = \dfrac{R_1(-1)}{R_2(-1)}$.

4.4.2 Method of solution

We substitute the expressions proposed for $\rho_1(\xi_1^{'}), \rho_2(\xi_2^{'})$ in the integral equations

$$\begin{aligned}\frac{2\pi}{\mu_1}\Delta\sigma_1(\xi_1) &= -\pi\sum_{n=1}^{\infty}\gamma_n U_{n-1}(\xi_1)\\ &- \Gamma\sum_{n=0}^{\infty}\gamma_n\int_{-1}^{+1}\frac{d\xi_1^{'}}{\sqrt{1-\xi_1^{'2}}}\frac{(\xi_1-\xi_1^{'})\sin^2\alpha+(\xi_1+\xi_1^{'}+2)\cos^2\alpha}{(\xi_1-\xi_1^{'})^2\sin^2\alpha+(\xi_1+\xi_1^{'}+2)^2\cos^2\alpha}T_n(\xi_1^{'})\\ &- \frac{2m}{1+m}\sum_{n=0}^{\infty}\beta_n\int_{-1}^{+1}\frac{d\xi_2^{'}}{\sqrt{1-\xi_2^{'2}}}\frac{(\xi_2^{'}+1)\cos\alpha+\dfrac{l_1}{l_2}(\xi_1+1)}{\left(\dfrac{l_1}{l_2}\right)^2(\xi_1+1)^2\sin^2\alpha+\left((\xi_2^{'}+1)+\dfrac{l_1}{l_2}(\xi_1+1)\cos\alpha\right)^2}T_n(\xi_2^{'})\end{aligned} \tag{4.70}$$

$$\begin{aligned}\frac{2\pi}{\mu_2}\Delta\sigma_2(\xi_2) &= -\pi\sum_{n=1}^{\infty}\beta_n U_{n-1}(\xi_2)+\Gamma\sum_{n=0}^{\infty}\beta_n\int_{-1}^{+1}\frac{d\xi_2^{'}}{\sqrt{1-\xi_2^{'2}}}\frac{T_n(\xi_2^{'})}{\xi_2+\xi_2^{'}+2}\\ &- \frac{2}{1+m}\sum_{n=0}^{\infty}\gamma_n\int_{-1}^{+1}\frac{d\xi_1^{'}}{\sqrt{1-\xi_1^{'2}}}\frac{(\xi_1^{'}+1)\cos\alpha+\dfrac{l_2}{l_1}(\xi_2+1)}{(\xi_1^{'}+1)^2\sin^2\alpha+\left((\xi_1^{'}+1)\cos\alpha+\dfrac{l_2}{l_1}(\xi_2+1)\right)^2}T_n(\xi_1^{'})\end{aligned} \tag{4.71}$$

For both the equations, the first term on second side has been obtained using the integral property (A.4) valid for Chebyshev polynomials of first kind. Multiplying equation (4.70) by $U_k(\xi_1)\sqrt{1-\xi_1^2}$ and integrating on the interval $-1, 1$ in the variable ξ_1 we obtain

$$\frac{\pi^2}{\mu_1}\Delta\sigma_k^{(1)} = -\frac{\pi^2}{2}\sum_{n=1}^{\infty}\gamma_n\delta_{k,n-1}-\Gamma\sum_{n=0}^{\infty}\gamma_n R_{11}(k,n)-\frac{2m}{1+m}\sum_{n=0}^{\infty}\beta_n R_{12}(k,n) \tag{4.72}$$

To write the first term on the second side we have used the orthogonality relation (A.3) relative to Chebyshev polynomials of second kind. $R_{11}(k,n)$ e $R_{12}(k,n)$ are double integrals and they have the following form

$$\begin{aligned}R_{11}(k,n) &= \int_{-1}^{+1}U_k(\xi_1)\sqrt{1-\xi_1^2}\left(\int_{-1}^{+1}\frac{d\xi_1^{'}}{\sqrt{1-\xi_1^{'2}}}\frac{(\xi_1-\xi_1^{'})\sin^2\alpha+(\xi_1+\xi_1^{'}+2)\cos^2\alpha}{(\xi_1-\xi_1^{'})^2\sin^2\alpha+(\xi_1+\xi_1^{'}+2)^2\cos^2\alpha}T_n(\xi_1^{'})\right)d\xi_1\\ R_{12}(k,n) &=\\ &= \int_{-1}^{+1}U_k(\xi_1)\sqrt{1-\xi_1^2}\left(\int_{-1}^{+1}\frac{d\xi_2^{'}}{\sqrt{1-\xi_2^{'2}}}\frac{(\xi_2^{'}+1)\cos\alpha+\dfrac{l_1}{l_2}(\xi_1+1)}{\left(\dfrac{l_1}{l_2}(\xi_1+1)\sin\alpha\right)^2+\left((\xi_2^{'}+1)+\dfrac{l_1}{l_2}(\xi_1+1)\cos\alpha\right)^2}T_n(\xi_2^{'})\right)d\xi_1\end{aligned} \tag{4.73}$$

In the same manner, if we multiply equation (4.71) by $U_k(\xi_2)\sqrt{1-\xi_2^2}$ and then integrate on the interval $-1, +1$ in the variable ξ_2 we obtain

$$\frac{\pi^2}{\mu_2}\Delta\sigma_k^{(2)} = -\frac{\pi^2}{2}\sum_{n=1}^{\infty}\beta_n\delta_{k,n-1}+\Gamma\sum_{n=0}^{\infty}\beta_n R_{22}(k,n)-\frac{2}{1+m}\sum_{n=0}^{\infty}\gamma_n R_{21}(k,n) \tag{4.74}$$

where double integrals $R_{21}(k,n), R_{22}(k,n)$ have this form

$$R_{22}(k,n) = \int_{-1}^{+1} U_k(\xi_2)\sqrt{1-\xi_2^2}\left(\int_{-1}^{+1} \frac{d\xi_2^{'}}{\sqrt{1-\xi_2^{'2}}}\frac{T_n(\xi_2^{'})}{\xi_2+\xi_2^{'}+2}\right)d\xi_2$$

$$R_{21}(k,n) =$$

$$= \int_{-1}^{+1} U_k(\xi_2)\sqrt{1-\xi_2^2}\left(\int_{-1}^{+1} \frac{d\xi_1^{'}}{\sqrt{1-\xi_1^{'2}}}\frac{(\xi_1^{'}+1)\cos\alpha+\frac{l_2}{l_1}(\xi_2+1)}{(\xi_1^{'}+1)^2\sin^2\alpha+\left((\xi_1^{'}+1)\cos\alpha+\frac{l_2}{l_1}(\xi_2+1)\right)^2}T_n(\xi_1^{'})\right)d\xi_2 \tag{4.75}$$

$\Delta\sigma_k^{(1)}, \Delta\sigma_k^{(2)}$ are the coefficients of the expansion in U_k polynomials of the stress drops $\Delta\sigma_1, \Delta\sigma_2$, respectively. If $\Delta\sigma_1, \Delta\sigma_2$ are constants then $\Delta\sigma_k^{(1)} = \Delta\sigma_k^{(2)} = \Delta\sigma\delta_{k0}$.
In order to provide an approximate solution to the crack problem, the infinite sums in (4.69)-(4.71), are truncated to a finite index N. More specifically, this means that in (4.70),(4.71) we take

1. $R_{ij}(k,n) = 0$ for $k > N-1 \wedge n > N$
2. $\Delta\sigma_k^{(1)} = \Delta\sigma_k^{(2)} = 0$ for $k > N-1$

Let $i = k+1, j = n+1$, we define the following matrix $(2N)\times(2N+2)$:

$$\Upsilon = \begin{pmatrix} G_{11} & G_{12} \\ G_{21} & G_{22} \end{pmatrix} \tag{4.76}$$

whose elements are the $(N)\times(N+1)$ matrices

$$\begin{cases} G_{11}(i,j) = -\frac{\mu_1}{\pi^2}\left(\frac{\pi^2}{2}\delta_{i-1,j-2} + \Gamma R_{11}(i-1,j-1)\right) \\ G_{12}(i,j) = -\frac{\mu_1}{\pi^2}\frac{2m}{1+m}R_{12}(i-1,j-1) \\ G_{21}(i,j) = -\frac{\mu_2}{\pi^2}\frac{2}{1+m}R_{21}(i-1,j-1) \\ G_{22}(i,j) = -\frac{\mu_2}{\pi^2}\left(\frac{\pi^2}{2}\delta_{i-1,j-2} - \Gamma R_{22}(i-1,j-1)\right) \end{cases}$$

In other terms, the matrix Υ_{ij}, with $i = 1,2,...,2N$ and $j = 1,2,...,2N+2$, is

$$\Upsilon_{ij} = \begin{cases} G_{11}(i,j) & \text{if } (1 \le i \le N) \wedge (1 \le j \le N+1) \\ G_{12}(i,j-(N+1)) & \text{if } (1 \le i \le N) \wedge (N+2 \le j \le 2N+2) \\ G_{21}(i-N,j) & \text{if } (N+1 \le i \le 2N) \wedge (1 \le j \le N+1) \\ G_{22}(i-N,j-(N+1)) & \text{if } (N+1 \le i \le 2N) \wedge (N+2 \le j \le 2N+2) \end{cases}$$

Furthermore, let η be a column vector with $2N+2$ components γ_n and β_n

$$\eta = [\gamma_0, ..., \gamma_N, \beta_0, ..., \beta_N]^T \tag{4.77}$$

and let χ be the $2N$ column vector containing the N components of $\Delta\sigma_1$ and the N components of $\Delta\sigma_2$

$$\chi = [\Delta\sigma_0^{(1)}, ..., \Delta\sigma_{N-1}^{(1)}, \Delta\sigma_0^{(2)}, ..., \Delta\sigma_{N-1}^{(2)}]^T \tag{4.78}$$

If $\Delta\sigma_1, \Delta\sigma_2$ are constants, only the first and the $(N+1)$th components of χ do not vanish. The solution of the truncated problem is given by the following system of $2N$ equations for the $2N+2$ unknowns η_j

$$\chi_i = \sum_{j=1}^{2N+2} \Upsilon_{ij}\eta_j, \qquad i = 1, ..., 2N \tag{4.79}$$

with the supplementary conditions derived from (4.67),(4.69).

$$l_1\eta_1 = l_2\eta_{N+2} \tag{4.80}$$

$$\sum_{j=1}^{N+1} (-1)^{j-1}\,\eta_j = Q \sum_{j=N+2}^{2N+2} (-1)^{j-(N+1)-1}\,\eta_j \tag{4.81}$$

4.4.3 Results

The computations have been performed assuming:

- $\nu_1 = \nu_2 = 0.25$ and $\mu_2 = 3\mu_1 = 30$ GPa
- $2l_1 = 2l_2 = 8$ km for the length of crack sections
- a stepwise constant stress drop profile with $\Delta\sigma_2 = 3$ MPa and $\Delta\sigma_1 = \dfrac{\Delta\sigma_2}{m}\cos(\alpha)$.

The non-vanishing stress components σ_{xy}, σ_{zy} induced by shear cracks corresponding to α=0, 22.5°, 45° are shown in Figure 4.4. If we compare cases (b) and (c) with the case of a planar shear crack (a), we observe an asymmetric stress release with respect to the negative z axis; the stress release is concentrated in the footwall block, while a minor release of σ_{xy} is observed in the opposite quadrant. Therefore we can expect that the region with minor release is candidated to host new fractures. Several field observations regarding the complex pattern of surface fractures connected with major transcurrent earthquakes could be explained in terms of such a mechanism. For instance, if we consider the case of the $M_s = 6.6$ earthquake of June 17-th, 2000 (Figure 4.6), the aftershock activity (dots) shows very well the NS orientation of the main fault, confirming the fault plane solution, while on the surface we can observe lines of fracture (double lines) parallel to the main fault and positioned on both sides, far from each other several kilometres. This kind of observations can be clearly interpreted as the result of near-surface segmentation of the fault plane into several en-echelon branches. In the next section we propose a model suitable to describe this kind of field observations.

In order to evaluate the accuracy of the approximate solution found, we show in Figure 4.5 the stress components σ_{xy}, σ_{zy} computed according to the displacement discontinuity method. This numerical technique does not involve a study of the singular nature (assuming equal to -1 the singularity at the ends of each boundary element) and therefore we can check the correctness of the results found with the crack model. The comparison of stress maps shown in Figures 4.4, 4.5 is satisfactory, since the maps obtained with the method of solution proposed are confirmed by the maps obtained with the boundary element approach.

4.5 Conclusions

In this chapter we have presented a model in order to describe strike-slip faulting in layered media. Bonafede et al. (2002) have studied the problem of a vertical shear crack crossing the interface between two media and a stress drop condition have been derived which have a considerable influence on the style of faulting in layered media. In fact there are several real cases in which such a condition cannot be fulfilled. The model proposed is able to describe strike-slip faulting across a structural discontinuity if the stress drop in the shallow layer is lower than the value prescribed by the stress drop condition pertinent to a vertical planar crack (e.g. the case of a recent deposit of sediments on top of a pre-stressed basement rock). The vertical dipping lower section can cross the interface if the upper section is suitably inclined according to the generalized stress drop condition derived. The asymptotic study of the singular behaviour of the dislocation density has shown that the density distribution has an algebraic singularity at the interface of degree ω between 0 and $-\frac{1}{2}$, depending on the inclination angle α of the upper crack section and on the rigidity contrast m between the two media. Furthermore, the inclination of the upper section determines an asymmetric stress release with respect to the negative z axis, therefore the region with minor release is candidate to host new fractures. Several field observations regarding the complex pattern of surface fractures connected with major transcurrent earthquakes could be explained in terms of such a mechanism. For instance, if we consider the case of the $M_s = 6.6$ earthquake of June 17-th, 2000 (Figure 4.6), the aftershocks (dots) show very well the NS orientation of the main fault, confirming the fault plane solution, while on the surface we can observe lines of fracture (double lines) parallel to the main fault and positioned on both sides, far from each other several kilometres. This kind of observations can be clearly interpreted as the result of near-surface segmentation of the fault plane into several en-echelon branches. In the

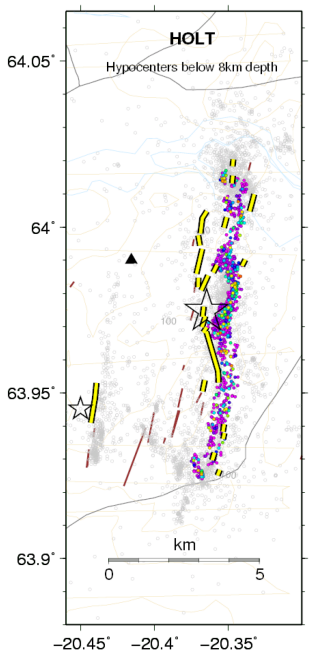

Figure 4.6: Aftershocks and pattern of surface fractures in the SISZ

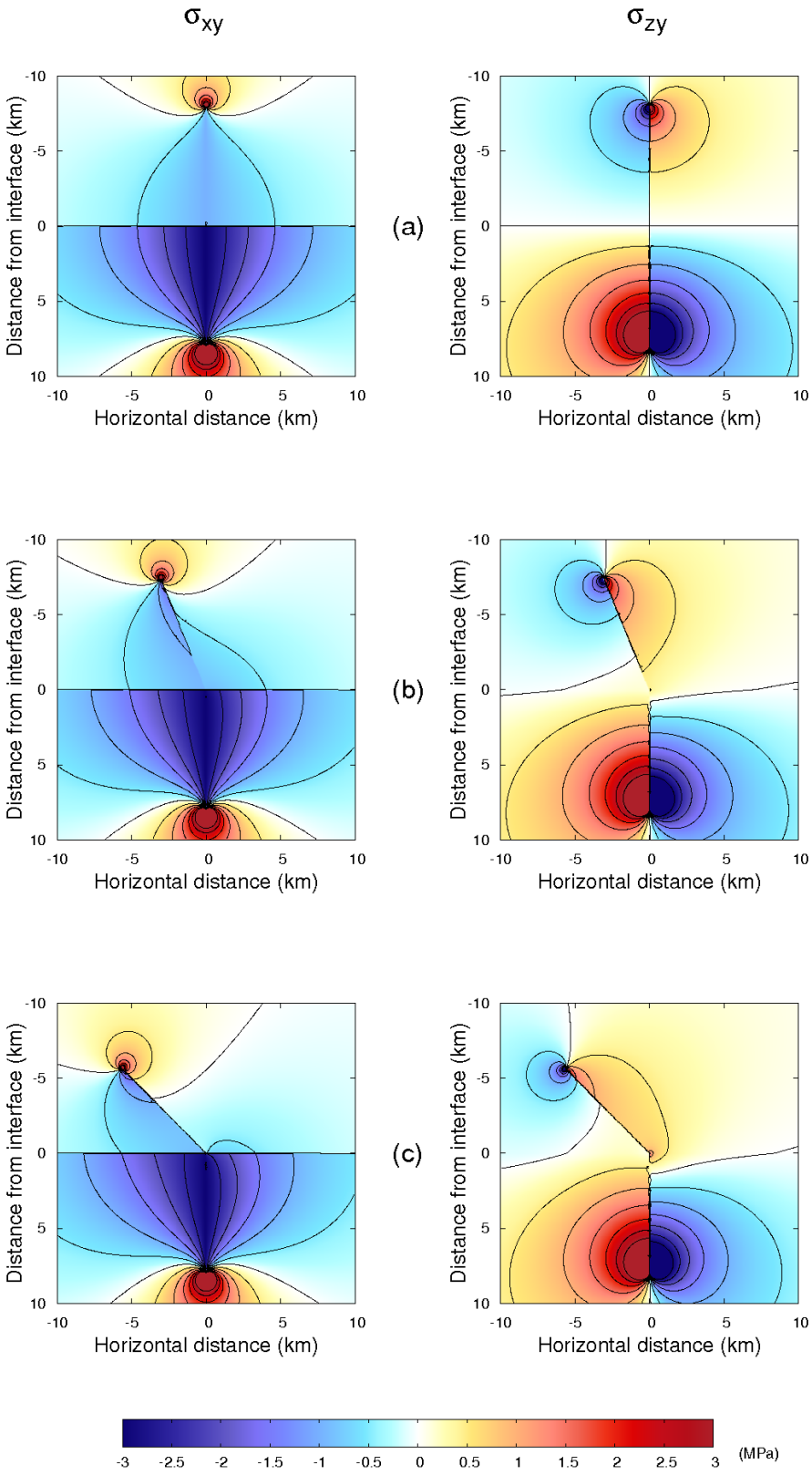

Figure 4.4: Non-vanishing stress components σ_{xy}, σ_{zy} induced by shear crack with:(a) $\alpha = 0°$, (b) $\alpha = 22.5°$, (c) $\alpha = 45°$

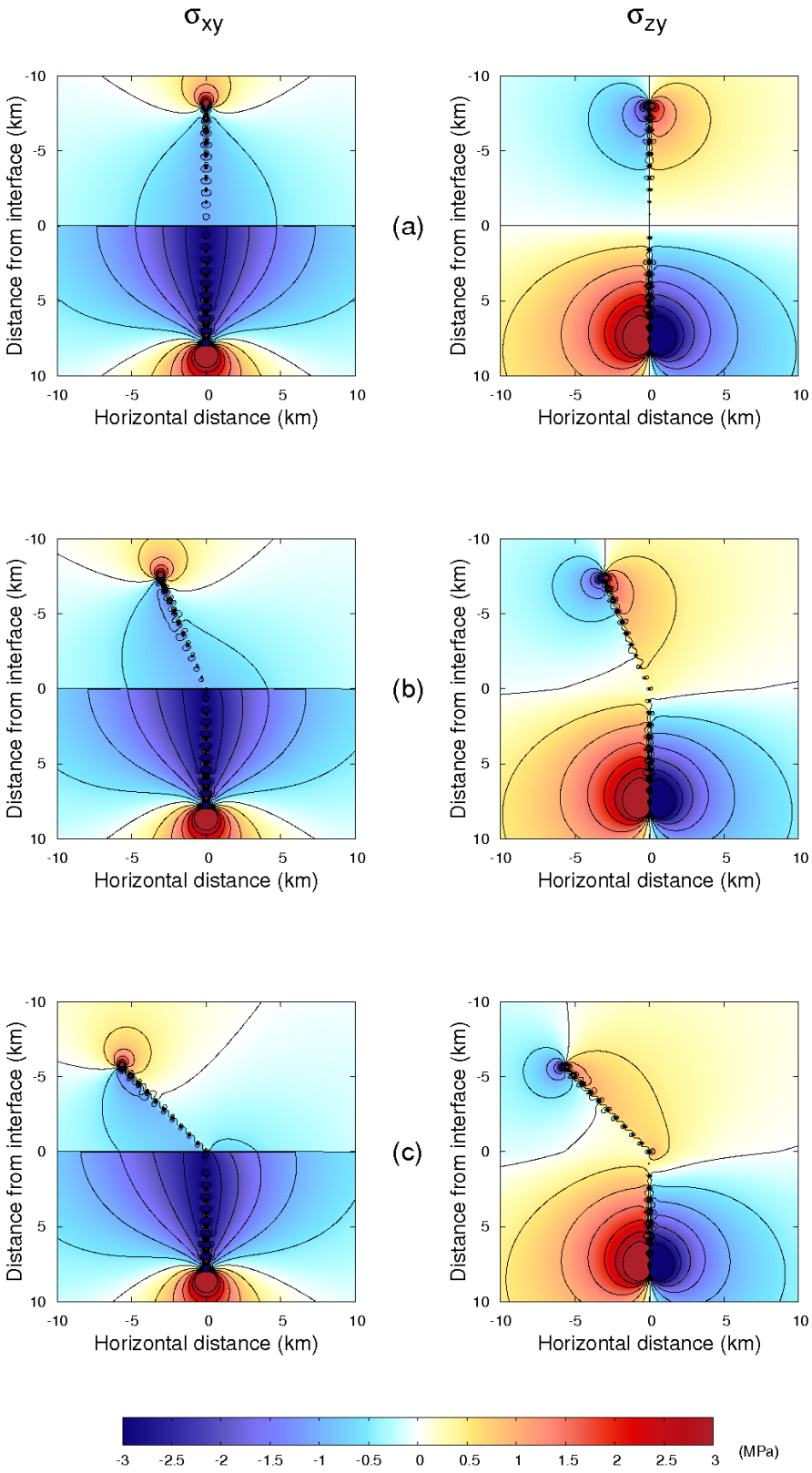

Figure 4.5: Non-vanishing stress components σ_{xy}, σ_{zy} computing according to the displacement discontinuity method:(a) $\alpha = 0°$, (b) $\alpha = 22.5°$, (c) $\alpha = 45°$

next chapter we propose a model of fault branching suitable to describe the observations here examined.

Chapter 5

Fault branching model

5.1 Model description

As in the previous model, we consider an elastic layer of thickness H and rigidity μ_1, bounded by a free surface and welded to an elastic half-space of rigidity μ_2. The origin of the reference system is placed at the intersection between the crack and the interface, with z axis pointing downward. We still consider an antiplane strain configuration in which the only non-vanishing component of the displacement field is $u_y(x, z)$, which is independent of the coordinate y.
With respect to the fault bending model, now the crack is splitted into three interacting sections, all open at the interface, but with sections 1a,1b embedded in the layer and section 2 embedded in the lower half-space. The sections 1a,1b have length $2l_{1a}, 2l_{1b}$, respectively; both sections are inclined with respect to the negative z axis ($-\frac{\pi}{2} < \alpha_{1a}, \alpha_{1b} < \frac{\pi}{2}$) and $\hat{n}_{1a} = (\cos\alpha_{1a}, 0, -\sin\alpha_{1a})$ represents the normal versor of section 1a, while $\hat{n}_{1b} = (\cos\alpha_{1b}, 0, -\sin\alpha_{1b})$ is the normal versor of section 1b. As in the previous model, section 2 is normal with respect to the interface and its length is equal to $2l_2$. A sketch of the model is presented in figure 5.1.

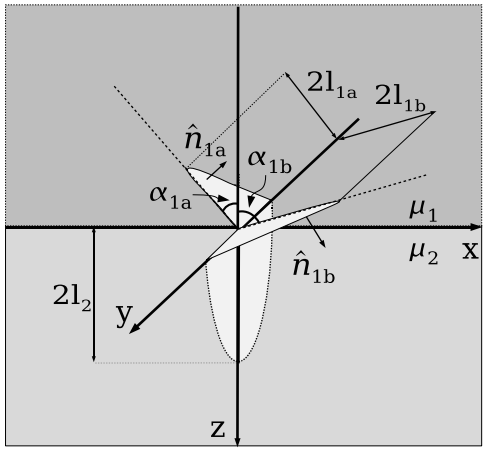

Figure 5.1: Fault branching model

Now we have to consider three equilibrium equation, one for each crack section

$$-\Delta\sigma_{1a}(\hat{x}_{1a},\hat{y}_{1a}) = (\sigma^c_{ny})^{1a}_{1a}(\hat{x}_{1a},\hat{y}_{1a}) + (\sigma^c_{ny})^{1b}_{1a}(\hat{x}_{1a},\hat{y}_{1a}) + (\sigma^c_{ny})^{2}_{1}(\hat{x}_{1a},\hat{y}_{1a}), \qquad \begin{cases}\hat{x}_{1a} = -\mathcal{S}_{1a}\cos\alpha_{1a}\\ \hat{y}_{1a} = -\mathcal{S}_{1a}\sin\alpha_{1a}\end{cases} \quad (0 < \mathcal{S}_{1a} < 2l_{1a})$$

$$-\Delta\sigma_{1b}(\hat{x}_{1b},\hat{y}_{1b}) = (\sigma^c_{ny})^{1a}_{1b}(\hat{x}_{1b},\hat{y}_{1b}) + (\sigma^c_{ny})^{1b}_{1b}(\hat{x}_{1b},\hat{y}_{1b}) + (\sigma^c_{ny})^{2}_{1}(\hat{x}_{1b},\hat{y}_{1b}), \qquad \begin{cases}\hat{x}_{1b} = -\mathcal{S}_{1b}\cos\alpha_{1b}\\ \hat{y}_{1b} = -\mathcal{S}_{1b}\sin\alpha_{1b}\end{cases} \quad (0 < \mathcal{S}_{1b} < 2l_{1b})$$

$$-\Delta\sigma_{2}(0,z) = (\sigma^c_{xy})^{1a}_{2}(0,z) + (\sigma^c_{xy})^{1b}_{2}(0,z) + (\sigma^c_{xy})^{2}_{2}(0,z) \quad (0 < z < 2l_2)$$

where $\Delta\sigma_{1a}(\hat{x}_{1a},\hat{y}_{1a})$ is the stress drop in a point of section 1a, being $(\mathcal{S}_{1a},\alpha_{1a})$ the polar coordinates of the point $(\hat{x}_{1a},\hat{y}_{1a})$, $\Delta\sigma_{1b}(\hat{x}_{1b},\hat{y}_{1b})$ is the stress drop in a point of section 1b, being $(\mathcal{S}_{1b},\alpha_{1b})$ the polar coordinates of the point $(\hat{x}_{1b},\hat{y}_{1b})$, and $\Delta\sigma_2(0,z)$ is the stress drop in a point of the vertical section.
The three crack sections are interagent, so the stress drop on each section is equal to to the sum of three contributions. $(\sigma^c_{ny})^{1a}_{1a}, (\sigma^c_{ny})^{1b}_{1a}, (\sigma^c_{ny})^{2}_{1a}$ are stress induced on section 1a, $(\sigma^c_{ny})^{1a}_{1b}, (\sigma^c_{ny})^{1b}_{1b}, (\sigma^c_{ny})^{2}_{1b}$ are stress induced on section 1b and $(\sigma^c_{xy})^{1a}_{2}, (\sigma^c_{xy})^{1b}_{2}, (\sigma^c_{xy})^{2}_{2}$ are stress induced on section 2 due to slip of section 1a, section 1b, section 2, respectively.
On the vertical section the stress component released is simply σ_{xy}, while the components released on section 1a and on section 1b must be evaluated using the Cauchy relation

$$\sigma_{ny} = T_y^{(\hat{n})} = \sigma_{iy}n_i = \cos\alpha\ \sigma_{xy} - \sin\alpha\ \sigma_{zy} \tag{5.1}$$

where $\hat{n} = \hat{n}_{1a}$ in case of section 1a and $\hat{n} = \hat{n}_{1b}$ in case of section 1b.
To define a crack model we have to employ suitable superimpositions of elementary solutions. Using a continuous distribution of elementary dislocations with dislocation lines contained in the interval $0 < S < 2l_{1a}$, a distribution with dislocation lines in the interval $0 < S < 2l_{1b}$ and a distribution with dislocation lines in the interval $0 < z < 2l_2$, the equilibrium equations can be rewritten in the following form

$$\begin{aligned}-\Delta\sigma_{1a}(\mathcal{S}_{1a}) = &\int_0^{2l_{1a}} (\sigma_{ny})^I_1(\mathcal{S}_{1a};S_0)\rho_{1a}(S_0)dS_0 + \int_0^{2l_{1b}} (\sigma_{ny})^I_1(\mathcal{S}_{1a};S_0)\rho_{1b}(S_0)dS_0\\ &+ \int_0^{2l_2} (\sigma_{ny})^{II}_1(\mathcal{S}_{1a};z_0)\rho_2(z_0)dz_0 \end{aligned} \tag{5.2a}$$

$$\begin{aligned}-\Delta\sigma_{1b}(\mathcal{S}_{1b}) = &\int_0^{2l_{1a}} (\sigma_{ny})^I_1(\mathcal{S}_{1b};S_0)\rho_{1a}(S_0)dS_0 + \int_0^{2l_{1b}} (\sigma_{ny})^I_1(\mathcal{S}_{1b};S_0)\rho_{1a}(S_0)dS_0\\ &+ \int_0^{2l_2} (\sigma_{ny})^{II}_1(\mathcal{S}_{1b};z_0)\rho_2(z_0)dz_0 \end{aligned} \tag{5.2b}$$

$$\begin{aligned}-\Delta\sigma_{2}(z) = &\int_0^{2l_{1a}} (\sigma_{xy})^I_2(z;S_0)\rho_{1a}(S_0)dS_0 + \int_0^{2l_{1b}} (\sigma_{xy})^I_2(z;S_0)\rho_{1b}(S_0)dS_0\\ &+ \int_0^{2l_2} (\sigma_{xy})^{II}_2(z;z_0)\rho_2(z_0)dz_0 \end{aligned} \tag{5.2c}$$

where the integrals must be evaluated in the principle-value sense.
In case of sections 1a and 1b, the integral kernels $(\sigma_{ny})^I_1, (\sigma_{xy})^I_2$ can be obtained using the analytical solutions for an elementary screw dislocation of arbitrary dip (Singh et al., 1994) embedded in the upper layer.

$$(\sigma_{xy})_1^I(x,z;S_0) = \frac{\mu_1}{2\pi}\left\{\frac{z+S_0\cos\alpha}{R^2} - \frac{z-S_0\cos\alpha+2H}{S^2} + \sum_{n=1}^{\infty}\Gamma^n\left[-\frac{z-S_0\cos\alpha-2(n-1)H}{T^2} + \frac{z+S_0\cos\alpha+2nH}{V^2} + \frac{z+S_0\cos\alpha-2nH}{U^2} - \frac{z-S_0\cos\alpha+2(n+1)H}{W^2}\right]\right\} \tag{5.3}$$

$$(\sigma_{zy})_1^I(x,z;S_0) = -\frac{\mu_1}{2\pi}(x+S_0\sin\alpha)\left\{\frac{1}{R^2} - \frac{1}{S^2} + \sum_{n=1}^{\infty}\Gamma^n\left[-\frac{1}{T^2} + \frac{1}{V^2} + \frac{1}{U^2} - \frac{1}{W^2}\right]\right\} \tag{5.4}$$

$$(\sigma_{xy})_2^I(x,z;S_0) = \frac{\mu_2}{2\pi}\frac{2}{1+m}\left\{\frac{z+S_0\cos\alpha}{R^2} - \frac{z-S_0\cos\alpha+2H}{S^2} + \sum_{n=1}^{\infty}\Gamma^n\left[\frac{z+S_0\cos\alpha+2nH}{V^2} - \frac{z-S_0\cos\alpha+2(n+1)H}{W^2}\right]\right\} \tag{5.5}$$

where

$$\begin{cases} R^2 = (x+S_0\sin\alpha)^2 + (z+S_0\cos\alpha)^2 \\ S^2 = (x+S_0\sin\alpha)^2 + (z-S_0\cos\alpha+2H)^2 \\ T^2 = (x+S_0\sin\alpha)^2 + (z-S_0\cos\alpha-2(n-1)H)^2 \\ U^2 = (x+S_0\sin\alpha)^2 + (z+S_0\cos\alpha-2nH)^2 \\ V^2 = (x+S_0\sin\alpha)^2 + (z+S_0\cos\alpha+2nH)^2 \\ W^2 = (x+S_0\sin\alpha)^2 + (z-S_0\cos\alpha+2(n+1)H)^2 \end{cases} \qquad \begin{cases} m = \dfrac{\mu_2}{\mu_1} \\ \\ \Gamma = \dfrac{1-m}{1+m} \end{cases} \tag{5.6}$$

In case of section 2, the integral kernels $(\sigma_{ny})_1^{II}$, $(\sigma_{xy})_2^{II}$ can be derived using the analytical solutions proper to a vertical screw dislocation (Rybicki , 1971).

$$(\sigma_{xy})_1^{II}(x,z;z_0) = \frac{\mu_1}{2\pi}\frac{2m}{1+m}\left[\sum_{n=0}^{\infty}\Gamma^n\left(\frac{z+z_0+2(n+1)H}{x^2+(z+z_0+2(n+1)H)^2} - \frac{z-z_0-2nH}{x^2+(z-z_0-2nH)^2}\right)\right] \tag{5.7}$$

$$(\sigma_{zy})_1^{II}(x,z;z_0) = -\frac{\mu_1}{2\pi}\frac{2m}{1+m}\left[\sum_{n=0}^{\infty}\Gamma^n\left(\frac{x}{x^2+(z+z_0+2(n+1)H)^2} - \frac{x}{x^2+(z-z_0-2nH)^2}\right)\right] \tag{5.8}$$

$$(\sigma_{xy})_2^{II}(z;z_0) = -\frac{\mu_2}{2\pi}\left[\frac{1}{z-z_0} + \Gamma\frac{1}{z+z_0} - \frac{4m}{(1+m)^2}\sum_{n=0}^{\infty}\Gamma^n\frac{1}{z+z_0+2(n+1)H}\right] \tag{5.9}$$

Once the stress drops $\Delta\sigma_{1a}, \Delta\sigma_{1b}, \Delta\sigma_2$ are assigned, the equilibrium equations become a system of coupled integral equations for the unknown functions $\rho_{1a}, \rho_{1b}, \rho_2$.
The unknown dislocation density distribution ρ is splitted into three subdomains

$$\rho = \begin{cases} \rho_{1a}(S_0), & 0 < S_0 < 2l_1 \\ \rho_{1b}(S_0), & 0 < S_0 < 2l_1 b \\ \rho_2(z_0), & 0 < z_0 < 2l_2 \end{cases} \tag{5.10}$$

where $\rho_{1a}, \rho_{1b}, \rho_2$ are defined through the displacement discontinuity over the crack plane

$$\rho_{1a} = \left[\frac{\partial \Delta u(S)}{\partial S}\right]_{S=S_0} \tag{5.11}$$

$$\rho_{1b} = \left[\frac{\partial \Delta u(S)}{\partial S}\right]_{S=S_0} \tag{5.12}$$

$$\rho_2 = \left[\frac{\partial \Delta u(z)}{\partial z}\right]_{z=z_0} \tag{5.13}$$

From (5.11), (5.12) and (5.13) we obtain

$$\Delta u_{1a}(S) = \int_0^S \rho(S_0) dS_0 + C_{1a}$$
$$\Delta u_{1b}(S) = \int_0^S \rho(S_0) dS_0 + C_{1b}$$
$$\Delta u_2(z) = \int_0^z \rho(z_0) dz_0 + C_2$$

where C_{1a}, C_{1b}, C_2 are constants that can be fixed imposing the condition of crack closure

$$\Delta u_{1a}(2l_{1a}) = 0$$
$$\Delta u_{1b}(2l_{1b}) = 0$$
$$\Delta u_2(2l_2) = 0$$

In fact, from the previous conditions, we obtain that $C_{1a}, C_{1b}, C_2 = 0$.
Once the dislocation density ρ is known, the solution of a crack problem is simply obtained by a superimposition of elementary solutions. In our case, if f denotes any elementary component of displacement or stress, the crack solution is given by

$$f^c(x,z) = \int_0^{2l_{1a}} f(x,z;S_0)\rho_{1a}(S_0)dS_0 + \int_0^{2l_{1b}} f(x,z;S_0)\rho_{1b}(S_0)dS_0 + \int_0^{2l_2} f(x,z;z_0)\rho_2(z_0)dz_0 \tag{5.14}$$

The first step in the study of the crack model is the derivation of the system of integral equations which describe the model presented. The details about the calculations performed are summarised in appendix C.1. The equilibrium equations (5.2) can be ex-

pressed in the following form

$$\begin{aligned}
\frac{2\pi}{\mu_1}\Delta\sigma_{1a}(S_a) = &\int_0^{2l_{1a}} \frac{\rho_{1a}(S_{0a})dS_{0a}}{S_a - S_{0a}} \\
&- \Gamma \int_0^{2l_{1a}} \frac{S_a + S_{0a}\cos(2\alpha_{1a})}{(S_a - S_{0a})^2 \sin^2\alpha_{1a} + (S_a + S_{0a})^2 \cos^2\alpha_{1a}} \rho_{1a}(S_{0a})dS_{0a} \\
&- \frac{2m}{1+m} \int_0^{2l_2} \frac{S_a + z_0 \cos\alpha_{1a}}{S_a^2 \sin^2\alpha_{1a} + (S_a\cos\alpha_{1a} + z_0)^2} \rho_2(z_0)dz_0 \\
&+ \int_0^{2l_{1b}} \frac{S_a - S_{0b}\cos(\alpha_{1a} - \alpha_{1b})}{(S_a\sin\alpha_{1a} - S_{0b}\sin\alpha_{1b})^2 + (S_a\cos\alpha_{1a} - S_{0b}\cos\alpha_{1b})^2} \rho_{1b}(S_{0b})dS_{0b} \\
&- \Gamma \int_0^{2l_{1b}} \frac{S_a + S_{0b}\cos(\alpha_{1a} + \alpha_{1b})}{(S_a\sin\alpha_{1a} - S_{0b}\sin\alpha_{1b})^2 + (S_a\cos\alpha_{1a} + S_{0b}\cos\alpha_{1b})^2} \rho_{1b}(S_{0b})dS_{0b} \\
&+ \int_0^{2l_{1a}} R_{1a,1a}(S_a; S_{0a})\rho_{1a}(S_{0a})dS_{0a} + \int_0^{2l_2} R_{1a,2}(S_a; z_0)\rho_2(z_0)dz_0 \\
&+ \int_0^{2l_{1b}} R_{1a,1b}(S_a; S_{0b})\rho_{1b}(S_{0b})dS_{0b}
\end{aligned}$$

$$\begin{aligned}
\frac{2\pi}{\mu_1}\Delta\sigma_{1b}(S_b) = &\int_0^{2l_{1b}} \frac{\rho_{1b}(S_{0b})dS_{0b}}{S_a - S_{0b}} \\
&- \Gamma \int_0^{2l_{1b}} \frac{S_b + S_{0b}\cos(2\alpha_{1b})}{(S_b - S_{0b})^2 \sin^2\alpha_{1b} + (S_b + S_{0b})^2 \cos^2\alpha_{1b}} \rho_{1b}(S_{0b})dS_{0b} \\
&- \frac{2m}{1+m} \int_0^{2l_2} \frac{S_b + z_0 \cos\alpha_{1b}}{S_b^2 \sin^2\alpha_{1b} + (S_b\cos\alpha_{1b} + z_0)^2} \rho_2(z_0)dz_0 \\
&+ \int_0^{2l_{1a}} \frac{S_a - S_{0a}\cos(\alpha_{1b} - \alpha_{1a})}{(S_a\sin\alpha_{1b} - S_{0a}\sin\alpha_{1a})^2 + (S_a\cos\alpha_{1b} - S_{0a}\cos\alpha_{1a})^2} \rho_{1a}(S_{0a})dS_{0a} \\
&- \Gamma \int_0^{2l_{1a}} \frac{S_a + S_{0a}\cos(\alpha_{1a} + \alpha_{1b})}{(S_a\sin\alpha_{1b} - S_{0a}\sin\alpha_{1a})^2 + (S_a\cos\alpha_{1b} + S_{0a}\cos\alpha_{1a})^2} \rho_{1a}(S_{0a})dS_{0a} \\
&+ \int_0^{2l_{1b}} R_{1b,1b}(S_b; S_{0b})\rho_{1b}(S_{0b})dS_{0b} + \int_0^{2l_2} R_{1b,2}(S_b; z_0)\rho_2(z_0)dz_0 \\
&+ \int_0^{2l_{1b}} R_{1b,1a}(S_b; S_{0a})\rho_{1a}(S_{0a})dS_{0a}
\end{aligned}$$

$$\begin{aligned}
\frac{2\pi}{\mu_2}\Delta\sigma_2(z) = &\int_0^{2l_2} \frac{\rho_2(z_0)dz_0}{z - z_0} + \Gamma \int_{-1}^{+1} \frac{\rho_2(z_0)dz_0}{z + z_0} \\
&- \frac{2}{1+m} \int_0^{2l_{1a}} \frac{z + S_{0a}\cos\alpha_{1a}}{S_{0a}^2 \sin^2\alpha_{1a} + (z + S_{0a}\cos\alpha_{1a})^2} \rho_{1a}(S_{0a})dS_{0a} \\
&- \frac{2}{1+m} \int_0^{2l_{1b}} \frac{z + S_{0b}\cos\alpha_{1b}}{S_{0b}^2 \sin^2\alpha_{1b} + (z + S_{0b}\cos\alpha_{1b})^2} \rho_{1b}(S_{0b})dS_{0b} \\
&+ \int_0^{2l_{1a}} R_{2,1a}(z; S_{0a})\rho_{1a}(S_{0a})dS_{0a} + \int_0^{2l_{1b}} R_{2,1b}(z; S_{0b})\rho_{1b}(S_{0b})dS_{0b} \\
&+ \int_0^{2l_2} R_{22}(z; z_0)\rho_2(z_0)dz_0
\end{aligned}$$

The terms present in the last raw of each integral equation are regular (Fredholm kernels), in fact these terms describe the effects induced by the presence of the free surface. Letting

$H \longrightarrow +\infty$ these integrals tend to 0, therefore the system so obtained describe the case of two half-spaces welded at the interface. Furthermore, if we consider the adimensional variables

$$\begin{cases} \xi_{1a} = \dfrac{S_a - l_{1a}}{l_{1a}} \\ \xi'_{1a} = \dfrac{S_{0a} - l_{1a}}{l_{1a}} \end{cases} \qquad \begin{cases} \xi_{1b} = \dfrac{S_b - l_{1b}}{l_{1b}} \\ \xi'_{1b} = \dfrac{S_{0b} - l_{1b}}{l_{1b}} \end{cases} \qquad \begin{cases} \xi_2 = \dfrac{z - l_2}{l_2} \\ \xi'_2 = \dfrac{z_0 - l_2}{l_2} \end{cases} \tag{5.15}$$

the system can be rewritten in the following way

$$\begin{aligned}
\frac{2\pi}{\mu_1}\Delta\sigma_{1a}(\xi_{1a}) &= \int_{-1}^{+1} \frac{\rho_{1a}(\xi'_{1a})d\xi'_{1a}}{\xi_{1a} - \xi'_{1a}} \\
&- \Gamma \int_{-1}^{+1} \frac{(\xi_{1a}+1) + (\xi'_{1a}+1)\cos(2\alpha_{1a})}{(\xi_{1a} - \xi'_{1a})^2 \sin^2\alpha_{1a} + (\xi_{1a} + \xi'_{1a} + 2)^2 \cos^2\alpha_{1a}} \rho_{1a}(\xi'_{1a})d\xi'_{1a} \\
&- \frac{2m}{1+m} \int_{-1}^{+1} \frac{\dfrac{l_{1a}}{l_2}(\xi_{1a}+1) + (\xi'_2+1)\cos\alpha_{1a}}{\left(\dfrac{l_{1a}}{l_2}\right)^2 (\xi_{1a}+1)^2 \sin^2\alpha_{1a} + \left(\dfrac{l_{1a}}{l_2}(\xi_{1a}+1)\cos\alpha_{1a} + (\xi'_2+1)\right)^2} \rho_2(\xi'_2)d\xi'_2 \\
&+ \int_{-1}^{+1} \frac{\dfrac{l_{1a}}{l_{1b}}(\xi_{1a}+1) - (\xi'_{1b}+1)\cos(\alpha_{1a} - \alpha_{1b})}{\left(\dfrac{l_{1a}}{l_{1b}}(\xi_{1a}+1)\sin\alpha_{1a} - (\xi'_{1b}+1)\sin\alpha_{1b}\right)^2 + \left(\dfrac{l_{1a}}{l_{1b}}(\xi_{1a}+1)\cos\alpha_{1a} - (\xi'_{1b}+1)\cos\alpha_{1b}\right)^2} \rho_{1b}(\xi'_{1b})d\xi'_{1b} \\
&- \Gamma \int_{-1}^{+1} \frac{\dfrac{l_{1a}}{l_{1b}}(\xi_{1a}+1) + (\xi'_{1b}+1)\cos(\alpha_{1a} + \alpha_{1b})}{\left(\dfrac{l_{1a}}{l_{1b}}(\xi_{1a}+1)\sin\alpha_{1a} - (\xi'_{1b}+1)\sin\alpha_{1b}\right)^2 + \left(\dfrac{l_{1a}}{l_{1b}}(\xi_{1a}+1)\cos\alpha_{1a} + (\xi'_{1b}+1)\cos\alpha_{1b}\right)^2} \rho_{1b}(\xi'_{1b})d\xi'_{1b}
\end{aligned}$$

$$\begin{aligned}
\frac{2\pi}{\mu_1}\Delta\sigma_{1b}(\xi_{1b}) &= \int_{-1}^{+1} \frac{\rho_{1b}(\xi'_{1b})d\xi'_{1b}}{\xi_{1a} - \xi'_{1b}} \\
&- \Gamma \int_{-1}^{+1} \frac{(\xi_{1b}+1) + (\xi'_{1b}+1)\cos(2\alpha_{1b})}{(\xi_{1b} - \xi'_{1b})^2 \sin^2\alpha_{1b} + (\xi_{1b} + \xi'_{1b} + 2)^2 \cos^2\alpha_{1b}} \rho_{1b}(\xi'_{1b})d\xi'_{1b} \\
&- \frac{2m}{1+m} \int_{-1}^{+1} \frac{\dfrac{l_{1b}}{l_2}(\xi_{1b}+1) + (\xi'_2+1)\cos\alpha_{1b}}{\left(\dfrac{l_{1b}}{l_2}\right)^2 (\xi_{1b}+1)^2 \sin^2\alpha_{1b} + \left(\dfrac{l_{1b}}{l_2}(\xi_{1b}+1)\cos\alpha_{1b} + (\xi'_2+1)\right)^2} \rho_2(\xi'_2)d\xi'_2 \\
&+ \int_{-1}^{+1} \frac{\dfrac{l_{1b}}{l_{1a}}(\xi_{1b}+1) - (\xi'_{1a}+1)\cos(\alpha_{1b} - \alpha_{1a})}{\left(\dfrac{l_{1b}}{l_{1a}}(\xi_{1b}+1)\sin\alpha_{1b} - (\xi'_{1a}+1)\sin\alpha_{1a}\right)^2 + \left(\dfrac{l_{1b}}{l_{1a}}(\xi_{1b}+1)\cos\alpha_{1b} - (\xi'_{1a}+1)\cos\alpha_{1a}\right)^2} \rho_{1a}(\xi'_{1a})d\xi'_{1a} \\
&- \Gamma \int_{-1}^{+1} \frac{\dfrac{l_{1b}}{l_{1a}}(\xi_{1b}+1) + (\xi'_{1a}+1)\cos(\alpha_{1a} + \alpha_{1b})}{\left(\dfrac{l_{1b}}{l_{1a}}(\xi_{1b}+1)\sin\alpha_{1b} - (\xi'_{1a}+1)\sin\alpha_{1a}\right)^2 + \left(\dfrac{l_{1b}}{l_{1a}}(\xi_{1b}+1)\cos\alpha_{1b} + (\xi'_{1a}+1)\cos\alpha_{1a}\right)^2} \rho_{1a}(\xi'_{1a})d\xi'_{1a}
\end{aligned}$$

$$\begin{aligned}
\frac{2\pi}{\mu_2}\Delta\sigma_2(\xi_2) &= \int_{-1}^{+1} \frac{\rho_2(\xi'_2)d\xi'_2}{\xi_2 - \xi'_2} + \Gamma \int_{-1}^{+1} \frac{\rho_2(\xi'_2)d\xi'_2}{\xi_2 + \xi'_2 + 2} \\
&- \frac{2}{1+m} \int_{-1}^{+1} \frac{\dfrac{l_2}{l_{1a}}(\xi_2+1) + (\xi'_{1a}+1)\cos\alpha_{1a}}{(\xi'_{1a}+1)^2 \sin^2\alpha_{1a} + \left(\dfrac{l_2}{l_{1a}}(\xi_2+1) + (\xi'_{1a}+1)\cos\alpha_{1a}\right)^2} \rho_{1a}(\xi'_{1a})d\xi'_{1a} \\
&- \frac{2}{1+m} \int_{-1}^{+1} \frac{\dfrac{l_2}{l_{1b}}(\xi_2+1) + (\xi'_{1b}+1)\cos\alpha_{1b}}{(\xi'_{1b}+1)^2 \sin^2\alpha_{1b} + \left(\dfrac{l_2}{l_{1b}}(\xi_2+1) + (\xi'_{1b}+1)\cos\alpha_{1b}\right)^2} \rho_{1b}(\xi'_{1b})d\xi'_{1b}
\end{aligned} \tag{5.16}$$

The integral equations can be written in this compact way

$$\frac{2\pi}{\mu_1}\Delta\sigma_{1a}(\xi_{1a}) = {I_1}^{1a} - \Gamma {I_2}^{1a} - (1-\Gamma)\,{I_3}^{1a} + {I_4}^{1a} - \Gamma {I_5}^{1a} \tag{5.17}$$

$$\frac{2\pi}{\mu_1}\Delta\sigma_{1b}(\xi_{1b}) = {I_1}^{1b} - \Gamma {I_2}^{1b} - (1-\Gamma)\,{I_3}^{1b} + {I_4}^{1b} - \Gamma {I_5}^{1b} \tag{5.18}$$

$$\frac{2\pi}{\mu_2}\Delta\sigma_{2}(\xi_{2}) = {I_1}^{2} + \Gamma {I_2}^{2} - (1+\Gamma)\,{I_3}^{2} - (1+\Gamma)\,{I_4}^{2} \tag{5.19}$$

where

$$\Gamma = \frac{1-m}{1+m}, \qquad m = \frac{\mu_2}{\mu_1} = \frac{1-\Gamma}{1+\Gamma}, \qquad 1-\Gamma = \frac{2m}{1+m}, \qquad 1+\Gamma = \frac{2}{1+m} \tag{5.20}$$

in order to refer more easily to the terms present on second side of both equations.
Now the study of the model proceeds

- we perform an asymptotic study in order to determine the singular nature of the dislocation density (Sec. 5.2)
- we study the relations between the bounded stress drops on the crack sections (Sec. 5.3)
- we search a numerical solution for the system of integral equations (Sec. 5.4)

5.2 Study of asymptotic behaviour

5.2.1 Singularities of ρ at crack tips

In order to obtain the singular behaviour of the dislocation density at crack tips, we generalise to the system of coupled equations (5.16) the method proposed by Erdogan et al. (1973), already described in section 3.3.2 on page 31. The details about the evaluation of the asymptotic behaviour of I integrals are described in appendix 5.2.
The asymptotic evaluation for the integral equations are assigned by the following expressions

$$\begin{aligned}
-\frac{2}{\mu_1}\Delta\sigma_{1a}(\xi) = {} & -R_{1a}(-1)2^{a_{1a}}\cot(\pi b_{1a})\,(\xi+1)^{b_{1a}} + R_{1a}(1)2^{b_{1a}}\cot(\pi b_{1a})\,(1-\xi)^{a_{1a}} \\
& - b_0 R_{1a}(-1)2^{a_{1a}}\frac{1}{\sin(\pi b_{1a})}\,(\xi+1)^{b_{1a}}\cos(2\alpha_{1a}(1+b_{1a})) \\
& - c_0 R_2(-1)2^{a_2}\frac{1}{\sin(\pi b_2)}\left[\frac{l_{1a}}{l_2}\,(\xi+1)\right]^{b_2}\cos(\alpha_{1a}(1+b_{1a})) \\
& - R_{1b}(-1)2^{a_{1b}}\frac{1}{\sin(\pi b_{1b})}\left[\frac{l_{1a}}{l_{1b}}\,(\xi+1)\right]^{b_{1b}}\cos(\pi b_{1b} + (\alpha_{1a}-\alpha_{1b})(1+b_{1b})) \\
& - b_0 R_{1b}(-1)2^{a_{1b}}\frac{1}{\sin(\pi b_{1b})}\left[\frac{l_{1a}}{l_{1b}}\,(\xi+1)\right]^{b_{1b}}\cos((\alpha_{1a}+\alpha_{1b})(1+b_{1b})) \\
& + F_{0a}(\xi) + F_{1a}(\xi) + \hat{F}_{1a}(\xi) + F_{Ia}(\xi) + F_{IIIa}(\xi)
\end{aligned} \tag{5.21}$$

$$
\begin{aligned}
-\frac{2}{\mu_1}\Delta\sigma_{1b}(\xi) = & -R_{1b}(-1)2^{a_{1b}}\cot(\pi b_{1b})\,(\xi+1)^{b_{1b}} + R_{1b}(1)2^{b_{1b}}\cot(\pi b_{1b})\,(1-\xi)^{a_{1b}} \\
& - b_0 R_{1b}(-1)2^{a_{1b}}\frac{1}{\sin(\pi b_{1b})}\,(\xi+1)^{b_{1b}}\cos(2\alpha_{1b}(1+b_{1b})) \\
& - c_0 R_2(-1)2^{a_2}\frac{1}{\sin(\pi b_2)}\left[\frac{l_{1b}}{l_2}\,(\xi+1)\right]^{b_2}\cos(\alpha_{1b}(1+b_{1b})) \\
& - R_{1a}(-1)2^{a_{1a}}\frac{1}{\sin(\pi b_{1a})}\left[\frac{l_{1b}}{l_{1a}}\,(\xi+1)\right]^{b_{1a}}\cos(\pi b_{1a}+(\alpha_{1b}-\alpha_{1a})(1+b_{1a})) \\
& - b_0 R_{1a}(-1)2^{a_{1a}}\frac{1}{\sin(\pi b_{1a})}\left[\frac{l_{1b}}{l_{1a}}\,(\xi+1)\right]^{b_{1a}}\cos((\alpha_{1a}+\alpha_{1b})(1+b_{1a})) \\
& + F_{0b}(\xi) + F_{1b}(\xi) + \hat{F}_{1b}(\xi) + F_{Ib}(\xi) + F_{IIIb}(\xi)
\end{aligned} \tag{5.22}
$$

$$
\begin{aligned}
-\frac{2}{\mu_2}\Delta\sigma_2(\xi) = & -R_2(-1)2^{a_2}\cot(\pi b_2)\,(\xi+1)^{b_2} + R_2(1)2^{b_2}\cot(\pi b_2)\,(1-\xi)^{a_2} \\
& - b_0^{'} R_2(-1)2^{a_2}\frac{1}{\sin(\pi b_2)}\,(\xi+1)^{b_2} \\
& - c_{0a}^{'} R_{1a}(-1)2^{a_{1a}}\frac{1}{\sin(\pi b_{1a})}\left[\frac{l_2}{l_{1a}}\,(\xi+1)\right]^{b_{1a}}\cos(\alpha_{1a}(1+b_{1a})) \\
& - c_{0a}^{'} R_{1b}(-1)2^{a_{1b}}\frac{1}{\sin(\pi b_{1b})}\left[\frac{l_2}{l_{1b}}\,(\xi+1)\right]^{b_{1b}}\cos(\alpha_{1b}(1+b_{1b})) \\
& + G_0(\xi) + G_1(\xi) + \hat{G}_{1a}(\xi) + \hat{G}_{1b}(\xi)
\end{aligned} \tag{5.23}
$$

where

$$
b_0 = \Gamma, \qquad c_0 = \frac{2m}{1+m} = 1-\Gamma, \qquad b_0^{'} = -\Gamma, \qquad c_{0a}^{'} = \frac{2}{1+m} = 1+\Gamma \tag{5.24}
$$

5.2.2 Singularity at $\xi = 1$

To study the singularity of ρ_{1a} in the upper tip of this crack section, we multiply both sides of equation (5.21) by $(1-\xi)^{-a_{1a}}$ and letting $\xi \to 1$ we find

$$
\cot(\pi a_{1a}) = 0 \quad \Longrightarrow \quad a_{1a} = -\frac{1}{2} \tag{5.25}
$$

In the same manner, multiplying both sides of equation (5.22) by $(1-\xi)^{-a_{1b}}$ and considering the limit $\xi \to 1$, we obtain for ρ_{1b}

$$
\cot(\pi a_{1b}) = 0 \quad \Longrightarrow \quad a_{1b} = -\frac{1}{2} \tag{5.26}
$$

Finally, multiplying both sides of equation (5.23) by $(1-\xi)^{-a_2}$ and considering the limit $\xi \to 1$, we obtain for ρ_2

$$\cot(\pi a_2) = 0 \quad \Longrightarrow \quad a_2 = -\frac{1}{2} \tag{5.27}$$

As expected, we have found that the singularity in the crack tips away from the interface is equal to $-\frac{1}{2}$, the value typical for a crack developing in an homogeneous medium.

5.2.3 Singularity at the interface

Multiplying both sides of equation (5.21) by $(\xi+1)^{-b_{1a}}$ and letting $\xi \to -1$, we obtain

$$\begin{aligned}
0 = & -R_{1a}(-1)2^{a_{1a}}\cot(\pi b_{1a}) \\
& - b_0 R_{1a}(-1)2^{a_{1a}}\frac{1}{\sin(\pi b_{1a})}\cos(2\alpha_{1a}(1+b_{1a})) \\
& - c_0 R_2(-1)2^{a_2}\frac{1}{\sin(\pi b_2)}\left(\frac{l_{1a}}{l_2}\right)^{b_2}(\xi+1)^{b_2-b_{1a}}\cos(\alpha_{1a}(1+b_{1a})) \\
& - R_{1b}(-1)2^{a_{1b}}\frac{1}{\sin(\pi b_{1b})}\left(\frac{l_{1a}}{l_{1b}}\right)^{b_{1b}}(\xi+1)^{b_{1b}-b_{1a}}\cos(\pi b_{1b}+(\alpha_{1a}-\alpha_{1b})(1+b_{1b})) \\
& - b_0 R_{1b}(-1)2^{a_{1b}}\frac{1}{\sin(\pi b_{1b})}\left(\frac{l_{1a}}{l_{1b}}\right)^{b_{1b}}(\xi+1)^{b_{1b}-b_{1a}}\cos((\alpha_{1a}+\alpha_{1b})(1+b_{1b}))
\end{aligned} \tag{5.28}$$

In order that (5.28) can be satisfied the following two inequalities must be fulfilled

$$b_2 \leq b_{1a}, \quad b_{1b} \leq b_{1a} \tag{5.29}$$

In the same manner, multiplying both sides of equation (5.22) by $(\xi+1)^{-b_{1b}}$ and considering the limit $\xi \to -1$, we obtain

$$\begin{aligned}
0 = & -R_{1b}(-1)2^{a_{1b}}\cot(\pi b_{1b}) \\
& - b_0 R_{1b}(-1)2^{a_{1b}}\frac{1}{\sin(\pi b_{1b})}\cos(2\alpha_{1b}(1+b_{1b})) \\
& - c_0 R_2(-1)2^{a_2}\frac{1}{\sin(\pi b_2)}\left(\frac{l_{1b}}{l_2}\right)^{b_2}(\xi+1)^{b_2-b_{1b}}\cos(\alpha_{1b}(1+b_{1b})) \\
& - R_{1a}(-1)2^{a_{1a}}\frac{1}{\sin(\pi b_{1a})}\left(\frac{l_{1b}}{l_{1a}}\right)^{b_{1a}}(\xi+1)^{b_{1a}-b_{1b}}\cos(\pi b_{1a}+(\alpha_{1b}-\alpha_{1a})(1+b_{1a})) \\
& - b_0 R_{1a}(-1)2^{a_{1a}}\frac{1}{\sin(\pi b_{1a})}\left(\frac{l_{1b}}{l_{1a}}\right)^{b_{1a}}(\xi+1)^{b_{1a}-b_{1b}}\cos((\alpha_{1a}+\alpha_{1b})(1+b_{1a}))
\end{aligned} \tag{5.30}$$

To satisfy the previous equation the following inequalities must be fulfilled

$$b_2 \leq b_{1b}, \quad b_{1a} \leq b_{1b} \tag{5.31}$$

Finally, multiplying both sides of equation (5.23) by $(\xi+1)^{-b_2}$ and letting $\xi \to -1$, we obtain

$$\begin{aligned}
0 = & -R_2(-1)2^{a_2}\cot(\pi b_2) \\
& - b_0^{'} R_2(-1)2^{a_2}\frac{1}{\sin(\pi b_2)} \\
& - c_{0a}^{'} R_{1a}(-1)2^{a_{1a}}\frac{1}{\sin(\pi b_{1a})}\left(\frac{l_2}{l_{1a}}\right)^{b_{1a}}(\xi+1)^{b_{1a}-b_2}\cos(\alpha_{1a}(1+b_{1a})) \\
& - c_{0a}^{'} R_{1b}(-1)2^{a_{1b}}\frac{1}{\sin(\pi b_{1b})}\left(\frac{l_2}{l_{1b}}\right)^{b_{1b}}(\xi+1)^{b_{1b}-b_2}\cos(\alpha_{1b}(1+b_{1b}))
\end{aligned} \tag{5.32}$$

The following two inequalities must be fulfilled in order that previous equation can be satisfied

$$b_{1a} \leq b_2, \quad b_{1b} \leq b_2 \tag{5.33}$$

Considering all the inequalities found, we conclude that

$$b_{1a} = b_{1b} = b_2 = \omega \tag{5.34}$$

The stress drop on the crack surface near the interface must be bounded, therefore we have to impose on each crack section that the sum of singular terms must vanish, and in this way we obtain the following system

$$\begin{aligned}
&\left(\frac{l_2}{l_{1a}}\right)^{\omega}\left[\cos(\pi\omega)+\Gamma\cos(2\alpha_{1a}(1+\omega))\right]R_{1a}(-1) \\
&\quad+\left(\frac{l_2}{l_{1b}}\right)^{\omega}\left[\cos(\pi\omega+(\alpha_{1a}-\alpha_{1b})(1+\omega))+\Gamma\cos((\alpha_{1a}+\alpha_{1b})(1+\omega))\right]R_{1b}(-1) \\
&\quad+(1-\Gamma)\cos(\alpha_{1a}(1+\omega))R_2(-1)=0
\end{aligned} \tag{5.35}$$

$$\begin{aligned}
&\left(\frac{l_2}{l_{1a}}\right)^{\omega}\left[\cos(\pi\omega+(\alpha_{1b}-\alpha_{1a})(1+\omega))+\Gamma\cos((\alpha_{1a}+\alpha_{1b})(1+\omega))\right]R_{1a}(-1) \\
&\quad+\left(\frac{l_2}{l_{1b}}\right)^{\omega}\left[\cos(\pi\omega)+\Gamma\cos(2\alpha_{1b}(1+\omega))\right]R_{1b}(-1) \\
&\quad+(1-\Gamma)\cos(\alpha_{1b}(1+\omega))R_2(-1)=0
\end{aligned} \tag{5.36}$$

$$\begin{aligned}
&\left(\frac{l_2}{l_{1a}}\right)^{\omega}(1+\Gamma)\cos(\alpha_{1a}(1+\omega))R_{1a}(-1) \\
&\quad+\left(\frac{l_2}{l_{1b}}\right)^{\omega}(1+\Gamma)\cos(\alpha_{1b}(1+\omega))R_{1b}(-1) \\
&\quad+\left[\cos(\pi\omega)-\Gamma\right]R_2(-1)=0
\end{aligned} \tag{5.37}$$

In order to have non-vanishing solutions $(R_{1a}(-1), R_{1b}(-1), R_2(-1) \neq 0)$ the determinant of the system must vanish. We can perform this calculation numerically and surprisingly we find that the determinant is identically equal to zero. Therefore we deduce that raws of the matrix are linearly dependent. With respect to the fault bending model, we cannot identify a value for ω and so this parameter still remains undetermined.
First we consider the case $\alpha_{1a} = \alpha_{1b}$; it's easy to verify that equations (5.35),(5.36) become identicals, so we have to consider the following system

$$\left(\frac{l_2}{l_{1a}}\right)^{\omega} [\cos(\pi\omega) + \Gamma\cos(2\alpha(1+\omega))]\, R_{1a}(-1) + \left(\frac{l_2}{l_{1b}}\right)^{\omega} [\cos(\pi\omega) + \Gamma\cos(2\alpha(1+\omega))]\, R_{1b}(-1) + (1-\Gamma)\cos(\alpha(1+\omega))R_2(-1) = 0 \tag{5.38}$$

$$\left(\frac{l_2}{l_{1a}}\right)^{\omega} (1+\Gamma)\cos(\alpha(1+\omega))R_{1a}(-1) + \left(\frac{l_2}{l_{1b}}\right)^{\omega} (1+\Gamma)\cos(\alpha(1+\omega))R_{1b}(-1) + [\cos(\pi\omega) - \Gamma]\, R_2(-1) = 0 \tag{5.39}$$

In order to obtain the reduced system, we perform the following transformation

$$L_1 \longrightarrow (1+\Gamma)\cos(\alpha(1+\omega))L_1 - [\cos(\pi\omega) + \Gamma\cos(2\alpha(1+\omega))]\, L_2 \tag{5.40}$$

The first equation can be so expressed

$$-\left\{[\cos(\pi\omega) + \Gamma\cos(2\alpha(1+\omega))] \cdot [\cos(\pi\omega) - \Gamma] - (1-\Gamma^2)\cos^2(\alpha(1+\omega))\right\} R_2(-1) = 0 \tag{5.41}$$

Being $R_2(-1) \neq 0$, the following condition must me satisfied

$$[\cos(\pi\omega) + \Gamma\cos(2\alpha(1+\omega))] \cdot [\cos(\pi\omega) - \Gamma] - (1-\Gamma^2)\cos^2(\alpha(1+\omega)) = 0 \tag{5.42}$$

The reduced system is equivalent to the initial system since

$$(1+\Gamma) = \frac{2}{1+m} > 0, \quad \forall m \in R^+ \tag{5.43}$$

$$\cos(\alpha(1+\omega)) \neq 0, \qquad \forall\omega \in]-1, 0] \tag{5.44}$$

If we divide for $R_2(-1)$, we obtain

$$\frac{1}{R_2(-1)}\left[\left(\frac{l_2}{l_{1a}}\right)^{\omega} R_{1a}(-1) + \left(\frac{l_2}{l_{1b}}\right)^{\omega} R_{1b}(-1)\right] = -\frac{\cos(\pi\omega) - \Gamma}{(1+\Gamma)\cdot\cos(\alpha(1+\omega))} \tag{5.45}$$

Furthermore, if $l_{1a} = l_{1b} = l_1$, we found of course the condition proper to the fault bending model.

$$\frac{R_1(-1)}{R_2(-1)} = \frac{R_{1a}(-1) + R_{1b}(-1)}{R_2(-1)} = -\left(\frac{l_1}{l_2}\right)^{\omega} \frac{\cos(\pi\omega) - \Gamma}{(1+\Gamma)\cdot\cos(\alpha(1+\omega))} \tag{5.46}$$

Now we consider the case $\alpha_{1a} \neq \alpha_{1b} \neq \alpha$ and using the following transformation

$$L_1 \longrightarrow AL_1 + BL_2 - CL_3 \tag{5.47}$$

where

$$A = \cos(\alpha_{1b}(1+\omega)) \left\{ [\cos(\pi\omega) + \Gamma\cos(2\alpha_{1b}(1+\omega))]\,[\cos(\pi\omega) - \Gamma] - (1-\Gamma^2)\cos^2(\alpha_{1b}(1+\omega)) \right\}$$

$$\begin{aligned} B = {} & \cos(\alpha_{1b}(1+\omega))\times \\ & \left\{ (1-\Gamma^2)\cos(\alpha_{1a}(1+\omega))\cos(\alpha_{1b}(1+\omega)) \right. \\ & \left. - [\cos(\pi\omega + (\alpha_{1a} - \alpha_{1b})(1+\omega)) + \Gamma\cos((\alpha_{1a} + \alpha_{1b})(1+\omega))]\,[\cos(\pi\omega) - \Gamma] \right\} \end{aligned}$$

$$\begin{aligned} C = {} & (1-\Gamma)\cos(\alpha_{1b}(1+\omega))\times \\ & \{\cos(\alpha_{1a}(1+\omega))\,[\cos(\pi\omega) + \Gamma\cos(2\alpha_{1b}(1+\omega))] \\ & - \cos(\alpha_{1b}(1+\omega))\,[\cos(\pi\omega + (\alpha_{1a} - \alpha_{1b})(1+\omega)) + \Gamma\cos((\alpha_{1a} + \alpha_{1b})(1+\omega))]\} \end{aligned}$$

we can eliminate the first equation from the linear system. To assure the equivalence of the system so obtained with the initial system, A must not vanish so the following conditions must be satisfied

$$\cos(\alpha_{1b}(1+\omega)) \neq 0, \qquad \forall\omega \in]-1, 0] \tag{5.48}$$

$$[\cos(\pi\omega) + \Gamma\cos(2\alpha_{1b}(1+\omega))]\cdot[\cos(\pi\omega) - \Gamma] - (1-\Gamma^2)\cos^2(\alpha_{1b}(1+\omega)) \neq 0 \tag{5.49}$$

Therefore we have to exclude the value of ω for which a single fracture develops in the upper medium.
It is possible to determinate numerically the roots of equation (Figure 5.2) and we can observe that the same value of ω corresponds to α_{1b} and $-\alpha_{1b}$.
After this premise, we consider the system

$$\begin{aligned} & \left(\frac{l_2}{l_{1a}}\right)^{\omega} [\cos(\pi\omega + (\alpha_{1b} - \alpha_{1a})(1+\omega)) + \Gamma\cos((\alpha_{1a} + \alpha_{1b})(1+\omega))] R_{1a}(-1) \\ & \quad + \left(\frac{l_2}{l_{1b}}\right)^{\omega} [\cos(\pi\omega) + \Gamma\cos(2\alpha_{1b}(1+\omega))]\, R_{1b}(-1) \\ & \quad + (1-\Gamma)\cos(\alpha_{1b}(1+\omega)) R_2(-1) = 0 \end{aligned} \tag{5.50}$$

$$\left(\frac{l_2}{l_{1a}}\right)^{\omega}(1+\Gamma)\cos(\alpha_{1a}(1+\omega))R_{1a}(-1) + \left(\frac{l_2}{l_{1b}}\right)^{\omega}(1+\Gamma)\cos(\alpha_{1b}(1+\omega))R_{1b}(-1) + [\cos(\pi\omega)-\Gamma]\,R_2(-1)=0 \tag{5.51}$$

Being $R_{1a}(-1), R_{1b}(-1), R_2(-1) \neq 0$ we can choose to divide for $R_2(-1)$ obtaining a non-homogeneous linear system whose unknowns are $\frac{R_{1a}(-1)}{R_2(-1)}$ and $\frac{R_{1b}(-1)}{R_2(-1)}$.
This system admits a solution only if the determinant of the associated matrix does not vanish and therefore the following condition must be fulfilled

$$\cos(\alpha_{1b}(1+\omega))\left[\cos(\pi\omega+(\alpha_{1b}-\alpha_{1a})(1+\omega))+\Gamma\cos((\alpha_{1a}+\alpha_{1b})(1+\omega))\right] - \cos(\alpha_{1a}(1+\omega))\left[\cos(\pi\omega)+\Gamma\cos(2\alpha_{1b}(1+\omega))\right]\neq 0 \tag{5.52}$$

The previous equation can be expressed as

$$\sin((\alpha_{1a}-\alpha_{1b})(1+\omega))\cdot[\sin(\pi\omega+\alpha_{1b}(1+\omega))-\Gamma\sin(\alpha_{1b}(1+\omega))]\neq 0 \tag{5.53}$$

Since $\alpha_{1a} \neq \alpha_{1b}$, $\omega = 0$ is the only root of the first factor, but the second factor can have further roots. If we search numerically the roots of equation (5.53) (Figure 5.3), it is possible to identify the roots of the second factor with the roots of (5.42) corresponding to positive values of α_{1b} (Figure 5.2).
Therefore equation (5.42) can be expressed as

$$-[\sin(\pi\omega+\alpha_{1b}(1+\omega))-\Gamma\sin(\alpha_{1b}(1+\omega))]\cdot[\sin(\pi\omega-\alpha_{1b}(1+\omega))+\Gamma\sin(\alpha_{1b}(1+\omega))]=0 \tag{5.54}$$

where if we substitute α_{1b} with $-\alpha_{1b}$ the two factors exchange their identities.
Using Kramer theorem we obtain finally the solution of the system

$$\begin{cases} \dfrac{R_{1a}(-1)}{R_2(-1)} = -\left(\dfrac{l_{1a}}{l_2}\right)^{\omega}\dfrac{\sin(\pi\omega-\alpha_{1b}(1+\omega))+\Gamma\sin(\alpha_{1b}(1+\omega))}{(1+\Gamma)\cdot\sin((\alpha_{1a}-\alpha_{1b})(1+\omega))} \\ \dfrac{R_{1b}(-1)}{R_2(-1)} = +\left(\dfrac{l_{1b}}{l_2}\right)^{\omega}\dfrac{\sin(\pi\omega-\alpha_{1a}(1+\omega))+\Gamma\sin(\alpha_{1a}(1+\omega))}{(1+\Gamma)\cdot\sin((\alpha_{1a}-\alpha_{1b})(1+\omega))} \end{cases} \tag{5.55}$$

5.3 Stress drop condition

In this section we compare again the stress released on each crack section near the interface, but now the target is to determine any condition relating the bounded stress drops $\Delta\sigma_{1a}, \Delta\sigma_{1b}, \Delta\sigma_2$ which must be assigned. The only unknown contributions are the ones given by ${I_{14}}^{1a}, {I_{15}}^{1a}, {I_{14}}^{1b}, {I_{15}}^{1b}$ since the other terms have been already evaluated considering the fault bending model. The details about the calculations performed are summarised in appendix C.3. The following expressions describe the bounded stress drop

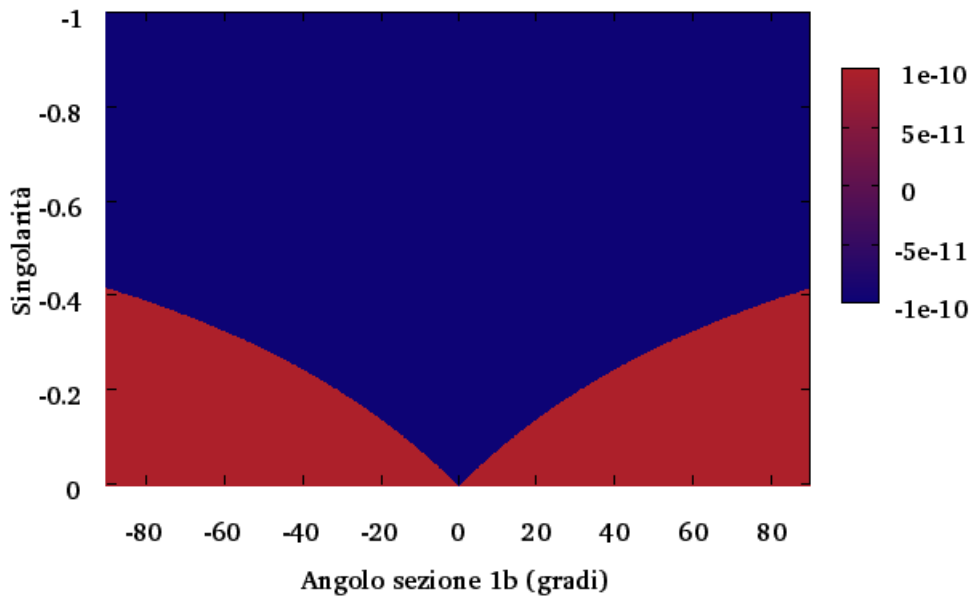

Figure 5.2: Roots of equation (5.42)

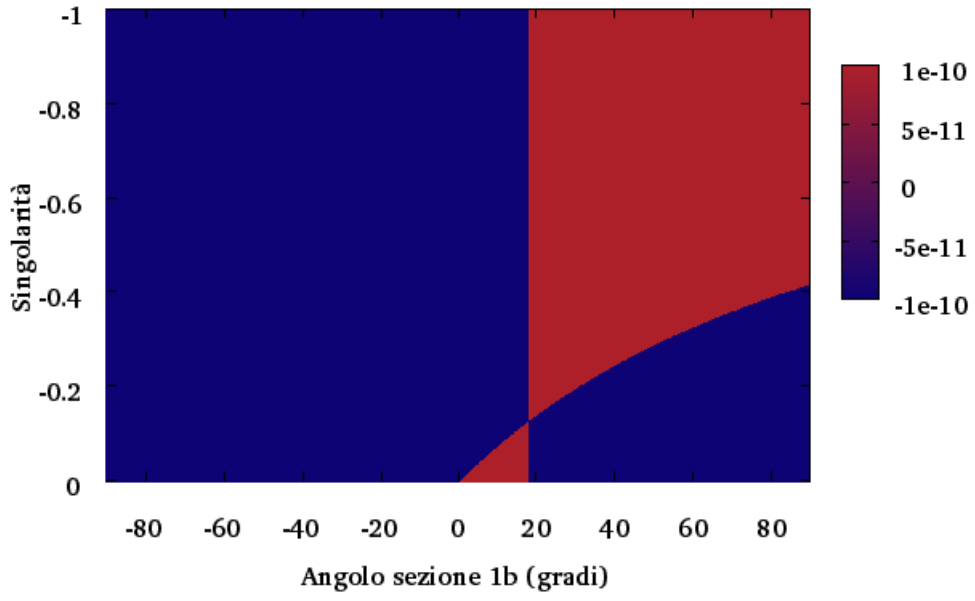

Figure 5.3: Roots of equation (5.53)

on each crack section

$$\frac{2\pi}{\mu_1}\Delta\sigma_{1a}(-1) = [1+\Gamma\cos(2\alpha_{1a})]\,\mathcal{S}_{1a} + (1-\Gamma)\cos\alpha_{1a}\mathcal{S} + [\cos(\alpha_{1a}-\alpha_{1b}) + \Gamma\cos(\alpha_{1a}+\alpha_{1b})]\,\mathcal{S}_{1b} \tag{5.56a}$$

$$\frac{2\pi}{\mu_1}\Delta\sigma_{1b}(-1) = [1+\Gamma\cos(2\alpha_{1b})]\,\mathcal{S}_{1b} + (1-\Gamma)\cos\alpha_{1b}\mathcal{S} + [\cos(\alpha_{1b}-\alpha_{1a}) + \Gamma\cos(\alpha_{1a}+\alpha_{1b})]\,\mathcal{S}_{1a} \tag{5.56b}$$

$$\frac{2\pi}{\mu_2}\Delta\sigma_{2}(-1) = (1-\Gamma)\,\mathcal{S} + (1+\Gamma)\,[\cos\alpha_{1a}\mathcal{S}_{1a} + \cos\alpha_{1b}\mathcal{S}_{1b}] \tag{5.56c}$$

where $\mathcal{S}_{1a}, \mathcal{S}_{1b}, \mathcal{S}$ are respectively

$$\mathcal{S}_{1a} = 2^{-\frac{1}{2}+\omega}\,\Gamma(\omega)\sum_{k=0}^{+\infty}\gamma_k^{(1a)}(-1)^k\frac{\mathbf{\Gamma}(k+1-\frac{1}{2})}{\mathbf{\Gamma}(k+1-\frac{1}{2}+\omega)} \tag{5.57}$$

$$\mathcal{S}_{1b} = 2^{-\frac{1}{2}+\omega}\,\Gamma(\omega)\sum_{k=0}^{+\infty}\gamma_k^{(1b)}(-1)^k\frac{\mathbf{\Gamma}(k+1-\frac{1}{2})}{\mathbf{\Gamma}(k+1-\frac{1}{2}+\omega)} \tag{5.58}$$

$$\mathcal{S} = 2^{-\frac{1}{2}+\omega}\,\Gamma(\omega)\sum_{k=0}^{+\infty}\beta_k(-1)^k\frac{\mathbf{\Gamma}(k+1-\frac{1}{2})}{\mathbf{\Gamma}(k+1-\frac{1}{2}+\omega)} \tag{5.59}$$

The following relations

$$\frac{\gamma_k^{(1a)}}{\beta_k} = -\left(\frac{l_{1a}}{l_2}\right)^{\omega}\frac{\sin(\pi\omega-\alpha_{1b}(1+\omega)) + \Gamma\sin(\alpha_{1b}(1+\omega))}{(1+\Gamma)\cdot\sin((\alpha_{1a}-\alpha_{1b})(1+\omega))} = Q_{1a} \tag{5.60}$$

$$\frac{\gamma_k^{(1b)}}{\beta_k} = +\left(\frac{l_{1b}}{l_2}\right)^{\omega}\frac{\sin(\pi\omega-\alpha_{1a}(1+\omega)) + \Gamma\sin(\alpha_{1a}(1+\omega))}{(1+\Gamma)\cdot\sin((\alpha_{1a}-\alpha_{1b})(1+\omega))} = Q_{1b} \tag{5.61}$$

$$\tag{5.62}$$

are valid for $k \geq 0$ so it is possible to rewrite equations (5.56a),(5.56b),(5.56c) in this form

$$\frac{2\pi}{\mu_1}\Delta\sigma_{1a}(-1) = \mathcal{S}(\omega)\left\{(1-\Gamma)\cos\alpha_{1a} + \frac{1+\Gamma\cos(2\alpha_{1a})}{1+\Gamma}Q_{1a} + \frac{\cos(\alpha_{1a}-\alpha_{1b}) + \Gamma\cos(\alpha_{1a}+\alpha_{1b})}{1+\Gamma}Q_{1b}\right\}$$

$$\frac{2\pi}{\mu_1}\Delta\sigma_{1b}(-1) = \mathcal{S}(\omega)\left\{(1-\Gamma)\cos\alpha_{1b} + \frac{1+\Gamma\cos(2\alpha_{1b})}{1+\Gamma}Q_{1b} + \frac{\cos(\alpha_{1a}-\alpha_{1b}) + \Gamma\cos(\alpha_{1a}+\alpha_{1b})}{1+\Gamma}Q_{1a}\right\}$$

$$\frac{2\pi}{\mu_2}\Delta\sigma_{2}(-1) = \mathcal{S}(\omega)\left\{(1-\Gamma) + \cos\alpha_{1a}\,Q_{1a} + \cos\alpha_{1b}\,Q_{1b}\right\}$$

Considering the following relations

$$\begin{aligned}\frac{1+\Gamma\cos(2\alpha)}{1+\Gamma} &= \frac{1}{1+\Gamma} + \frac{\Gamma}{1+\Gamma}\cos(2\alpha)\\ &= \frac{1+m}{2} + \frac{1-m}{2}\cos(2\alpha)\\ &= \frac{1}{2}(1+\cos(2\alpha)) + \frac{1}{2}(1-\cos(2\alpha))m\\ &= \cos^2\alpha + m\sin^2\alpha\end{aligned} \tag{5.63}$$

$$\begin{aligned}\frac{\cos(\alpha_{1a}-\alpha_{1b})+\Gamma\cos(\alpha_{1a}+\alpha_{1b})}{1+\Gamma} &= \\ &= \frac{1}{1+\Gamma}\cos(\alpha_{1a}-\alpha_{1b})+\frac{\Gamma}{1+\Gamma}\cos(\alpha_{1a}+\alpha_{1b}) \\ &= \left(\frac{1}{1+\Gamma}+\frac{\Gamma}{1+\Gamma}\right)\cos\alpha_{1a}\cos\alpha_{1b}+\left(\frac{1}{1+\Gamma}-\frac{\Gamma}{1+\Gamma}\right)\sin\alpha_{1a}\sin\alpha_{1b} \\ &= \cos\alpha_{1a}\cos\alpha_{1b}+m\sin\alpha_{1a}\sin\alpha_{1b}\end{aligned}$$

stress drops on section 1a and 1b can be rewritten in terms of the stress drop corresponding to the vertical section of the crack.

$$\Delta\sigma_{1a}(-1)=\cos\alpha_{1a}\cdot\frac{\Delta\sigma_2(-1)}{m}-\sin\alpha_{1a}\,F_1(\alpha_{1a},\alpha_{1b},m) \tag{5.64}$$

$$\Delta\sigma_{1b}(-1)=\cos\alpha_{1b}\cdot\frac{\Delta\sigma_2(-1)}{m}-\sin\alpha_{1b}\,F_1(\alpha_{1a},\alpha_{1b},m) \tag{5.65}$$

where the function $F_1(\alpha_{1a},\alpha_{1b},m)$ has this form

$$F_1(\alpha_{1a},\alpha_{1b},m)=\frac{\mu_1}{2\pi}\frac{2m}{1+m}\,2^{-\frac{1}{2}+\omega}\,\Gamma(\omega)\cdot G(\alpha_{1a},\alpha_{1b})$$

$$G(\alpha_{1a},\alpha_{1b})=\sin\alpha_{1a}\sum_{k=0}^{+\infty}\gamma_k^{(1a)}(-1)^k\frac{\mathbf{\Gamma}(k+1-\frac{1}{2})}{\mathbf{\Gamma}(k+1-\frac{1}{2}+\omega)}-\sin\alpha_{1b}\sum_{k=0}^{+\infty}\gamma_k^{(1b)}(-1)^k\frac{\mathbf{\Gamma}(k+1-\frac{1}{2})}{\mathbf{\Gamma}(k+1-\frac{1}{2}+\omega)}$$

Relations (5.64),(5.65) are analogues to the condition (4.54) derived considering the fault bending model. $F_1(\alpha,m),F_2(\alpha,m)$ are the σ_{zy} stress components induced by section 1a and section 1b, respectively; so if we consider the case of a purely transform domain, the initial state of stress is

$$\begin{cases}\sigma_{xy}^0=\sigma^0\\ \sigma_{zy}^0=0\end{cases} \tag{5.66}$$

and the stress drop conditions become

$$\frac{\Delta\sigma_{1a}(-1)}{\mu_1}=\cos\alpha_{1a}\,\frac{\Delta\sigma_2(-1)}{\mu_2}, \tag{5.67}$$

$$\frac{\Delta\sigma_{1b}(-1)}{\mu_1}=\cos\alpha_{1b}\,\frac{\Delta\sigma_2(-1)}{\mu_2} \tag{5.68}$$

since no σ_{zy} stress component have to be released and therefore $F_1(\alpha,m),F_2(\alpha,m)$ must vanish. These stress drop conditions can be fulfilled if the stress drop in the upper medium is lower than required for a planar through-going surface. Therefore a vertical dipping strike-slip fault at depth may cross the interface and fault branching can take place within the sedimentary layer, provided that the shallower sections are suitably inclined.

5.4 Numerical solution

The asymptotic study shows that finite stress release is obtained over both crack sections if the exponents are $a_{1a}=a_{1b}=a_2=-\frac{1}{2}$ and $b_{1a}=b_{1b}=b_2=\omega$, but $\omega\in)-1,0]$ is still

undetermined. In order to obtain informations about the singular nature of dislocations density at the interface, here it is useful to adopt a different approach. We choose to use the displacement discontinuity method since this numerical technique can be applied without any previous knowledge about the singular nature at crack tips. Considering Figure 5.4, we observe that no singularity seems to be present at crack tips $\xi = -1$ (the origin of the reference system) and if we perform a more detailed calculation with a higher resolution in proximity of the interface (Figure 5.4) this conclusion is confirmed. Now the indeterminacy of ω can be interpreted from a mathematical point of view. At the interface the dislocation density is not singular, nevertheless the function can be expanded using $P_k(-1/2, \beta)$ polynomials with $\beta \neq 0$, since the only price we pay is a slower convergence. Hereafter we will consider $\omega = 0$.

Now the form of the singular factors suggests expanding $R(\xi)$ in Jacobi polynomials $P_n^{-1/2,0}(\xi)$, which are orthogonal if the weight function $w(\xi) = (1-\xi)^{-1/2}$ is employed.

$$\rho_{1a}(\xi_{1a}) = \frac{1}{\sqrt{1-\xi_{1a}}} \sum_{k=0}^{\infty} c_k P_k^{(-1/2,0)}(\xi_{1a}), \qquad -1 < \xi_{1a} < 1 \tag{5.69a}$$

$$\rho_{1b}(\xi_{1b}) = \frac{1}{\sqrt{1-\xi_{1b}}} \sum_{k=0}^{\infty} d_k P_k^{(-1/2,0)}(\xi_{1b}), \qquad -1 < \xi_{1b} < 1 \tag{5.69b}$$

$$\rho_2(\xi_2) = \frac{1}{\sqrt{1-\xi_2}} \sum_{k=0}^{\infty} e_k P_k^{(-1/2,0)}(\xi_2), \qquad -1 < \xi_2 < 1 \tag{5.69c}$$

Each crack section is open at the interface, therefore we must supply three supplementary conditions in order that the problem may yield a unique solution.

5.4.1 Supplementary conditions

The first supplementary condition is easily derived from the continuity condition of crack slip at the interface between the media.

$$\Delta u_{1a}\left(\xi_{1a} = -1\right) + \Delta u_{1b}\left(\xi_{1b} = -1\right) = \Delta u_2\left(\xi_2 = -1\right)$$
$$\Longrightarrow \quad l_{1a} \int_{-1}^{1} \rho_{1a}(\xi_{1a}^{'}) d\xi_{1a}^{'} + l_{1b} \int_{-1}^{1} \rho_{1b}(\xi_{1b}^{'}) d\xi_{1b}^{'} = l_2 \int_{-1}^{1} \rho_2(\xi_2^{'}) d\xi_2^{'} \tag{5.70}$$

Let us consider the dislocation density ρ_2; Jacobi polynomials in (5.69c) can be expressed in terms of Legendre polynomials using interrelations among orthogonal polynomials

$$P_k^{(-1/2,0)}(\xi_2) = (-1)^k P_k^{(0,-1/2)}(-\xi_2) = (-1)^k C_{2k}^{1/2}(t_2) = (-1)^k P_{2k}(t_2), \qquad t_2 = \sqrt{\frac{1-\xi_2}{2}} \tag{5.71}$$

where $C_k^{(\alpha)}(t)$ are ultraspherical polynomials that, if $\alpha = \frac{1}{2}$, reproduce Legendre polynomials $P_k(t)$. The normalized dislocation density $\rho_2(\xi_2)$ can then be rewritten in the following form

$$\rho_2(t_2) = \frac{1}{t_2} \sum_{k=0}^{\infty} \beta_k P_{2k}(t_2), \qquad -1 < \xi_2 < 1, \qquad 0 < t_2 < 1 \tag{5.72}$$

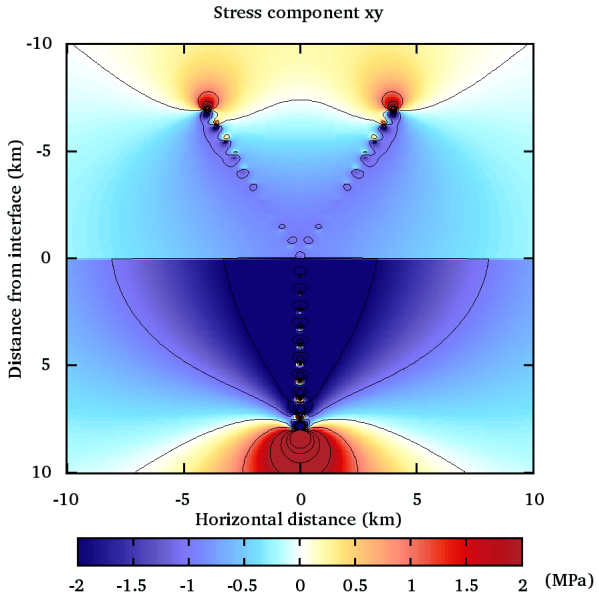

Figure 5.4: Stress component σ_{xy} computed according to the displacement discontinuity method with $N = 10$ boundary elements for each crack section. The calculations have been performed assuming $\alpha_{1a} = 30°$, $\alpha_{1b} = -30°$.

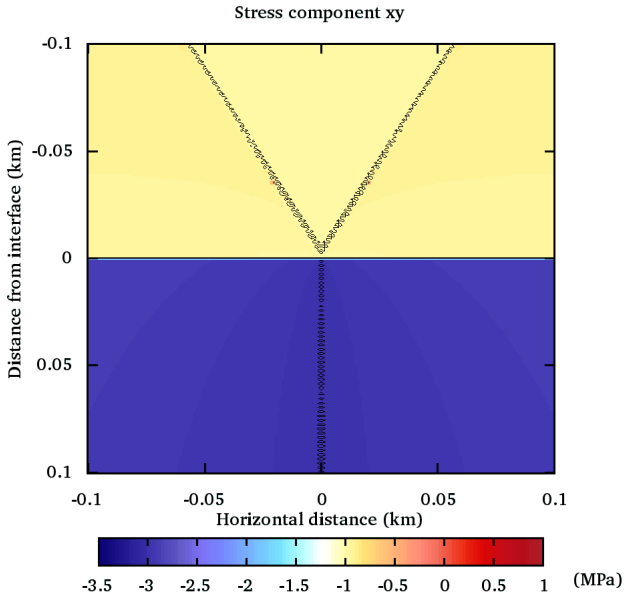

Figure 5.5: Stress component σ_{xy} in the region of 200 m $\times$ 200 m surrounding the intersection of the crack with the interface. The displacement discontinuity method have been applied choosing a more refined distribution of boundary elements near the origin.

where β_k coefficients differ from e_k in equation (5.69c) by a factor of $(-1)^k/\sqrt{2}$. The presence of the singular factor ${t_2}^{-1}$ in equation (5.72) should be of no concern, since ρ_2 always appears through integrals when observable quantities are considered and $d\xi_2 = -4t_2 dt_2$. For instance, if we compute displacement discontinuity Δu_2, we obtain

$$\Delta u_2(\xi_2) = l_2 \int_{-1}^{\xi_2} \rho_2(\xi_2) d\xi_2 + C = 4l_2 \int_{t_2}^{1} \sum_{k=0}^{\infty} \beta_k P_{2k}(t_2) dt + C = -4l_2 \int_{0}^{t_2} \sum_{k=0}^{\infty} \beta_k P_{2k}(t_2) dt \quad (5.73)$$

where, in the last equality, the closure condition $\Delta u_2(\xi_2 = 1)$ has been employed to fix the integration constant C. The slip amplitude at the interface $\xi_2 = -1$ can be easily computed from equation (5.73), using the property that $P_{2k}(t)$ polynomials are even functions and are orthogonal over $(-1, 1)$ to $P_0 = 1$ if $k \neq 0$

$$\Delta u_2(\xi_2 = -1) = -4l_2 \int_{0}^{1} \sum_{k=0}^{\infty} \beta_k P_{2k}(t_2) dt + C = -2l_2 \int_{0}^{t_2} \sum_{k=0}^{\infty} \beta_k \int_{-1}^{1} P_{2k}(t_2) dt = -4l_2 \beta_0 \quad (5.74)$$

Employing the same method, the dislocation densities $\rho_{1a}(\xi_{1a}), \rho_{1b}(\xi_{1b})$ can be written through expansions similar to (5.72)

$$\rho_{1a}(t_{1a}) = \frac{1}{t_{1a}} \sum_{k=0}^{\infty} \gamma_k^{(1a)} P_{2k}(t_{1a}), \qquad -1 < \xi_{1a} < 1, \qquad 0 < t_{1a} < 1 \quad (5.75)$$

$$\rho_{1b}(t_{1b}) = \frac{1}{t_{1b}} \sum_{k=0}^{\infty} \gamma_k^{(1b)} P_{2k}(t_{1b}), \qquad -1 < \xi_{1b} < 1, \qquad 0 < t_{1b} < 1 \quad (5.76)$$

and the crack slip at the interface for section 1a and 1b are respectively

$$\Delta u_{1a}(\xi_{1a} = -1) = -4l_{1a}\gamma_0^{(1a)} \quad (5.77)$$

$$\Delta u_{1b}(\xi_{1b} = -1) = -4l_{1b}\gamma_0^{(1b)} \quad (5.78)$$

So the first supplementary condition assumes this form

$$l_2\beta_0 = l_{1a}\gamma_0^{(1a)} + l_{1b}\gamma_0^{(1b)} \quad (5.79)$$

The other two supplementary conditions are needed to provide finite stress values over the crack plane near the interface ($z = 0$) and for $w = 0$ we have

$$\begin{cases} \dfrac{R_{1a}(-1)}{R_2(-1)} = \dfrac{\rho_{1a}(-1)}{\rho_2(-1)} = m\dfrac{\sin(\alpha_{1b})}{\sin(\alpha_{1a} - \alpha_{1b})} = Q_{1a} \\ \\ \dfrac{R_{1b}(-1)}{R_2(-1)} = \dfrac{\rho_{1b}(-1)}{\rho_2(-1)} = -m\dfrac{\sin(\alpha_{1a})}{\sin(\alpha_{1a} - \alpha_{1b})} = Q_{1b} \end{cases} \quad (5.80)$$

Since $P_{2k}(1)$ and considering equations (5.75),(5.76),(5.72), we obtain a relation between $\gamma_k^{(1a)}, \beta_k$ coefficients and a relation between $\gamma_k^{(1b)}, \beta_k$ coefficients

$$\sum_{k=0}^{\infty} \gamma_k^{(1a)} = Q_{1a} \sum_{k=0}^{\infty} \beta_k \tag{5.81}$$

$$\sum_{k=0}^{\infty} \gamma_k^{(1b)} = Q_{1b} \sum_{k=0}^{\infty} \beta_k \tag{5.82}$$

5.4.2 Method of solution

The following infinite systems

$$\begin{aligned}\frac{\pi^2}{\mu_1}\Delta\sigma_k^{(1a)} =& \sum_{n=0}^{\infty} \gamma_n^{(1a)} R_{11}(k,n) - \Gamma \sum_{n=0}^{\infty} \gamma_n^{(1a)} R_{12}(k,n) - (1-\Gamma) \sum_{n=0}^{\infty} \beta_n R_{13}(k,n) \\ &+ \sum_{n=1}^{\infty} \gamma_n^{(1b)} R_{14}(k,n) - \Gamma \sum_{n=1}^{\infty} \gamma_n^{(1b)} R_{15}(k,n)\end{aligned} \tag{5.83}$$

$$\begin{aligned}\frac{\pi^2}{\mu_1}\Delta\sigma_k^{(1b)} =& \sum_{n=0}^{\infty} \gamma_n^{(1b)} R_{21}(k,n) - \Gamma \sum_{n=0}^{\infty} \gamma_n^{(1b)} R_{22}(k,n) - (1-\Gamma) \sum_{n=0}^{\infty} \beta_n R_{23}(k,n) \\ &+ \sum_{n=1}^{\infty} \gamma_n^{(1a)} R_{24}(k,n) - \Gamma \sum_{n=1}^{\infty} \gamma_n^{(1a)} R_{25}(k,n)\end{aligned} \tag{5.84}$$

$$\begin{aligned}\frac{\pi^2}{\mu_2}\Delta\sigma_k^{(2)} =& \sum_{n=1}^{\infty} \beta_n R_{31}(k,n) + \Gamma \sum_{n=0}^{\infty} \beta_n R_{32}(k,n) - (1+\Gamma) \sum_{n=0}^{\infty} \gamma_n^{(1a)} R_{33}(k,n) \\ &- (1+\Gamma) \sum_{n=0}^{\infty} \gamma_n^{(1b)} R_{34}(k,n)\end{aligned} \tag{5.85}$$

can be obtained following these steps

1. substitution of (5.72),(5.75),(5.76) in the integral equations
2. use of the integral relation (A.5) to perform analytically the first integration
3. each equation have to be multiplied by $U_k\sqrt{1-\xi^2}$ and integrated on the interval $-1, 1$ in the variable ξ

The details about the double integrals $R_{ij}(k,n)$ are described in appendix C.4 on page 142. $\Delta\sigma_k^{(1a)}, \Delta\sigma_k^{(1b)}, \Delta\sigma_k^{(2)}$ are the coefficients of the expansion in U_k polynomials of the stress drops $\Delta\sigma_{1a}, \Delta\sigma_{1b}, \Delta\sigma_2$, respectively. If $\Delta\sigma_{1a}, \Delta\sigma_{1b}, \Delta\sigma_2$ are constants then $\Delta\sigma_k^{(1a)} = \Delta\sigma_k^{(1a)} = \Delta\sigma_k^{(2)} = \Delta\sigma\delta_{k0}$.
In order to provide an approximate solution to the crack problem, the infinite sums in (5.81)-(5.85), are truncated to a finite index N. More specifically, this means that in (5.83)-(5.85) we take

1. $R_{ij}(k,n) = 0$ for $k > N-1 \wedge n > N$
2. $\Delta\sigma_k^{(1a)} = \Delta\sigma_k^{(1b)} = \Delta\sigma_k^{(2)} = 0$ for $k > N-1$

Let $i = k + 1, j = n + 1$, we define the following matrix $(3N) \times (3N + 3)$:

$$\Upsilon = \begin{pmatrix} G_{11} & G_{12} & G_{13} \\ G_{21} & G_{22} & G_{23} \\ G_{31} & G_{32} & G_{33} \end{pmatrix} \tag{5.86}$$

whose elements are the $(N) \times (N + 1)$ matrices

$$\begin{cases} G_{11}(i,j) = \frac{\mu_1}{\pi^2}\left(R_{11}(i-1,j-1) - \Gamma R_{12}(i-1,j-1)\right) \\ G_{12}(i,j) = \frac{\mu_1}{\pi^2}\left(R_{14}(i-1,j-1) - \Gamma R_{15}(i-1,j-1)\right) \\ G_{13}(i,j) = -\frac{\mu_1}{\pi^2}(1-\Gamma)R_{13}(i-1,j-1) \\ G_{21}(i,j) = \frac{\mu_1}{\pi^2}\left(R_{21}(i-1,j-1) - \Gamma R_{22}(i-1,j-1)\right) \\ G_{22}(i,j) = \frac{\mu_1}{\pi^2}\left(R_{24}(i-1,j-1) - \Gamma R_{25}(i-1,j-1)\right) \\ G_{23}(i,j) = -\frac{\mu_1}{\pi^2}(1-\Gamma)R_{23}(i-1,j-1) \\ G_{31}(i,j) = -\frac{\mu_2}{\pi^2}(1+\Gamma)R_{33}(i-1,j-1) \\ G_{32}(i,j) = -\frac{\mu_2}{\pi^2}(1+\Gamma)R_{34}(i-1,j-1) \\ G_{33}(i,j) = \frac{\mu_2}{\pi^2}\left(R_{31}(i-1,j-1) + \Gamma R_{32}(i-1,j-1)\right) \end{cases}$$

In other terms, the matrix Υ_{ij}, with $i = 1, 2, ..., 3N$ and $j = 1, 2, ..., 3N + 3$, is

$$\Upsilon_{ij} = \begin{cases} G_{11}(i,j) & \text{if } (1 \le i \le N) \wedge (1 \le j \le N+1) \\ G_{12}(i, j-(N+1)) & \text{if } (1 \le i \le N) \wedge (N+2 \le j \le 2N+2) \\ G_{13}(i, j-2(N+1)) & \text{if } (1 \le i \le N) \wedge (2N+3 \le j \le 3N+3) \\ G_{21}(i-N, j) & \text{if } (N+1 \le i \le 2N) \wedge (1 \le j \le N+1) \\ G_{22}(i-N, j-(N+1)) & \text{if } (N+1 \le i \le 2N) \wedge (N+2 \le j \le 2N+2) \\ G_{23}(i-N, j-2(N+1)) & \text{if } (N+1 \le i \le 2N) \wedge (2N+3 \le j \le 3N+3) \\ G_{31}(i-2N, j) & \text{if } (2N+1 \le i \le 3N) \wedge (1 \le j \le N+1) \\ G_{32}(i-2N, j-(N+1)) & \text{if } (2N+1 \le i \le 3N) \wedge (N+2 \le j \le 2N+2) \\ G_{32}(i-2N, j-2(N+1)) & \text{if } (2N+1 \le i \le 3N) \wedge (2N+3 \le j \le 3N+3) \end{cases}$$

Furthermore, let η be a column vector with $3N + 3$ components $\gamma_n^{(1a)}, \gamma_n^{(1b)}, \beta_n$

$$\eta = [\gamma_0^{(1a)}, ..., \gamma_N^{(1a)}, \gamma_0^{(1b)}, ..., \gamma_N^{(1b)}, \beta_0, ..., \beta_N]^T \tag{5.87}$$

and let χ be the $3N$ column vector containing the N components of $\Delta\sigma_{1a}$, the N components of $\Delta\sigma_{1b}$ and the N components of $\Delta\sigma_2$

$$\chi = [\Delta\sigma_0^{(1a)}, ..., \Delta\sigma_{N-1}^{(1a)}, \Delta\sigma_0^{(1b)}, ..., \Delta\sigma_{N-1}^{(1b)}, \Delta\sigma_0^{(2)}, ..., \Delta\sigma_{N-1}^{(2)}]^T \tag{5.88}$$

If $\Delta\sigma_{1a}, \Delta\sigma_{1b}, \Delta\sigma_2$ are constants, only the first, the $(N+1)$th and the $(2N+1)$th components of χ do not vanish.
The solution of the truncated problem is given by the following system of $3N$ equations for the $3N+3$ unknowns η_j

$$\chi_i = \sum_{j=1}^{3N+3} \Upsilon_{ij}\eta_j, \qquad i = 1, ..., 3N \tag{5.89}$$

with the supplementary conditions derived from (5.79),(5.81),(5.82)

$$l_{1a}\eta_1 + l_{1a}\eta_{N+2} = l_2\eta_{2N+3} \tag{5.90}$$

$$\sum_{j=1}^{N+1} \eta_j = Q_{1a} \sum_{j=2N+3}^{3N+3} \eta_j \tag{5.91}$$

$$\sum_{j=N+2}^{2N+2} \eta_j = Q_{1b} \sum_{j=2N+3}^{3N+3} \eta_j \tag{5.92}$$

5.4.3 Results

The computations have been performed assuming:

- $\nu_1 = \nu_2 = 0.25$ and $\mu_2 = 3\mu_1 = 30$ GPa
- $2l_1 = 2l_2 = 8$ km for the length of crack sections
- a stepwise constant stress drop profile with $\Delta\sigma_2 = 3$ MPa and
  - $\Delta\sigma_{1a} = \dfrac{\Delta\sigma_2}{m}\cos(\alpha_{1a})$
  - $\Delta\sigma_{1b} = \dfrac{\Delta\sigma_2}{m}\cos(\alpha_{1b})$

In Figure 5.7, we show the stress drop and the crack slip corresponding to the following three cases:

I $\alpha_{1a} = 30, \alpha_{1b} = -30$

II $\alpha_{1a} = 30, \alpha_{1b} = -15$

III $\alpha_{1a} = 30, \alpha_{1b} = +15$

The approximate solutions reproduce with great accuracy the stress drop profile if the infinite sums in $(5.75), (5.76), (5.72)$ are truncated to $N = 10$. In case I (Figure 5.7a) the stress drop over crack section 1a and over crack section 1b have the same value and furthermore Figures 5.7b and Figures 5.7c are identicals since the stress drop on section 1b have the same value in both cases.
As expected, the crack slip on the inclined sections has the same profile when the sections are symmetric with respect to the negative z axis (Figure 5.7b), while in cases II-III the crack slip is significantly affected by the relative position of sections 1a and 1b (Figure 5.7d, Figure 5.7f). First, we can note that the crack slip is split up between section 1a and section 1b so that the major slip is observed on the less inclined section, since the other section feels more the higher rigidity of the lower media (Figure 5.7d). If both sections are in the same quadrant (Figure 5.7e), the effect is amplified so that the crack slip has very different trends on section 1a and on section 1b.

To evaluate the accuracy of the approximate solution found, we show in Figure 4.5 the stress component σ_{xy} computed according to the displacement discontinuity method. The comparison is very satisfactory since the stress map obtained with the boundary element approach is reproduced with great accuracy. Observing the stress maps corresponding to cases I-III (Figure 5.8), we note that when the inclined sections are in opposite quadrants (cases I-II), the release of the σ_{xy} stress component affects a wider region, while in case I the pattern of stress release is similar to that obtained in the case of a single inclined section, where no significant stress release is observed in the opposite quadrant. Further we can observe that the presence of two inclined sections determine a very variable pattern for the stress component σ_{zy}, since this component change of sign at each crack section and in correspondence of the negative z axis.

The method of solution proposed involves the expansion of the dislocation density in Legendre polynomials since we have assumed $\omega = 0$. The asymptotic study shows that the singularity degree can assume all the values in the interval $]-1, 0]$. Therefore a solution can be derived considering another value for ω and in Figure 5.9 we show the stress drop computed according to the expansion of the dislocation density in Chebyshev polynomials, the method used in the previous chapter. As expected, this method of solution has a slower convergence, since now for $N = 10$ (Figure 5.9a) the stress drop is very variable and even increasing the order of truncation to $N = 100$ (Figure 5.9b) the accuracy decreases approaching the interface.

5.5 Conclusions

The model proposed is suitable to describe fault branching in a shallow layer. Strike-slip faulting across a structural discontinuity can be described within the framework of this model when the stress drop in the shallow layer is lower than the value prescribed by the stress drop discontinuity condition proper to a vertical planar crack. In fact two new stress drop conditions have been derived which account for a minor stress drop in the upper layer

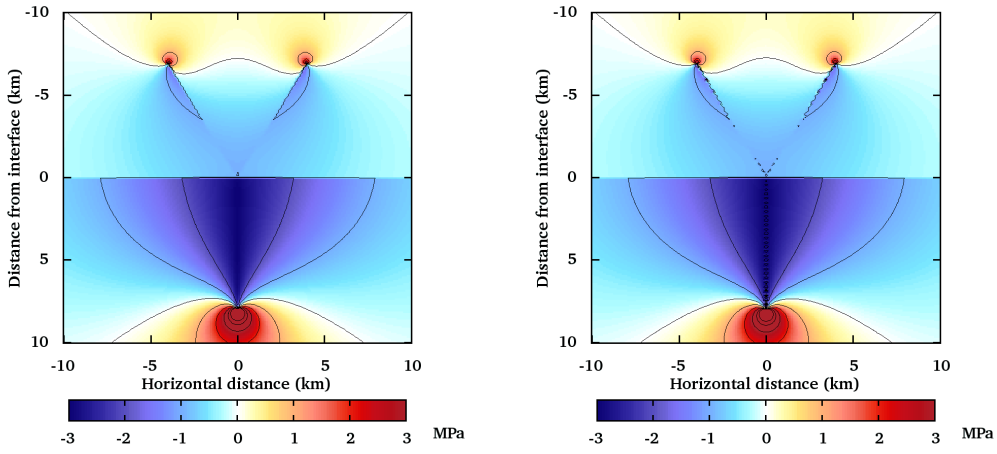

Figure 5.6: Stress

if this sections are suitably inclined.

If an inclined section is already present in the upper layer, as described by the fault bending model (Chapter 4), a second inclined section can develop in order to release further stress in the shallow layer. Such a mechanism is able to describe several field observations regarding the complex pattern of surface fractures associated with major transcurrent tectonic earthquakes.

The study of the asympthotic behaviour leaves the singular degree of the dislocation density undetermined, with $\omega \in]-1, 0]$. This indeterminacy has only a mathematical character and it can be interpreted in terms of a further degree of freedom introduced by the presence of the third crack surface. From a physical point of view, the simplest explanation is that no singularity is present at the interface and in fact this guess is confirmed by results obtained with a boundary element approach.

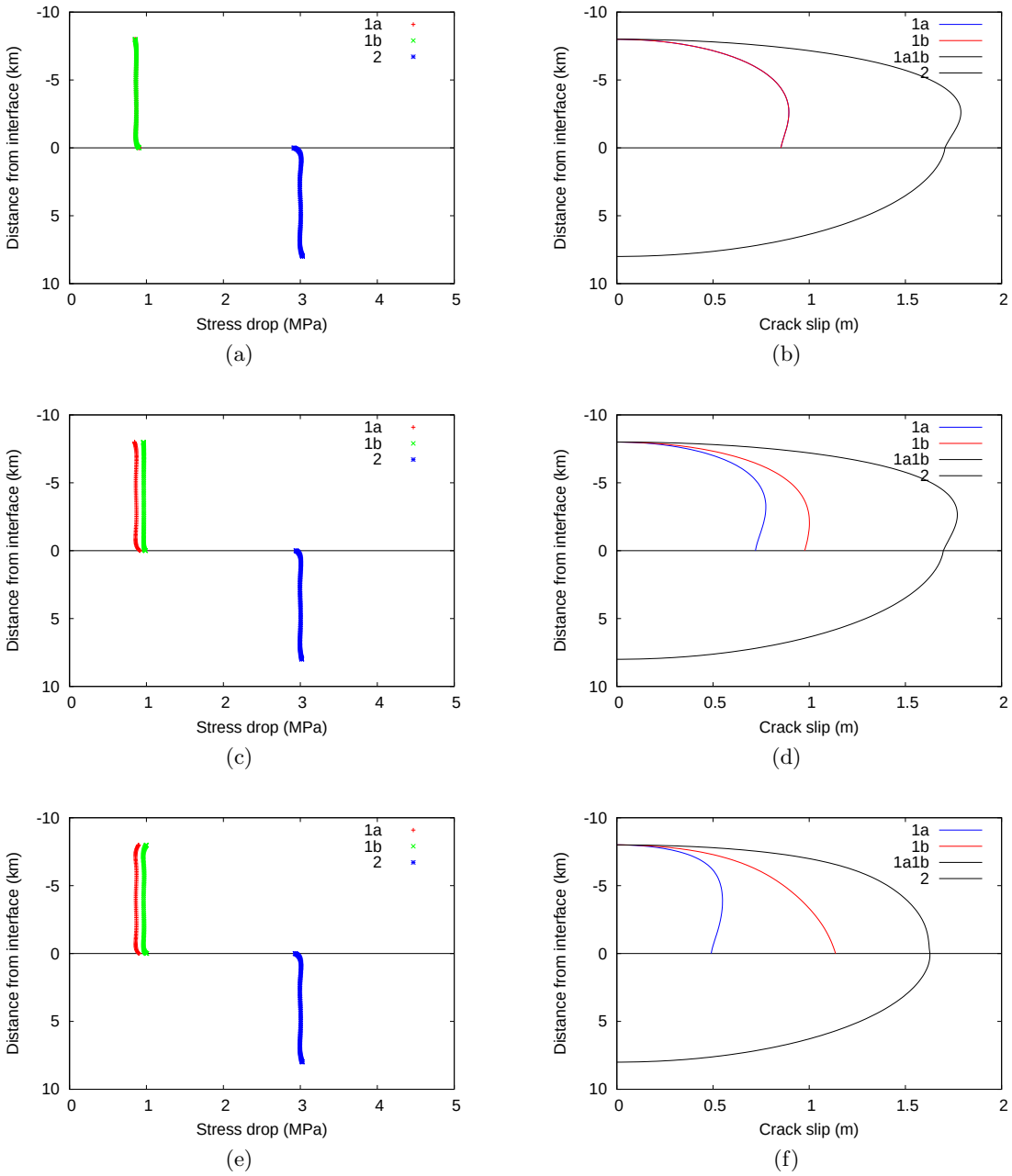

Figure 5.7: Stress drop and crack slip on crack sections

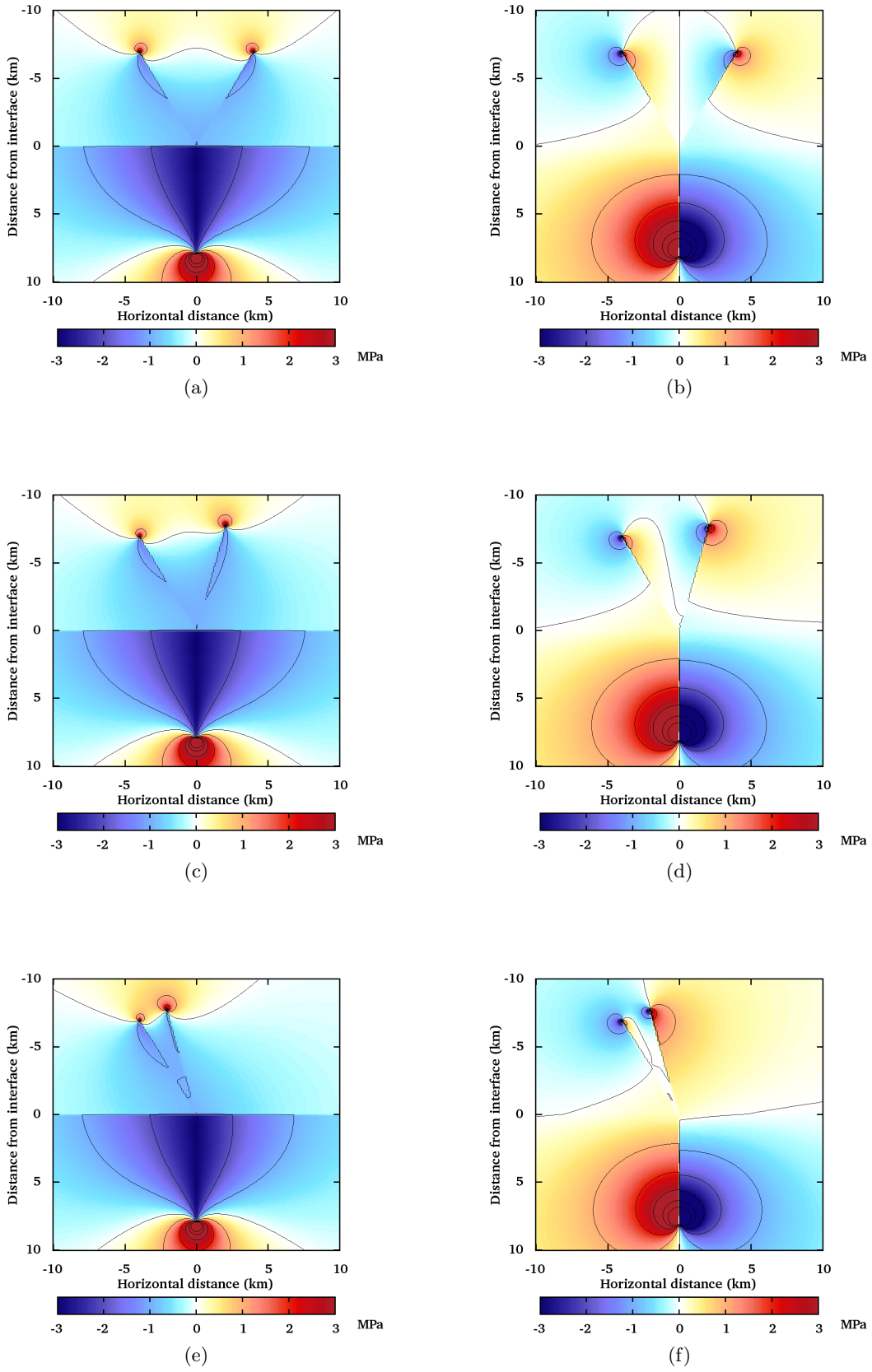

Figure 5.8: Stress maps

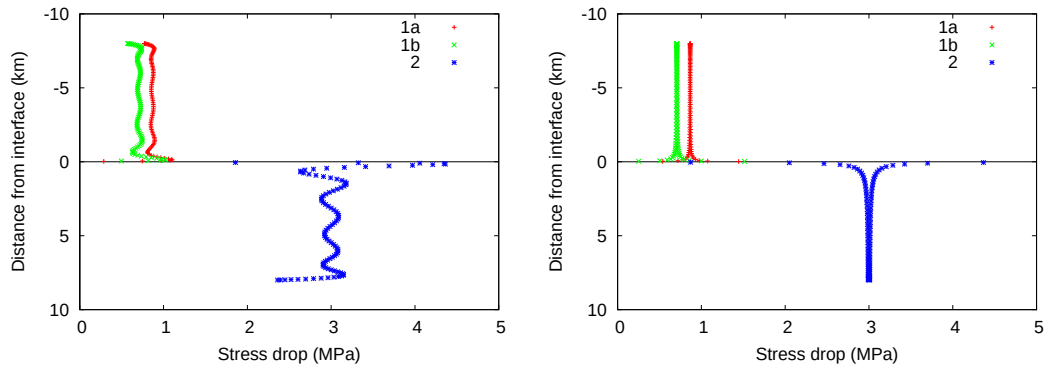

Figure 5.9: Stress drop on crack sections computed according to the expansion in Chebyshev polynomials of the dislocation density

Chapter 6

Modelling of interface unwelding

The models proposed in Chaps. 4-5 are suitable to describe strike-slip faulting in elastic layered media when the stress drop in the shallow layer is lower than prescribed by the stress drop condition proper to a planar crack surface. Instead, if $\Delta\sigma_1/\Delta\sigma_1 > \mu_1/\mu_2$, which may be the case when anelastic processes relax deviatoric stress in layer 2, alternative solutions must be considered. In such a case, one through-going crack cannot fulfil the welded boundary conditions and unwelding of the interface may take place. We have solved this problem within the theory of fracture mechanics, employing the boundary element method.

6.1 Model description

We consider a system in which a shallow elastic layer is separated by a thin plastic layer from the deeper brittle crust. The low rigidity upper layer can represent a sedimentary deposit, while the ductile layer can represent a solidified lava flow subjected to anelastic deformation. The release of stress in the plastic layer may determine the decoupling between the shallow layer and the deeper crust. Neglecting the thickness of the plastic layer, this decoupling can be described in terms of the unwelding of the interface between the layer and a lower half-space (Figure 6.1).

The origin of the reference system is at the free surface and the interface between the shallow layer and the half-space is at the depth H. A deviatoric stress field proper to a transform domain is imposed at remote distance, with a compressive component (-1 MPa) in direction SW, and a tensile component (+1 MPa) acting NW. An antiplane strain configuration is considered, in which the only non-vanishing component of the displacement field is $u_y(x, z)$, which is independent of the coordinate y, so the only non-vanishing components induced by crack slip are σ_{xy}, σ_{zy} and the principle axis of the stress tensor remain unchanged, being the bisectors of the quadrants in the xy plane (Figure 6.2). The main fault (MF) considered is a transcurrent dextral fault and the unwelding is described in terms of two horizontal dislocations ($hd+, hd-$), slipping in opposite directions, at the interface from $x = l_1$ to $x = l_2$ and from $x = -l_2$ to $x = -l_1$ (Figure 6.1). In order

to determine l_1, l_2, the σ_{zy} stress component induced by the MF are compared with the frictional threshold $f(\rho_r - \rho_w)gH$. The dimension of the unwelded region is studied in terms of the model parameter.

In order to compute the stress components σ_{xy}, σ_{zy} we use the expressions given by Rybicki (1971) for a long vertical strike-slip fault and the expressions for an inclined strike-slip fault in a layered media (Singh et al., 1994). To identify the stress components we use the following notation

$$(\sigma_{ij})_{1,2}^{I,II}(x, z; x_0, z_0) \tag{6.1}$$

where

- x, z is the point where the component is evaluated
- x_0, z_0 identify the position of a dislocation line parallel to the y axis
- i, j are used to identify the stress component σ_{xy}, σ_{zy}
- I, II tell us if the dislocation is in the upper layer or in the half-space
- $1, 2$ indicates if the component is pertinent to the layer or to the lower half-space

Horizontal dislocation

$$(\sigma_{xy})_1^I(x, z; x_0, z_0) = \frac{\mu_1}{2\pi}\left\{\frac{z - z_0}{R^2} - \frac{z + z_0}{S^2} + \sum_{n=1}^{\infty}\Gamma^n\left[-\frac{z + z_0 - 2nH}{T^2} + \frac{z - z_0 + 2nH}{V^2} + \frac{z - z_0 - 2nH}{U^2} - \frac{z + z_0 + 2nH}{W^2}\right]\right\} \tag{6.2}$$

$$(\sigma_{zy})_1^I(x, z; x_0, z_0) = -\frac{\mu_1}{2\pi}(x - x_0)\left\{\frac{1}{R^2} - \frac{1}{S^2} + \sum_{n=1}^{\infty}\Gamma^n\left[-\frac{1}{T^2} + \frac{1}{V^2} + \frac{1}{U^2} - \frac{1}{W^2}\right]\right\} \tag{6.3}$$

$$(\sigma_{xy})_2^I(x, z; x_0, z_0) = \frac{\mu_2}{2\pi}\frac{2}{1 + m}\left\{\frac{z - z_0}{R^2} - \frac{z + z_0}{S^2} + \sum_{n=1}^{\infty}\Gamma^n\left[\frac{z - z_0 + 2nH}{V^2} - \frac{z + z_0 + 2nH}{W^2}\right]\right\} \tag{6.4}$$

$$(\sigma_{zy})_2^I(x, z; x_0, z_0) = -\frac{\mu_2}{2\pi}\frac{2}{1 + m}(x - x_0)\left\{\frac{1}{R^2} - \frac{1}{S^2} + \sum_{n=1}^{\infty}\Gamma^n\left[\frac{1}{V^2} - \frac{1}{W^2}\right]\right\} \tag{6.5}$$

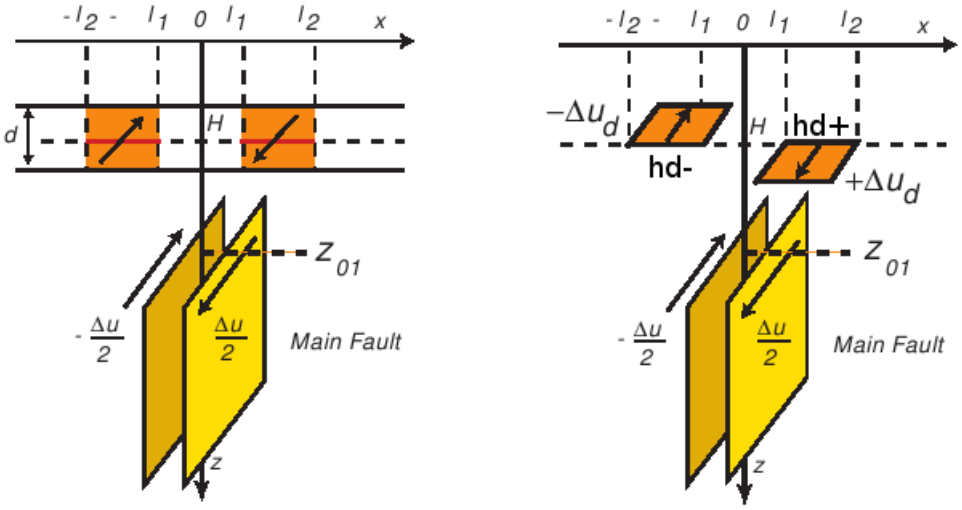

Figure 6.1: Sketch of the model

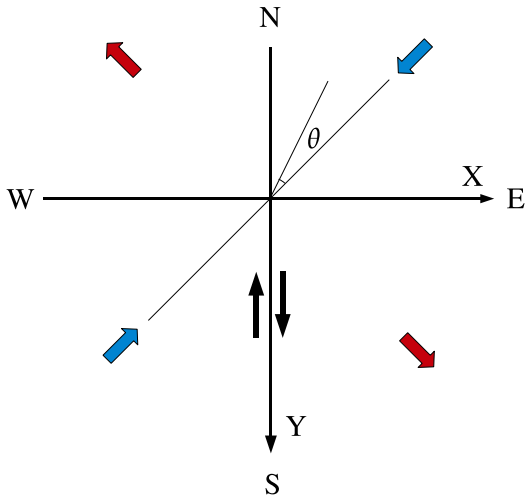

Figure 6.2: Orientation of the optimal plane

where

$$\begin{cases} R^2 = (x-x_0)^2 + (z-z_0)^2 \\ S^2 = (x-x_0)^2 + (z+z_0)^2 \\ T^2 = (x-x_0)^2 + (z+z_0-2nH)^2 \\ U^2 = (x-x_0)^2 + (z-z_0-2nH)^2 \\ V^2 = (x-x_0)^2 + (z-z_0+2nH)^2 \\ W^2 = (x-x_0)^2 + (z+z_0+2nH)^2 \end{cases} \tag{6.6}$$

Vertical dislocation

$$(\sigma_{xy})_1^{II}(x,z;x_0,z_0) = \\ = -\frac{\mu_1}{2\pi}\frac{2m}{1+m}\sum_{n=0}^{\infty}\Gamma^n\left(\frac{z-z_0-2nH}{(x-x_0)^2+(z-z_0-2nH)^2} - \frac{z+z_0+2nH}{(x-x_0)^2+(z+z_0+2nH)^2}\right) \tag{6.7}$$

$$(\sigma_{zy})_1^{II}(x,z;x_0,z_0) = \\ = \frac{\mu_1}{2\pi}\frac{2m}{1+m}\sum_{n=0}^{\infty}\Gamma^n\left(\frac{x-x_0}{(x-x_0)^2+(z-z_0-2nH)^2} - \frac{x-x_0}{(x-x_0)^2+(z+z_0+2nH)^2}\right) \tag{6.8}$$

$$(\sigma_{xy})_2^{II}(x,z;x_0,z_0) = \\ = -\frac{\mu_2}{2\pi}\left[\frac{z-z_0}{(x-x_0)^2+(z-z_0)^2} + \Gamma\frac{z+z_0-2H}{(x-x_0)^2+(z+z_0-2H)^2}\right. \\ \left. -\frac{4m}{(1+m)^2}\sum_{n=0}^{\infty}\Gamma^n\frac{z+z_0+2nH}{(x-x_0)^2+(z+z_0+2nH)^2}\right] \tag{6.9}$$

$$(\sigma_{zy})_2^{II}(x,z;x_0,z_0) = \\ = \frac{\mu_2}{2\pi}\left[\frac{x-x_0}{(x-x_0)^2+(z-z_0)^2} + \Gamma\frac{x-x_0}{(x-x_0)^2+(z+z_0-2H)^2}\right. \\ \left. -\frac{4m}{(1+m)^2}\sum_{n=0}^{\infty}\Gamma^n\frac{x-x_0}{(x-x_0)^2+(z+z_0+2nH)^2}\right] \tag{6.10}$$

6.1.1 Opening of secondary fractures

To study if the unwelding can determine the opening of secondary shear fractures we compute the *Coulomb failure function*

$$CFF = |\tau| + f(\sigma_n + p) \tag{6.11}$$

where

- τ, shear stress
- f, friction coefficient

- σ_n, normal stress
- $p = \rho_w g z$, pore pressure

The modified Coulomb failure criterion states that opening of shear fractures takes place on the plane where the traction overcomes the frictional threshold. In presence of friction the optimal plane is not the one where the shear stress is highest. The orientation of this plane is influenced by the normal stress acting on its surface, since a tensile stress reduces friction. Considering a bidimensional state of stress, the orientation of the vertical plane is identified by θ (Figure 6.2), the angle formed by the plane with the compressive axis

$$\theta = \frac{1}{2}\arctan(1/f) \qquad \text{(Turcotte et al., 2002)} \tag{6.12}$$

If $f = 0$ we have $\theta = \frac{\pi}{4}$, so the optimal plane agrees with the plane where the shear traction is highest; if $f >> 1$ we have $\theta \simeq 0$, so the opening of secondary shear fractures will be favoured on the plane normal to tensile principle stress, because on this plane the effect of friction is reduced.
To study if unwelding can determine the opening of tensile fractures, we compute instead the *maximum opening stress* (MOS), which is defined as the principle tensile stress σ_3 of the stress tensor given by the sum of lithostatic stress and the stress change induced by the MF and the two horizontal dislocations $hd+, hd-$.

6.2 Volterra dislocations

The easier way to model the main fault and the horizontal dislocations is to use Volterra dislocations; this is an oversimplified approach, nevertheless it is useful since it can be used to determine some informations about the behaviour of the system. In fact this model will be used to obtain a fir ts estimate for

1. the distance between the MF upper tip and the interface in order that unwelding can effectively take place
2. the extension of the two unwelded regions
3. the entity Δu_d of the unwelding

To estimate Δu_d, we have considered the point on the interface where the stress component σ_{zy} induced by the MF takes its maximum value and we have determined the slip of the horizontal dislocation necessary to release the stress in excess with respect to the threshold value.
Computations have been performed assuming:

- $\Delta u_s = 1$ m
- $m = \mu_2/\mu_1 = 3$ with $\mu_2 = 10$ GPa

f	H (m)	z_{01} (m)	l_1 (m)	l_2 (m)	Δu_d (m)
0.2	0.02	0.05	0.1	307.5	0.37
,,	,,	0.1	0.9	401.8	0.46
,,	,,	0.15	3.3	455.6	0.68
,,	,,	0.2	8.1	481.9	0.88
,,	0.1	0.15	0.9	429.8	0.41
,,	,,	0.2	3.8	475.6	0.33
,,	,,	0.25	9.5	505.0	0.26
,,	,,	0.3	18.8	529.8	0.21
0.84	0.02	0.05	0.4	190.8	0.35
,,	,,	0.1	3.7	238.1	0.35
,,	,,	0.15	13.8	253.8	0.30
,,	,,	0.2	36.4	245.8	0.13
,,	0.1	0.15	3.6	254.7	0.32
,,	,,	0.2	16.2	261.2	0.16
,,	,,	0.25	43.6	245.7	0.05
,,	,,	0.3	114.2	182.3	0.00

Table 6.1: Trends of Δu_d,l_1,l_2 as function of f, H, z_{01} when $MF, hd+, hd-$ are modelled as Volterra dislocations

- $\rho = 2300$ kg/m^3, if $z < 500$ m, $\rho = 2600$ kg/m^3, if $z > 500$ m
- $p(z) = \rho_w g z$, hydrostatic trend for pore pressure
- $z_{02} = 12$ km, depth of the MF lower tip

In table 6.1, we report the trends of Δu_d, l_1, l_2 for different values of the model parameters f, H, z_{01}. Observing the results summarised in the table, we can see that the dimensions of the unwelded regions are substantially controlled by the coefficient of friction. In fact the increase of friction from 0.2 to 0.84 determines an increase of friction threshold that approximately halves the width of the unwelded region. Further we see that complete unwelding takes place before the MF touche the interface. This result can be explained in terms of the unphysical strong singularities that effects the stress induced by Volterra dislocations. We must conclude that more realistic models are necessary in order to study the conditions for unwelding.

6.3 Somigliana dislocations

A more realistic way to model the main fault (MF) and the horizontal dislocations ($hd+, hd-$) is to use Somigliana dislocations, which are characterised by a non-uniform displacement discontinuity over the dislocation surface. Here we assume that the MF is characterised by a uniform stress drop and that unwelding takes place with variable slip in order to release stress in excess of the frictional threshold. To solve the inverse dislocation problem we use the displacement discontinuity method. The implementation of this numerical technique involves the decomposition of MF, $hd+$ and $hd-$ in boundary

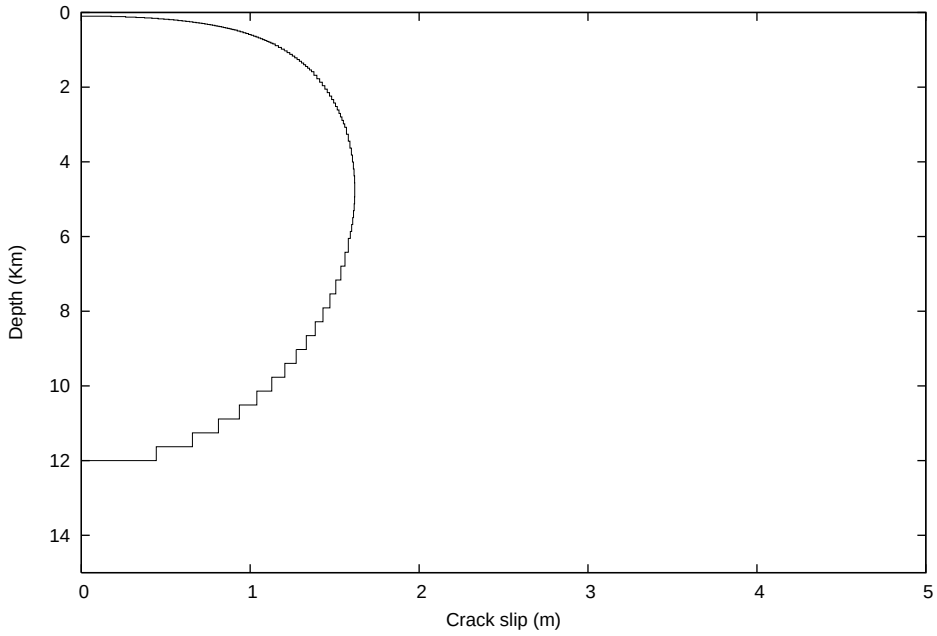

Figure 6.3: Non-uniform decomposition in boundary elements

elements. An uniform decomposition is not suitable for the system we consider since we want to evaluate the stress induced in the thin ($\sim 10^2$ m) shallow layer, but to obtain a sufficiently detailed solution, the boundary elements near the interface must be sufficiently small. In fact the result obtained with the displacement discontinuity method have a non-uniform resolution, which is optimal in the regions far from the boundary, while in the near-field the solution obtained is not representative. Since the MF is very long ($\sim 10^4$ m), than a very refined decomposition ($N \sim 10^4$ boundary elements) is necessary in order that the solution can have the required resolution in the region of interest. The implementation of the uniform decomposition is quite simple, but the required number of boundary elements imply a too long computational time. Therefore we have chosen to adopt a non-uniform decomposition. The boundary elements are selected according to an algorithm that increases the density of these elements approaching the interface. In this way we obtain the best resolution in the shallow layer, since the length of each boundary element is selected according to its distance from the interface (Figure 6.3).

Two different approaches have been considered describing the MF and the two horizontal dislocations $hd+, hd-$ as Somigliana dislocations

Case I in the first approach we neglect the back-interaction exerted by $hd+, hd-$ on the

MF

$$t^i_{s+} = -\Delta t^i_{s+} = \sum_{j=1}^{M} A^{ij}_{s+s+} D^j_{s+} + \sum_{j=1}^{M} A^{ij}_{s+s-} D^j_{s-}$$
$$t^i_{s-} = -\Delta t^i_{s-} = \sum_{j=1}^{M} A^{ij}_{s-s+} D^j_{s+} + \sum_{j=1}^{M} A^{ij}_{s-s-} D^j_{s-}$$
$$i = 1, ..., M$$

where

$$\begin{cases} \Delta t^i_{s+} = t^i_{s+} - f(\rho - \rho_w) g h \\ \Delta t^i_{s-} = -(t^i_{s-} - f(\rho - \rho_w) g h) \end{cases}$$

$\Delta t^i_{s+}, \Delta t^i_{s+}$ are the amounts of σ_{zy} stress component that overcome the frictional threshold on i-th boundary of $hd+$ and $hd-$, respectively. $A^{ij}_{s+s+}, A^{ij}_{s+s-}, A^{ij}_{s-s+}, A^{ij}_{s-s-}$ are $(M \times M)$ matrix containing the influence coefficients of the traction that are computed according to equations (6.2)-(6.5).

Case II in the second approach the effect of the back-interaction is considered

$$t^i_{s+} = -\Delta t^i_{s+} = \sum_{j=1}^{M} A^{ij}_{s+s+} D^j_{s+} + \sum_{j=1}^{M} A^{ij}_{s+s-} D^j_{s-} + \sum_{k=1}^{N} A^{ik}_{s+s} D^j_s$$
$$t^i_{s-} = -\Delta t^i_{s-} = \sum_{j=1}^{M} A^{ij}_{s-s+} D^j_{s+} + \sum_{j=1}^{M} A^{ij}_{s-s-} D^j_{s-} + \sum_{k=1}^{N} A^{ik}_{s-s} D^j_s$$
$$t^i_s = -\Delta t^i_s = \sum_{j=1}^{M} A^{kj}_{ss+} D^j_{s+} + \sum_{j=1}^{M} A^{kj}_{ss-} D^j_{s-} + \sum_{k=1}^{N} A^{kk}_{ss} D^j_s$$
$$i = 1, ..., M$$
$$k = 1, ..., N$$

where

$$\begin{cases} \Delta t^i_{s+} = -f(\rho - \rho_w) g h & 1 \le i \le M \\ \Delta t^i_{s-} = f(\rho - \rho_w) g h) & 1 \le i \le M \\ \Delta t^k_s = \Delta\sigma & 1 \le k \le N \end{cases}$$

$\Delta t^i_{s+}, \Delta t^i_{s-}$ are the frictional threshold on the i-th boundary element of $hd+$ and $hd-$,respectively and Δt^k_s is the uniform stress drop imposed on each boundary elementary of the MF. $A^{ij}_{s+s+}, A^{ij}_{s+s-}, A^{ij}_{s-s+}, A^{ij}_{s-s-}$ are $(M \times M)$ matrices and $A^{ik}_{ss+}, A^{ik}_{ss-}$ are $(N \times M)$ containing the influence coefficients of the traction that are computed according to equations (6.2)-(6.5). $A^{ki}_{s+s}, A^{ki}_{s+s}$ are $(M \times N)$ matrices and A^{kk}_{ss} is a $(N \times N)$ matrix, containing the influence coefficients of the traction that are computed according to equations (6.7)-(6.10).

f	H (m)	z_{01} (m)	l_1 (m)	l_2 (m)
0.2	0.02	0.02	0.0	401.1
,,	,,	0.05	0.3	458.7
,,	,,	0.1	2.9	481.1
,,	,,	0.15	10.0	483.6
,,	0.1	0.1	0.0	478.1
,,	,,	0.15	2.9	499.8
,,	,,	0.2	11.5	495.8
,,	,,	0.25	27.6	484.8
0.84	0.02	0.02	0.0	200.3
,,	,,	0.05	1.2	223.8
,,	,,	0.1	12.2	217.9
,,	,,	0.15	49.6	178.1
,,	0.1	0.1	0.0	250.7
,,	,,	0.15	12.7	225.0
,,	,,	0.2	63.5	165.5
,,	,,	0.25	x	x

Table 6.2: Trends of l_1,l_2 as function of f, H, z_{01} when $MF, hd+, hd-$ are modelled as Somigliana dislocations

Of course, it's easy to predict that the accuracy of the results obtained with the first approach decreases when the MF approaches the interface, since the back-interaction is stronger. Therefore we expect that the results obtained with the two methods coincide until the MF is sufficiently far from the interface, while they should differ substantially when the MF touches the interface. Computations have been performed assuming:

- $\Delta\sigma = 1$ MPa
- $m = \mu_2/\mu_1 = 3$ with $\mu_2 = 10$ GPa
- $\rho = 2300$ kg/m^3, if $z < 500$ m, $\rho = 2600$ kg/m^3, if $z > 500$ m
- $p(z) = \rho_w g z$, hydrostatic trend for pore pressure
- $z_{02} = 12$ km, depth of the MF lower tip

We have studied the dependence from the following parameters of the stress induced in the shallow layer:

- f, frictional coefficient
- H, depth of the interface
- z_{01}, depth of the upper tip of the MF.

In Table 6.2, we show the computed values for l_1, l_2 for different reference configurations when back-interaction is considered (Case II). In the last raw, x indicates that unwelding does not take place since the frictional threshold has not been exceeded. Observing the results summarised in Table 6.2, first we can remark that the extension of the unwelding

region is very similar to that predicted by the Volterra dislocation model. Secondly we can observe that complete unwelding takes place only when the MF touches the interface. Somigliana model reproduces the result obtained with the Volterra model and furthermore it permits to describe unwelding in a more correct way, since the solutions obtained are no more affected by unphysical singularities. We consider now Figure 6.4, where results corresponding to Case I and Case II are compared. As expected, if the MF terminates at the interface, the results obtained with the two different approaches differ substantially. In fact, if back-interaction is neglected (Case I), the behaviour of the system is not reproduced correctly, since the three crack considered are closed at the contact point of the MF with the interface (left column of Figure 6.4a). Instead, if back-interaction is not neglected (Case II), the cracks are all open in this point and furthermore the condition of continuity of crack-slip is automatically satisfied (right column of Figure 6.4a). In Figure 6.4b, both the shear stress induced separately by the MF and the horizontal dislocations, and the total shear stress induced in the upper layer are shown. Comparing again the results pertinent to Case I and Case II, we see that the stress concentration below the interface is very high and localized in a narrow region if back-interaction is neglected and we must remark that this feature is very difficult to reconcile with observations. Instead, if back-interaction is considered, a wide stripe of high and nearly uniform shear stress develops above the welded interface, whose width is controlled by the extension of unwelding. Below the interface we don't observe any concentration of stress and so we overcome the problem met neglecting back-interaction.

The opening of secondary fractures in the upper medium is possible only when the MF touches the interface, since a concentration of deviatoric stress above the interface is observed only when complete unwelding takes place. In Figure 6.3, the results for the total shear stress (XY total), for the Coulomb failure function (CFF) and for the maximum opening stress (MOS) are shown. The calculations are performed on the optimal oriented plane and two different values for the friction coefficient are considered, (a) $f = 0.2$ and (b) $f = 0.84$. The orientation of the optimal plane can be calculated using the relation (6.12). For $f = 0.2$ the optimal plane makes an angle $\alpha_1 = \frac{\pi}{4} - \theta_1 = 5.7°$ with the strike direction (NS) of the main fault, while for $f = 0.84$ this plane makes an angle $\alpha_2 = \frac{\pi}{4} - \theta_2 = 20°$ with the same direction (broken lines in Figure 6.3a).

The results for the CFF and the MOS are similar to those obtained for the total induced stress, since they assume their highest values (~ 10 MPa) only above the unwelded interface (Figures 6.3b-6.3c). If we assume ~ 1 MPa as minimum values for the tensile strength of surface rocks, we observe that the opening of open fractures is confined in the shallow layer, since below the interface the maximum opening stress vanishes. In order to study shear failure, we assume instead $C_0 = 2$ MPa, where C_0 is the cohesion value in shear. The shear failure is expected when the CFF overcomes the rock cohesion value. Observing Figures 6.3b-6.3c, we conclude that shear fractures can develop only above the unwelding region, as already observed for the open fractures. As final remark, we observe that the width of the region where secondary (shear and open) fractures can develop is controlled

only by the value of the friction coefficient.

6.4 Conclusions

The model proposed in this chapter provides preliminary insight into the problem of a blind strike-slip fault terminating within a plastic media above it. The presence of the plastic layer can be used to model the presence of an intermediate layer (pyroclastic material) that decouples a surface brittle layer (lava fields) from the deeper brittle crust. Anelastic deformation in the plastic layer keeps the deviatoric stress below a frictional threshold and deformation takes place at a constant deviatoric stress. In this case the models presented in Chapters 4-5 are not suitable to describe the behaviour of the system since $\Delta\sigma_1/\Delta\sigma_1 > \mu_1/\mu_2$ and so we guess that unwelding can take place. The modelling results suggest that in order to have unwelding the main fault must terminate at shallow depth (< 100 m) and against the interface (or within ~ 100 m below it). This result can be simply interpreted in terms of the effect induced by lithostatic stress. Deeper it is the interface, higher it is the frictional threshold to overcome. Therefore the stress induced by the main fault is able to overcome the frictional threshold only when its upper tip arrives in proximity of the surface. When unwelding takes place the main fault does not break directly to the surface since stress diffuses laterally above the unwelded surface. In this context, the model proposed can be interpreted as a generalization of the fault branching model, since the two unwelding regions ($hd+, hd-$) can be considered as two inclined sections that develop on the interface when the main fault cannot break in the shallow layer. The effect of the unwelding is a redistribution of stress, which determines high deviatoric stress over a wide region in the shallow layer. The study of the Coulumb failure function and of the maximum opening stress has shown than open fractures and shear fractures may open in the shallow layer up to 500 m off-strike from the main fault and further the maximum depth of these secondary surface fractures is confined above the unwelding interface.

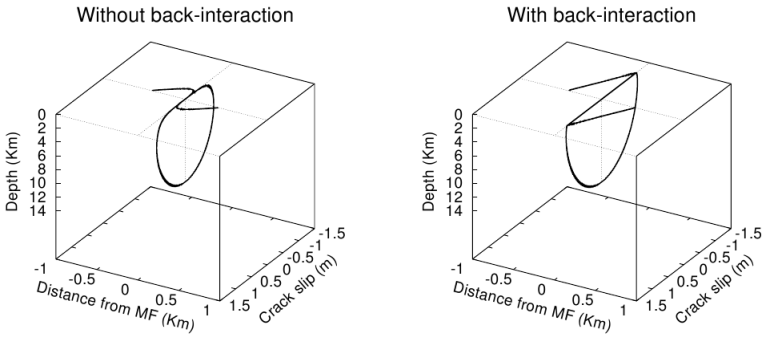
Without back-interaction
With back-interaction
Depth (Km)
Distance from MF (Km)
Crack slip (m)

(a)

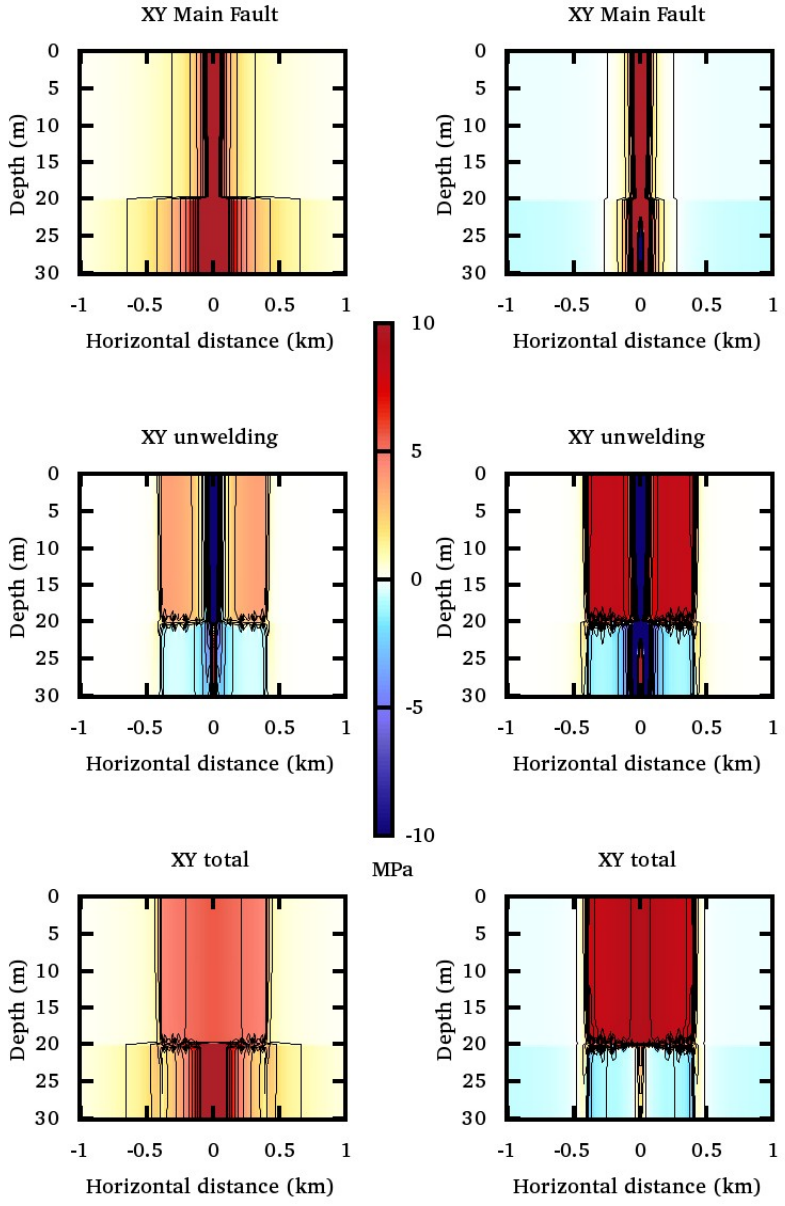
XY Main Fault
XY Main Fault
XY unwelding
XY unwelding
XY total
XY total
Depth (m)
Horizontal distance (km)
MPa
10
5
0
-5
-10

(b)

Figure 6.4

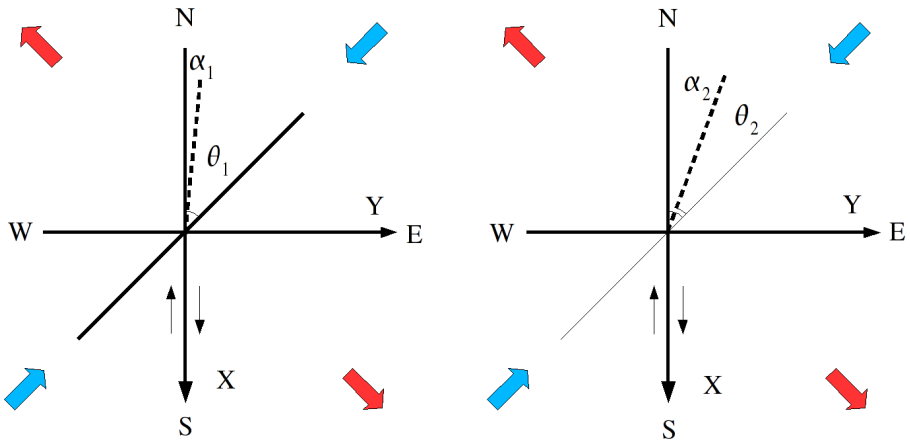
N
α1
θ1
W
Y
E
X
S
N
α2
θ2
W
Y
E
X
S

(a)

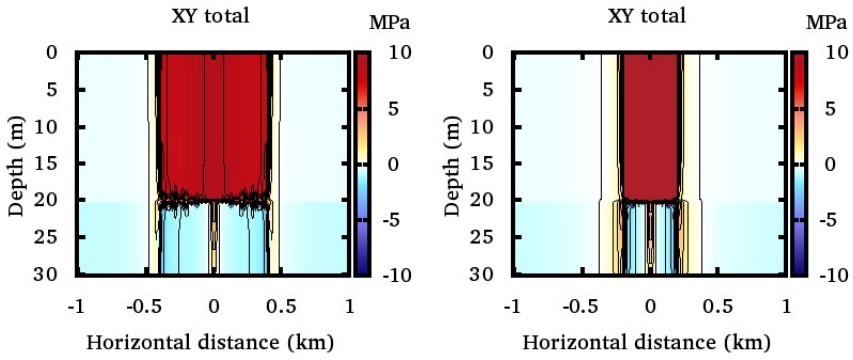
XY total
MPa
Depth (m)
Horizontal distance (km)
XY total
MPa
Depth (m)
Horizontal distance (km)

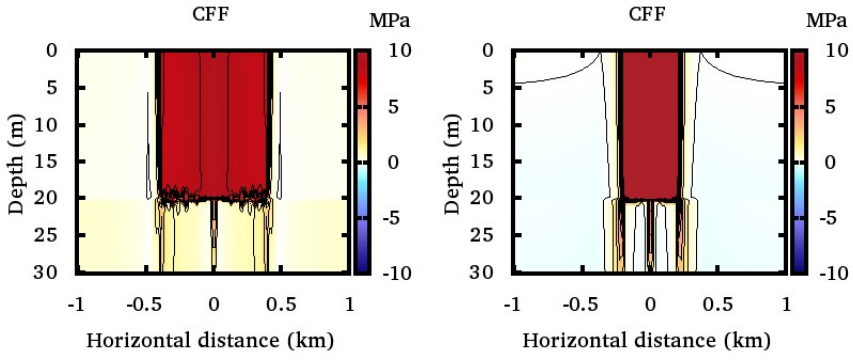
CFF
MPa
Depth (m)
Horizontal distance (km)
CFF
MPa
Depth (m)
Horizontal distance (km)

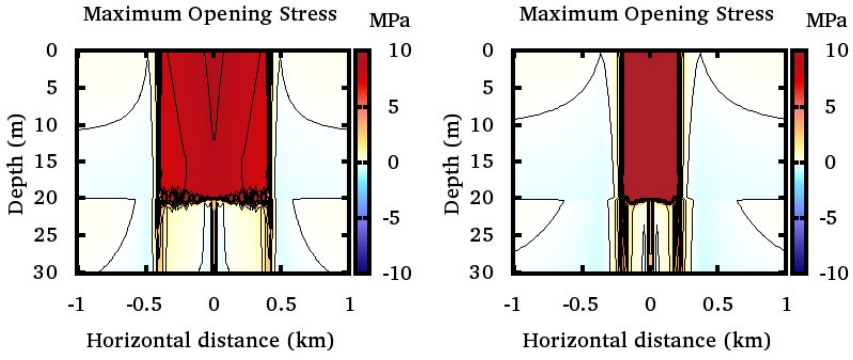
Maximum Opening Stress
MPa
Depth (m)
Horizontal distance (km)
Maximum Opening Stress
MPa
Depth (m)
Horizontal distance (km)

(b) (c)

Chapter 7

Conclusions

The study of crustal heterogeneities is important in order to achieve a better understanding of fault processes and in this work two different types of these heterogeneities have been considered.

The first type involves the concept of asperity, briefly introduced in Section 1.1 on page 1, and here applied to interpret the anomalous features of the $M_s = 6.6$ earthquake of June 17-th, 2000 in the South Iceland Seismic Zone. The type of asperity invoked to explain these feature is different from the usual concept of asperity used in seismology. The common feature of previous asperity models was the interpretation of such a heterogeneity as a "strong" region, whose rupture determines a high moment release. In our context, instead, the presence of the asperity is suggested not only to explain the high magnitude of the earthquake with respect to the estimated fault dimensions, but also the change of seismicity pattern before and after the mainshock. The study of the first model (Elastic model) has confirmed that the presence of a structural discontinuity in the form of a spherical inclusion was able to explain both the intriguing features associated with the mainshock. Nevertheless, the nature of the asperity as a structural discontinuity is not supported by tomographic studies in the SISZ and so this have imposed a more elaborated discussion about the nature of the asperity. From this discussion we have elaborated a model (Viscoelastic model) in which the asperity must not be considered as a permanent feature of the fault zone, since it is the result of a formation process in which high pressure fluids ascending from the brittle-ductile transition play a preeminent role. The asperity must be considered as a low fractured region surrounded by high fractured regions in which the ascent of high pressure fluids is started and then reinforced. Therefore these regions can have similar short-term rigidities (accounting for the similar seismic velocities), but considering long time deformation processes the asperity can show a very different effective rigidity with the respect to the surrounding media, since pressure solution processes (e.g. Poirier (1985)) or else the widespread presence of shear cracks (generated seismically or growing subcritically according to the stress-corrosion mechanisms) can explain a low effective rigidity for the surrounding medium.

In the second part of our work we have investigated the complexities of fault processes

induced by the layered structure of the shallow crust. The first model proposed (fault bending model) shows that, when the stress drop in the shallow layer is lower than the value prescribed by a vertical planar crack, fault bending in the shallow layer can take place if the upper section of the crack is suitably inclined accordingly to the generalized stress drop condition derived. Furthermore the asymmetric stress release with respect to the negative z axis suggests that other fractures can develop in the opposite quadrant. About this possibility, a second model (fault branching model) have been considered in which fault branching in the shallow layer is examined. As the previous model, the second model can be applied only when the stress drop in the shallow layer is lower than the value prescribed for a vertical planar crack. The indeterminacy of the singular degree of the dislocation density at the interface represents an unexpected result, but it simply means that however a first section is inclined in the shallow layer, a second fracture can develop with a suitable inclination in order to release stress in excess in the same layer. The last model proposed consider instead the case in which the stress drop in the upper layer is higher than the value prescribed by a vertical planar crack. In this case we guess that unwelding can take place and the conditions for unwelding have been studied employing a dislocation model. The study of this model has shown that complete unwelding can take place only if the main fault arrives in proximity of the interface and in this case the stress diffusion over the unwelding region can determine the opening of secondary (shear and open) fractures which are confined in the shallow layer. Therefore such a mechanism can be invoked to explain the complex surface pattern of faulting (e.g. double en-echelon structures) observed in the SISZ and in other several regions characterized by a transcurrent tectonics.

Appendix A

Orthogonal polynomials

A.1 Chebyshev polynomials

Taken $x = \cos\theta$, we define Chebyshev polynomial of first kind

$$T_n(x) = \cos n\theta, \qquad 0 \le \theta \le \pi, \quad -1 \le x \le 1.$$

Here we report the first three polynomials ($n = 0, 1, 2$)

$$\begin{aligned} T_0(x) &= 1 \\ T_1(x) &= x \\ T_2(x) &= 2x^2 - 1 \end{aligned} \tag{A.1}$$

The polynomials obey this recurrence relation

$$T_{n+1}(x) = 2xT_n(x) - T_{n-1}(x)$$

from which can be easily deduced that T_n are effectively polynomials in the variable $x = \cos\theta$.
T_n are orthogonal on the interval $(-1, 1)$ with weight function $(1 - x^2)^{-1/2}$

$$\int_{-1}^{1} T_n(x)T_k(x)\frac{dx}{\sqrt{1-x^2}} = \begin{cases} \pi & \text{if } n = k = 0, \\ (\pi/2)\,\delta_{nk} & \text{instead} \end{cases}$$

We define Chebyshev polynomial of second kind in the variable $x = \cos\theta$

$$U_n(x) = \frac{\sin(n+1)\theta}{\sin\theta}, \qquad 0 \le \theta \le \pi, \quad -1 \le x \le 1$$

The first three polynomials have this aspect ($n = 0, 1, 2$)

$$\begin{aligned} U_0(x) &= 1 \\ U_1(x) &= 2x \\ U_2(x) &= 4x^2 - 1 \end{aligned} \tag{A.2}$$

These polynomials obey the same recurrence relation

$$U_{n+1}(x) = 2xU_n(x) - U_{n-1}(x)$$

and satisfy the following orthogonality relation with weight function $(1-x^2)^{1/2}$

$$\int_{-1}^{1} U_n(x)U_k(x)\sqrt{1-x^2}dx = \frac{\pi}{2}\delta_{nk}. \tag{A.3}$$

$U_n(x)$ polynomials obey to these integral properties

$$\int_{-1}^{x} T_n(x')\frac{dx'}{\sqrt{1-x'^2}} = \begin{cases} (\pi/2) + \arcsin x & \text{if } n = 0, \\ -\frac{1}{n}U_{n-1}(x)\sqrt{1-x^2} & \text{if } n > 0 \end{cases}$$

In fracture theory the following relations valid for T_n polynomials play a central role

$$\fint_{-1}^{1} \frac{T_n(x')}{x'-x}\frac{dx'}{\sqrt{1-x'^2}} = \begin{cases} 0 & \text{if } n = 0, \\ \pi U_{n-1}(x) & \text{if } n > 0 \end{cases} \qquad |x| < 1 \tag{A.4}$$

while for $|x| > 1$ we have

$$\int_{-1}^{1} \frac{T_n(x')}{x'-x}\frac{dx'}{\sqrt{1-x'^2}} = \begin{cases} -\pi\dfrac{(x-\sqrt{x^2-1})^n}{\sqrt{x^2-1}} & \text{if } x > 1, \\ \pi\dfrac{(x+\sqrt{x^2-1})^n}{\sqrt{x^2-1}} & \text{if } x < -1 \end{cases}$$

A.2 Jacobi polynomials

Jacobi Polynomials $P_n^{(\alpha,\beta)}$ are the solution of the differential equation

$$\left(1-x^2\right)\frac{d^2y}{dx^2} + \left(\beta - \alpha - (\alpha+\beta+2)\,x\right)\frac{d^2y}{dx^2} + n\,(n+\alpha+\beta+1) = 0$$

The explicit expression for these polynomials is

$$P_n^{(\alpha,\beta)}(x) = \frac{\mathbf{\Gamma}\,(\alpha+n+1)}{n!\,\mathbf{\Gamma}\,(\alpha+\beta+n+1)}\sum_{m=0}^{n}\binom{n}{m}\frac{\mathbf{\Gamma}\,(\alpha+\beta+n+m+1)}{\mathbf{\Gamma}\,(\alpha+m+1)}\left(\frac{x-1}{2}\right)^m$$

where $\mathbf{\Gamma}$ is the Gamma function.
$P_n^{(\alpha,\beta)}$ are orthogonal with weight function $w(x) = (1-x)^\alpha(1+x)^\beta$

$$\int_{-1}^{1}(1-x)^\alpha(1+x)^\beta P_n^{(\alpha,\beta)}(x)P_k^{(\alpha,\beta)}(x)dx =$$

$$= \frac{2^{\alpha+\beta+1}}{2n+\alpha+\beta+1}\frac{\mathbf{\Gamma}\,(n+\alpha+1)\;\mathbf{\Gamma}\,(n+\beta+1)}{\mathbf{\Gamma}\,(n+\alpha+\beta+1)\;n!}\,\delta_{nk}$$

$$\alpha > -1, \beta > -1$$

and satisfy the following integral relation

$$\int_{-1}^{+1}(x-t)^{-1}(1-t)^{\alpha}(1+t)^{\beta}P_n^{(\alpha,\beta)}(t)dt = 2(x-1)^{\alpha}(x+1)^{\beta}Q_n^{(\alpha,\beta)}(x) \tag{A.5}$$

where $Q_n^{(\alpha,\beta)}(x)$ are Jacobi functions of second type and x belong to the complex plane cut along the segment (-1,1).
Functions $Q_n^{(\alpha,\beta)}(x)$ can be expressed in terms of $P_n^{(\alpha,\beta)}(x)$ as shown here

$$\begin{aligned} Q_n^{(\alpha,\beta)}(x) = &-\frac{\pi}{2}\csc(\pi\beta)e^{i\pi(\alpha+\beta)}P_n^{(\alpha,\beta)}(x) \\ &+ 2^{\alpha+\beta-1}(x-1)^{-\alpha}(x+1)^{-\beta}(-1)^n\frac{\mathbf{\Gamma}(\beta)\mathbf{\Gamma}(n+1+\alpha)}{\mathbf{\Gamma}(n+1+\alpha+\beta)}\,F\Big(n+1,-n-\alpha-\beta;1-\beta;\frac{1}{2}(1+x)\Big) \end{aligned} \tag{A.6}$$

where F is the hypergeometric function

$$F(a,b;c;x) = \sum_{k=0}^{\infty}\frac{(a)_k(b)_k}{(c)_k}\frac{z^k}{k!} = \frac{\mathbf{\Gamma}(c)}{\mathbf{\Gamma}(a)\mathbf{\Gamma}(b)}\sum_{k=0}^{\infty}\frac{\mathbf{\Gamma}(a+k)\mathbf{\Gamma}(b+k)}{\mathbf{\Gamma}(c+k)}\frac{x^k}{k!}$$

characterized by these properties

- it's a regular solution of hypergeometric equation if $c \neq 0, -1, -2, ..$
- F absolutely converges in the unit circle if $a, b \neq 0, -1, -2, ..$

Appendix B

Details about fault bending model

B.1 Stress drop evaluation

B.1.1 Stress drop on section 1

Contribution of section 1 on the same section

To evaluate the stress component $(\sigma_{ny})_1^I$ we have to use the following expression

$$(\sigma_{ny})_1^I(S;S_0) = \cos\alpha\,(\sigma_{xy})_1^I(S;S_0) - \sin\alpha\,(\sigma_{zy})_1^I(S;S_0) \tag{B.1}$$

This component must be calculated in an arbitrary point of section 1

$$\begin{cases} x = -S\sin\alpha \\ z = -S\cos\alpha \end{cases} \qquad 0 < S < 2l_1 \tag{B.2}$$

If we insert (B.2) in equations (4.4),(4.5) the components $(\sigma_{xy})_1^I$, $(\sigma_{zy})_1^I$ can be written in this form

$$\begin{aligned}(\sigma_{xy})_1^I(S;S_0) = -\frac{\mu_1}{2\pi}\Bigg\{&\frac{(S-S_0)\cos\alpha}{R^2} - \Gamma\frac{(S+S_0)\cos\alpha}{T_0^2} \\ &+\sum_{n=1}^{\infty}\Gamma^n\left[-\Gamma\frac{(S+S_0)\cos\alpha+2nH}{T^2} + \frac{(S-S_0)\cos\alpha-2nH}{V^2}\right. \\ &\left.+\frac{(S-S_0)\cos\alpha+2nH}{U^2} - \Gamma^{-1}\frac{(S+S_0)\cos\alpha-2nH}{W^2}\right]\Bigg\}\end{aligned} \tag{B.3}$$

$$(\sigma_{zy})_1^I(S;S_0) = \frac{\mu_1}{2\pi}(S-S_0)\sin\alpha\left\{\frac{1}{R^2} - \frac{\Gamma}{T_0^2} + \sum_{n=1}^{\infty}\Gamma^n\left[-\frac{\Gamma}{T^2} + \frac{1}{V^2} + \frac{1}{U^2} - \frac{\Gamma^{-1}}{W^2}\right]\right\} \tag{B.4}$$

Combining the expressions (B.3), (B.4) as indicated by (B.1) we obtain

$$(\sigma_{ny})_1^I(S;S_0) = -\frac{\mu_1}{2\pi}\left\{\frac{1}{S-S_0} - \Gamma\frac{(S-S_0)\sin^2\alpha + (S+S_0)\cos^2\alpha}{(S-S_0)^2\sin^2\alpha + (S+S_0)^2\cos^2\alpha} + \mathcal{R}_{11}(S;S_0)\right\} \tag{B.5}$$

where $\mathcal{R}_{11}(S;S_0)$ represents the sum of the terms describing the effects determined by the presence of the free surface

$$\mathcal{R}_{11}(S;S_0)=\sum_{n=1}^{\infty}\Gamma^n\left[-\Gamma\frac{S+S_0\cos(2\alpha)+2nH\cos\alpha}{T^2}+\frac{S-S_0-2nH\cos\alpha}{V^2}\right.$$
$$\left.+\frac{S-S_0+2nH\cos\alpha}{U^2}-\Gamma^{-1}\frac{S+S_0\cos(2\alpha)-2nH\cos\alpha}{W^2}\right]$$

$$\begin{cases}R^2=(S-S_0)^2\sin^2\alpha+(S-S_0)^2\cos^2\alpha=(S-S_0)^2\\ T_0^2=(S-S_0)^2\sin^2\alpha+((S+S_0)\cos\alpha)^2\\ T^2=(S-S_0)^2\sin^2\alpha+((S+S_0)\cos\alpha+2nH)^2\\ U^2=(S-S_0)^2\sin^2\alpha+((S-S_0)\cos\alpha+2nH)^2\\ V^2=(S-S_0)^2\sin^2\alpha+((S-S_0)\cos\alpha-2nH)^2\\ W^2=(S-S_0)^2\sin^2\alpha+((S+S_0)\cos\alpha-2nH)^2\end{cases}\tag{B.6}$$

The contribution to stress drop on section 1 produced by the same section can be finally written in this way

$$-\frac{2\pi}{\mu_1}\int_0^{2l_1}(\sigma_{ny})_1^I(S;S_0)\rho_1(S_0)dS_0=$$
$$=\int_0^{2l_1}\frac{\rho_1(S_0)dS_0}{S-S_0}-\Gamma\int_0^{2l_1}\frac{(S-S_0)\sin^2\alpha+(S+S_0)\cos^2\alpha}{(S-S_0)^2\sin^2\alpha+(S+S_0)^2\cos^2\alpha}\rho_1(S_0)dS_0\tag{B.7}$$
$$+\int_0^{2l_1}\mathcal{R}_{11}(S;S_0)\rho_1(S_0)dS_0$$

Contribution of section 2 on section 1

To calculate this contribution we follow the same procedure used in the last section. Therefore we have to evaluate $(\sigma_{ny})_1^{II}$ according to this expression

$$(\sigma_{ny})_1^{II}(S;z_0)=\cos\alpha\,(\sigma_{xy})_1^{II}(S;z_0)-\sin\alpha\,(\sigma_{zy})_1^{II}(S;z_0)\tag{B.8}$$

Given

$$\begin{cases}x=-S\sin\alpha\\ z=-S\cos\alpha\end{cases}\tag{B.9}$$

the stress components (4.8),(4.10) evaluated in an arbitrary point of section 1 assume this form

$$(\sigma_{xy})_1^{II}(S;z_0)=$$
$$=\frac{\mu_1}{2\pi}\frac{2m}{1+m}\sum_{n=0}^{\infty}\Gamma^n\left(\frac{z_0+2(n+1)H-S\cos\alpha}{S^2\sin^2\alpha+(z_0+2(n+1)H-S\cos\alpha)^2}+\frac{z_0+2nH+S\cos\alpha}{S^2\sin^2\alpha+(z_0+2nH+S\cos\alpha)^2}\right)$$
$$(\sigma_{zy})_1^{II}(S;z_0)$$
$$=\frac{\mu_1}{2\pi}\frac{2m}{1+m}\sum_{n=0}^{\infty}\Gamma^n\left(\frac{S\sin\alpha}{S^2\sin^2\alpha+(z_0+2(n+1)H-S\cos\alpha)^2}-\frac{S\sin\alpha}{S^2\sin^2\alpha+(z_0+2nH+S\cos\alpha)^2}\right)$$

(B.10)

Combining the expression found for $(\sigma_{xy})_1^{II}, (\sigma_{zy})_1^{II}$ according to (B.8) we find

$$(\sigma_{ny})_1^{II}(S;z_0) = -\frac{\mu_1}{2\pi}\left\{-\frac{2m}{1+m}\frac{z_0\cos\alpha+S}{S^2\sin^2\alpha+(z_0+S\cos\alpha)^2}+\mathcal{R}_{12}(S;z_0)\right\} \tag{B.11}$$

where

$$\mathcal{R}_{12}(S;z_0) = \\ = -\frac{2m}{1+m}\sum_{n=0}^{\infty}\Gamma^n\left(\frac{[z_0+2(n+1)H]\cos\alpha-S}{S^2\sin^2\alpha+(z_0+2(n+1)H-S\cos\alpha)^2}+\Gamma\frac{[z_0+2(n+1)H]\cos\alpha+S}{S^2\sin^2\alpha+(z_0+2(n+1)H+S\cos\alpha)^2}\right) \tag{B.12}$$

Therefore the stress induced on section 1 by slip of section 2 is assigned by the following expression

$$\begin{aligned}-\frac{2\pi}{\mu_1}\int_0^{2l_2}(\sigma_{ny})_1^{II}(S;z_0)\rho_2(z_0)dz_0 = -\frac{2m}{1+m}\int_0^{2l_2}\frac{z_0\cos\alpha+S}{S^2\sin^2\alpha+(z_0+S\cos\alpha)^2}\rho_2(z_0)dz_0 \\ +\int_0^{2l_2}\mathcal{R}_{12}(S;z_0)\rho_2(z_0)dz_0\end{aligned} \tag{B.13}$$

B.1.2 Stress drop on section 2

Contribution of section 2 on the same section

In this case, both the Cauchy kernel and the generalized Cauchy kernel are already explicit

$$(\sigma_{xy})_2^{II}(z;z_0) = -\frac{\mu_2}{2\pi}\left\{\frac{1}{z-z_0}+\Gamma\frac{1}{z+z_0}+\mathcal{R}_{22}(z;z_0)\right\} \tag{B.14}$$

where

$$\mathcal{R}_{22}(z;z_0) = -\frac{4m}{(1+m)^2}\sum_{n=0}^{\infty}\Gamma^n\frac{1}{z+z_0+2(n+1)H} \tag{B.15}$$

Therefore the stress induced on section 2 by slip of the same section is equal to

$$\begin{aligned}-\frac{2\pi}{\mu_2}\int_0^{2l_2}(\sigma_{xy})_2^{II}(z;z_0)\rho_2(z_0)dz_0 = \int_0^{2l_2}\frac{\rho_2(z_0)dz_0}{z-z_0}+\Gamma\int_0^{2l_2}\frac{\rho_2(z_0)dz_0}{z+z_0} \\ +\int_0^{2l_2}\mathcal{R}_{22}(z;z_0)\rho_2(z_0)dz_0\end{aligned} \tag{B.16}$$

Contribution of section 1 on section 2

The stress component $(\sigma_{xy})_2^I$ induced in a point of section 2 by slip of section 1 has this form

$$\begin{aligned}(\sigma_{xy})_2^I(z;S_0) = \\ = \frac{\mu_2}{2\pi}\frac{2}{1+m}\left\{\frac{S_0\cos\alpha+z}{S_0^2\sin^2\alpha+(S_0\cos\alpha+z)^2}+\frac{S_0\cos\alpha-z-2H}{S_0^2\sin^2\alpha+(S_0\cos\alpha-z-2H)^2}\right. \\ \left.+\sum_{n=1}^{\infty}\Gamma^n\left[\frac{S_0\cos\alpha+z+2nH}{S_0^2\sin^2\alpha+(S_0\cos\alpha+z+2nH)^2}+\frac{S_0\cos\alpha-z-2(n+1)H}{S_0^2\sin^2\alpha+(S_0\cos\alpha-z-2(n+1)H)^2}\right]\right\}\end{aligned} \tag{B.17}$$

The previous expression can be rewritten in order to explicit the term corresponding to the generalized Cauchy kernel

$$(\sigma_{xy})_2^I(z;S_0) = -\frac{\mu_2}{2\pi}\left\{-\frac{2}{1+m}\frac{S_0\cos\alpha+z}{S_0^2\sin^2\alpha+(S_0\cos\alpha+z)^2}+\mathcal{R}_{12}(z;S_0)\right\} \tag{B.18}$$

where

$$\begin{aligned}\mathcal{R}_{12}(z;S_0) = \\ = -\frac{2}{1+m}\sum_{n=1}^{\infty}\Gamma^n\left[\frac{S_0\cos\alpha-z-2nH}{S_0^2\sin^2\alpha+(S_0\cos\alpha-z-2nH)^2}+\Gamma^{-1}\frac{S_0\cos\alpha+z+2nH}{S_0^2\sin^2\alpha+(S_0\cos\alpha+z+2nH)^2}\right]\end{aligned} \tag{B.19}$$

The stress induced by section 1 on section 2 is assigned by this expression

$$\begin{aligned}-\frac{2\pi}{\mu_2}\int_0^{2l_1}(\sigma_{xy})_2^I(z;S_0)\rho_1(S_0)dS_0 = -\frac{2}{1+m}\int_0^{2l_1}\frac{S_0\cos\alpha+z}{S_0^2\sin^2\alpha+(S_0\cos\alpha+z)^2}\rho_1(S_0)dS_0 \\ +\int_0^{2l_1}\mathcal{R}_{12}(z;S_0)\rho_1(S_0)dS_0\end{aligned} \tag{B.20}$$

B.2 Study of asymptotic behaviour

B.2.1 Cauchy kernels

To evaluate the asymptotic behaviour of I_{11}, I_{21} we have to use the Plemelj formula

$$\frac{1}{\pi}\int_{-1}^{1}\frac{\rho(t)}{t-\xi}\,dt = \frac{1}{2}\left[\Phi^+(\xi)+\Phi^-(\xi)\right], \qquad -1<\xi<1 \tag{B.21}$$

because the point ξ lies on the cut of the complex plane.

Integral I_{11}

Using 4.23 and the Plemelj formula, we obtain

$$\frac{1}{\pi}\int_{-1}^{1}\frac{\rho(t)}{t-\xi_1}\,dt = -R_1(-1)2^{a_1}\cot(\pi b_1)(\xi_1+1)^{b_1} + R_1(+1)2^{b_1}\cot(\pi a_1)(1-\xi_1)^{a_1} + F_0(\xi) \tag{B.22}$$

where the behaviour of F_0 near $\xi_1 = -1$ is similar to that of Φ_0.

Integral I_{21}

Using the same procedure, we obtain

$$\frac{1}{\pi}\int_{-1}^{1}\frac{\rho(t)}{t-\xi_2}\,dt = -R_2(-1)2^{a_1}\cot(\pi b_1)(\xi_2+1)^{b_1} + R_2(+1)2^{b_1}\cot(\pi a_1)(1-\xi_2)^{a_1} + G_0(\xi) \tag{B.23}$$

where the behaviour of G_0 near $\xi_2 = -1$ is similar to that of Φ_0.

B.2.2 Generalized Cauchy kernels

The general form of a generalized Cauchy kernel is

$$\sum_{k=0}^{n} c_k\,(\xi+1)^k\,\frac{d^k}{d\xi^k}(\xi' - z_1(\xi))^{-1}, \qquad z_1(\xi) = -1 + (\xi+1)e^{i\theta_1}, \qquad 0 < \theta_1 < 2\pi$$

When c_0 is the only coefficient different form 0, the kernel assumes its simplest form

$$\frac{c_0}{\xi' - z_1(\xi)}, \qquad z_1(\xi) = -1 + (\xi+1)e^{i\theta_1} \tag{B.24}$$

In this section we will show that the integral kernels corresponding to $I_{12}, I_{13}, I_{22}, I_{13}$ can be expressed in this form.

Integral I_{12}

Considering the second term in the first integral equation

$$\int_{-1}^{+1}\frac{(\xi_1-\xi_1^{'})\sin^2\alpha + (\xi_1+\xi_1^{'}+2)\cos^2\alpha}{(\xi_1-\xi_1^{'})^2\sin^2\alpha + (\xi_1+\xi_1^{'}+2)^2\cos^2\alpha}\rho_1(\xi_1^{'})d\xi_1^{'} \tag{B.25}$$

we have to prove the integral kernel is a generalized Cauchy kernel, so we have to rewrite this term as indicated in (B.24).

We try to split the integral kernel as indicated below

$$\begin{aligned}
&\frac{(\xi_1-\xi_1^{'})\sin^2\alpha+(\xi_1+\xi_1^{'}+2)\cos^2\alpha}{(\xi_1-\xi_1^{'})^2\sin^2\alpha+(\xi_1+\xi_1^{'}+2)^2\cos^2\alpha}= \\
=&\frac{A}{(\xi_1-\xi_1^{'})\sin\alpha-i(\xi_1+\xi_1^{'}+2)\cos\alpha}+\frac{B}{(\xi_1-\xi_1^{'})\sin\alpha+i(\xi_1+\xi_1^{'}+2)\cos\alpha} \\
=&\frac{\Big[(\xi_1-\xi_1^{'})\sin\alpha+i(\xi_1+\xi_1^{'}+2)\cos\alpha\Big]A+\Big[(\xi_1-\xi_1^{'})\sin\alpha-i(\xi_1+\xi_1^{'}+2)\cos\alpha\Big]B}{\big((\xi_1-\xi_1^{'})\sin\alpha-i(\xi_1+\xi_1^{'}+2)\cos\alpha\big)\cdot\big((\xi_1-\xi_1^{'})\sin\alpha+i(\xi_1+\xi_1^{'}+2)\cos\alpha\big)} \\
=&\frac{(\xi_1-\xi_1^{'})\sin\alpha\cdot[A+B]+(\xi_1+\xi_1^{'}+2)\cos\alpha\cdot[iA-iB]}{(\xi_1-\xi_1^{'})^2\sin^2\alpha+(\xi_1+\xi_1^{'}+2)^2\cos^2\alpha}
\end{aligned} \tag{B.26}$$

Comparing the first and the last raw in (B.26) we find the following system for A, B

$$\begin{cases} A+B=\sin\alpha \\ \\ iA-iB=\cos\alpha \end{cases} \tag{B.27}$$

The system can be easily solved and its solution is given by

$$\begin{cases} A=\frac{1}{2}e^{-i\left(\frac{\pi}{2}-\alpha\right)} \\ \\ B=\frac{1}{2}e^{i\left(\frac{\pi}{2}-\alpha\right)} \end{cases} \tag{B.28}$$

Using the expression found for A, we can rewrite the term corresponding to this coefficient in the second raw of (B.26) as indicated here

$$\begin{aligned}
&\frac{A}{(\xi_1-\xi_1^{'})\sin\alpha-i(\xi_1+\xi_1^{'}+2)\cos\alpha}= \\
=&\frac{-A}{(\xi_1^{'}+1)(\sin\alpha+i\cos\alpha)-(\xi_1+1)(\sin\alpha-i\cos\alpha)} \\
=&\frac{-Ae^{-i\left(\frac{\pi}{2}-\alpha\right)}}{\xi_1^{'}+1+e^{2i\alpha}(\xi_1+1)} \\
=&\frac{A^{'}}{\xi_1^{'}-z_1(\xi_1)}
\end{aligned} \tag{B.29}$$

where

$$\begin{cases} A^{'}=-Ae^{-i\left(\frac{\pi}{2}-\alpha\right)}=-\frac{1}{2}e^{-2i\left(\frac{\pi}{2}-\alpha\right)}=\frac{1}{2}e^{2i\alpha} \\ \\ z_1(\xi_1)=-1-(\xi_1+1)e^{2i\alpha} \end{cases} \tag{B.30}$$

Using the same procedure for the term corresponding to B in the second raw of (B.26) we find

$$\begin{aligned}
&\frac{B}{(\xi_1-\xi_1^{'})\sin\alpha+i(\xi_1+\xi_1^{'}+2)\cos\alpha}= \\
=&\frac{-B}{(\xi_1^{'}+1)(\sin\alpha-i\cos\alpha)-(\xi_1+1)(\sin\alpha+i\cos\alpha)} \\
=&\frac{-Be^{i\left(\frac{\pi}{2}-\alpha\right)}}{\xi_1^{'}+1+e^{-2i\alpha}(\xi_1+1)} \\
=&\frac{B^{'}}{\xi_1^{'}-z_1^{'}(\xi_1)}
\end{aligned} \tag{B.31}$$

where

$$\begin{cases}
B^{'}=-\dfrac{1}{2}e^{2i\left(\frac{\pi}{2}-\alpha\right)}=\dfrac{1}{2}e^{-2i\alpha}=\overline{A^{'}} \\
\\
z_1^{'}(\xi_1)=-1-(\xi_1+1)e^{-2i\alpha}=\overline{z_1}(\xi_1)
\end{cases} \tag{B.32}$$

With the procedure shown, we can rewrite integral I_{12} as the sum of two integrals with generalized Cauchy kernels

$$\begin{aligned}
&\int_{-1}^{+1}\frac{(\xi_1-\xi_1^{'})\sin^2\alpha+(\xi_1+\xi_1^{'}+2)\cos^2\alpha}{(\xi_1-\xi_1^{'})^2\sin^2\alpha+(\xi_1+\xi_1^{'}+2)^2\cos^2\alpha}\rho_1(\xi_1^{'})d\xi_1^{'}= \\
&\quad=A^{'}\int_{-1}^{+1}\frac{\rho_1(\xi_1^{'})d\xi_1^{'}}{\xi_1^{'}-z_1(\xi_1)}+\overline{A^{'}}\int_{-1}^{+1}\frac{\rho_1(\xi_1^{'})d\xi_1^{'}}{\xi_1^{'}-\overline{z_1}(\xi_1)}
\end{aligned} \tag{B.33}$$

The asymptotic behaviour of these integrals can be evaluated defining

$$\frac{1}{\pi}\int_{-1}^{1}\frac{\rho(\xi')}{\xi'-z_1(\xi_1)}\,d\xi'=\Phi(z_1(\xi_1)) \tag{B.34}$$

$$\frac{1}{\pi}\int_{-1}^{1}\frac{\rho(\xi')}{\xi'-\overline{z_1}(\xi_1)}\,d\xi'=\Phi(\overline{z_1}(\xi_1)) \tag{B.35}$$

Substituting $z_1+1=e^{i\pi}(\xi_1+1)e^{2i\alpha}$ for (B.34) and $\overline{z_1}+1$ for (B.35) in equation (4.23) we obtain

$$\Phi(z_1(\xi_1))=-R_1(-1)2^{a_1}\frac{(\xi_1+1)^{b_1}}{\sin(\pi b_1)}e^{2i\alpha b_1}+F_1^{'}(\xi_1) \tag{B.36}$$

$$\Phi(\overline{z_1}(\xi_1))=-R_1(-1)2^{a_1}\frac{(\xi_1+1)^{b_1}}{\sin(\pi b_1)}e^{-2i\alpha b_1}+F_1^{''}(\xi_1) \tag{B.37}$$

where the behaviour of F_1', F_1'' near $\xi_1 = -1$ is similar to that of Φ_0.
Combining this results we can finally find the asymptotic behaviour of I_{12}

$$\begin{aligned}
&-\frac{1}{\pi}\int_{-1}^{+1}\frac{(\xi_1-\xi_1^{'})\sin^2\alpha+(\xi_1+\xi_1^{'}+2)\cos^2\alpha}{(\xi_1-\xi_1^{'})^2\sin^2\alpha+(\xi_1+\xi_1^{'}+2)^2\cos^2\alpha}\rho_1(\xi_1^{'})d\xi_1^{'}= \\
&\quad=-\left(A^{'}\Phi(z_1(\xi_1))+\overline{A^{'}}\Phi(\overline{z_1}(\xi_1))\right) \\
&\quad=R_1(-1)2^{a_1}\frac{(\xi_1+1)^{b_1}}{\sin(\pi b_1)}\left[\frac{1}{2}\left(e^{2i\alpha(1+b_1)}+e^{-2i\alpha(1+b_1)}\right)\right]+F_1(\xi_1) \\
&\quad=R_1(-1)2^{a_1}\frac{(\xi_1+1)^{b_1}}{\sin(\pi b_1)}\cos(2\alpha(1+b_1))+F_1(\xi_1)
\end{aligned} \tag{B.38}$$

where F_1 has behaviour near $\xi_1 = -1$ similar to that of Φ_0, being a linear combination of F_1', F_1''.

Integral I_{13}

We consider now the term describing the stress induced on the inclined section by slip of the vertical section

$$\int_{-1}^{+1}\frac{(\xi_2^{'}+1)\cos\alpha+\dfrac{l_1}{l_2}(\xi_1+1)}{\left(\dfrac{l_1}{l_2}\right)^2(\xi_1+1)^2\sin^2\alpha+\left((\xi_2^{'}+1)+\dfrac{l_1}{l_2}(\xi_1+1)\cos\alpha\right)^2}\rho_2(\xi_2^{'})d\xi_2^{'} \tag{B.39}$$

In order to write the integral kernel in the form of a generalized Cauchy kernel we proceed with the same procedure used for the integral I_{12}

$$\begin{aligned}
&\frac{(\xi_2^{'}+1)\cos\alpha+\dfrac{l_1}{l_2}(\xi_1+1)}{\left((\xi_2^{'}+1)+\dfrac{l_1}{l_2}(\xi_1+1)\cos\alpha\right)^2+\left(\dfrac{l_1}{l_2}(\xi_1+1)\sin\alpha\right)^2}= \\
&=\frac{\hat{A}}{\left((\xi_2^{'}+1)+\dfrac{l_1}{l_2}(\xi_1+1)\cos\alpha\right)-i\left(\dfrac{l_1}{l_2}(\xi_1+1)\sin\alpha\right)} \\
&\qquad+\frac{\hat{B}}{\left((\xi_2^{'}+1)+\dfrac{l_1}{l_2}(\xi_1+1)\cos\alpha\right)+i\left(\dfrac{l_1}{l_2}(\xi_1+1)\sin\alpha\right)}= \\
&=\frac{\left[\left((\xi_2^{'}+1)+\dfrac{l_1}{l_2}(\xi_1+1)\cos\alpha\right)+i\left(\dfrac{l_1}{l_2}(\xi_1+1)\sin\alpha\right)\right]\hat{A}}{\left((\xi_2^{'}+1)+\dfrac{l_1}{l_2}(\xi_1+1)\cos\alpha\right)^2+\left(\dfrac{l_1}{l_2}(\xi_1+1)\sin\alpha\right)^2} \\
&\qquad+\frac{\left[\left((\xi_2^{'}+1)+\dfrac{l_1}{l_2}(\xi_1+1)\cos\alpha\right)-i\left(\dfrac{l_1}{l_2}(\xi_1+1)\sin\alpha\right)\right]\hat{B}}{\left((\xi_2^{'}+1)+\dfrac{l_1}{l_2}(\xi_1+1)\cos\alpha\right)^2+\left(\dfrac{l_1}{l_2}(\xi_1+1)\sin\alpha\right)^2}= \\
&=\frac{(\xi_2^{'}+1)\left[\hat{A}+\hat{B}\right]+\dfrac{l_1}{l_2}(\xi_1+1)\left[(\cos\alpha+i\sin\alpha)\hat{A}+(\cos\alpha-i\sin\alpha)\hat{B}\right]}{\left((\xi_2^{'}+1)-\dfrac{l_1}{l_2}(\xi_1+1)\cos\alpha\right)^2+\left(\dfrac{l_1}{l_2}(\xi_1+1)\sin\alpha\right)^2}
\end{aligned}$$

(B.40)

To find $\hat{A}, \hat{B}$ we have to solve the system

$$\begin{cases} \hat{A} + \hat{B} = \cos\alpha \\ \\ e^{i\alpha}\hat{A} + e^{-i\alpha}\hat{B} = 1 \end{cases} \tag{B.41}$$

whose solution is

$$\begin{cases} \hat{A} = \dfrac{1}{2}e^{-i\alpha} \\ \\ \hat{B} = \dfrac{1}{2}e^{i\alpha} \end{cases} \tag{B.42}$$

The term corresponding to $\hat{A}$ can be rewritten in the following way

$$\begin{aligned} &\frac{\hat{A}}{\left((\xi_2'+1) + \dfrac{l_1}{l_2}(\xi_1+1)\cos\alpha\right) - i\left(\dfrac{l_1}{l_2}(\xi_1+1)\sin\alpha\right)} = \\ =&\frac{\hat{A}}{\xi_2'+1+\dfrac{l_1}{l_2}(\cos\alpha - i\sin\alpha)(\xi_1+1)} \\ =&\frac{\hat{A}}{\xi_2'+1+\dfrac{l_1}{l_2}e^{-i\alpha}(\xi_1+1)} \\ =&\frac{\hat{A}}{\xi_2' - \hat{z}_1(\xi_1)} \end{aligned} \tag{B.43}$$

where

$$\begin{cases} \hat{A} = \dfrac{1}{2}e^{-i\alpha} \\ \\ \hat{z}_1(\xi_1) = -1 - \dfrac{l_1}{l_2}(\xi_1+1)e^{-i\alpha} \end{cases} \tag{B.44}$$

Following the same procedure we can rewrite the term corresponding to $\hat{B}$

$$\begin{aligned} &\frac{\hat{B}}{\left((\xi_2'+1) + \dfrac{l_1}{l_2}(\xi_1+1)\cos\alpha\right) + i\left(\dfrac{l_1}{l_2}(\xi_1+1)\sin\alpha\right)} = \\ =&\frac{\hat{B}}{\xi_2'+1+\dfrac{l_1}{l_2}(\cos\alpha + i\sin\alpha)(\xi_1+1)} \\ =&\frac{\hat{B}}{\xi_2'+1+\dfrac{l_1}{l_2}e^{i\alpha}(\xi_1+1)} \\ =&\frac{\hat{B}}{\xi_2' - \hat{z}_1'(\xi_1)} \end{aligned} \tag{B.45}$$

where

$$\begin{cases} \hat{B} = \dfrac{1}{2}e^{i\alpha} = \overline{\hat{A}} \\ \\ \hat{z}_1^{'}(\xi_1) = -1 - \dfrac{l_1}{l_2}(\xi_1+1)e^{i\alpha} = \overline{\hat{z}_1}(\xi_1) \end{cases} \tag{B.46}$$

Therefore the integral I_{23} can be expressed as the sum of two integrals with generalized Cauchy kernels

$$\begin{aligned} &\int_{-1}^{+1} \frac{(\xi_2^{'}+1)\cos\alpha + \dfrac{l_1}{l_2}(\xi_1+1)}{\left(\dfrac{l_1}{l_2}\right)^2(\xi_1+1)^2\sin^2\alpha + \left((\xi_2^{'}+1) + \dfrac{l_1}{l_2}(\xi_1+1)\cos\alpha\right)^2}\rho_2(\xi_2^{'})d\xi_2^{'} = \\ &= \hat{A}\int_{-1}^{+1}\frac{\rho_2(\xi_2^{'})d\xi_2^{'}}{\xi_2^{'}-\hat{z}_1(\xi_1)} + \overline{\hat{A}}\int_{-1}^{+1}\frac{\rho_2(\xi_2^{'})d\xi_2^{'}}{\xi_2^{'}-\overline{\hat{z}_1}(\xi_1)} \end{aligned} \tag{B.47}$$

The asymptotic behaviour of these integrals can be evaluated defining

$$\frac{1}{\pi}\int_{-1}^{1}\frac{\rho(\xi')}{\xi'-\hat{z}_1(\xi_1)}\,d\xi' = \Phi(\hat{z}_1(\xi_1)) \tag{B.48}$$

$$\frac{1}{\pi}\int_{-1}^{1}\frac{\rho(\xi')}{\xi'-\overline{\hat{z}_1}(\xi_1)}\,d\xi' = \Phi(\overline{\hat{z}_1}(\xi_1)) \tag{B.49}$$

Substituting $\hat{z}_1+1 = e^{i\pi}\dfrac{l_1}{l_2}(\xi_1+1)e^{-i\alpha}$ for (B.48) and $\overline{\hat{z}_1}+1$ for (B.49) in equation (4.23), we obtain

$$\Phi(\hat{z}_1(\xi_1)) = -R_2(-1)2^{a_2}\frac{1}{\sin(\pi b_2)}\left[\frac{l_1}{l_2}(\xi_1+1)\right]^{b_2}e^{-i\alpha b_2} + \hat{F}_1^{'}(\xi_1) \tag{B.50}$$

$$\Phi(\overline{\hat{z}_1}(\xi_1)) = -R_2(-1)2^{a_2}\frac{1}{\sin(\pi b_2)}\left[\frac{l_1}{l_2}(\xi_1+1)\right]^{b_2}e^{i\alpha b_2} + \hat{F}_1^{''}(\xi_1) \tag{B.51}$$

where the behaviour of $\hat{F}_1', \hat{F}_1''$ near $\xi_1 = -1$ is similar to that of Φ_0.
Therefore, combining (B.50),(B.51) as indicated by (B.47), we find the asymptotic evaluation for I_{13}

$$\begin{aligned} &-\frac{1}{\pi}\int_{-1}^{+1}\frac{(\xi_2^{'}+1)\cos\alpha + \dfrac{l_1}{l_2}(\xi_1+1)}{\left(\dfrac{l_1}{l_2}\right)^2(\xi_1+1)^2\sin^2\alpha + \left((\xi_2^{'}+1) + \dfrac{l_1}{l_2}(\xi_1+1)\cos\alpha\right)^2}\rho_2(\xi_2^{'})d\xi_2^{'} = \\ &= -\left(\hat{A}\Phi(\hat{z}_1(\xi_1)) + \overline{\hat{A}}\Phi(\overline{\hat{z}_1}(\xi_1))\right) \\ &= R_2(-1)2^{a_2}\frac{1}{\sin(\pi b_2)}\left[\frac{l_1}{l_2}(\xi_1+1)\right]^{b_2}\left[\frac{1}{2}\left(e^{-i\alpha(1+b_2)} + e^{i\alpha(1+b_2)}\right)\right] + \hat{F}_1(\xi_1) \\ &= R_2(-1)2^{a_2}\frac{1}{\sin(\pi b_2)}\left[\frac{l_1}{l_2}(\xi_1+1)\right]^{b_2}\cos(\alpha(1+b_2)) + \hat{F}_1(\xi_1) \end{aligned} \tag{B.52}$$

where $\hat{F}_1$ has behaviour near $\xi_1 = -1$ similar to that of F_1', F_1''.

Integral I_{22}

In this case the term can be immediately written as a generalized Cauchy kernel

$$\int_{-1}^{+1} \frac{\rho_2(\xi_2^{'})d\xi_2^{'}}{\xi_2+\xi_2^{'}+2} = \int_{-1}^{+1} \frac{\rho_2(\xi_2^{'})d\xi_2^{'}}{\xi_2^{'}-z_2(\xi_2)}, \qquad z_2(\xi_2) = -1-(\xi_2+1)$$

Therefore we find

$$-\frac{1}{\pi}\int_{-1}^{+1} \frac{\rho_2(\xi_2^{'})d\xi_2^{'}}{\xi_2+\xi_2^{'}+2} = -\Phi(z_2(\xi_2)) = R_2(-1)2^{a_2}\frac{(\xi_2+1)^{b_2}}{\sin(\pi b_2)} + G_1(\xi_2) \tag{B.53}$$

where the behaviour of G_1 near $\xi_1 = -1$ is similar to that of Φ_0.

Integral I_{23}

The last term to be considered is the one describing the stress induced on the vertical section by slip on the inclined section

$$\int_{-1}^{+1} \frac{(\xi_1^{'}+1)\cos\alpha + \frac{l_2}{l_1}(\xi_2+1)}{(\xi_1^{'}+1)^2\sin^2\alpha + \left((\xi_1^{'}+1)\cos\alpha + \frac{l_2}{l_1}(\xi_2+1)\right)^2}\rho_1(\xi_1^{'})d\xi_1^{'} \tag{B.54}$$

As done for the other terms we try to express the integral kernel as the sum of two generalized Cauchy kernels

$$\begin{aligned}
&\frac{(\xi_1^{'}+1)\cos\alpha + \frac{l_2}{l_1}(\xi_2+1)}{(\xi_1^{'}+1)^2\sin^2\alpha + \left((\xi_1^{'}+1)\cos\alpha + \frac{l_2}{l_1}(\xi_2+1)\right)^2} = \\
=&\frac{\tilde{A}}{(\xi_1^{'}+1)\sin\alpha - i\left((\xi_1^{'}+1)\cos\alpha + \frac{l_2}{l_1}(\xi_2+1)\right)} \\
&+ \frac{\tilde{B}}{(\xi_1^{'}+1)\sin\alpha + i\left((\xi_1^{'}+1)\cos\alpha + \frac{l_2}{l_1}(\xi_2+1)\right)} = \\
=&\frac{\left[(\xi_1^{'}+1)\sin\alpha + i\left((\xi_1^{'}+1)\cos\alpha + \frac{l_2}{l_1}(\xi_2+1)\right)\right]\tilde{A}}{(\xi_1^{'}+1)^2\sin^2\alpha + \left((\xi_1^{'}+1)\cos\alpha + \frac{l_2}{l_1}(\xi_2+1)\right)^2} \\
&+ \frac{\left[(\xi_1^{'}+1)\sin\alpha - i\left((\xi_1^{'}+1)\cos\alpha + \frac{l_2}{l_1}(\xi_2+1)\right)\right]\tilde{B}}{(\xi_1^{'}+1)^2\sin^2\alpha + \left((\xi_1^{'}+1)\cos\alpha + \frac{l_2}{l_1}(\xi_2+1)\right)^2} = \\
=&\frac{(\xi_1^{'}+1)\left[(\sin\alpha + i\cos\alpha)\tilde{A} + (\sin\alpha - i\cos\alpha)\tilde{B}\right] + \frac{l_2}{l_1}(\xi_2+1)\left[i\tilde{A} - i\tilde{B}\right]}{(\xi_1^{'}+1)^2\sin^2\alpha + \left((\xi_1^{'}+1)\cos\alpha + \frac{l_2}{l_1}(\xi_2+1)\right)^2}
\end{aligned} \tag{B.55}$$

Therefore $\tilde{A}, \tilde{B}$ must satisfy the following system

$$\begin{cases} e^{i\left(\frac{\pi}{2}-\alpha\right)}\tilde{A} + e^{-i\left(\frac{\pi}{2}-\alpha\right)}\tilde{B} = \cos\alpha \\ \\ i\tilde{A} - i\tilde{B} = 1 \end{cases} \tag{B.56}$$

whose solution is

$$\begin{cases} \tilde{A} = \frac{1}{2}e^{-i\frac{\pi}{2}} \\ \\ \tilde{B} = \frac{1}{2}e^{i\frac{\pi}{2}} \end{cases} \tag{B.57}$$

Following the usual procedure, we consider now the term corresponding to A in the first raw of equation (B.55)

$$\begin{aligned} &\frac{\tilde{A}}{(\xi_1'+1)\sin\alpha - i\left((\xi_1'+1)\cos\alpha + \dfrac{l_2}{l_1}(\xi_2+1)\right)} = \\ =&\frac{\tilde{A}}{(\xi_1'+1)(\sin\alpha - i\cos\alpha) - i\dfrac{l_2}{l_1}(\xi_2+1)} \\ =&\frac{\tilde{A}}{(\xi_1'+1)e^{-i\left(\frac{\pi}{2}-\alpha\right)} + \dfrac{l_2}{l_1}e^{-i\frac{\pi}{2}}(\xi_2+1)} \\ =&\frac{\tilde{A}e^{i\left(\frac{\pi}{2}-\alpha\right)}}{\xi_1'+1+\dfrac{l_2}{l_1}e^{-i\alpha}(\xi_2+1)} \\ =&\frac{\tilde{A}'}{\xi_1' - z_2(\xi_2)} \end{aligned} \tag{B.58}$$

where

$$\begin{cases} \tilde{A}' = \tilde{A}e^{i\left(\frac{\pi}{2}-\alpha\right)} = \dfrac{1}{2}e^{-i\frac{\pi}{2}}e^{i\left(\frac{\pi}{2}-\alpha\right)} = \dfrac{1}{2}e^{-i\alpha} \\ \\ \hat{z_2}(\xi_2) = -1 - \dfrac{l_2}{l_1}(\xi_2+1)e^{-i\alpha} \end{cases} \tag{B.59}$$

The term corresponding to B assumes instead this form

$$\begin{aligned}
&\frac{\tilde{B}}{(\xi_1^{'}+1)\sin\alpha + i\left((\xi_1^{'}+1)\cos\alpha + \frac{l_2}{l_1}(\xi_2+1)\right)} = \\
=&\frac{\tilde{B}}{(\xi_1^{'}+1)(\sin\alpha + i\cos\alpha) + i\frac{l_2}{l_1}(\xi_2+1)} \\
=&\frac{\tilde{B}}{(\xi_1^{'}+1)e^{i\left(\frac{\pi}{2}-\alpha\right)} + \frac{l_2}{l_1}e^{i\frac{\pi}{2}}(\xi_2+1)} \\
=&\frac{\tilde{B}e^{-i\left(\frac{\pi}{2}-\alpha\right)}}{\xi_1^{'}+1+\frac{l_2}{l_1}e^{i\alpha}(\xi_2+1)} \\
=&\frac{\tilde{B}^{'}}{\xi_1^{'}-\hat{z}_2^{'}(\xi_2)}
\end{aligned} \tag{B.60}$$

where

$$\begin{cases}
\tilde{B}^{'} = \tilde{B}e^{-i\left(\frac{\pi}{2}-\alpha\right)} = \dfrac{1}{2}e^{i\frac{\pi}{2}}e^{-i\left(\frac{\pi}{2}-\alpha\right)} = \dfrac{1}{2}e^{i\alpha} = \overline{\tilde{A}^{'}} \\
\\
\hat{z}_2^{'}(\xi_2) = -1 - \dfrac{l_2}{l_1}(\xi_2+1)e^{i\alpha} = \overline{\hat{z}_2}(\xi_2)
\end{cases} \tag{B.61}$$

Therefore I_{23} can be expressed in the following way

$$\begin{aligned}
&\int_{-1}^{+1} \frac{(\xi_1^{'}+1)\cos\alpha + \frac{l_2}{l_1}(\xi_2+1)}{(\xi_1^{'}+1)^2\sin^2\alpha + \left((\xi_1^{'}+1)\cos\alpha + \frac{l_2}{l_1}(\xi_2+1)\right)^2}\rho_1(\xi_1^{'})d\xi_1^{'} = \\
=&\tilde{A}^{'}\int_{-1}^{+1}\frac{\rho_1(\xi_1^{'})d\xi_1^{'}}{\xi_1^{'}-\hat{z}_2(\xi_2)} + \overline{\tilde{A}^{'}}\int_{-1}^{+1}\frac{\rho_1(\xi_1^{'})d\xi_1^{'}}{\xi_1^{'}-\overline{\hat{z}_2}(\xi_2)}
\end{aligned} \tag{B.62}$$

The asymptotic behaviour of these integrals can be evaluated defining

$$\frac{1}{\pi}\int_{-1}^{1}\frac{\rho(\xi')}{\xi'-\hat{z}_2(\xi_2)}\,d\xi' = \Phi(\hat{z}_2(\xi_2)) \tag{B.63}$$

$$\frac{1}{\pi}\int_{-1}^{1}\frac{\rho(\xi')}{\xi'-\overline{\hat{z}_2}(\xi_2)}\,d\xi' = \Phi(\overline{\hat{z}_1}(\xi_2)) \tag{B.64}$$

Substituting $\hat{z}_2+1 = e^{i\pi}\dfrac{l_2}{l_1}(\xi_2+1)e^{-i\alpha}$ for (B.63) and $\overline{\hat{z}_2}+1$ for (B.64) in equation (4.23), we obtain

$$\Phi(\hat{z}_2(\xi_2)) = -R_1(-1)2^{a_1}\frac{1}{\sin(\pi b_1)}\left[\frac{l_2}{l_1}(\xi_2+1)\right]^{b_1}e^{-i\alpha b_1} + \hat{G}_1^{'}(\xi_2) \tag{B.65}$$

$$\Phi(\overline{\hat{z}_2}(\xi_2)) = -R_1(-1)2^{a_1}\frac{1}{\sin(\pi b_1)}\left[\frac{l_2}{l_1}(\xi_2+1)\right]^{b_1}e^{i\alpha b_1} + \hat{G}_1^{''}(\xi_2) \tag{B.66}$$

where the behaviour of $\hat{G}_1', \hat{G}_1''$ near $\xi_1 = -1$ is similar to that of Φ_0.
Combining (B.65),(B.66) as indicated by (B.62), we find the asymptotic evaluation for I_{23}

$$\begin{aligned}
&-\frac{1}{\pi}\int_{-1}^{+1} \frac{(\xi_1^{'}+1)\cos\alpha + \dfrac{l_2}{l_1}(\xi_2+1)}{(\xi_1^{'}+1)^2\sin^2\alpha + \left((\xi_1^{'}+1)\cos\alpha + \dfrac{l_2}{l_1}(\xi_2+1)\right)^2}\rho_1(\xi_1^{'})d\xi_1^{'} = \\
&\quad = -\left(\tilde{A}'\int_{-1}^{+1}\frac{\rho_1(\xi_1^{'})d\xi_1^{'}}{\xi_1^{'}-\hat{z}_2(\xi_2)} + \overline{\tilde{A}'}\int_{-1}^{+1}\frac{\rho_1(\xi_1^{'})d\xi_1^{'}}{\xi_1^{'}-\overline{\hat{z}_2}(\xi_2)}\right) \\
&\quad = R_1(-1)2^{a_1}\frac{1}{\sin(\pi b_1)}\left[\frac{l_2}{l_1}(\xi_2+1)\right]^{b_1}\left[\frac{1}{2}\left(e^{-i\alpha(1+b_1)}+e^{i\alpha(1+b_1)}\right)\right] + \hat{G}_1(\xi_2) \\
&\quad = R_1(-1)2^{a_1}\frac{1}{\sin(\pi b_1)}\left[\frac{l_2}{l_1}(\xi_2+1)\right]^{b_1}\cos(\alpha(1+b_1)) + \hat{G}_1(\xi_2)
\end{aligned} \tag{B.67}$$

where $\hat{G}_1$ has behaviour near $\xi_1 = -1$ similar to that of Φ_0, being a linear combination of $\hat{G}_1', \hat{G}_1''$.

B.3 Stress drop condition

In order to evaluate the integrals I_{ij} we can use the following integral relation

$$\int_{-1}^{+1}(x-t)^{-1}(1-t)^{\alpha}(1+t)^{\beta}P_n^{(\alpha,\beta)}(t)dt = 2(x-1)^{\alpha}(x+1)^{\beta}Q_n^{(\alpha,\beta)}(x) \tag{B.68}$$

and to determine bounded and singular terms of the integrals we will use the following representation for the Jacobi functions of second type

$$\begin{aligned}
Q_n^{(\alpha,\beta)}(x) = &-\frac{\pi}{2}\csc(\pi\beta)e^{i\pi(\alpha+\beta)}P_n^{(\alpha,\beta)}(x) \\
&+ 2^{\alpha+\beta-1}(x-1)^{-\alpha}(x+1)^{-\beta}(-1)^n\frac{\mathbf{\Gamma}(\beta)\mathbf{\Gamma}(n+1+\alpha)}{\mathbf{\Gamma}(n+1+\alpha+\beta)}\,F\Big(n+1,-n-\alpha-\beta;1-\beta;\frac{1}{2}(1+x)\Big)
\end{aligned} \tag{B.69}$$

For mathematical details please refer to appendix A.2.

B.3.1 Crack section 1

Integral I_{11}

If we substitute ρ_1 in I_{11}, we obtain

$$I_{11} = \int_{-1}^{+1}\frac{\rho_1(\xi_1^{'})d\xi_1^{'}}{\xi_1-\xi_1^{'}} = \sum_{k=0}^{+\infty}\gamma_k\int_{-1}^{+1}(\xi_1-\xi_1^{'})^{-1}(1-\xi_1^{'})^{-\frac{1}{2}}(1+\xi_1^{'})^{\omega}P_k^{(-\frac{1}{2},\omega)}(\xi_1^{'})d\xi_1^{'} \tag{B.70}$$

We have to determine its value in a point $\xi \in (-1,1)$, but the complex plane is cut along this segment and so we have to proceed in the following way

$$\int_{-1}^{+1} (\xi_1 - \xi_1')^{-1}(1-\xi_1')^{-\frac{1}{2}}(1+\xi_1')^{\omega} P_k^{(-\frac{1}{2},\omega)}(\xi_1')d\xi_1' = \\ = \frac{1}{2}\left[2(\xi_1{}^+ - 1)^{-\frac{1}{2}}(\xi_1{}^+ + 1)^{\omega} Q_k^{(-\frac{1}{2},\omega)}(\xi_1{}^+) + 2(\xi_1{}^- - 1)^{-\frac{1}{2}}(\xi_1{}^- + 1)^{\omega} Q_k^{(-\frac{1}{2},\omega)}(\xi_1{}^-)\right]$$

That is, we calculate the integrals in $\xi_1{}^+ = \zeta + i0, \xi_1{}^- = \zeta - i0$ corresponding to the opposite borders of the cut and take the mean of these values as the result of the integral. Regarding the arguments to assign to $\xi_1 - 1, \xi_1 + 1$:

- in $\xi_1{}^+$ we take $\arg(\xi_1{}^+ - 1) = \pi$, $\arg(\xi_1{}^+ + 1) = 0$
- in $\xi_1{}^-$ we instead take $\arg(\xi_1{}^- - 1) = -\pi$, $\arg(\xi_1{}^- + 1) = 2\pi$

Following the procedure described before, we ordain

$$I_{11} = \int_{-1}^{+1} \frac{\rho_1(\xi_1^{'})d\xi_1^{'}}{\xi_1 - \xi_1^{'}} = I_{11}{}^S + I_{11}{}^B \tag{B.71}$$

where

$$I_{11}{}^S = -\pi\,(1-\xi_1)^{-\frac{1}{2}}\,(1+\xi_1)^{\omega}\cot(\pi\omega)\sum_{k=0}^{+\infty}\gamma_k P_k^{(-\frac{1}{2},\omega)}(\xi_1)$$

$$I_{11}{}^B = 2^{-\frac{1}{2}+\omega}\,\mathbf{\Gamma}(\omega)\sum_{k=0}^{+\infty}\gamma_k(-1)^k\frac{\mathbf{\Gamma}\left(k+1-\frac{1}{2}\right)}{\mathbf{\Gamma}\left(k+1-\frac{1}{2}+\omega\right)}\,F\left(k+1,-k+\frac{1}{2}-\omega;1-\omega;\frac{1}{2}(1+\xi_1)\right) \tag{B.72}$$

We can observe that $I_{11}{}^S$ corresponds to a singular term for the stress near the crack tips, while $I_{11}{}^B$ remains bounded approaching the ends of the crack.
Letting $\xi_1 \to -1$ we obtain that

$$(1+\xi_1)^{-\omega}\cdot I_{11}{}^S \xrightarrow{\xi_1\to-1} -\pi 2^{-\frac{1}{2}}\cot(\pi\omega)\sum_{k=0}^{+\infty}\gamma_k P_k^{(-\frac{1}{2},\omega)}(-1) \tag{B.73}$$

$$I_{11}{}^B \xrightarrow{\xi_1\to-1} 2^{-\frac{1}{2}+\omega}\,\mathbf{\Gamma}(\omega)\sum_{k=0}^{+\infty}\gamma_k(-1)^k\frac{\mathbf{\Gamma}\left(k+1-\frac{1}{2}\right)}{\mathbf{\Gamma}\left(k+1-\frac{1}{2}+\omega\right)} \tag{B.74}$$

Integral I_{12}

The integral can be rewritten in the following way

$$\begin{aligned} I_{12} &= \int_{-1}^{+1} \frac{(\xi_1 - \xi_1^{'})\sin^2\alpha + (\xi_1 + \xi_1^{'} + 2)\cos^2\alpha}{(\xi_1 - \xi_1^{'})^2\sin^2\alpha + (\xi_1 + \xi_1^{'} + 2)^2\cos^2\alpha}\rho_1(\xi_1^{'})d\xi_1^{'} \\ &= -\left(A_1\int_{-1}^{+1}\frac{\rho_1(\xi_1^{'})d\xi_1^{'}}{z_1(\xi_1) - \xi_1^{'}} + \overline{A_1}\int_{-1}^{+1}\frac{\rho_1(\xi_1^{'})d\xi_1^{'}}{\overline{z_1}(\xi_1) - \xi_1^{'}}\right) \\ &= -\Big[\cos(2\alpha)\ \mathrm{Re}\left\{J_{12}\right\} - \sin(2\alpha)\ \mathrm{Im}\left\{J_{12}\right\}\Big] \end{aligned} \tag{B.75}$$

where

$$J_{12} = \int_{-1}^{+1}\frac{\rho_1(\xi_1^{'})d\xi_1^{'}}{z_1(\xi_1) - \xi_1^{'}}, \qquad \begin{cases} A_1 = \dfrac{1}{2}e^{2i\alpha} \\ z_1(\xi_1) = -1 - e^{2i\alpha}(\xi_1 + 1) \end{cases} \tag{B.76}$$

If we evaluate the integral J_{12}, the integral relation (B.68) can be applied without any further considerations, because z_1 does not lie on the cut of the complex plane.

$$\int_{-1}^{+1}\frac{\rho_1(\xi_1^{'})d\xi_1^{'}}{z_1(\xi_1) - \xi_1^{'}} = 2\left(z_1(\xi_1) - 1\right)^{-\frac{1}{2}}\left(z_1(\xi_1) + 1\right)^{\omega}\sum_{k=0}^{+\infty}\gamma_k Q_k^{\left(-\frac{1}{2},\omega\right)}\left(z_1(\xi_1)\right) \tag{B.77}$$

Using the relation (B.69) we can represent the result in this way

$$J_{12} = {J_{12}}^S + {J_{12}}^B \tag{B.78}$$

where

$$\begin{aligned} {J_{12}}^S =& -e^{2i\alpha\omega}\left(2 + e^{2i\alpha}(\xi_1 + 1)\right)^{-\frac{1}{2}}(\xi_1 + 1)^{\omega}\frac{\pi}{\sin(\pi\omega)}\sum_{k=0}^{+\infty}\gamma_k P_k^{\left(-\frac{1}{2},\omega\right)}\left(-1 - e^{2i\alpha}(\xi_1 + 1)\right) \\ {J_{12}}^B =& 2^{-\frac{1}{2}+\omega}\,\mathbf{\Gamma}(\omega)\sum_{k=0}^{+\infty}\gamma_k(-1)^k\frac{\mathbf{\Gamma}(k + 1 - \frac{1}{2})}{\mathbf{\Gamma}(k + 1 - \frac{1}{2} + \omega)}\,F\left(k+1, -k + \frac{1}{2} - \omega; 1 - \omega; -\frac{1}{2}e^{2i\alpha}(\xi_1 + 1)\right) \end{aligned}$$

Now if we define

$${I_{12}}^S = -\left[\cos(2\alpha)\,\mathrm{Re}\left\{{J_{12}}^S\right\} - \sin(2\alpha)\left\{{J_{12}}^S\right\}\right] \tag{B.79}$$

$${I_{12}}^B = -\left[\cos(2\alpha)\,\mathrm{Re}\left\{{J_{12}}^B\right\} - \sin(2\alpha)\left\{{J_{12}}^B\right\}\right] \tag{B.80}$$

and letting $\xi_1 \to -1$ we obtain

$$(1 + \xi_1)^{-\omega}\cdot {I_{12}}^S \xrightarrow{\xi_1 \to -1} \pi 2^{-\frac{1}{2}}\frac{1}{\sin(\pi\omega)}\left(\sum_{k=0}^{+\infty}\gamma_k P_k^{(-\frac{1}{2},\omega)}(-1)\right)\cos(2\alpha(1 + \omega)) \tag{B.81}$$

because $e^{2i\alpha\omega}$ is the only factor that remains complex in this limit, therefore to obtain the previous result is sufficient to apply the following trigonometry identity

$$\cos(2\alpha\omega)\cos(2\alpha) - \sin(2\alpha\omega)\sin(2\alpha) = \cos(2\alpha(1 + \omega)) \tag{B.82}$$

Considering the second term, we obtain

$$I_{12}{}^{B} \xrightarrow{\xi_1 \to -1} -2^{-\frac{1}{2}+\omega}\,\mathbf{\Gamma}(\omega)\left(\sum_{k=0}^{+\infty}\gamma_k(-1)^k\frac{\mathbf{\Gamma}\left(k+1-\frac{1}{2}\right)}{\mathbf{\Gamma}\left(k+1-\frac{1}{2}+\omega\right)}\right)\cos(2\alpha) \tag{B.83}$$

because in this limit J_{12} become real.

Integral I_{13}

Now we consider the integral

$$\begin{aligned} I_{13} &= \int_{-1}^{+1}\frac{(\xi_2^{'}+1)\cos\alpha+\dfrac{l_1}{l_2}(\xi_1+1)}{\left(\dfrac{l_1}{l_2}\right)^2(\xi_1+1)^2\sin^2\alpha+\left((\xi_2^{'}+1)+\dfrac{l_1}{l_2}(\xi_1+1)\cos\alpha\right)^2}\rho_2(\xi_2^{'})d\xi_2^{'} \\ &= -\left(\hat{A}_1\int_{-1}^{+1}\frac{\rho_1(\xi_1^{'})d\xi_1^{'}}{\hat{z}_1(\xi_1)-\xi_1^{'}}+\overline{\hat{A}_1}\int_{-1}^{+1}\frac{\rho_1(\xi_1^{'})d\xi_1^{'}}{\overline{\hat{z}_1}(\xi_1)-\xi_1^{'}}\right) \\ &= -\Big[\cos\alpha\ \mathrm{Re}\left\{J_{13}\right\}+\sin\alpha\ \mathrm{Im}\left\{J_{13}\right\}\Big] \end{aligned} \tag{B.84}$$

where

$$J_{13}=\int_{-1}^{+1}\frac{\rho_1(\xi_1^{'})d\xi_1^{'}}{\hat{z}_1(\xi_1)-\xi_1^{'}},\qquad \begin{cases}\hat{A}_1=\dfrac{1}{2}e^{-i\alpha}\\ \hat{z}_1(\xi_1)=-1-e^{-i\alpha}\dfrac{l_1}{l_2}(\xi_1+1)\end{cases} \tag{B.85}$$

$\hat{z}_1$ is not on the cut of the complex plane, so J_{13} can be evaluated without any further considerations using equation (B.68)

$$\int_{-1}^{+1}\frac{\rho_1(\xi_1^{'})d\xi_1^{'}}{\hat{z}_1(\xi_1)-\xi_1^{'}}=2\left(\hat{z}_1(\xi_1)-1\right)^{-\frac{1}{2}}\left(\hat{z}_1(\xi_1)+1\right)^{\omega}\sum_{k=0}^{+\infty}\gamma_k Q_k^{\left(-\frac{1}{2},\omega\right)}\left(\hat{z}_1(\xi_1)\right) \tag{B.86}$$

Using relation (B.69), we can express the solution in this form

$$J_{13}=J_{13}{}^{S}+J_{13}{}^{B} \tag{B.87}$$

where

$$J_{13}{}^{S}=-e^{-i\alpha\omega}\left(2+\frac{l_1}{l_2}e^{-i\alpha}(\xi_1+1)\right)^{-\frac{1}{2}}\left[\frac{l_1}{l_2}(\xi_1+1)\right]^{\omega}\frac{\pi}{\sin(\pi\omega)}\sum_{k=0}^{+\infty}\beta_k P_k^{\left(-\frac{1}{2},\omega\right)}\left(-1-e^{-i\alpha}\frac{l_1}{l_2}(\xi_1+1)\right)$$

$$J_{13}{}^{B}=2^{-\frac{1}{2}+\omega}\,\mathbf{\Gamma}(\omega)\sum_{k=0}^{+\infty}\beta_k(-1)^k\frac{\mathbf{\Gamma}(k+1-\frac{1}{2})}{\mathbf{\Gamma}(k+1-\frac{1}{2}+\omega)}\,F\left(k+1,-k+\frac{1}{2}-\omega;1-\omega;-\frac{1}{2}e^{-i\alpha}\frac{l_1}{l_2}(\xi_1+1)\right)$$

Defining

$$I_{13}{}^{S}=-\left[\cos(\alpha)\,\mathrm{Re}\left\{J_{13}{}^{S}\right\}-\sin(\alpha)\left\{J_{13}{}^{S}\right\}\right] \tag{B.88}$$

$$I_{13}{}^{B}=-\left[\cos(\alpha)\,\mathrm{Re}\left\{J_{13}{}^{B}\right\}-\sin(\alpha)\left\{J_{13}{}^{B}\right\}\right] \tag{B.89}$$

and letting $\xi_1 \to -1$, for ${I_{13}}^S$ we obtain

$$(1+\xi_1)^{-\omega} \cdot {I_{13}}^S \xrightarrow{\xi_1 \to -1} \pi 2^{-\frac{1}{2}} \frac{1}{\sin(\pi\omega)} \left(\frac{l_1}{l_2}\right)^{\omega} \left(\sum_{k=0}^{+\infty} \beta_k P_k^{(-\frac{1}{2},\omega)}(-1)\right) \cos(\alpha(1+\omega)) \quad \text{(B.90)}$$

considering the following trigonometry relation

$$\cos(\alpha\omega)\cos(\alpha) - \sin(\alpha\omega)\sin(\alpha) = \cos(\alpha(1+\omega)) \quad \text{(B.91)}$$

while for ${I_{13}}^B$ we obtain

$${I_{13}}^B \xrightarrow{\xi_1 \to -1} -2^{-\frac{1}{2}+\omega}\, \mathbf{\Gamma}(\omega) \left(\sum_{k=0}^{+\infty} \beta_k (-1)^k \frac{\mathbf{\Gamma}\left(k+1-\frac{1}{2}\right)}{\mathbf{\Gamma}\left(k+1-\frac{1}{2}+\omega\right)}\right) \cos\alpha \quad \text{(B.92)}$$

B.3.2 Crack section 2

Integral I_{21}

Using the same procedure adopted for the integral I_{11}

$$I_{21} = \int_{-1}^{+1} \frac{\rho_2(\xi_2')d\xi_2'}{\xi_2 - \xi_2'} = {I_{21}}^S + {I_{21}}^B \quad \text{(B.93)}$$

where

$$\begin{aligned} {I_{21}}^S &= -\pi\,(1-\xi_2)^{-\frac{1}{2}}\,(1+\xi_2)^{\omega}\cot(\pi\omega)\sum_{k=0}^{+\infty}\beta_k P_k^{(-\frac{1}{2},\omega)}(\xi_2) \\ {I_{21}}^B &= 2^{-\frac{1}{2}+\omega}\,\mathbf{\Gamma}(\omega)\sum_{k=0}^{+\infty}\beta_k(-1)^k \frac{\mathbf{\Gamma}\left(k+1-\frac{1}{2}\right)}{\mathbf{\Gamma}\left(k+1-\frac{1}{2}+\omega\right)}\, F\left(k+1,-k+\frac{1}{2}-\omega;1-\omega;\frac{1}{2}(1+\xi_2)\right) \end{aligned} \quad \text{(B.94)}$$

Letting $\xi_2 \to -1$ we obtain

$$(1+\xi_2)^{-\omega}\cdot{I_{21}}^S \xrightarrow{\xi_2 \to -1} -\pi 2^{-\frac{1}{2}}\cot(\pi\omega)\sum_{k=0}^{+\infty}\beta_k P_k^{(-\frac{1}{2},\omega)}(-1) \quad \text{(B.95)}$$

$${I_{21}}^B \xrightarrow{\xi_2 \to -1} 2^{-\frac{1}{2}+\omega}\,\mathbf{\Gamma}(\omega)\sum_{k=0}^{+\infty}\beta_k(-1)^k \frac{\mathbf{\Gamma}\left(k+1-\frac{1}{2}\right)}{\mathbf{\Gamma}\left(k+1-\frac{1}{2}+\omega\right)} \quad \text{(B.96)}$$

Integral I_{22}

This integral can be so expressed

$$I_{22} = \int_{-1}^{+1} \frac{\rho_2(\xi_2^{'})d\xi_2^{'}}{\xi_2 + \xi_2^{'} + 2} = -\int_{-1}^{+1} \frac{\rho_2(\xi_2^{'})d\xi_2^{'}}{z_2\left(\xi_2\right) - \xi_2^{'}}, \qquad z_2(\xi_2) = -1 - (\xi_2 + 1) \tag{B.97}$$

So using the integral relation (B.68) and equation (B.69), we obtain

$$I_{22} = {I_{22}}^S + {S_{22}}^B \tag{B.98}$$

where

$$\begin{aligned} {I_{22}}^S &= (1-\xi_2)^{-\frac{1}{2}} (1+\xi_2)^{\omega} \frac{\pi}{\sin(\pi\omega)} \sum_{k=0}^{+\infty} \beta_k P_k^{(-\frac{1}{2},\omega)}(-1-(\xi_2+1)) \\ {I_{22}}^B &= -2^{-\frac{1}{2}+\omega}\, \mathbf{\Gamma}(\omega) \sum_{k=0}^{+\infty} \beta_k (-1)^k \frac{\mathbf{\Gamma}\left(k+1-\frac{1}{2}\right)}{\mathbf{\Gamma}\left(k+1-\frac{1}{2}+\omega\right)} F\left(k+1, -k+\frac{1}{2}-\omega; 1-\omega; -\frac{1}{2}(1+\xi_2)\right) \end{aligned} \tag{B.99}$$

Letting $\xi_2 \to -1$, we obtain

$$(1+\xi_2)^{-\omega} \cdot {I_{22}}^S \xrightarrow{\xi_2 \to -1} \pi 2^{-\frac{1}{2}} \frac{1}{\sin(\pi\omega)} \sum_{k=0}^{+\infty} \beta_k P_k^{(-\frac{1}{2},\omega)}(-1) \tag{B.100}$$

$${I_{22}}^B \xrightarrow{\xi_2 \to -1} -2^{-\frac{1}{2}+\omega}\, \mathbf{\Gamma}(\omega) \sum_{k=0}^{+\infty} \beta_k (-1)^k \frac{\mathbf{\Gamma}\left(k+1-\frac{1}{2}\right)}{\mathbf{\Gamma}\left(k+1-\frac{1}{2}+\omega\right)} \tag{B.101}$$

Integral I_{23}

The integral can be rewritten in the following way

$$\begin{aligned} I_{23} &= \int_{-1}^{+1} \frac{(\xi_1^{'}+1)\cos\alpha + \dfrac{l_2}{l_1}(\xi_2+1)}{(\xi_1^{'}+1)^2 \sin^2\alpha + \left((\xi_1^{'}+1)\cos\alpha + \dfrac{l_2}{l_1}(\xi_2+1)\right)^2} \rho_1(\xi_1^{'}) d\xi_1^{'} \\ &= -\left(\hat{A}_2 \int_{-1}^{+1} \frac{\rho_1(\xi_1^{'})d\xi_1^{'}}{\hat{z}_2\left(\xi_1\right) - \xi_1^{'}} + \overline{\hat{A}_2} \int_{-1}^{+1} \frac{\rho_1(\xi_1^{'})d\xi_1^{'}}{\overline{\hat{z}_2}\left(\xi_2\right) - \xi_1^{'}} + \right) \\ &= -\Big[\cos\alpha\ \mathrm{Re}\left\{J_{23}\right\} + \sin\alpha\ \mathrm{Im}\left\{J_{23}\right\} \Big] \end{aligned} \tag{B.102}$$

where

$$J_{23} = \int_{-1}^{+1} \frac{\rho_1(\xi_1^{'})d\xi_1^{'}}{\hat{z}_2\left(\xi_2\right) - \xi_1^{'}}, \qquad \begin{cases} \hat{A}_2 = \dfrac{1}{2} e^{-i\alpha} \\ \hat{z}_2(\xi_2) = -1 - e^{-i\alpha} \dfrac{l_2}{l_1}(\xi_2+1) \end{cases} \tag{B.103}$$

The point $\hat{z}_2$ is not on the cut of the complex plane, so using (A.5) we obtain

$$\int_{-1}^{+1} \frac{\rho_1(\xi_1^{'})d\xi_1^{'}}{\hat{z}_2\left(\xi_2\right)-\xi_1^{'}} = 2\left(\hat{z}_2\left(\xi_2\right)-1\right)^{-\frac{1}{2}}\left(\hat{z}_2\left(\xi_2\right)+1\right)^{\omega}\sum_{k=0}^{+\infty}\gamma_k Q_k^{\left(-\frac{1}{2},\omega\right)}\left(\hat{z}_1\left(\xi_2\right)\right) \tag{B.104}$$

Using (B.69), the solution can be so expressed

$$J_{23} = {J_{23}}^S + {J_{23}}^B \tag{B.105}$$

where

$${J_{23}}^S = -e^{-i\alpha\omega}\left(2+\frac{l_2}{l_1}e^{-i\alpha}\left(\xi_2+1\right)\right)^{-\frac{1}{2}}\left[\frac{l_2}{l_1}\left(\xi_2+1\right)\right]^{\omega}\frac{\pi}{\sin(\pi\omega)}\sum_{k=0}^{+\infty}\gamma_k P_k^{\left(-\frac{1}{2},\omega\right)}\left(-1-e^{-i\alpha}\frac{l_2}{l_1}\left(\xi_2+1\right)\right)$$

$${J_{23}}^B = 2^{-\frac{1}{2}+\omega}\,\mathbf{\Gamma}(\omega)\sum_{k=0}^{+\infty}\gamma_k(-1)^k\frac{\mathbf{\Gamma}(k+1-\frac{1}{2})}{\mathbf{\Gamma}(k+1-\frac{1}{2}+\omega)}\,F\left(k+1,-k+\frac{1}{2}-\omega;1-\omega;-\frac{1}{2}e^{-i\alpha}\frac{l_2}{l_1}(\xi_2+1)\right)$$

Now if we define

$${I_{23}}^S = -\left[\cos(\alpha)\,\mathrm{Re}\left\{{J_{23}}^S\right\}-\sin(\alpha)\left\{{J_{23}}^S\right\}\right] \tag{B.106}$$

$${I_{23}}^B = -\left[\cos(\alpha)\,\mathrm{Re}\left\{{J_{23}}^B\right\}-\sin(\alpha)\left\{{J_{23}}^B\right\}\right] \tag{B.107}$$

Letting $\xi_2 \to -1$, for ${I_{23}}^S$ we obtain

$$(1+\xi_2)^{-\omega}\cdot{I_{23}}^S \xrightarrow{\xi_2\to-1} \pi 2^{-\frac{1}{2}}\frac{1}{\sin(\pi\omega)}\left(\frac{l_2}{l_1}\right)^{\omega}\left(\sum_{k=0}^{+\infty}\gamma_k P_k^{(-\frac{1}{2},\omega)}(-1)\right)\cos(\alpha(1+\omega)) \tag{B.108}$$

using the trigonometry relation

$$\cos(\alpha\omega)\cos(\alpha)-\sin(\alpha\omega)\sin(\alpha)=\cos(\alpha(1+\omega)) \tag{B.109}$$

For the bounded term ${I_{23}}^B$, we obtain

$${I_{23}}^B \xrightarrow{\xi_2\to-1} -2^{-\frac{1}{2}+\omega}\,\mathbf{\Gamma}(\omega)\left(\sum_{k=0}^{+\infty}\gamma_k(-1)^k\frac{\mathbf{\Gamma}\left(k+1-\frac{1}{2}\right)}{\mathbf{\Gamma}\left(k+1-\frac{1}{2}+\omega\right)}\right)\cos\alpha \tag{B.110}$$

B.4 Numerical solution

B.4.1 Evaluation of $R_{ij}(k,n)$ coefficients

The integrals $R_{ij}(k,n)$ can be rewritten in the following way

$$\begin{aligned}
&R_{11}(k,n) = \\
&\quad = \int_{-1}^{+1} U_k(\xi_1)\sqrt{1-\xi_1^2}\left(A_{11}\int_{-1}^{+1}\frac{d\xi_1^{'}}{\sqrt{1-\xi_1^{'2}}}\frac{T_n(\xi_1^{'})}{\xi_1^{'}+\upsilon_{11}} + \overline{A_{11}}\int_{-1}^{+1}\frac{d\xi_1^{'}}{\sqrt{1-\xi_1^{'2}}}\frac{T_n(\xi_1^{'})}{\xi_1^{'}+\overline{\upsilon_{11}}}\right)d\xi_1 \\
&R_{12}(k,n) = \\
&\quad = \int_{-1}^{+1} U_k(\xi_1)\sqrt{1-\xi_1^2}\left(A_{12}\int_{-1}^{+1}\frac{d\xi_2^{'}}{\sqrt{1-\xi_2^{'2}}}\frac{T_n(\xi_2^{'})}{\xi_2^{'}+\upsilon_{12}} + \overline{A_{12}}\int_{-1}^{+1}\frac{d\xi_1^{'}}{\sqrt{1-\xi_2^{'2}}}\frac{T_n(\xi_2^{'})}{\xi_2^{'}+\overline{\upsilon_{12}}}\right)d\xi_1 \\
&R_{21}(k,n) = \\
&\quad = \int_{-1}^{+1} U_k(\xi_2)\sqrt{1-\xi_2^2}\left(A_{21}\int_{-1}^{+1}\frac{d\xi_1^{'}}{\sqrt{1-\xi_1^{'2}}}\frac{T_n(\xi_1^{'})}{\xi_1^{'}+\upsilon_{21}} + \overline{A_{21}}\int_{-1}^{+1}\frac{d\xi_1^{'}}{\sqrt{1-\xi_1^{'2}}}\frac{T_n(\xi_1^{'})}{\xi_1^{'}+\overline{\upsilon_{21}}}\right)d\xi_2 \\
&R_{22}(k,n) = \\
&\quad = \int_{-1}^{+1} U_k(\xi_2)\sqrt{1-\xi_2^2}\left(\int_{-1}^{+1}\frac{d\xi_2^{'}}{\sqrt{1-\xi_2^{'2}}}\frac{T_n(\xi_2^{'})}{\xi_2^{'}+\upsilon_{22}}\right)d\xi_2
\end{aligned} \tag{B.111}$$

where

$$\begin{aligned}
A_{11} &= \frac{1}{2}e^{2i\alpha}, & \upsilon_{11} &= 1 + e^{2i\alpha}(\xi_1+1) \\
A_{12} &= \frac{1}{2}e^{-i\alpha}, & \upsilon_{12} &= 1 + \frac{l_1}{l_2}e^{-i\alpha}(\xi_1+1) \\
A_{21} &= \frac{1}{2}e^{-i\alpha}, & \upsilon_{21} &= 1 + \frac{l_2}{l_1}e^{-i\alpha}(\xi_2+1) \\
& & \upsilon_{22} &= \xi_2 + 2
\end{aligned}$$

We are using the non-dimensional variables $\xi, \xi' \in (-1,1)$, so we can consider the following changes of variable

$$\begin{cases} \xi^{'} = \cos(\theta) \\ \xi \ = \cos(\varphi) \end{cases} \tag{B.112}$$

Using (B.112) in (B.111), we obtain

$$R_{11}(k,n) = \int_0^\pi \sin((k+1)\varphi)\sin(\varphi)\left(A_{11}\int_0^\pi \frac{\cos(n\theta)d\theta}{\cos(\theta)+\upsilon_{11}} + \overline{A_{11}}\int_0^\pi \frac{\cos(n\theta)d\theta}{\cos(\theta)+\overline{\upsilon_{11}}}\right)d\varphi$$
$$= \int_0^\pi \sin((k+1)\varphi)\sin(\varphi)J_{11}(\varphi,n)d\varphi$$

$$R_{12}(k,n) = \int_0^\pi \sin((k+1)\varphi)\sin(\varphi)\left(A_{12}\int_0^\pi \frac{\cos(n\theta)d\theta}{\cos(\theta)+\upsilon_{12}} + \overline{A_{12}}\int_0^\pi \frac{\cos(n\theta)d\theta}{\cos(\theta)+\overline{\upsilon_{12}}}\right)d\varphi$$
$$= \int_0^\pi \sin((k+1)\varphi)\sin(\varphi)J_{12}(\varphi,n)d\varphi$$

$$R_{21}(k,n) = \int_0^\pi \sin((k+1)\varphi)\sin(\varphi)\left(A_{21}\int_0^\pi \frac{\cos(n\theta)d\theta}{\cos(\theta)+\upsilon_{21}} + \overline{A_{21}}\int_0^\pi \frac{\cos(n\theta)d\theta}{\cos(\theta)+\overline{\upsilon_{21}}}\right)d\varphi$$
$$= \int_0^\pi \sin((k+1)\varphi)\sin(\varphi)J_{21}(\varphi,n)d\varphi$$

$$R_{22}(k,n) = \int_0^\pi \sin((k+1)\varphi)\sin(\varphi)\left(\int_0^\pi \frac{\cos(n\theta)d\theta}{\cos(\theta)+\upsilon_{22}}\right)d\varphi$$
$$= \int_0^\pi \sin((k+1)\varphi)\sin(\varphi)J_{22}(\varphi,n)d\varphi$$

where the integrals $J_{ij}(\varphi,n)$ can be solved analytically; in fact, if we take $z = e^{i\theta}$

$$\frac{1}{2i}\int_{z=|1|} \frac{\left(z^{2n}+1\right)dz}{z^n\left(z^2+2\upsilon_{ij}z+1\right)} = \frac{1}{2i}\left[\int_{z=|1|} \frac{z^n dz}{\left(z^2+2\upsilon_{ij}z+1\right)} + \int_{z=|1|} \frac{dz}{z^n\left(z^2+2\upsilon_{ij}z+1\right)}\right] \quad \text{(B.113)}$$

both the integrals can be evaluated using the residual theorem.
In the first integral, the integrand function $f_1(z)$ has only one singular point inside the unit circle

$$z_1 = -\upsilon_{ij} + \sqrt{\upsilon_{ij}^2 - 1} \quad \text{(B.114)}$$

This singularity is a simple pole and the corresponding residual is equal to

$$Res\left[f_1(z), z_1\right] = \frac{\left(-\upsilon_{ij} + \sqrt{\upsilon_{ij}^2-1}\right)^n}{2\sqrt{\upsilon_{ij}^2-1}} \quad \text{(B.115)}$$

Considering the second integral, in this case we have two singular points, a pole of order n in $z = 0$ and a simple pole in z_1. It's easy to verify that for every n, the sum of the corresponding residuals is equal to $Res\left[f_1(z), z_1\right]$ and so we obtain that

$$\frac{1}{2i}\int_{z=|1|} \frac{\left(z^{2n}+1\right)dz}{z^n\left(z^2+2\upsilon_{ij}z+1\right)} = \pi\frac{\left(-\upsilon_{ij} + \sqrt{\upsilon_{ij}^2-1}\right)^n}{\sqrt{\upsilon_{ij}^2-1}} \quad \text{(B.116)}$$

The integrals $J_{ij}(\varphi, n)$ are here reported

$$
\begin{aligned}
&J_{11}(\varphi,n) = \\
&\quad = \frac{1}{2}\left[e^{2i\alpha}\left(\frac{1}{2i}\int_{z=|1|}\frac{\left(z^{2n}+1\right)dz}{z^n\left(z^2+2\upsilon_{11}z+1\right)}\right)+e^{-2i\alpha}\left(\frac{1}{2i}\int_{z=|1|}\frac{\left(z^{2n}+1\right)dz}{z^n\left(z^2+2\overline{\upsilon_{11}}z+1\right)}\right)\right] \\
&\quad = \pi\left[\cos(2\alpha)\,\mathrm{Re}\left\{\frac{\left(-\upsilon_{11}+\sqrt{\upsilon_{11}^2-1}\right)^n}{\sqrt{\upsilon_{11}^2-1}}\right\}-\sin(2\alpha)\,\mathrm{Im}\left\{\frac{\left(-\upsilon_{11}+\sqrt{\upsilon_{11}^2-1}\right)^n}{\sqrt{\upsilon_{11}^2-1}}\right\}\right]
\end{aligned}
$$

$$
\begin{aligned}
&J_{12}(\varphi,n) = \\
&\quad = \frac{1}{2}\left[e^{-i\alpha}\left(\frac{1}{2i}\int_{z=|1|}\frac{\left(z^{2n}+1\right)dz}{z^n\left(z^2+2\upsilon_{12}z+1\right)}\right)+e^{i\alpha}\left(\frac{1}{2i}\int_{z=|1|}\frac{\left(z^{2n}+1\right)dz}{z^n\left(z^2+2\overline{\upsilon_{12}}z+1\right)}\right)\right] \\
&\quad = \pi\left[\cos\alpha\,\mathrm{Re}\left\{\frac{\left(-\upsilon_{12}+\sqrt{\upsilon_{12}^2-1}\right)^n}{\sqrt{\upsilon_{12}^2-1}}\right\}+\sin\alpha\,\mathrm{Im}\left\{\frac{\left(-\upsilon_{12}+\sqrt{\upsilon_{12}^2-1}\right)^n}{\sqrt{\upsilon_{12}^2-1}}\right\}\right]
\end{aligned}
$$

$$
\begin{aligned}
&J_{21}(\varphi,n) = \\
&\quad = \frac{1}{2}\left[e^{-i\alpha}\left(\frac{1}{2i}\int_{z=|1|}\frac{\left(z^{2n}+1\right)dz}{z^n\left(z^2+2\upsilon_{21}z+1\right)}\right)+e^{i\alpha}\left(\frac{1}{2i}\int_{z=|1|}\frac{\left(z^{2n}+1\right)dz}{z^n\left(z^2+2\overline{\upsilon_{21}}z+1\right)}\right)\right] \\
&\quad = \pi\left[\cos\alpha\,\mathrm{Re}\left\{\frac{\left(-\upsilon_{21}+\sqrt{\upsilon_{21}^2-1}\right)^n}{\sqrt{\upsilon_{21}^2-1}}\right\}+\sin\alpha\,\mathrm{Im}\left\{\frac{\left(-\upsilon_{21}+\sqrt{\upsilon_{21}^2-1}\right)^n}{\sqrt{\upsilon_{21}^2-1}}\right\}\right]
\end{aligned}
$$

$$
\begin{aligned}
&J_{22}(\varphi,n) = \\
&\quad = \int_{z=|1|}\frac{z^n dz}{i\left(z^2+2\upsilon_{11}z+1\right)} = \pi\frac{\left(-\upsilon_{22}+\sqrt{\upsilon_{22}^2-1}\right)^n}{\sqrt{\upsilon_{22}^2-1}}
\end{aligned}
$$

Appendix C

Details about fault branching model

C.1 Stress drop evaluation

C.1.1 Contribution of section 1b on section 1a

To evaluate $(\sigma_{n_a y})_1^I$, we use the following relation

$$(\sigma_{n_a y})_1^I (S_a; S_{0b}) = \cos\alpha_{1a} (\sigma_{xy})_1^I (S_a; S_{0b}) - \sin\alpha_{1a} (\sigma_{zy})_1^I (S_a; S_{0b}) \tag{C.1}$$

Given that

$$\begin{cases} x = -S_a \sin\alpha_{1a} \\ z = -S_a \cos\alpha_{1a} \end{cases} \tag{C.2}$$

stress components $(\sigma_{xy})_1^I$, $(\sigma_{zy})_1^I$ can be written in this form

$$\begin{aligned} (\sigma_{xy})_1^I(S_a; S_{0b}) = \\ = -\frac{\mu_1}{2\pi} \Bigg\{ & \frac{S_a\cos\alpha_{1a} - S_{0b}\cos\alpha_{1b}}{R^2} - \Gamma\frac{S_a\cos\alpha_{1a} + S_{0b}\cos\alpha_{1b}}{T_0^2} \\ & + \sum_{n=1}^{\infty} \Gamma^n \Bigg[-\Gamma\frac{S_a\cos\alpha_{1a} + S_{0b}\cos\alpha_{1b} + 2nH}{T^2} + \frac{S_a\cos\alpha_{1a} - S_{0b}\cos\alpha_{1b} - 2nH}{V^2} \\ & + \frac{S_a\cos\alpha_{1a} - S_{0b}\cos\alpha_{1b} + 2nH}{U^2} - \Gamma^{-1}\frac{S_a\cos\alpha_{1a} + S_{0b}\cos\alpha_{1b} - 2nH}{W^2} \Bigg] \Bigg\} \end{aligned} \tag{C.3}$$

$$(\sigma_{zy})_1^I (S_a; S_{0b}) = \frac{\mu_1}{2\pi} (S_a \sin\alpha_{1a} - S_{0b} \sin\alpha_{1b}) \left\{ \frac{1}{R^2} - \frac{\Gamma}{T_0^2} + \sum_{n=1}^{\infty} \Gamma^n \left[-\frac{\Gamma}{T^2} + \frac{1}{V^2} + \frac{1}{U^2} - \frac{\Gamma^{-1}}{W^2} \right] \right\} \tag{C.4}$$

where

$$\begin{cases} R^2 = (S_a \sin\alpha_{1a} - S_{0b}\sin\alpha_{1b})^2 + (S_a\cos\alpha_{1a} - S_{0b}\cos\alpha_{1b})^2 \\ T_0^2 = (S_a \sin\alpha_{1a} - S_{0b}\sin\alpha_{1b})^2 + (S_a\cos\alpha_{1a} + S_{0b}\cos\alpha_{1b})^2 \\ T^2 = (S_a \sin\alpha_{1a} - S_{0b}\sin\alpha_{1b})^2 + (S_a\cos\alpha_{1a} + S_{0b}\cos\alpha_{1b} + 2nH)^2 \\ V^2 = (S_a \sin\alpha_{1a} - S_{0b}\sin\alpha_{1b})^2 + (S_a\cos\alpha_{1a} - S_{0b}\cos\alpha_{1b} - 2nH)^2 \\ U^2 = (S_a \sin\alpha_{1a} - S_{0b}\sin\alpha_{1b})^2 + (S_a\cos\alpha_{1a} - S_{0b}\cos\alpha_{1b} + 2nH)^2 \\ W^2 = (S_a \sin\alpha_{1a} - S_{0b}\sin\alpha_{1b})^2 + (S_a\cos\alpha_{1a} + S_{0b}\cos\alpha_{1b} - 2nH)^2 \end{cases}$$

Evaluating $(\sigma_{n_a y})_1^I$ we obtain this expression

$$\begin{aligned} &(\sigma_{n_a y})_1^I (S_a; S_{0b}) = \\ &\quad = -\frac{\mu_1}{2\pi}\left\{ \frac{S_a - S_{0b}\cos(\alpha_{1a}-\alpha_{1b})}{(S_a\sin\alpha_{1a} - S_{0b}\sin\alpha_{1b})^2 + (S_a\cos\alpha_{1a} - S_{0b}\cos\alpha_{1b})^2} \right. \\ &\qquad \left. -\Gamma\frac{S_a + S_{0b}\cos(\alpha_{1a}+\alpha_{1b})}{(S_a\sin\alpha_{1a} - S_{0b}\sin\alpha_{1b})^2 + (S_a\cos\alpha_{1a} + S_{0b}\cos\alpha_{1b})^2} + R_{1a,1b}(S_a; S_{0b}) \right\} \end{aligned}$$

where $R_{1a,1b}(S_a; S_{0b})$ has the following form

$$\begin{aligned} &R_{1a,1b}(S_a; S_{0b}) = \\ &= \sum_{n=1}^{\infty}\Gamma^n \left[-\Gamma\frac{S_a + S_{0b}\cos(\alpha_{1a}+\alpha_{1b}) + 2nH\cos\alpha_{1a}}{T^2} + \frac{S_a - S_{0b}\cos(\alpha_{1a}-\alpha_{1b}) - 2nH\cos\alpha_{1a}}{V^2} \right. \\ &\qquad \left. + \frac{S_a - S_{0b}\cos(\alpha_{1a}-\alpha_{1b}) + 2nH\cos\alpha_{1a}}{U^2} - \Gamma^{-1}\frac{S_a + S_{0b}\cos(\alpha_{1a}+\alpha_{1b}) - 2nH\cos\alpha_{1a}}{W^2} \right] \end{aligned}$$

The stress induced on section $1a$ due to slip on section 1b is equal to

$$\begin{aligned} &-\frac{2\pi}{\mu_1}\int_0^{2l_{1b}} (\sigma_{n_a y})_1^I (S_a; S_{0b})\rho_{1b}(S_{0b})dS_{0b} = \\ &\quad = \int_0^{2l_{1b}} \frac{S_a - S_{0b}\cos(\alpha_{1a}-\alpha_{1b})}{(S_a\sin\alpha_{1a} - S_{0b}\sin\alpha_{1b})^2 + (S_a\cos\alpha_{1a} - S_{0b}\cos\alpha_{1b})^2}\rho_{1b}(S_{0b})dS_{0b} \\ &\qquad - \Gamma\int_0^{2l_{1b}} \frac{S_a + S_{0b}\cos(\alpha_{1a}+\alpha_{1b})}{(S_a\sin\alpha_{1a} - S_{0b}\sin\alpha_{1b})^2 + (S_a\cos\alpha_{1a} + S_{0b}\cos\alpha_{1b})^2}\rho_{1b}(S_{0b})dS_{0b} \\ &\qquad + \int_0^{2l_{1b}} R_{1a,1b}(S_a; S_{0b})\rho_{1b}(S_{0b})dS_{0b} \end{aligned} \tag{C.5}$$

C.2 Study of asymptotic behaviour

C.2.1 Generalized Cauchy kernels

Integral $I_4{}^{1a}$

Consider the first further integral corresponding to a generalized Cauchy kernel

$$\int_{-1}^{+1} \frac{\frac{l_{1a}}{l_{1b}}(\xi_{1a}+1)-(\xi_{1b}^{'}+1)\cos(\alpha_{1a}-\alpha_{1b})}{\left(\frac{l_{1a}}{l_{1b}}(\xi_{1a}+1)\sin\alpha_{1a}-(\xi_{1b}^{'}+1)\sin\alpha_{1b}\right)^2+\left(\frac{l_{1a}}{l_{1b}}(\xi_{1a}+1)\cos\alpha_{1a}-(\xi_{1b}^{'}+1)\cos\alpha_{1b}\right)^2}\rho_{1b}(\xi_{1b}^{'})d\xi_{1b}^{'} \tag{C.6}$$

We try to split the integral in the following way

$$\frac{\frac{l_{1a}}{l_{1b}}(\xi_{1a}+1)-(\xi_{1b}^{'}+1)\cos(\alpha_{1a}-\alpha_{1b})}{\left(\frac{l_{1a}}{l_{1b}}(\xi_{1a}+1)\sin\alpha_{1a}-(\xi_{1b}^{'}+1)\sin\alpha_{1b}\right)^2+\left(\frac{l_{1a}}{l_{1b}}(\xi_{1a}+1)\cos\alpha_{1a}-(\xi_{1b}^{'}+1)\cos\alpha_{1b}\right)^2}=$$

$$=\frac{A_1}{\left(\frac{l_{1a}}{l_{1b}}(\xi_{1a}+1)\sin\alpha_{1a}-(\xi_{1b}^{'}+1)\sin\alpha_{1b}\right)-i\left(\frac{l_{1a}}{l_{1b}}(\xi_{1a}+1)\cos\alpha_{1a}-(\xi_{1b}^{'}+1)\cos\alpha_{1b}\right)}+$$
$$\frac{B_1}{\left(\frac{l_{1a}}{l_{1b}}(\xi_{1a}+1)\sin\alpha_{1a}-(\xi_{1b}^{'}+1)\sin\alpha_{1b}\right)+i\left(\frac{l_{1a}}{l_{1b}}(\xi_{1a}+1)\cos\alpha_{1a}-(\xi_{1b}^{'}+1)\cos\alpha_{1b}\right)}=$$

$$=\frac{\left[\left(\frac{l_{1a}}{l_{1b}}(\xi_{1a}+1)\sin\alpha_{1a}-(\xi_{1b}^{'}+1)\sin\alpha_{1b}\right)+i\left(\frac{l_{1a}}{l_{1b}}(\xi_{1a}+1)\cos\alpha_{1a}-(\xi_{1b}^{'}+1)\cos\alpha_{1b}\right)\right]A_1}{\left(\frac{l_{1a}}{l_{1b}}(\xi_{1a}+1)\sin\alpha_{1a}-(\xi_{1b}^{'}+1)\sin\alpha_{1b}\right)^2+\left(\frac{l_{1a}}{l_{1b}}(\xi_{1a}+1)\cos\alpha_{1a}-(\xi_{1b}^{'}+1)\cos\alpha_{1b}\right)^2}+ \tag{C.7}$$
$$\frac{\left[\left(\frac{l_{1a}}{l_{1b}}(\xi_{1a}+1)\sin\alpha_{1a}-(\xi_{1b}^{'}+1)\sin\alpha_{1b}\right)-i\left(\frac{l_{1a}}{l_{1b}}(\xi_{1a}+1)\cos\alpha_{1a}-(\xi_{1b}^{'}+1)\cos\alpha_{1b}\right)\right]B_1}{\left(\frac{l_{1a}}{l_{1b}}(\xi_{1a}+1)\sin\alpha_{1a}-(\xi_{1b}^{'}+1)\sin\alpha_{1b}\right)^2+\left(\frac{l_{1a}}{l_{1b}}(\xi_{1a}+1)\cos\alpha_{1a}-(\xi_{1b}^{'}+1)\cos\alpha_{1b}\right)^2}=$$

$$=\frac{\frac{l_{1a}}{l_{1b}}(\xi_{1a}+1)\left[e^{i\left(\frac{\pi}{2}-\alpha_{1a}\right)}A_1+e^{-i\left(\frac{\pi}{2}-\alpha_{1a}\right)}B_1\right]-(\xi_{1b}^{'}+1)\left[e^{i\left(\frac{\pi}{2}-\beta_{a}\right)}A_1+e^{-i\left(\frac{\pi}{2}-\beta_{a}\right)}B_1\right]}{\left(\frac{l_{1a}}{l_{1b}}(\xi_{1a}+1)\sin\alpha_{1a}-(\xi_{1b}^{'}+1)\sin\alpha_{1b}\right)^2+\left(\frac{l_{1a}}{l_{1b}}(\xi_{1a}+1)\cos\alpha_{1a}-(\xi_{1b}^{'}+1)\cos\alpha_{1b}\right)^2}$$

If we compare the first and the last raw of equation (C.7) we find that A_1, B_1 must satisfy this system

$$\begin{cases} e^{i\left(\frac{\pi}{2}-\alpha_{1a}\right)}A_1+e^{-i\left(\frac{\pi}{2}-\alpha_{1a}\right)}B_1=1 \\ \\ e^{i\left(\frac{\pi}{2}-\beta_{a}\right)}A_1+e^{-i\left(\frac{\pi}{2}-\beta_{a}\right)}B_1=\cos(\alpha_{1a}-\alpha_{1b}) \end{cases} \tag{C.8}$$

Solving the system, we find that coefficients A_1, B_1 are respectively

$$\begin{cases} A_1 = \frac{1}{2}e^{-i\left(\frac{\pi}{2}-\alpha_{1a}\right)} \\ \\ B_1 = \frac{1}{2}e^{i\left(\frac{\pi}{2}-\alpha_{1a}\right)} \end{cases} \tag{C.9}$$

We can now manipulate the term corresponding to A_1 in (C.7) and obtain

$$\begin{aligned} &\frac{A_1}{\left(\frac{l_{1a}}{l_{1b}}(\xi_{1a}+1)\sin\alpha_{1a} - (\xi'_{1b}+1)\sin\alpha_{1b}\right) - i\left(\frac{l_{1a}}{l_{1b}}(\xi_{1a}+1)\cos\alpha_{1a} - (\xi'_{1b}+1)\cos\alpha_{1b}\right)} = \\ &\frac{A_1}{\frac{l_{1a}}{l_{1b}}(\xi_{1a}+1)(\sin\alpha_{1a} - i\cos\alpha_{1a}) - (\xi'_{1b}+1)(\sin\alpha_{1b} - i\cos\alpha_{1b})} = \\ &\frac{-A_1 e^{i\left(\frac{\pi}{2}-\alpha_{1b}\right)}}{\xi'_{1b}+1-\frac{l_{1a}}{l_{1b}}e^{i(\alpha_{1a}-\alpha_{1b})}(\xi_{1a}+1)} = \\ &\frac{A'_1}{\xi'_{1b} - z_1(\xi_{1a})} \end{aligned} \tag{C.10}$$

where

$$\begin{cases} A'_1 = -A_1 e^{i\left(\frac{\pi}{2}-\alpha_{1b}\right)} = -\frac{1}{2}e^{i(\alpha_{1a}-\alpha_{1b})} = \frac{1}{2}e^{i(\pi+\alpha_{1a}-\alpha_{1b})} \\ \\ z_1(\xi_{1a}) = -1 - \frac{l_{1a}}{l_{1b}}(\xi_{1a}+1)e^{i(\pi+\alpha_{1a}-\alpha_{1b})} \end{cases} \tag{C.11}$$

Using the same procedure, we can now rewrite the term corresponding to B_1

$$\begin{aligned} &\frac{B_1}{\left(\frac{l_{1a}}{l_{1b}}(\xi_{1a}+1)\sin\alpha_{1a} - (\xi'_{1b}+1)\sin\alpha_{1b}\right) + i\left(\frac{l_{1a}}{l_{1b}}(\xi_{1a}+1)\cos\alpha_{1a} - (\xi'_{1b}+1)\cos\alpha_{1b}\right)} = \\ &\frac{B_1}{\frac{l_{1a}}{l_{1b}}(\xi_{1a}+1)(\sin\alpha_{1a} + i\cos\alpha_{1a}) - (\xi'_{1b}+1)(\sin\alpha_{1b} + i\cos\alpha_{1b})} = \\ &\frac{-B_1 e^{-i\left(\frac{\pi}{2}-\alpha_{1b}\right)}}{\xi'_{1b}+1-\frac{l_{1a}}{l_{1b}}e^{-i(\alpha_{1a}-\alpha_{1b})}(\xi_{1a}+1)} = \\ &\frac{B'_1}{\xi'_{1b} - (z_{1a})_{II}(\xi_{1a})} \end{aligned} \tag{C.12}$$

where

$$\begin{cases} B'_1 = -B_1 e^{-i\left(\frac{\pi}{2}-\alpha_{1b}\right)} = -\frac{1}{2}e^{-i(\alpha_{1a}-\alpha_{1b})} = \frac{1}{2}e^{-i(\pi+\alpha_{1a}-\alpha_{1b})} = \overline{A'_1} \\ \\ z_2(\xi_{1a}) = -1 - \frac{l_{1a}}{l_{1b}}(\xi_{1a}+1)e^{-i(\pi+\alpha_{1a}-\alpha_{1b})} = \overline{z_1}(\xi_{1a}) \end{cases} \tag{C.13}$$

We have found that the integral ${I_4}^{1a}$ can be expressed in the following way

$$\int_{-1}^{+1} \frac{\frac{l_{1a}}{l_{1b}}(\xi_{1a}+1)-(\xi_{1b}^{'}+1)\cos(\alpha_{1a}-\alpha_{1b})}{\left(\frac{l_{1a}}{l_{1b}}(\xi_{1a}+1)\sin\alpha_{1a}-(\xi_{1b}^{'}+1)\sin\alpha_{1b}\right)^2+\left(\frac{l_{1a}}{l_{1b}}(\xi_{1a}+1)\cos\alpha_{1a}-(\xi_{1b}^{'}+1)\cos\alpha_{1b}\right)^2}\rho_{1b}(\xi_{1b}^{'})d\xi_{1b}^{'}=$$
$$=A_1^{'}\int_{-1}^{+1}\frac{\rho_{1b}(\xi_{1b}^{'})d\xi_{1b}^{'}}{\xi_{1b}^{'}-z_1(\xi_{1a})}+\overline{A_1^{'}}\int_{-1}^{+1}\frac{\rho_{1b}(\xi_{1b}^{'})d\xi_{1b}^{'}}{\xi_{1b}^{'}-\overline{z_1}(\xi_{1a})} \tag{C.14}$$

The asymptotic behaviour of these integrals can be evaluated defining

$$\frac{1}{\pi}\int_{-1}^{1}\frac{\rho(\xi')}{\xi'-z_1(\xi_1)}\,d\xi'=\Phi(z_1) \tag{C.15}$$
$$\frac{1}{\pi}\int_{-1}^{1}\frac{\rho(\xi')}{\xi'-\overline{z_1}(\xi_1)}\,d\xi'=\Phi(\overline{z_1}) \tag{C.16}$$

Substituting $z_1+1=-1+e^{i\pi}\frac{l_{1a}}{l_{1b}}(\xi_{1a}+1)e^{i(\pi+\alpha_{1a}-\alpha_{1b})}$ for (C.15) and $\overline{z_1}+1$ for (C.16) in equation (4.23) we obtain

$$\Phi(z_1(\xi_{1a}))=-R_{1b}(-1)2^{a_{1b}}\frac{1}{\sin(\pi b_{1b})}\left[\frac{l_{1a}}{l_{1b}}(\xi_{1a}+1)\right]^{b_{1b}}e^{i(\pi+\alpha_{1a}-\alpha_{1b})b_{1b}}+F_1^{'}(\xi_{1a}) \tag{C.17}$$
$$\Phi(\overline{z_1}(\xi_{1a}))=-R_{1b}(-1)2^{a_{1b}}\frac{1}{\sin(\pi b_{1b})}\left[\frac{l_{1a}}{l_{1b}}(\xi_{1a}+1)\right]^{b_{1b}}e^{-i(\pi+\alpha_{1a}-\alpha_{1b})b_{1b}}+F_1^{''}(\xi_{1a}) \tag{C.18}$$

where the behaviour of F_1', F_1'' near $\xi_{1a}=-1$ is similar to that of Φ_0.
Combining this results as indicated by equation (C.14) we find the asymptotic evaluation corresponding to ${I_{14}}^{1a}$

$$-\frac{1}{\pi}\int_{-1}^{+1}\frac{\frac{l_{1a}}{l_{1b}}(\xi_{1a}+1)-(\xi_{1b}^{'}+1)\cos(\alpha_{1a}-\alpha_{1b})}{\left(\frac{l_{1a}}{l_{1b}}(\xi_{1a}+1)\sin\alpha_{1a}-(\xi_{1b}^{'}+1)\sin\alpha_{1b}\right)^2+\left(\frac{l_{1a}}{l_{1b}}(\xi_{1a}+1)\cos\alpha_{1a}-(\xi_{1b}^{'}+1)\cos\alpha_{1b}\right)^2}\rho_{1b}(\xi_{1b}^{'})d\xi_{1b}^{'}=$$
$$=-\left(A_1^{'}\Phi(z_1(\xi_{1a}))+\overline{A_1^{'}}\Phi(\overline{z_1}(\xi_{1a}))\right)=$$
$$=R_{1b}(-1)2^{a_{1b}}\frac{1}{\sin(\pi b_{1b})}\left[\frac{l_{1a}}{l_{1b}}(\xi_{1a}+1)\right]^{b_{1b}}\left[\frac{1}{2}\left(e^{i(\pi+\alpha_{1a}-\alpha_{1b})(1+b_{1b})}+e^{-i(\pi+\alpha_{1a}-\alpha_{1b})(1+b_{1b})}\right)\right]+F_1(\xi_{1a})=$$
$$=R_{1b}(-1)2^{a_{1b}}\frac{1}{\sin(\pi b_{1b})}\left[\frac{l_{1a}}{l_{1b}}(\xi_{1a}+1)\right]^{b_{1b}}\cos((\pi+\alpha_{1a}-\alpha_{1b})(1+b_{1b}))+F_1(\xi_{1a})=$$
$$=-R_{1b}(-1)2^{a_{1b}}\frac{1}{\sin(\pi b_{1b})}\left[\frac{l_{1a}}{l_{1b}}(\xi_{1a}+1)\right]^{b_{1b}}\cos(\pi b_{1b}+(\alpha_{1a}-\alpha_{1b})(1+b_{1b}))+F_1(\xi_{1a}) \tag{C.19}$$

where F_1 has behaviour near $\xi_1=-1$ similar to that of Φ_0, being a linear combination of F_1', F_1''.

Integral ${I_5}^{1a}$

Consider now the second of the further integral corresponding to a generalized Cauchy kernel

$$\int_{-1}^{+1} \frac{\frac{l_{1a}}{l_{1b}}(\xi_{1a}+1)+(\xi_{1b}^{'}+1)\cos(\alpha_{1a}+\alpha_{1b})}{\left(\frac{l_{1a}}{l_{1b}}(\xi_{1a}+1)\sin\alpha_{1a}-(\xi_{1b}^{'}+1)\sin\alpha_{1b}\right)^2+\left(\frac{l_{1a}}{l_{1b}}(\xi_{1a}+1)\cos\alpha_{1a}+(\xi_{1b}^{'}+1)\cos\alpha_{1b}\right)^2}\rho_{1b}(\xi_{1b}^{'})d\xi_{1b}^{'} \tag{C.20}$$

We split the integral kernel in the following way

$$\frac{\frac{l_{1a}}{l_{1b}}(\xi_{1a}+1)+(\xi_{1b}^{'}+1)\cos(\alpha_{1a}+\alpha_{1b})}{\left(\frac{l_{1a}}{l_{1b}}(\xi_{1a}+1)\sin\alpha_{1a}-(\xi_{1b}^{'}+1)\sin\alpha_{1b}\right)^2+\left(\frac{l_{1a}}{l_{1b}}(\xi_{1a}+1)\cos\alpha_{1a}+(\xi_{1b}^{'}+1)\cos\alpha_{1b}\right)^2}=$$

$$=\frac{A_2}{\left(\frac{l_{1a}}{l_{1b}}(\xi_{1a}+1)\sin\alpha_{1a}-(\xi_{1b}^{'}+1)\sin\alpha_{1b}\right)-i\left(\frac{l_{1a}}{l_{1b}}(\xi_{1a}+1)\cos\alpha_{1a}+(\xi_{1b}^{'}+1)\cos\alpha_{1b}\right)}+$$
$$\frac{B_2}{\left(\frac{l_{1a}}{l_{1b}}(\xi_{1a}+1)\sin\alpha_{1a}-(\xi_{1b}^{'}+1)\sin\alpha_{1b}\right)+i\left(\frac{l_{1a}}{l_{1b}}(\xi_{1a}+1)\cos\alpha_{1a}+(\xi_{1b}^{'}+1)\cos\alpha_{1b}\right)}=$$

$$=\frac{\left[\left(\frac{l_{1a}}{l_{1b}}(\xi_{1a}+1)\sin\alpha_{1a}-(\xi_{1b}^{'}+1)\sin\alpha_{1b}\right)+i\left(\frac{l_{1a}}{l_{1b}}(\xi_{1a}+1)\cos\alpha_{1a}+(\xi_{1b}^{'}+1)\cos\alpha_{1b}\right)\right]A_2}{\left(\frac{l_{1a}}{l_{1b}}(\xi_{1a}+1)\sin\alpha_{1a}-(\xi_{1b}^{'}+1)\sin\alpha_{1b}\right)^2+\left(\frac{l_{1a}}{l_{1b}}(\xi_{1a}+1)\cos\alpha_{1a}+(\xi_{1b}^{'}+1)\cos\alpha_{1b}\right)^2}+ \tag{C.21}$$
$$\frac{\left[\left(\frac{l_{1a}}{l_{1b}}(\xi_{1a}+1)\sin\alpha_{1a}-(\xi_{1b}^{'}+1)\sin\alpha_{1b}\right)-i\left(\frac{l_{1a}}{l_{1b}}(\xi_{1a}+1)\cos\alpha_{1a}+(\xi_{1b}^{'}+1)\cos\alpha_{1b}\right)\right]B_2}{\left(\frac{l_{1a}}{l_{1b}}(\xi_{1a}+1)\sin\alpha_{1a}-(\xi_{1b}^{'}+1)\sin\alpha_{1b}\right)^2+\left(\frac{l_{1a}}{l_{1b}}(\xi_{1a}+1)\cos\alpha_{1a}+(\xi_{1b}^{'}+1)\cos\alpha_{1b}\right)^2}=$$

$$=\frac{\frac{l_{1a}}{l_{1b}}(\xi_{1a}+1)\left[e^{i\left(\frac{\pi}{2}-\alpha_{1a}\right)}A_2+e^{-i\left(\frac{\pi}{2}-\alpha_{1a}\right)}B_2\right]+(\xi_{1b}^{'}+1)\left[e^{i\left(\frac{\pi}{2}+\alpha_{1b}\right)}A_2+e^{-i\left(\frac{\pi}{2}+\alpha_{1b}\right)}B_2\right]}{\left(\frac{l_{1a}}{l_{1b}}(\xi_{1a}+1)\sin\alpha_{1a}-(\xi_{1b}^{'}+1)\sin\alpha_{1b}\right)^2+\left(\frac{l_{1a}}{l_{1b}}(\xi_{1a}+1)\cos\alpha_{1a}+(\xi_{1b}^{'}+1)\cos\alpha_{1b}\right)^2}$$

Comparing the first and the last raw we find that A_2 and B_2 must satisfy the following conditions

$$\begin{cases} e^{i\left(\frac{\pi}{2}-\alpha_{1a}\right)}A_1+e^{-i\left(\frac{\pi}{2}-\alpha_{1a}\right)}B_1=1 \\ \\ e^{i\left(\frac{\pi}{2}+\beta_a\right)}A_1+e^{-i\left(\frac{\pi}{2}+\beta_a\right)}B_1=\cos(\alpha_{1a}+\alpha_{1b}) \end{cases} \tag{C.22}$$

Solving the system we can determine coefficients A_2, B_2

$$\begin{cases} A_2=\frac{1}{2}e^{-i\left(\frac{\pi}{2}-\alpha_{1a}\right)} \\ \\ B_2=\frac{1}{2}e^{i\left(\frac{\pi}{2}-\alpha_{1a}\right)} \end{cases} \tag{C.23}$$

The term corresponding to A can be rearranged in this way

$$\begin{aligned}
&\frac{A_2}{\left(\frac{l_{1a}}{l_{1b}}(\xi_{1a}+1)\sin\alpha_{1a}-(\xi_{1b}^{'}+1)\sin\alpha_{1b}\right)-i\left(\frac{l_{1a}}{l_{1b}}(\xi_{1a}+1)\cos\alpha_{1a}+(\xi_{1b}^{'}+1)\cos\alpha_{1b}\right)}=\\
&\frac{A_2}{\frac{l_{1a}}{l_{1b}}(\xi_{1a}+1)(\sin\alpha_{1a}-i\cos\alpha_{1a})-(\xi_{1b}^{'}+1)(\sin\alpha_{1b}+i\cos\alpha_{1b})}=\\
&\frac{-A_2e^{i\left(\frac{\pi}{2}-\alpha_{1b}\right)}}{\xi_{1b}^{'}+1+\frac{l_{1a}}{l_{1b}}e^{i(\alpha_{1a}+\alpha_{1b})}(\xi_{1a}+1)}=\\
&\frac{A_2^{'}}{\xi_{1b}^{'}-z_1(\xi_{1a})}
\end{aligned}\tag{C.24}$$

where

$$\begin{cases}
A_2^{'}=-A_2e^{-i\left(\frac{\pi}{2}-\alpha_{1b}\right)}=\dfrac{1}{2}e^{i(\alpha_{1a}+\alpha_{1b})}\\[2ex]
z_3(\xi_{1a})=-1-\dfrac{l_{1a}}{l_{1b}}(\xi_{1a}+1)e^{i(\alpha_{1a}+\alpha_{1b})}
\end{cases}\tag{C.25}$$

For the term corresponding to B we obtain the following expression

$$\begin{aligned}
&\frac{B_2}{\left(\frac{l_{1a}}{l_{1b}}(\xi_{1a}+1)\sin\alpha_{1a}-(\xi_{1b}^{'}+1)\sin\alpha_{1b}\right)+i\left(\frac{l_{1a}}{l_{1b}}(\xi_{1a}+1)\cos\alpha_{1a}+(\xi_{1b}^{'}+1)\cos\alpha_{1b}\right)}=\\
&\frac{B_2}{\frac{l_{1a}}{l_{1b}}(\xi_{1a}+1)(\sin\alpha_{1a}+i\cos\alpha_{1a})+(\xi_{1b}^{'}+1)(-\sin\alpha_{1b}+i\cos\alpha_{1b})}=\\
&\frac{B_2e^{-i\left(\frac{\pi}{2}+\alpha_{1b}\right)}}{\xi_{1b}^{'}+1+\frac{l_{1a}}{l_{1b}}e^{-i(\alpha_{1a}+\alpha_{1b})}(\xi_{1a}+1)}=\\
&\frac{B_2^{'}}{\xi_{1b}^{'}-z_4(\xi_{1a})}
\end{aligned}\tag{C.26}$$

where

$$\begin{cases}
B_2^{'}=B_2e^{-i\left(\frac{\pi}{2}+\alpha_{1b}\right)}=\dfrac{1}{2}e^{-i(\alpha_{1a}+\alpha_{1b})}=\overline{A_2^{'}}\\[2ex]
z_4(\xi_{1a})=-1-\dfrac{l_{1a}}{l_{1b}}(\xi_{1a}+1)e^{-i(\alpha_{1a}+\alpha_{1b})}=\overline{z_3}(\xi_{1a})
\end{cases}\tag{C.27}$$

We rewrite now ${I_5}^{1a}$ as the sum of the two generalized integral kernels found

$$\begin{aligned}
&\int_{-1}^{+1}\frac{\frac{l_{1a}}{l_{1b}}(\xi_{1a}+1)+(\xi_{1b}^{'}+1)\cos(\alpha_{1a}+\alpha_{1b})}{\left(\frac{l_{1a}}{l_{1b}}(\xi_{1a}+1)\sin\alpha_{1a}-(\xi_{1b}^{'}+1)\sin\alpha_{1b}\right)^2+\left(\frac{l_{1a}}{l_{1b}}(\xi_{1a}+1)\cos\alpha_{1a}+(\xi_{1b}^{'}+1)\cos\alpha_{1b}\right)^2}\rho_{1b}(\xi_{1b}^{'})d\xi_{1b}^{'}\\
&=A_2^{'}\int_{-1}^{+1}\frac{\rho_{1b}(\xi_{1b}^{'})d\xi_{1b}^{'}}{\xi_{1b}^{'}-z_3(\xi_{1a})}+\overline{A_2^{'}}\int_{-1}^{+1}\frac{\rho_{1b}(\xi_{1b}^{'})d\xi_{1b}^{'}}{\xi_{1b}^{'}-\overline{z_3}(\xi_{1a})}
\end{aligned}\tag{C.28}$$

The asymptotic behaviour of these integrals can be evaluated defining

$$\frac{1}{\pi}\int_{-1}^{1}\frac{\rho(\xi')}{\xi'-z_3(\xi_1)}\,d\xi' = \Phi(z_3) \tag{C.29}$$

$$\frac{1}{\pi}\int_{-1}^{1}\frac{\rho(\xi')}{\xi'-\overline{z_3}(\xi_1)}\,d\xi' = \Phi(\overline{z_3}) \tag{C.30}$$

Substituting $z_3+1 = -1+e^{i\pi}\dfrac{l_{1a}}{l_{1b}}(\xi_{1a}+1)e^{i(\alpha_{1a}+\alpha_{1b})}$ for (C.29) and $\overline{z_3}+1$ for (C.30) in equation (4.23) we obtain

$$\Phi(z_3(\xi_{1a})) = -R_{1b}(-1)2^{a_{1b}}\frac{1}{\sin(\pi b_{1b})}\left[\frac{l_{1a}}{l_{1b}}(\xi_{1a}+1)\right]^{b_{1b}} e^{i(\alpha_{1a}+\alpha_{1b})b_{1b}} + F_3^{'}(\xi_{1a}) \tag{C.31}$$

$$\Phi(\overline{z_3}(\xi_{1a})) = -R_{1b}(-1)2^{a_{1b}}\frac{1}{\sin(\pi b_{1b})}\left[\frac{l_{1a}}{l_{1b}}(\xi_{1a}+1)\right]^{b_{1b}} e^{-i(\alpha_{1a}+\alpha_{1b})b_{1b}} + F_3^{''}(\xi_{1a}) \tag{C.32}$$

where the behaviour of F_3', F_3'' near $\xi_{1a}=-1$ is similar to that of Φ_0.
Combining this results as indicated by equation (C.28) we find the asymptotic evaluation corresponding to ${I_1}_4^{1a}$

$$\begin{aligned}
&-\frac{1}{\pi}\int_{-1}^{+1}\frac{\dfrac{l_{1a}}{l_{1b}}(\xi_{1a}+1)+(\xi_{1b}^{'}+1)\cos(\alpha_{1a}+\alpha_{1b})}{\left(\dfrac{l_{1a}}{l_{1b}}(\xi_{1a}+1)\sin\alpha_{1a}-(\xi_{1b}^{'}+1)\sin\alpha_{1b}\right)^2+\left(\dfrac{l_{1a}}{l_{1b}}(\xi_{1a}+1)\cos\alpha_{1a}+(\xi_{1b}^{'}+1)\cos\alpha_{1b}\right)^2}\rho_{1b}(\xi_{1b}^{'})d\xi_{1b}^{'} = \\
&\quad = -\left(A_2^{'}\Phi(z_3(\xi_{1a}))+\overline{A_2^{'}}\Phi(\overline{z_3}(\xi_{1a}))\right) = \\
&\quad = R_{1b}(-1)2^{a_{1b}}\frac{1}{\sin(\pi b_{1b})}\left[\frac{l_{1a}}{l_{1b}}(\xi_{1a}+1)\right]^{b_{1b}}\left[\frac{1}{2}\left(e^{i(\alpha_{1a}+\alpha_{1b})(1+b_{1b})}+e^{-i(\alpha_{1a}+\alpha_{1b})(1+b_{1b})}\right)\right]+F_3(\xi_{1a}) = \\
&\quad = R_{1b}(-1)2^{a_{1b}}\frac{1}{\sin(\pi b_{1b})}\left[\frac{l_{1a}}{l_{1b}}(\xi_{1a}+1)\right]^{b_{1b}}\cos((\alpha_{1a}+\alpha_{1b})(1+b_{1b}))+F_3(\xi_{1a})
\end{aligned}$$

C.3 Stress drop condition

C.3.1 Integrale ${I_4}^{1a}$

The integral can be rewritten in the following form

$$\begin{aligned}
&\int_{-1}^{+1}\frac{\dfrac{l_{1a}}{l_{1b}}(\xi_{1a}+1)-(\xi_{1b}^{'}+1)\cos(\alpha_{1a}-\alpha_{1b})}{\left(\dfrac{l_{1a}}{l_{1b}}(\xi_{1a}+1)\sin\alpha_{1a}-(\xi_{1b}^{'}+1)\sin\alpha_{1b}\right)^2+\left(\dfrac{l_{1a}}{l_{1b}}(\xi_{1a}+1)\cos\alpha_{1a}-(\xi_{1b}^{'}+1)\cos\alpha_{1b}\right)^2}\rho_{1b}(\xi_{1b}^{'})d\xi_{1b}^{'} \\
&\quad = -\left(A_1^{'}\int_{-1}^{+1}\frac{\rho_{1b}(\xi_{1b}^{'})d\xi_{1b}^{'}}{z_1(\xi_{1a})-\xi_{1b}^{'}}+\overline{A_1^{'}}\int_{-1}^{+1}\frac{\rho_{1b}(\xi_{1b}^{'})d\xi_{1b}^{'}}{\overline{z_1}(\xi_{1a})-\xi_{1b}^{'}}\right)
\end{aligned}$$

$$= \cos(\alpha_{1a}-\alpha_{1b})\,\mathrm{Re}\left\{{J_4}^{1a}\right\}-\sin(\alpha_{1a}-\alpha_{1b})\,\mathrm{Im}\left\{{J_4}^{1a}\right\}$$

where

$${J_4}^{1a} = \int_{-1}^{+1}\frac{\rho_{1b}(\xi_{1b}^{'})d\xi_{1b}^{'}}{\xi_{1b}^{'}-z_1(\xi_{1a})}, \qquad \begin{cases} A_1^{'} = -\dfrac{1}{2}e^{i(\alpha_{1a}-\alpha_{1b})} \\ z_1(\xi_{1a}) = -1+\dfrac{l_{1a}}{l_{1b}}e^{i(\alpha_{1a}-\alpha_{1b})}(\xi_{1a}+1) \end{cases} \tag{C.33}$$

If $\alpha_{1a} \neq \alpha_{1b}$ the point $z_1(\xi_{1a})$ is not on the cut of the complex plane so we can proceed using the integral relation (A.5) without any further consideration

$$\int_{-1}^{+1} \frac{\rho_{1b}(\xi_{1b}^{'})d\xi_{1b}^{'}}{\xi_{1b}^{'} - z_1(\xi_{1a})} = 2\left(z_1\left(\xi_{1a}\right) - 1\right)^{-\frac{1}{2}}\left(z_1\left(\xi_{1a}\right) + 1\right)^{\omega} \sum_{k=0}^{+\infty} \gamma_k Q_k^{\left(-\frac{1}{2},\omega\right)}\left(z_1\left(\xi_{1a}\right)\right) \tag{C.34}$$

Then using relation (A.6) we can express the solution of the integral in this way

$$J_4{}^{1a} = J_4{}^{S} + J_4{}^{B} \tag{C.35}$$

where

$$\begin{aligned} J_4{}^{S} =& -e^{i(\pi+\alpha_{1a}-\alpha_{1b})\omega}\left(2 - e^{i(\alpha_{1a}-\alpha_{1b})}\frac{l_{1a}}{l_{1b}}\left(\xi_{1a}+1\right)\right)^{-\frac{1}{2}}\left[\left(\frac{l_{1a}}{l_{1b}}\right)\left(\xi_{1a}+1\right)\right]^{\omega}\frac{\pi}{\sin(\pi\omega)} \\ & \times \sum_{k=0}^{+\infty}\gamma_k P_k^{\left(-\frac{1}{2},\omega\right)}\left(-1 + e^{i(\alpha_{1a}-\alpha_{1b})}\frac{l_{1a}}{l_{1b}}\left(\xi_{1a}+1\right)\right) \\ J_4{}^{B} =& 2^{-\frac{1}{2}+\omega}\,\Gamma(\omega)\sum_{k=0}^{+\infty}\gamma_k(-1)^k\frac{\Gamma(k+1-\frac{1}{2})}{\Gamma(k+1-\frac{1}{2}+\omega)}\,F\left(k+1,-k+\frac{1}{2}-\omega;1-\omega;\frac{1}{2}e^{i(\alpha_{1a}-\alpha_{1b})}\frac{l_{1a}}{l_{1b}}(\xi_{1a}+1)\right) \end{aligned}$$

Defining

$$I_4{}^{S} = \cos(\alpha_{1a}-\alpha_{1b})\,\mathrm{Re}\left\{J_4{}^{S}\right\} - \sin(\alpha_{1a}-\alpha_{1b})\left\{J_4{}^{S}\right\} \tag{C.36}$$

$$I_4{}^{B} = \cos(\alpha_{1a}-\alpha_{1b})\,\mathrm{Re}\left\{J_4{}^{B}\right\} - \sin(\alpha_{1a}-\alpha_{1b})\left\{J_4{}^{B}\right\} \tag{C.37}$$

and letting $\xi_{1a} \to -1$, for $I_4{}^{S}$ we obtain

$$(1+\xi_{1a})^{-\omega}\cdot I_4{}^{S} \xrightarrow{\xi_{1a}\to-1} -\pi 2^{-\frac{1}{2}}\frac{1}{\sin(\pi\omega)}\left(\frac{l_{1a}}{l_{1b}}\right)^{\omega}\left(\sum_{k=0}^{+\infty}\gamma_k P_k^{(-\frac{1}{2},\omega)}(-1)\right)\cos(\pi\omega+(\alpha_{1a}-\alpha_{1b})(1+\omega)) \tag{C.38}$$

using the following trigonometry relation

$$\cos((\pi+\alpha_{1a}-\alpha_{1b})\omega)\cos(\alpha_{1a}-\alpha_{1b}) - \sin((\pi+\alpha_{1a}-\alpha_{1b})\omega)\sin(\alpha_{1a}-\alpha_{1b}) = \cos(\pi\omega+(\alpha_{1a}-\alpha_{1b})(1+\omega)) \tag{C.39}$$

For $I_4{}^{B}$ we obtain

$$I_4{}^{B} \xrightarrow{\xi_{1a}\to-1} 2^{-\frac{1}{2}+\omega}\,\Gamma(\omega)\left(\sum_{k=0}^{+\infty}\gamma_k(-1)^k\frac{\Gamma\left(k+1-\frac{1}{2}\right)}{\Gamma\left(k+1-\frac{1}{2}+\omega\right)}\right)\cos(\alpha_{1a}-\alpha_{1b}) \tag{C.40}$$

Instead if $\alpha_{1a} = \alpha_{1b}$ to evaluate the integral we must use the following relation

$$\begin{aligned} &\int_{-1}^{+1}(x-t)^{-1}(1-t)^{\alpha}(1+t)^{\beta}P_k^{(\alpha,\beta)}(t)dt = \\ &\qquad = \frac{1}{2}\left[2(x_1-1)^{\alpha}(x_1+1)^{\beta}Q_k^{(\alpha,\beta)}(x_1) + 2(x_2-1)^{\alpha}(x_2+1)^{\beta}Q_k^{(\alpha,\beta)}(x_2)\right] \end{aligned} \tag{C.41}$$

because now the point lies on the cut and so we calculate the integral in $x_1 = \zeta + i0$ and $x_2 = \zeta - i0$ and take the mean as the result of ${I_4}^{1a}$

$$\int_{-1}^{+1} \frac{\rho_{1b}(\xi_{1b}^{'})d\xi_{1b}^{'}}{\xi_{1b}^{'} - z_1(\xi_{1a})} = 2\left(z_1\left(\xi_{1a}\right) - 1\right)^{-\frac{1}{2}}\left(z_1\left(\xi_{1a}\right) + 1\right)^{\omega}\sum_{k=0}^{+\infty}\gamma_k Q_k^{\left(-\frac{1}{2},\omega\right)}\left(z_1\left(\xi_{1a}\right)\right) \tag{C.42}$$

Using relation (A.6) we can still express the solution in this way

$${J_4}^{1a} = {J_4}^{S} + {J_4}^{B} \tag{C.43}$$

where now

$$\begin{aligned}
{J_4}^{S} =& -\pi\left(2 - \frac{l_{1a}}{l_{1b}}\left(\xi_{1a}+1\right)\right)^{-\frac{1}{2}}\left[\left(\frac{l_{1a}}{l_{1b}}\right)\left(\xi_{1a}+1\right)\right]^{\omega}\cot(\pi\omega)\sum_{k=0}^{+\infty}\gamma_k P_k^{\left(-\frac{1}{2},\omega\right)}\left(-1 + \frac{l_{1a}}{l_{1b}}\left(\xi_{1a}+1\right)\right)\\
{J_4}^{B} =& 2^{-\frac{1}{2}+\omega}\,\Gamma(\omega)\sum_{k=0}^{+\infty}\gamma_k(-1)^k\frac{\Gamma(k+1-\frac{1}{2})}{\Gamma(k+1-\frac{1}{2}+\omega)}\,F\left(k+1,-k+\frac{1}{2}-\omega;1-\omega;\frac{1}{2}\frac{l_{1a}}{l_{1b}}(\xi_{1a}+1)\right)
\end{aligned}$$

For ${I_4}^{S}$ now we obtain

$$(1+\xi_1)^{-\omega}\cdot {I_4}^{S} \xrightarrow{\xi_1\to -1} -\pi 2^{-\frac{1}{2}}\cot(\pi\omega)\left(\frac{l_{1a}}{l_{1b}}\right)^{\omega}\sum_{k=0}^{+\infty}\gamma_k P_k^{(-\frac{1}{2},\omega)}(-1) \tag{C.44}$$

while for ${I_4}^{B}$ we obtain

$${I_4}^{B} \xrightarrow{\xi_1\to -1} 2^{-\frac{1}{2}+\omega}\,\Gamma(\omega)\sum_{k=0}^{+\infty}\gamma_k(-1)^k\frac{\Gamma\left(k+1-\frac{1}{2}\right)}{\Gamma\left(k+1-\frac{1}{2}+\omega\right)} \tag{C.45}$$

It's easy to verify that results corresponding to the case $\alpha_{1a} = \alpha_{1b}$ can be obtained directly considering the limit $\alpha_{1a} \to \alpha_{1b}$ of the results obtained taking $\alpha_{1a} \neq \alpha_{1b}$.

C.3.2 Integrale ${I_5}^{1a}$

This integral can be expressed in the following way

$$\begin{aligned}
&\int_{-1}^{+1}\frac{\frac{l_{1a}}{l_{1b}}(\xi_{1a}+1) + (\xi_{1b}^{'}+1)\cos(\alpha_{1a}+\alpha_{1b})}{\left(\frac{l_{1a}}{l_{1b}}(\xi_{1a}+1)\sin\alpha_{1a} - (\xi_{1b}^{'}+1)\sin\alpha_{1b}\right)^2 + \left(\frac{l_{1a}}{l_{1b}}(\xi_{1a}+1)\cos\alpha_{1a} + (\xi_{1b}^{'}+1)\cos\alpha_{1b}\right)^2}\rho_{1b}(\xi_{1b}^{'})d\xi_{1b}^{'}\\
&= -\left(A_2^{'}\int_{-1}^{+1}\frac{\rho_{1b}(\xi_{1b}^{'})d\xi_{1b}^{'}}{z_3(\xi_{1a}) - \xi_{1b}^{'}} + \overline{A_2^{'}}\int_{-1}^{+1}\frac{\rho_{1b}(\xi_{1b}^{'})d\xi_{1b}^{'}}{\overline{z_3}(\xi_{1a}) - \xi_{1b}^{'}}\right)\\
&= -\left(\cos(\alpha_{1a}+\alpha_{1b})\,\mathrm{Re}\left\{{J_5}^{1a}\right\} - \sin(\alpha_{1a}+\alpha_{1b})\,\mathrm{Im}\left\{{J_5}^{1a}\right\}\right)
\end{aligned}$$

where

$$\int_{-1}^{+1}{J_5}^{1a} = \frac{\rho_{1b}(\xi_{1b}^{'})d\xi_{1b}^{'}}{\xi_{1b}^{'} - z_3(\xi_{1a})}, \qquad \begin{cases} A_2^{'} = \dfrac{1}{2}e^{i(\alpha_{1a}+\alpha_{1b})} \\ z_3(\xi_{1a}) = -1 - \dfrac{l_{1a}}{l_{1b}}e^{i(\alpha_{1a}+\alpha_{1b})}(\xi_{1a}+1) \end{cases} \tag{C.46}$$

The point $z_3(\xi_{1a})$ does not lie on the cut of the complex plane so using relation (A.5) we can write

$$\int_{-1}^{+1} \frac{\rho_{1b}(\xi_{1b}^{'})d\xi_{1b}^{'}}{\xi_{1b}^{'} - z_3(\xi_{1a})} = 2\left(z_3\left(\xi_{1a}\right)-1\right)^{-\frac{1}{2}}\left(z_3\left(\xi_{1a}\right)+1\right)^{\omega}\sum_{k=0}^{+\infty}\gamma_k Q_k^{\left(-\frac{1}{2},\omega\right)}\left(z_3\left(\xi_{1a}\right)\right) \tag{C.47}$$

Using relation (B.69), we can express the solution in this form

$$J_5 = {J_5}^S + {J_5}^B \tag{C.48}$$

where

$$\begin{aligned}
{J_5}^S =& -e^{i(\alpha_{1a}+\alpha_{1b})\omega}\left(2+e^{i(\alpha_{1a}+\alpha_{1b})}\frac{l_{1a}}{l_{1b}}\left(\xi_{1a}+1\right)\right)^{-\frac{1}{2}}\left[\left(\frac{l_{1a}}{l_{1b}}\right)\left(\xi_{1a}+1\right)\right]^{\omega}\frac{\pi}{\sin(\pi\omega)} \\
&\times\sum_{k=0}^{+\infty}\gamma_k P_k^{\left(-\frac{1}{2},\omega\right)}\left(-1+e^{i(\alpha_{1a}+\alpha_{1b})}\frac{l_{1a}}{l_{1b}}\left(\xi_{1a}+1\right)\right) \\
{J_5}^S =& 2^{-\frac{1}{2}+\omega}\,\Gamma(\omega)\sum_{k=0}^{+\infty}\gamma_k(-1)^k\frac{\Gamma(k+1-\frac{1}{2})}{\Gamma(k+1-\frac{1}{2}+\omega)}\,F\left(k+1,-k+\frac{1}{2}-\omega;1-\omega;\frac{1}{2}e^{i(\alpha_{1a}+\alpha_{1b})}\frac{l_{1a}}{l_{1b}}(\xi_{1a}+1)\right)
\end{aligned}$$

Defining

$${I_5}^S = -\left[\cos(\alpha_{1a}+\alpha_{1b})\,\mathrm{Re}\left\{{J_5}^S\right\} - \sin(\alpha_{1a}+\alpha_{1b})\left\{{J_5}^S\right\}\right] \tag{C.49}$$

$${I_5}^B = -\left[\cos(\alpha_{1a}+\alpha_{1b})\,\mathrm{Re}\left\{{J_5}^B\right\} - \sin(\alpha_{1a}+\alpha_{1b})\left\{{J_5}^B\right\}\right] \tag{C.50}$$

and letting $\xi_{1a}\to -1$, for ${I_5}^S$ we obtain

$$(1+\xi_{1a})^{-\omega}\cdot {I_5}^{1a} \xrightarrow{\xi_{1a}\to -1} \pi 2^{-\frac{1}{2}}\frac{1}{\sin(\pi\omega)}\left(\frac{l_{1a}}{l_{1b}}\right)^{\omega}\left(\sum_{k=0}^{+\infty}\gamma_k P_k^{\left(-\frac{1}{2},\omega\right)}(-1)\right)\cos((\alpha_{1a}+\alpha_{1b})(1+\omega)) \tag{C.51}$$

derived using the following trigonometrical relation

$$\cos((\alpha_{1a}+\alpha_{1b})\omega)\cos(\alpha_{1a}+\alpha_{1b}) - \sin((\alpha_{1a}+\alpha_{1b})\omega)\sin(\alpha_{1a}+\alpha_{1b}) = \cos((\alpha_{1a}+\alpha_{1b})(1+\omega)) \tag{C.52}$$

while for ${I_5}^B$ we obtain

$${I_5}^B \xrightarrow{\xi_{1a}\to -1} -2^{-\frac{1}{2}+\omega}\,\Gamma(\omega)\left(\sum_{k=0}^{+\infty}\gamma_k(-1)^k\frac{\Gamma\left(k+1-\frac{1}{2}\right)}{\Gamma\left(k+1-\frac{1}{2}+\omega\right)}\right)\cos(\alpha_{1a}+\alpha_{1b}) \tag{C.53}$$

C.4 Numerical solution

C.4.1 $R_{ij}(k,n)$ coefficients

The double integrals $R_{ij}(k,n)$ have the following form

$$
\begin{aligned}
R_{11}(k,n) &= \int_{-1}^{+1} U_k(\xi_{1a})\sqrt{1-\xi_{1a}^2}\, J_{11}\, d\xi_{1a} \\
R_{12}(k,n) &= \\
&= -\int_{-1}^{+1} U_k(\xi_{1a})\sqrt{1-\xi_{1a}^2}\,[\cos(2\alpha_{1a})\,\mathrm{Re}\,\{J_{12}\} - \sin(2\alpha_{1a})\,\mathrm{Im}\,\{J_{12}\}]\, d\xi_{1a} \\
R_{13}(k,n) &= \\
&= -\int_{-1}^{+1} U_k(\xi_{1a})\sqrt{1-\xi_{1a}^2}\,[\cos(\alpha_{1a})\,\mathrm{Re}\,\{J_{13}\} + \sin(\alpha_{1a})\,\mathrm{Im}\,\{J_{13}\}]\, d\xi_{1a} \\
R_{14}(k,n) &= \\
&= \int_{-1}^{+1} U_k(\xi_{1a})\sqrt{1-\xi_{1a}^2}\,[\cos(\alpha_{1a}-\alpha_{1b})\,\mathrm{Re}\,\{J_{14}\} - \sin(\alpha_{1a}-\alpha_{1b})\,\mathrm{Im}\,\{J_{14}\}]\, d\xi_{1a} \\
R_{15}(k,n) &= \\
&= -\int_{-1}^{+1} U_k(\xi_{1a})\sqrt{1-\xi_{1a}^2}\,[\cos(\alpha_{1a}+\alpha_{1b})\,\mathrm{Re}\,\{J_{15}\} - \sin(\alpha_{1a}+\alpha_{1b})\,\mathrm{Im}\,\{J_{15}\}]\, d\xi_{1a} \\
R_{21}(k,n) &= \int_{-1}^{+1} U_k(\xi_{1b})\sqrt{1-\xi_{1b}^2}\, J_{21}\, d\xi_{1b} \\
R_{22}(k,n) &= \\
&= -\int_{-1}^{+1} U_k(\xi_{1b})\sqrt{1-\xi_{1b}^2}\,[\cos(2\alpha_{1b})\,\mathrm{Re}\,\{J_{22}\} - \sin(2\alpha_{1b})\,\mathrm{Im}\,\{J_{22}\}]\, d\xi_{1b} \\
R_{23}(k,n) &= \\
&= -\int_{-1}^{+1} U_k(\xi_{1b})\sqrt{1-\xi_{1b}^2}\,[\cos(\alpha_{1b})\,\mathrm{Re}\,\{J_{23}\} + \sin(\alpha_{1b})\,\mathrm{Im}\,\{J_{23}\}]\, d\xi_{1b} \\
R_{24}(k,n) &= \\
&= \int_{-1}^{+1} U_k(\xi_{1b})\sqrt{1-\xi_{1b}^2}\,[\cos(\alpha_{1a}-\alpha_{1b})\,\mathrm{Re}\,\{J_{24}\} - \sin(\alpha_{1a}-\alpha_{1b})\,\mathrm{Im}\,\{J_{24}\}]\, d\xi_{1b} \\
R_{25}(k,n) &= \\
&= -\int_{-1}^{+1} U_k(\xi_{1b})\sqrt{1-\xi_{1b}^2}\,[\cos(\alpha_{1a}+\alpha_{1b})\,\mathrm{Re}\,\{J_{25}\} - \sin(\alpha_{1a}+\alpha_{1b})\,\mathrm{Im}\,\{J_{25}\}]\, d\xi_{1b} \\
R_{31}(k,n) &= \int_{-1}^{+1} U_k(\xi_2)\sqrt{1-\xi_2^2}\, J_{33}\, d\xi_2 \\
R_{32}(k,n) &= -\int_{-1}^{+1} U_k(\xi_2)\sqrt{1-\xi_2^2}\, J_{34}\, d\xi_2 \\
R_{33}(k,n) &= \\
&= -\int_{-1}^{+1} U_k(\xi_2)\sqrt{1-\xi_2^2}\,[\cos\alpha_{1a}\,\mathrm{Re}\,\{J_{31}\} + \sin\alpha_{1a}\,\mathrm{Im}\,\{J_{31}\}]\, d\xi_2 \\
R_{34}(k,n) &= \\
&= -\int_{-1}^{+1} U_k(\xi_2)\sqrt{1-\xi_2^2}\,[\cos\alpha_{1b}\,\mathrm{Re}\,\{J_{32}\} + \sin\alpha_{1b}\,\mathrm{Im}\,\{J_{32}\}]\, d\xi_2
\end{aligned}
\tag{C.54}
$$

The integrals J_{ij} have been evaluated analytically, exploiting the even property of P_{2k} polynomials, and the integral formula

$$\int_{-1}^{1} \frac{P_k(t)}{t-t'} dt' = 2Q_k(t) \tag{C.55}$$

where $Q_k(t)$ are Legendre functions of second type, which possess a logarithmic singularity at $t = \pm 1$.

$$J_{11} = -\frac{2}{t_{1a}} \sum_{k=0}^{\infty} \gamma_k^{(1a)} Q_{2k}(t_{1a}), \qquad t_{1a} = \sqrt{\frac{1-\xi_{1a}}{2}} \tag{C.56}$$

$$J_{12} = -\frac{2}{u_{1a}} \sum_{k=0}^{\infty} \gamma_k^{(1a)} Q_{2k}(u_{1a}), \qquad u_{1a} = \sqrt{1+\frac{1}{2}(1+\xi_{1a})e^{2i\alpha_{1a}}} \tag{C.57}$$

$$J_{13} = -\frac{2}{v_{1a}} \sum_{k=0}^{\infty} \beta_k Q_{2k}(v_{1a}), \qquad v_{1a} = \sqrt{1+\frac{1}{2}\frac{l_{1a}}{l_2}(1+\xi_{1a})e^{-i\alpha_{1a}}} \tag{C.58}$$

$$J_{14} = -\frac{2}{r_{1a}} \sum_{k=0}^{\infty} \gamma_k^{(1b)} Q_{2k}(r_{1a}), \qquad r_{1a} = \sqrt{1+\frac{1}{2}\frac{l_{1a}}{l_{1b}}(1+\xi_{1a})e^{i(\alpha_{1a}-\alpha_{1b})}} \tag{C.59}$$

$$J_{15} = -\frac{2}{s_{1a}} \sum_{k=0}^{\infty} \gamma_k^{(1b)} Q_{2k}(s_{1a}), \qquad s_{1a} = \sqrt{1+\frac{1}{2}\frac{l_{1a}}{l_{1b}}(1+\xi_{1a})e^{i(\alpha_{1a}+\alpha_{1b})}} \tag{C.60}$$

$$J_{21} = -\frac{2}{t_{1b}} \sum_{k=0}^{\infty} \gamma_k^{(1a)} Q_{2k}(t_{1b}), \qquad t_{1b} = \sqrt{\frac{1-\xi_{1b}}{2}} \tag{C.61}$$

$$J_{22} = -\frac{2}{u_{1b}} \sum_{k=0}^{\infty} \gamma_k^{(1a)} Q_{2k}(u_{1b}), \qquad u_{1b} = \sqrt{1+\frac{1}{2}(1+\xi_{1b})e^{2i\alpha_{1b}}} \tag{C.62}$$

$$J_{23} = -\frac{2}{v_{1b}} \sum_{k=0}^{\infty} \beta_k Q_{2k}(v_{1b}), \qquad v_{1b} = \sqrt{1+\frac{1}{2}\frac{l_{1b}}{l_2}(1+\xi_{1b})e^{-i\alpha_{1b}}} \tag{C.63}$$

$$J_{24} = -\frac{2}{r_{1b}} \sum_{k=0}^{\infty} \gamma_k^{(1b)} Q_{2k}(r_{1b}), \qquad r_{1b} = \sqrt{1+\frac{1}{2}\frac{l_{1b}}{l_{1a}}(1+\xi_{1b})e^{i(\alpha_{1b}-\alpha_{1a})}} \tag{C.64}$$

$$J_{25} = -\frac{2}{s_{1b}} \sum_{k=0}^{\infty} \gamma_k^{(1b)} Q_{2k}(s_{1b}), \qquad s_{1b} = \sqrt{1+\frac{1}{2}\frac{l_{1b}}{l_{1a}}(1+\xi_{1b})e^{i(\alpha_{1a}+\alpha_{1b})}} \tag{C.65}$$

$$J_{31} = -\frac{2}{t_2} \sum_{k=0}^{\infty} \beta_k Q_{2k}(t_2), \qquad t_2 = \sqrt{\frac{1-\xi_2}{2}} \tag{C.66}$$

$$J_{32} = -\frac{2}{u_2} \sum_{k=0}^{\infty} \beta_k Q_{2k}(u_2), \qquad u_2 = \sqrt{1+\frac{1}{2}(1+\xi_2)} \tag{C.67}$$

$$J_{33} = -\frac{2}{r_2} \sum_{k=0}^{\infty} \gamma_k^{(1a)} Q_{2k}(r_2), \qquad r_2 = \sqrt{1+\frac{1}{2}\frac{l_2}{l_{1a}}(1+\xi_2)e^{-i\alpha_{1a}}} \tag{C.68}$$

$$J_{34} = -\frac{2}{s_2} \sum_{k=0}^{\infty} \gamma_k^{(1b)} Q_{2k}(s_2), \qquad s_2 = \sqrt{1+\frac{1}{2}\frac{l_2}{l_{1b}}(1+\xi_2)e^{-i\alpha_{1b}}} \tag{C.69}$$

Bibliography

Arnadóttir, Th., S. Jonsson, R. Pedersen and G. Gudmundsson (2003), *Coulomb stress changes in the South Iceland Seismic Zone due to two large earthquakes in June 2000*, Geophys. Res. Lett., 30, doi:10.1029/2002GL016495.

Arnadóttir, Th., S. Jonsson, F.F. Pollitz, W. Jiang and K.L. Feigl. 2005, *Postseismic deformation following the June 2000 earthquake sequence in the south Iceland seismic zone*, J. Geophys. Res., 110, B12308.

Bonafede, M. and E. Rivalta (1999), *On tensile cracks close to and across the interface between two welded elastic half-spaces*, Geophys. J. Intern., 138(2), 410-434. doi: 10.1046/j.1365-246X.1999.00880.x.

Bonafede, M., B. Parenti, and E. Rivalta, *On strike slip faulting in layered media*, Geophys. J. Int., Volume 149 Issue 3 Page 698-723, June 2002.

Bonafede, M., C. Ferrari, F. Maccaferri, and R. Stefansson (2007), *On the preparatory processes of the M6.6 earthquake of June 17th, 2000, in Iceland*, Geophys. Res. Lett., 34, L24305, doi:10.1029/2007GL031391.

Chiodini G., C. Cardellini, A. Amato, E. Boschi, S. Caliro, F. Frondini, G. Ventura (2004), *Carbon dioxide Earth degassing and seismogenesis in central and southern Italy*, Geophys. Res. Lett., 31, L07615, doi:10.1029/2004GL019480.

Crouch S L, Starfield A M., *Boundary Element Method in Solid Mechanics*, ALLEN and UNWIN, INC., 1983.

Das, S. and Kostrov, B. 1983. *Breaking of a single asperity: Rupture process and seismic radiation.* J. Geophys. Res. 88: 4277-88.

DeMets, C., R.G. Gordon, D.F. Argus, and S. Stein (1994), *Effect of recent revisions to the geomagnetic reversal time scale on estimates of currentm plate motions*, Geophys. Research Lett., 21, 2191-2194.

Einarsson, P. (1991), *Earthquakes and present-day tectonism in Iceland.* Tectonophysics, 189, 261-279.

Erdogan, F., Gupta, G.D. and Cook, T.S, *Numerical solution of singular integral equation*, Mech. of fracture, 1 (1973).

Goodier, J. N. (1933), *Concentration of Stress Around Spherical and Cylindrical Inclusions and Flaws*, J. Appl. Mech., Vol. 55, 1933, p. A39.

Hersir, G.P., A. Björnsson and L.B. Pedersen (1984), *Magnetotelluric survey across the active spreading zone in Southwest Iceland*. J. Volc. Geotherm. Res., 20, 253-265.

Ito, G., J. Lin, and D. Graham (2002), *Observational and theoretical studies of the dynamics of mantle plume-mid ocean ridge interaction*, Rev. Geophys., 41(4), doi:10.1029/2002RG000117.

Jaeger, J.C. and Cook, N.G.W. (1976), *Fundamentals of Rock Mechanics*, Chapman and Hall, London.

Jonsson, S. , P. Segall, R. Pedersen and Bjornsson, G. (2003), *Post-earthquake ground movements correlated to pore-pressure transients*, Nature 424, 179-183 (10 July 2003), doi:10.1038/nature01776.

Lay, T., Ruff, L., and Kanamori, H., 1980, *The asperity model and the nature of large earthquakes in subduction zones*, Earthquake Pred. Res. 1:3-71.

Lay, T., and Kanamori, H., 1981, *An asperity model of great earthquake sequences*, Earthquake Prediction - An International Review, AGU Geophys. Mono.: Washington, D.C., p. 14.

Lund,B., R. Slunga and R. Bödvarsson (2005), *Spatial and temporal variations of the stress field in the South Iceland seismic zone before and after the two M = 6.5 earthquakes of June 2000*, Geophysical Research Abstracts, 7, 06666.

Miller, S.A., C. Collettini, L. Chiaraluce, M. Cocco, M. Barchi and B.J.P. Kaus (2004), *Aftershocks driven by a high-pressure CO2 source at depth*, Nature 427, 724-727.

Muskhelishvili, N.I., *Singular Integral Equations*, Noordhoff, Groningen, 1953.

Poirier, J.P. (1985), *Creep of crystals*, Cambridge University Press, Cambridge, 260 pp.

Rivalta, E., W. Mangiavillano and M. Bonafede (2002), *The edge dislocation problem in a layered elastic medium*, Geophys. J. Intern., 149(2), 508-523. doi: 10.1046/j.1365-246X.2002.01649.x

Roth, F. (2004), *Stress changes modelled for the sequence of strong earthquakes in the South Iceland seismic zone since 1706*. Pageoph. 161(7), 1305-1327, doi:10.1007/s00024-004-2506-5.

Rybicki, K.R., 1971, *The elastic residual eld of a very long strike-slip fault in the presence of a discontinuity*, Bull. seism. Soc. Am., 61, 7992.

Singh, S.J. and Rani, S., 1994, *Litospheric deformation associated with two-dimensional strike-slip faulting*, J. Phys. Earth, 42, 197-220, 1994.

Stefánsson, R. and P. Halldorsson (1988), *Strain release and strain build-up in the South Iceland seismic zone*, Tectonophys. 159, 267-276.

Stefánsson, R., R. Bödvarsson, R. Slunga, P. Einarsson, S.S. Jakobsdóttir, H. Bungum, S. Gregersen, J. Havskov, J. Hjelme and H. Korhonen (1993), *Earthquake prediction research in the South Iceland seismic zone and the SIL project*. Bull. Seism. Soc. Am. 83(3), 696- 716.

Stefánsson, R., G. Gudmundsson, M. Bonafede (2007), *Earthquake prediction research and the year 2000 earthquakes in SISZ*. Bull. Seism. Soc. Am. Submitted.

Tryggvason, A., S. Th. Rögnvaldsson and O. G. Flovennz (2002), *Three-dimensional imaging of the P- and S-wave velocity structure and earthquake locations beneath Southwest Iceland*, Geophys. J. Int. (2002) 151, 848-866.

Turcotte, D.L. and G.Schubert, *Geodynamics-Applications of Continuum Physics to Geological Problems*, pp. 354-357, John Wiley, New York, 1982

Wells, D.L. and K.J. Coppersmith (1994), *New empirical relationships among magnitude, rupture length, rupture width, rupture area, and surface displacement*, Bull. Seism. Soc. Am., 84, 974-1002.

Wyss, M. and R. Stefánsson (2006), *Nucleation points of recent main shocks in southern Iceland mapped by b-values*. Bull. Seism. Soc. Am., 96 , 599-608.

Zencher, F., M. Bonafede and R. Stefánsson (2006), *Near-lithostatic pore pressure at seismogenic depths: a thermoporoelastic model*, Geophysical Journal International, 166 (3), 1318-1334.